PERFORMANCE, EMISSION AND COMBUSTION CHARACTERISTICS OF A BIODIESEL FUELLED DIESEL ENGINE

A Thesis submitted to the Delhi Technological University, Delhi in fulfillment of the requirements for the award of the degree of

DOCTOR OF PHILOSOPHY

in

Mechanical Engineering

by

HARVEER SINGH PALI

(2K12/PhD/ME/04)

Under the Supervision of

Dr. NAVEEN KUMAR

(Professor)

Mechanical Engineering Department

Delhi Technological University

Shahbad Daulatpur Bawana Road

Delhi – 110042, INDIA

JULY, 2016

DECLARATION

I hereby declare that the thesis entitled "**PERFORMANCE, EMISSION AND COMBUSTION CHARACTERISTICS OF A BIODIESEL FUELLED DIESEL ENGINE"** is an original work carried out by me under the supervision of Dr. Naveen Kumar, Professor, Department of Mechanical Engineering, Delhi Technological University, Delhi. This thesis has been prepared in conformity with the rules and regulations of the Delhi Technological University, Delhi. The research work reported and results presented in the thesis have not been submitted either in part or full to any other university or institute for the award of any other degree or diploma.

Harveer Singh Pali

(2K12/PhD/ME/04)
Research Scholar
Mechanical Engineering Department
Delhi Technological University,
Delhi

Date: 21.07.2016

Place: Delhi

CERTIFICATE

This is to certify that the work embodied in the thesis entitled **"PERFORMANCE, EMISSION AND COMBUSTION CHARACTERISTICS OF A BIODIESEL FUELLED DIESEL ENGINE"** by **Harveer Singh Pali, (**Roll No.**-2K12/PhD/ME/04)** in partial fulfillment of requirements for the award of Degree of **DOCTOR OF PHILOSOPHY in Mechanical Engineering**, is an authentic record of student's own work carried by him under my supervision.

This is also certified that this work has not been submitted to any other Institute or University for the award of any other diploma or degree.

(Dr. Naveen Kumar)
Professor
Mechanical Engineering Department
Delhi Technological University
Delhi- 110042.

Dedicated to My parents & family

ACKNOWLEDGEMENTS

The present research work was carried out under the esteemed supervision of my guide Prof. Naveen Kumar. It is my honour and privilege to express a deep sense of gratitude to him for his panegyric efforts, ever helping attitude, critical and valuable comments and constant inspiration. His mentorship helped me become a good researcher which I always dreamed. His words of solace and encouragement especially during difficult times shall ever be remembered by me. I also acknowledge the blessing by Smt. Sumeeta Garg who always cared for me during my stay in Delhi. I will be highly indebted to her for her affection.

I am also grateful to Dr. R. S. Mishra, Professor & Head, Dr. R. C. Singh, Associate Professor, Dr. Rajiv Chaudhari, Associate Professor, Dr. Rangnath M.S., Associate Professor and Mr. Raghvendra Gautam, Assistant Professor, Department of Mechanical Engineering, DTU Delhi for their help, encouragement and valuable suggestions.

I owe gratitude to the esteemed colleagues of the Centre for Advanced Studies and Research in Automotive Engineering (**CASRAE**), Delhi Technological University; particularly my research fellow Mr. Alhassan Yahaya and Mr. Parvesh Kumar for their excellent support and valuable suggestions.

I am thankful to Mr. Kamal Nain and Mr. Manoj Kumar for providing all laboratory assistance. I am also thankful for Mr. Surendra Singh and Smt. Neetu Mishra, the supporting staff of CASRAE, DTU, Delhi.

I am grateful to management of at Noida Institute of Engineering and Technology, Greater Noida, particularly Dr. O. P. Aggrawal, Managing Director, Dr. Neema Aggrawal, Asstt. Managing Director, Mr. Raman Batra, Executive Vice President, Dr. Ajay Kumar, Director and Dr. P. Pachauri, Head, Department of Mechanical Engineering for providing all possible support and relieving me from the official duties, which has enabled me to focus on the present work.

There are some friends and colleagues who have helped me along the way for the successful completion of this research work. I take this opportunity to thank Mr. Chinmaya Mishra, Assistant Professor, KIIT University, Mr. S.P. Diwedi, Assistant Professor, NIET, Gr. Noida and Dr. Vipin Kumar, Assistant Professor, NIET, Gr. Noida, Dr. Chandan Kumar, Professor, NIET Gr. Noida, Mr. Amardeep, Assistant Professor, IEC, Gr. Noida and Mr. Siddarth Bansal, Assistant Professor, MAIT, Delhi.

I shall ever cherish the affection and blessings showered on me by my parents. Whatever I have achieved in my professional life; it is all because of them. I cannot express in words their efforts put by them to nurture me. I am also indebted to my younger brothers Mr. Munesh Pal and Mr. Devendra Pal who always extended help whenever required. I place my sincere respect and a deep sense of gratitude to other family members, specially, my fathers in law Shri Y. N. Singh and Shri Surendra Singh.

Finally, I am unable to express my sincere gratitude in words for the affection, encouragement and moral support by my wife during the entire research work. I am ever beholden to my wife Seema Pal, son Chetan Anand Pali and daughter Kanishka Pali for not giving due attention and time during the present work.

There are many more persons who have helped me directly or indirectly to complete this research work. I take this opportunity to thank all of them and apologize for their names not being here.

Last but not the least; I thank the Almighty for giving me strength and patience to complete this work in all respects and leading to the path of success.

(Harveer Singh Pali)

New Delhi

July, 2016

ABSTRACT

India's economy is essentially diesel driven, and diesel consumption is almost four to five times higher than that of gasoline. So, biodiesel has proved its utility as a promising renewable and sustainable alternative to the petroleum diesel in the last two decades. One of the main barriers for commercialization of biodiesel is the cost of biodiesel as it is commonly derived from vegetable oils. Hence, the use of low-cost oils as biodiesel feedstocks is very much essential. In this context, Government of India approved the National Policy on Biofuels in December 2009 to substitute 20% of mineral diesel consumption by biodiesel from non-edible oils. However, the ambitious plan of producing sufficient biodiesel to meet the mandate of 20 percent diesel substitution by the year 2017 has not been realized. Excessive reliance on Jatropha curcas as the only feedstock and the inability to produce sufficient quantity has been one of the major reasons for not attaining the mandate. In the light of the above, the present research deals with the comprehensive study of other potential alternative tree borne oil seeds; Sal (Shorea robusta) and Kusum (Schleichera oleosa) for biodiesel production. In India, both feedstocks are potentially available and grossly unexplored for biodiesel production. The main objective of this research work is to produce Sal methyl ester (SME) and Kusum methyl ester (KME) and carry out combustion, performance and emission studies in a small capacity diesel engine with these biodiesel.

The research work has been divided into four major sections. In the first part, production of biodiesel (fatty acid methyl ester) from Sal oil and Kusum oil using either single-stage or two-stage transesterification was carried. A four factor central composite design (CCD) based on response surface methodology was employed for both single stage (esterification) and second stage(transesterification) processes to produce biodiesel from the high free fatty acid (FFA) vegetable oil. The process parameters like catalyst concentration,

reaction time, reaction temperature and methanol to oil molar ratio were taken as factors in the design. Based on the CCD designed test matrix, the experiments were carried out and the results were analysed. Kusum oil has high FFA content (approx 8%) therefore two stage transesterification was used whereas Sal oil has less than 2 % FFA, so single stage transesterification was employed. The optimum conditions for the acid catalysed esterification of Kusum biodiesel were 0.927 % catalyst concentration, 62.11°C reaction temperature, 67.82 minutes reaction time and 6.4 molar ratio. For the alkaline stage, 1.13 % catalyst, 63.18°C temperature, 79.2 minutes reaction time and 8.16 methanol/oil molar ratio; resulted in an optimal yield of 97.41% biodiesel. Based upon the optimum conditions, the confirmation tests were conducted and biodiesel yield achieved was 96.92% for Sal biodiesel and 96.5% Kusum biodiesel.

In the second stage of the research work, fatty acid profile and various physico-chemical properties of SME and KME were experimentally evaluated. The results of the Gas chromatography–mass spectrometry (GC-MS) study indicated that SME composition laid down between C-16 to C-20, where 61% saturated and 39% unsaturated of the total mixture whereas KME composed of C-16 to C-22 and it has 31% saturated and 69% unsaturated fatty acids. Properties like viscosity, density, calorific value, flash point, etc. were measured and found to be within the limits of ASTM standards. Presence of 61% saturated compounds of SME makes it highly susceptible to poor cold flow properties. On the other hand, KME has significant portion of unsaturated acids like oleic acid (C18:1) and eicosenoic acid (20:1). So Kusum biodiesel has poor oxidation stability.

The third stage of the study is related to the evaluation of cold flow properties and oxidation stability of both biodiesel using additives. The chemical additives for the improvement in cold flow properties are synonymously referred to as pour point depressants

(PDD). Application of the PPDs showed improved cold filter plugging point (CFPP) for all the test fuels. Among all additives, CRISTOL showed best results for both biodiesels. Storage stability for one year has suggested that some of the physico-chemical properties of both the biodiesel (SME and KME) changed slightly with time. The rate of change of different physico-chemical properties was found to be lower for both the biodiesel with an additive.

The fourth stage of the study comprised of fuel blend preparation, test rig development and study of the engine performance, exhaust emissions and combustion characteristics with biodiesel-diesel blends up to 40% and comparison of results with baseline diesel (D100). Various test fuels for the engine trials were Sal biodiesel (SME10, SME20, SME30 and SME40) and Kusum biodiesel (KME10, KME20, KME30 and KME40) with 10%, 20%, 30% and 40% volume wise substitution of D100 with biodiesel. The results indicated higher engine performance up to 20% blending of biodiesel in diesel as compared to baseline diesel. Other higher blends showed a marginal reduction in engine performance. Both biodiesel blends exhibited lower emissions of carbon monoxide (up to 63.77%), total hydrocarbon (up to 33.39%) and smoke opacity (up to 48%). However, emissions of oxides of nitrogen were increased with increase in biodiesel volume fraction in the test fuel. A notable observations of both the biodiesel were noticed in the combustion study that the trend of in-cylinder gas pressure and heat release rate (70.71 J/°CA for KME 20)increases with increase in biodiesel volume fraction up to 20% volume of biodiesel. Further increase in volume fraction of biodiesel showed diminishing trends for both SME and KME biodiesel. At the same time decrease in pressure rise rate (13.5%) and ignition delay period was observed (25%)with increasing biodiesel content up 40 % in biodiesel-diesel blends as compared to the baseline results. With increase in volume fraction of SME and KME in the blend, ignition delay was reduced from 11°CA for D100 to 8.2°CA for SME40 and 8.3°CA for KME40. Another

notable observation was that cumulative heat release of SME10 and KME 10 were higher than other test fuels.

As an outcome of an exhaustive engine trial and the subsequent analyses, it may be stated that Sal methyl ester and Kusum methyl ester are an excellent diesel engine fuel. Up to 20% blend of SME and KME with diesel may be used in any unmodified diesel engine with improved performance, emission (except NO_x) and combustion characteristics.

LIST OF CONTENTS

LIST OF FIGURES

LIST OF PLATES

LIST OF TABLES

NOMENCLATURE

@	At the rate
A/F	Air to Fuel
AN	Acid Number
API	American Petroleum Institute
ASTM	American Society for Testing and Materials
ATDC	After Top Dead Center
AVL-437	AVL-437 Smoke Meter
AV	Acid Value
B10	10% Biodiesel/90% Diesel
B20	20% Biodiesel/80% Diesel
B50	50% Biodiesel/50% Diesel
B100	Pure Biodiesel
BHA	Butylated Hydroxyanisole
BHT	Butylated Hydro-toluene
BIS	Bureau of Indian Standard
BMEP	Break Mean Effective Pressure
BSEC	Brake Specific Energy Consumption
BSFC	Brake Specific Fuel Consumption
BTE	Brake Thermal Efficiency
BTDC	Before Top Dead Center
C	Carbon
^{o}C	Degree Celsius
^{o}CA	Degree Cranck Angle
cc	Cubic centimeter
CCD	Central Composite Design
CFPP	Cold Filter Plugging Point
CH_3	Methyl
CH_4	Methane
CHN	Carbon, Hydrogen, Nitrogen
CI	Compression Ignition
cm^{-1}	Per Centimeter

CN	Cetane Number
CO	Carbon Monoxide
CO_2	Carbon Dioxide
CP	Cold Point
cSt	Centi Stoke
CV	Calorific Value
D100	Neat Diesel or Baseline
DI	Direct Injection
DPF	Diesel Particulate Filter
$dQ/d\Theta$	Rate of Heat Transfer in the Engine Cylinder
$dQ_w/d\Theta$	Rate of Heat Transfer from the Wall
DTBHQ	Di-tert Butyl Hydroquinone
EGR	Exhaust Gas Circulation
EN	European Union Standard
EOC	End of Combustion
EOI	End of Injection
^oF	Degree Fahrenheit
F/A	Fuel to Air
FBP	Final Boiling Point
FFA	Free Fatty Acid
FID	Flame Ionisation Detector
FIP	Fuel Injection Pump
FTIR	Fourier Transform Infra red
g	Gram
g/cc	Gram per cubic centimeter
GC	Gas Chromatography
GCMS	Gas Chromatography Mass Spectrometry
GLC	Gas Liquid Chromatographer
h	Hour
HC	Hydrocarbon
HCl	Hydrochloric Acid
HFRR	High Frequency Reciprocating Rig
H_2O	Water

HP	Horse Power
H_2SO_4	Sulphuric Acid
I_2	Iodine
IBP	Initial Boiling Point
IC	Internal Combustion
IDI	Indirect Injection
IR	Infra Red
IS	Indian standard
K	Potassium
KI	Potassium Iodide
KME	Kusum Methyl Ester or Kusum Biodiesel
KME 10	10%Kusum Methyl Ester/90% diesel
KME 20	20%Kusum Methyl Ester/80% diesel
KME 30	30%Kusum Methyl Ester/70% diesel
KME 40	40%Kusum Methyl Ester/60% diesel
KOH	Potassium Hydroxide
KVA	Kilo Volt Ampere
kW	Kilo Watt
kW-h	Kilo Watt Hour
LSD	Low Sulphur Diesel
lph	Liter per Hour
m	Meter
m*	Mass flow rate of fue
1M	1 Mole
meq/kg	Milli equivalent per Kilogram
Mg	Magnesium
Min.	Minute
ml	Milliliter
mm	Millimeter
Mt	Million Tonnes
Mtoe	Million Tonne of Oil Equivalent
Na	Sodium
NaI	Sodium Iodide

NaOH	Sodium Hydroxide
$Na_2S_2O_3$	Sodium Thiosulphate
$Na_2S_4O_6$	Sodium Dithionate
NaX	Sodium Halide
NMB	National Biodiesel Mission
NO	Nitric Oxide
Nos.	Numbers
NO_2	Nitrogen Di-oxide
NO_x	Oxides of Nitrogen
nPAH	Nitro Poly Aromatic Hydrocarbon
O_2	Oxygen
P	Instantaneous Cylinder gas Pressure, Pa
PAH	Poly aromatic Hydrocarbon
Pb	Lead
PC	Personal Computer
PDD	Pour Point Depressants
PM	Particulate Matter
PP	Pour Point
ppm	Parts per million
P-θ	Pressure – Crank Angle
PVC	Poly Vinyl Chloride
rpm	Revolutions Per Minute
SAE	Society of Automobile Engineering
SCR	Selective Catalyst Regenerative
sfc	Specific Fuel Consumption
SI	Spark Ignition
SME	Sal Methyl Ester or Sal Biodiesel
SME 10	10% Sal Methyl Ester/ 90% diesel
SME 20	20% Sal Methyl Ester/ 80% diesel
SME 30	30% Sal Methyl Ester/ 70% diesel
SME 40	40% Sal Methyl Ester/ 60% diesel
SOC	Start of Combustion
SOF	Soluble Organic Fraction

SOI	Start of Injection
ROH	Alkanol
R-OOH	Carboxylic Acid
R/P	Reserve to Production
RSM	Response Surface Metthodology
SO_2	Sulphur Dioxide
SO_x	Oxides of Sulphur
Sp.	Specific
T	Tonnes
TAN	Total Acid Number
TBN	Total Base Number
TBHQ	Tert-Butyl Hydroquinone
TCD	Thermal Conductivity Detector
TDC	Top Dead Center
TG	Tri- Glycerides
THC	Total Hydrocarbon
ULSD	Ultra-Low Sulphur Diesel
UBHC	Unburnt Hydrocarbon
V	Instantaneous Cylinder Volume, m^3
vs	Versus
v/v	Volume/ Volume
w	weigh
wt/wt	Weight/Weight
γ	Ratio of Specific heat,
ρ	Density
%	Percent
μ	Dynamic Viscosity
η	Efficiency

CHAPTER 1

INTRODUCTION

1.1 Motivation

The issues of climate change and energy security are considered most important in the present scenario, and a quest for sustainable energy sources in the light of the environmental problems and fluctuating energy prices has always been given utmost attention. Diesel engines are considered work horse in the Indian economy and have proven their utility in transportation, agriculture and power sectors, etc. Therefore, the diesel consumption in India is four to five times than that of petrol, so biodiesel as a substitute for diesel fuel will be an economically better option for a developing country like India. Biodiesel is a promising alternative fuel for diesel engines and the interest for utilizing biodiesel in the engine has increased substantially. The present work aims at exploring and developing indigenous fuels from existing sustainable energy resources of India as a substitute for mineral diesel for mitigating climate change.

1.2 Energy Scenario of India

Energy is one of the key drivers for socio-economic development, and most of the energy produced nowadays is derived from petroleum based fuels. The issues of climate change and energy security have become much higher priorities in modern times and the quest for sustainable energy sources in light of the environmental problems and escalating energy prices. This has resulted in increase global support for biofuels production as an alternative source of energy in Asian countries. Several alternative technologies are available as a solution to environmental and energy problems: biofuels, alcohols, compressed natural gas or hydrogen-fuelled vehicles. However, uncertainties about long term supplies of these fuels, price volatility and environmental degradation due to an indiscriminate burning of these fuels are some areas of concerns[1].

Among these alternative technologies, the use of bioenergy is proving to be particularly attractive and viable and, therefore, is receiving desirable consideration. The simplicity of production and use and price advantages, liquid biofuels appear to have a head start in this race. The current energy situation has stimulated active research interest in non-petroleum based, renewable, and non-polluting fuels. The quest of biofuels around the world is spurred largely by energy security and environmental concerns and a wide range of market mechanisms, incentives and subsidies have been put in place to facilitate their commercialization [2].

The domestic crude oil production in India has almost stagnated and not keeping pace with either burgeoning population or increase in energy requirement. India has 17% of the world's population and just 0.8% of the world's known oil and natural gas reserves [2]. Moreover, concerns about global warming (Post-Kyoto Protocol) due to emissions produced during combustion of fossil fuels also require improved engine technologies or use of environmental friendly fuels [3].

India's crude oil requirement in 2014-15 was 228.4 million tonnes whereas production was only about 20 % of total need. As India does not have a huge petroleum reserve, dependence on the import of crude petroleum is seriously affecting India's economy and has been the main reason for foreign exchange outflow. The expenditure for importing crude oil is rising considerably each year, and the country spent $112.748 billion (Rs 6.88 lakh crore) in 2014-2015 [4,5]. Figure 1.1 highlights the India's crude oil production and demand in last five years which clearly suggests that self-reliance is decreasing almost every year.

India is growing at a faster rate and consuming more energy than it ever did in its millennium civilization. Therefore, India needs abundant and sustainable energy supply in the foreseen future to maintain the momentum for economic growth and progressive social transformation, without jeopardizing the environment. Unfortunately, it is not able to diversify into new energy sources to ensure sustainability and to tackle issues concerning

environment. This can simply explain the reliability of the Indian energy sector on non-renewable energy resources such as fossil fuels [5- 7].

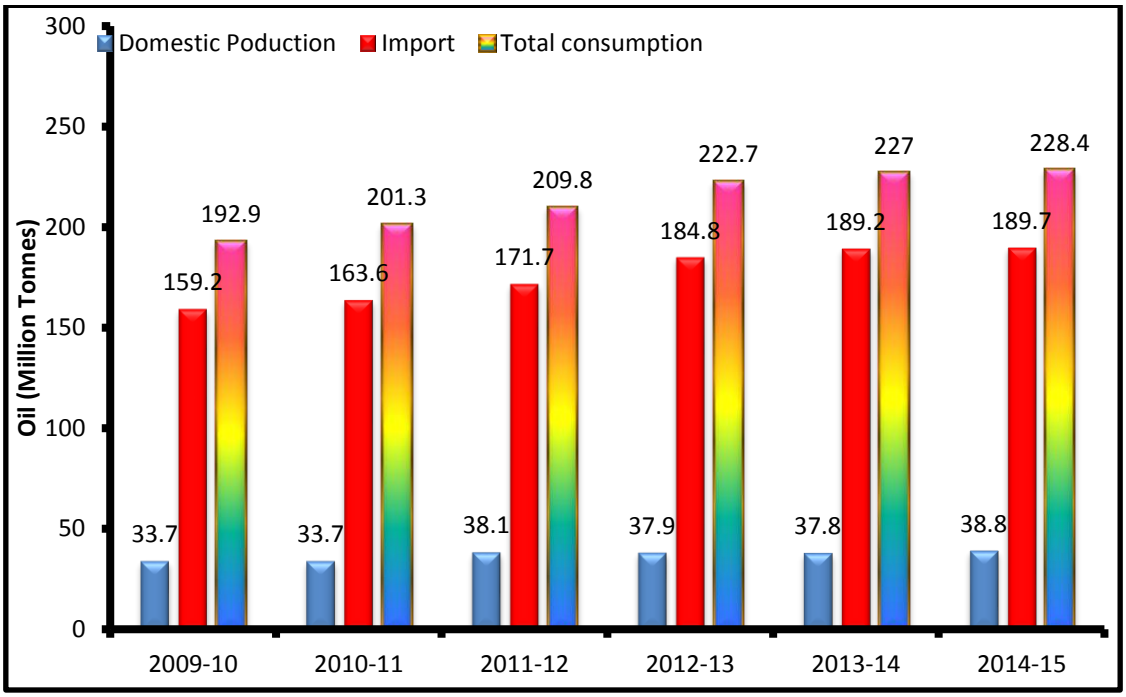

Figure 1.1: India's Crude Oil Production and Demand in last Five Years[4]

Diesel engines play significant roles in the Indian economy as they are used in heavy trucks, city transport buses, locomotives, electric generators, farm equipment and underground mining equipment [7]. Consequently, diesel consumption in India is nearly 4-5 times greater than that of gasoline [8]. However, such engines are also contributors towards harmful emissions, and there is an urgent need to search for alternatives to petroleum-derived diesel to reduce these harmful emissions in the environment [9].

1.3 Environmental Issues

Recently, technology development encourages innovations that are aimed at reducing harmful emissions or discharge into the environment. Such concepts referred to as green technologies are targeted towards reducing adverse effects on the environment. It is established that emissions from diesel Engine are sources of air pollution, having adverse implications on health and air quality. For example; Lead, carbon monoxide, nitrogen oxides, particulate matter, carbon dioxide and hydrocarbons are the main components of an internal

combustion engines exhaust gasses [10,11]. The absence of sulphur results in the reduction of acid rain formation by sulphate emissions which generate sulphuric acid in the atmosphere. The reduced sulphur in the blend also decreases the levels of corrosive sulphuric acid accumulating in the engine crankcase oil over time [12].

Emission tests from I.C. Engines have shown the presence of environmentally degrading components from a variety of renewable fuels such as hydrogen, alcohols, biogas, producer gas and biodiesel. However, in the Indian context, the biofuels such as alcohols, vegetable oils, biodiesel and biogas can contribute significantly towards these twin problems of fuel crises and environmental degradation [2,13,14]. The use of biodiesel in a conventional diesel engine substantially reduces emissions of unburned hydrocarbons, sulphates, polycyclic aromatic hydrocarbons, nitrated polycyclic aromatic hydrocarbons, and particulate matter [15–17].

Biofuels are very promising as these are essentially non-petroleum based fuels and result in energy security and environmental benefits. Biofuels in recent times have emerged as the most viable and sustainable fuels for reducing air pollution and providing sustainable energy supplies[18,19]. Nowadays, biofuels are increasingly used in providing affordable and inexhaustible energy in rural communities in line with the Sustainable Development [20].

Interest in biodiesel is continuing to increase in the world. This impetus is due to concerns about greenhouse gas (GHG) emissions and global climate change, an interest for renewable and sustainable energy sources and a strong desire to develop domestic and more secured fuel supplies. In recent years, several countries have embarked on legislative or regulatory pathways that encourage increased use of biodiesel using both incentives and prescriptive volumetric requirements [21].

1.4 Biodiesel Scenario in India

The Government of India (GOI) had launched the National Biodiesel Mission (NBM) identifying Jatropha as the most suitable non-edible oilseed for biodiesel production.

The Planning Commission of India had set an ambitious target of planting 11.2 to 13.4 million hectares to Jatropha by the end of 11th round of Five-Year Plan (2011-12). The central government and several state governments provide fiscal incentives for supporting planting of Jatropha and other inedible oilseeds. Several public institutions, government departments, state biofuel boards, state agricultural universities and cooperative sectors are also supporting the biofuel mission in various capacities.

India imports more than 40% of its edible oils requirement; hence non-edible oils are used for biodiesel. India as an agrarian nation and has rich plant biodiversity which can support the development of biodiesel. India also has a vast geographical area with agricultural lands as well as wastelands on which oil bearing plants can be planted. Indigenous non-edible oil bearing plants and trees include Jatropha, Karanja, Mahua, Neem, Kusum, etc. The oil yields from these species at present are insufficient to meet the demand for raw material on large scale production of biodiesel. Hence, there has been government initiatives and interest from few private firms to enhance the production and distribution facilities of biodiesel throughout the country.

For example, the Petroleum Ministry has set a target for biodiesel to meet 20% of India's diesel demand. Government's initiative has resulted in large scale plantation of Jatropha curcas in the state of Andhra Pradesh. Oil and Natural Gas Corporation (ONGC) has planned to build an export oriented refinery at Kakinada in Andhra Pradesh with an annual production capacity of 5.5–7.5 million tones.

As noted above, Jatropha production never achieved the desired level of commercialization and production of Jatropha-based biodiesel has failed. As a result, researchers are gradually shifted their focus to produce biodiesel from tree-borne oilseeds such as Karanja (*Pongamia pinnata*), Neem (*Azadirachta indica*), Kusum (*Schleichera oleosa*), Mahua (*Madhuca indica*), as well as waste edible oils and multiple feedstocks.

According to Global Agricultural Information Network report [22], India has six large capacity production plants (10,000 to 250,000 MT per year) with the installed capacity to produce 115-130 million liters of biodiesel from multiple feedstocks such as vegetable oils, waste cooking oils, animal fats and others as shown in Table 1.1.

Table 1.1: India's Biodiesel production from multiple feedstocks (million liters) [22]

Calendar Year	**2010**	**2011**	**2012**	**2013**	**2014**	**2015**
Beginning Stocks	45	38	42	45	45	50
Production	90	102	115	120	130	135
Imports	0	0	0	0	0	0
Exports	0	0	0	0	0	0
Consumption	52	60	70	75	80	90
Ending Stocks	38	42	45	45	50	45
Production Capacity						
Number of Bio-refineries	5	5	5	6	6	6
Capacity	450	450	460	465	480	480
Capacity Use (%)	20.00%	22.70%	25.00%	25.80%	27.10%	28.10%
Feedstock Use (1000 MT)*						
Used Cooking Oil	38	42	48	49	50	50
Animal Fats and Tallow's	6	6	7	7	6	5
Other Oils	50	58	65	70	75	85

Market Penetration						
Biodiesel, on road use	26	30	35	38	40	45
Diesel, on road use	42625	45520	49343	49354	49605	53284
Blend Rate (%)	0.06	0.07	0.07	0.08	0.08	0.08
Diesel, total use	71041	75866	82238	82256	82674	88807

Footnote: * Used cooking oil includes vegetable oils such as rice bran oil, palm stearine, cotton seed oil and fatty acid oils while 'other oils' include tree oils, palm sludge etc.

Currently, researchers investigated several topics such as policy drivers, biodiesel feedstocks, production technologies, fuel properties and specifications, storage stability, engine applications, combustion, performance, emissions impacts, and life-cycle analyses. A search in the Elsevier database at the end of 2015 with the term 'biodiesel' returned more than 3500 papers that contain this word in the article's keywords. Figure 1.2 presents the last ten years database taken for research in particularly on diesel engine.

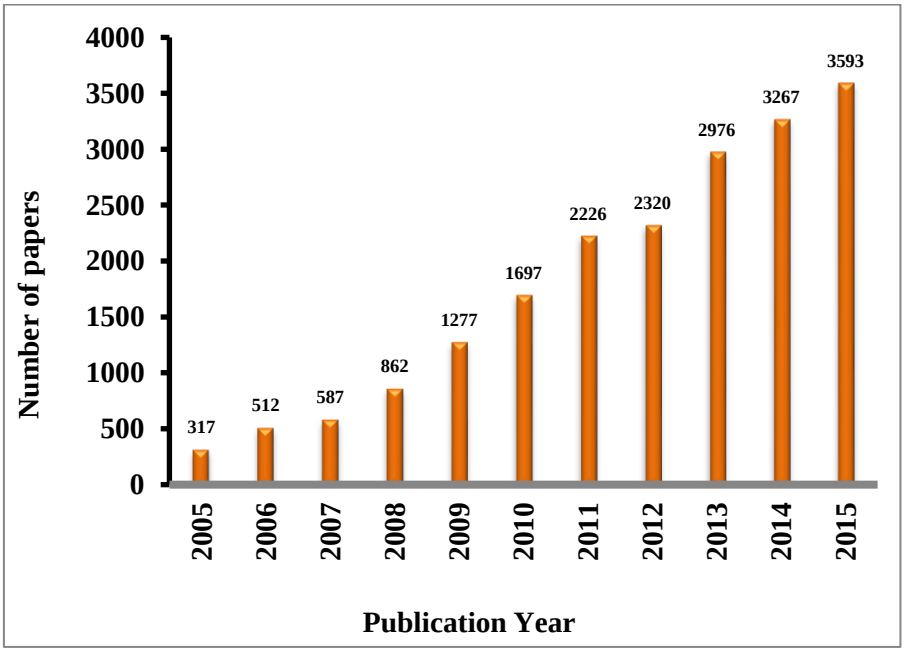

Figure 1.2: Year wise research publications

Biodiesel can also be used in its pure form (B100), but may require certain engine modifications to avoid maintenance and performance problems. The most investigated biodiesel blends are B20 as shown in Figure 1.3 [23]. Biodiesel has higher cetane number as compared to petroleum diesel. This exhibits its ability to improve diesel combustion.

Blends of 20 percent biodiesel with 80 percent petroleum diesel (B20) can generally be used in unmodified diesel engines. Diesel-biodiesel blend (B20) also has superior lubricity, which reduces wear in the engine and can increase the life of fuel injection systems as well as the other engine components.

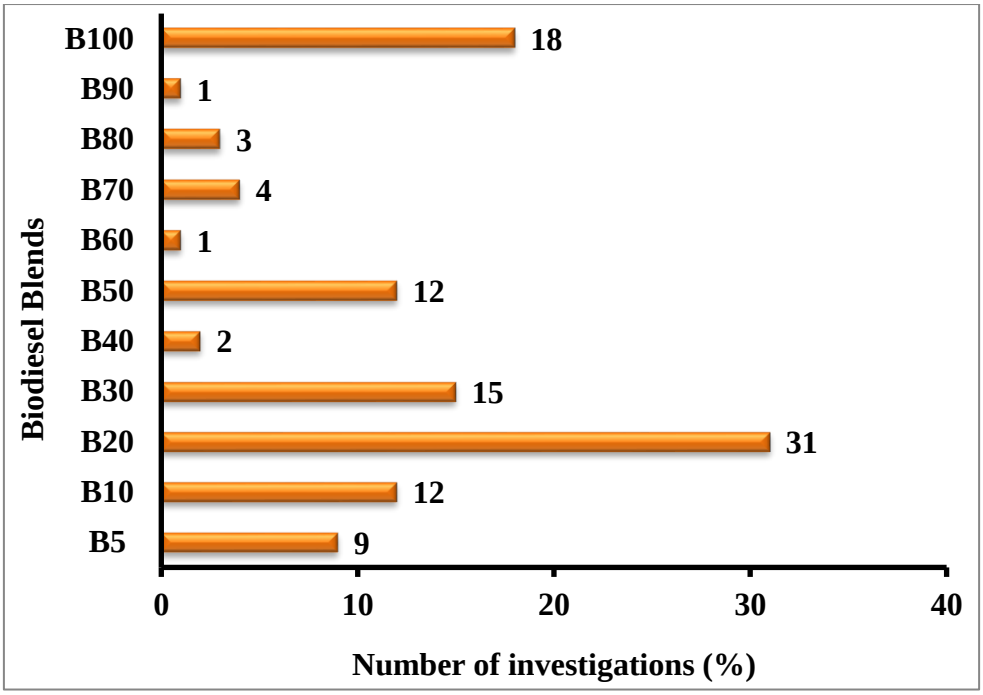

Figure 1.3: Roll of biodiesel/diesel blends on reported investigations (%)

Lots of research work has shown that biodiesel can be used in diesel engines without major modification [24–26]. In fact, its energy density is quite closer to mineral diesel and similarities between the combustion properties of biodiesel and petroleum-derived diesel have made the former one of the most promising renewable and sustainable fuels for the diesel engines [27–29]. Excessive dependence on Jatropha curcas for biodiesel production, lack of sufficient feedstocks, and lack of comprehensive research and development activities have been some of the major stumbling blocks cited by government agencies [30–32].

Therefore, use of other potential non-edible oil feedstocks for biodiesel production and integrated research and development to address the multifaceted challenges of biodiesel production and usage may supplement government's biofuel policy and also increase the feedstock availability substantially [33].

In this context, the present research work focuses on biodiesel production from tree borne non-edible oilseeds known as Sal (*Shorea robusta*) and Kusum (*Schleichera oleosa*) to evaluate their potential as alternatives fuels in the diesel engines.

1.5 Organization of Thesis

The thesis entitled, "**Performance, emission and combustion characteristics of a biodiesel fuelled diesel engine**" gives an outline of the utilization of sal biodiesel and kusum biodiesel in single cylinder four stroke diesel engine.This thesis is made up of five chapters. The organization of the chapters is as follows:

CHAPTER 1: INTRODUCTION -This chapter gives the background of the research. It starts by giving the motivations of the research and subsequently an introduction into the energy scenario of India and environmental issues associated with the application of biodiesel. Also, its heights the recent biodiesel scenario of India and finally, the chapter outlined the organization of thesis.

CHAPTER 2: LITERATURE REVIEW- This chapter highlighted general review of the roles of the diesel engine in India and reported the recent emerging sources of biodiesel fuels. In addition, the chapter reviewed the biodiesel feedstocks in India as well as the production technologies for biodiesel production, biodiesel standards and characterization, properties of biodiesel and its blends. This chapter also enumerated the performance, emission and combustion potentials of different feedstocks of Indian origin. The outcome of the exhaustive literature reviewed is also highlighted in the chapter. Finally, the research gap, problem statement and objectives of the research are outlined.

CHAPTER 3: SYSTEM DEVELOPMENT AND METHODOLOGY – It explains the procedure for biodiesel production of both Sal and Kusum oils and the methods for the evaluation of their physico-chemical properties. Detailed procedure for the biodiesel production, including its optimization using response surface methodology (RSM) and long term storage stability are discussed. Also, the system development for the engine trials has been described in details. The chapter also described the procedures for the calculations of heat release rate, mass friction burnt, and the exhaustive engine trials. Finally, the accuracy and uncertainties of measurements are also reported in this chapter.

CHAPTER 4: RESULTS AND DISCUSSION – This chapter discussed all the results obtained from the experimental work and statistical calculations, and presented the findings of the study followed by detailed argument and analysis of these findings besides comparing them with the existing results included in the literature. Results herein are presented in tables, graphs, and plates as the case may be.

CHAPTER 5: CONCLUSION –It provides a summary of the key findings in the light of the research and put logical conclusions supported by facts and figures obtained in this research. Finally, some recommendations for the future studies have been included in this chapter.

Lastly, the thesis also contained detailed references, appendices, and list of publications.

CHAPTER 2

LITERATURE REVIEW

2.1 Introduction

This chapter highlighted general review of the roles of the diesel engine in India and reported the recent emerging sources of biodiesel fuels. In addition, the chapter reviewed the biodiesel feedstocks in India as well as the production technologies for biodiesel production, biodiesel standards and characterization, properties of biodiesel and its blends. This chapter also enumerated the performance, emission and combustion potentials of different feedstocks. The outcome of the exhaustive literature reviewed is also highlighted in the chapter. Finally, the research gap, problem statement and objectives of the research are outlined.

2.2 Role of diesel engine in India

Diesel engines have been widely used in agriculture machinery, automobiles, railway locomotives and shipping power equipment due to their excellent performance and economy. In India, almost all irrigation pumps, farm implements, mechanized farm machinery and heavy transportation vehicle are powered by diesel engines. The diesel engine continues to dominate the agriculture sector in India and have always been preferred widely because of power developed, specific fuel consumption and durability. India is an agriculture based economy and agriculture is an energy transformation process as energy is produced and consumed in it. Figure 2.1 shows a glimpse of the diesel consumption in sectors where diesel is used as a primary input to run the prime mover. Road constituted 48% of the diesel consumption, while agriculture constituted 18%. The dual problem of fast depletion of petroleum based fuels and air pollution can be judiciously handled by switching from fossil fuel based economy to renewable source of energy.

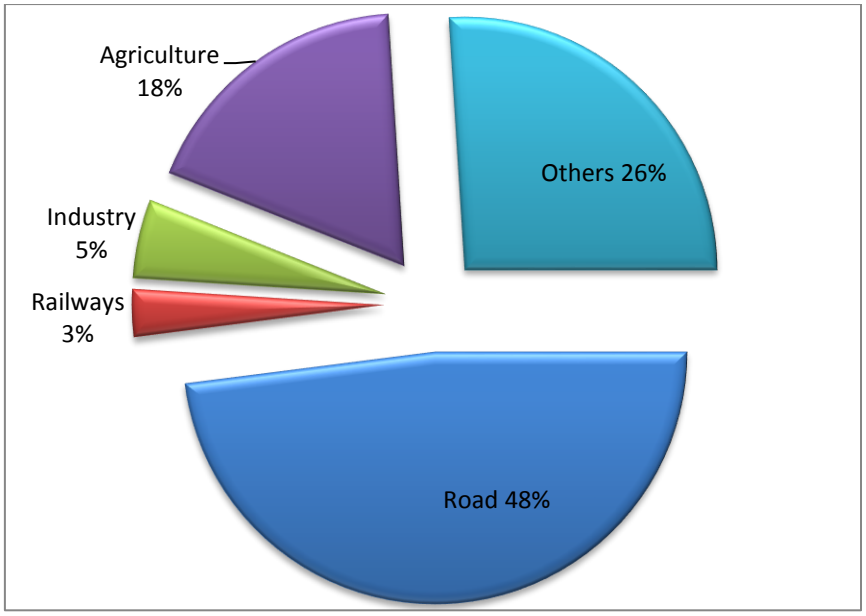

Figure 2.1: Percentage share of Diesel Consumption [8]

2.3 Emerging Energy Source of Diesel fuel: Biodiesel

The awareness on energy issues and environmental problems associated with burning fossil fuels has encouraged many researchers throughout the globe to investigate alternative sources of energy instead of fossil fuels and its derivatives. Among them, biodiesel seems very promising for several reasons. It is highly biodegradable and has minimal toxicity, it can replace diesel fuel in applications such as boilers and CI engines without modifications. A marginally decrease in performances is reported, resulting in almost zero emissions of sulphates, aromatic compounds and other chemical substances, that are destructive to the environment. These including; net contribution of carbon dioxide (CO_2), whole life-cycle is completed (including cultivation, production of oil and conversion to biodiesel) and it appears to cause significant improvement in rural economic potential [28,34].

The invention of the vegetable oil fuelled engine by Sir Rudolf Diesel dated back in the 1912. However, full exploration of biodiesel came into light in the 1973 as a result of renewed interest in renewable energy sources for reducing greenhouse gas (GHG) emissions, and alleviating the depletion of fossil fuel reserves.

Biodiesel is defined as mono-alkyl esters of long chain fatty acids derived from vegetable oils or animal fats and alcohol with or without catalyst [35–37]. Compared to diesel fuel, biodiesel produces less sulphur, carbon dioxide, carbon monoxide, particulate matters, smoke and hydrocarbons emission and more oxygen. More free oxygen leads to the complete combustion and reduced emission [38,39].

Biodiesel has been in use in many countries such as United States of America, Argentina, Indonesia, Brazil, China, Thailand and other European countries as shown in Figure 2.2. However, the potential for its production and application is much more. It has potential to be part of a sustainable energy mix in the future.

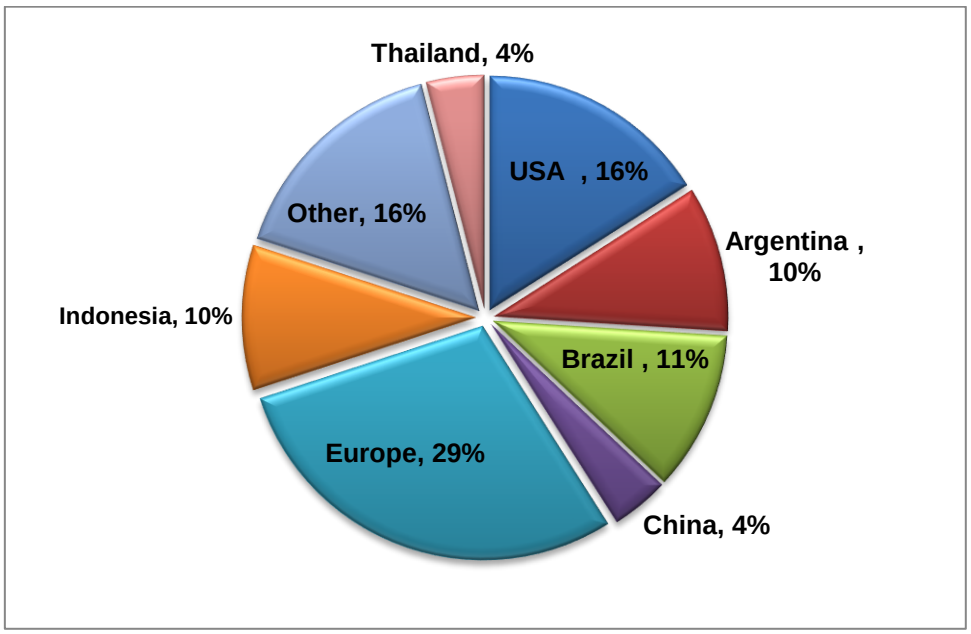

Figure 2.2: Biodiesel share of different countries

2.3.1 Biodiesel demand and accessibility in India

Approximately, 20 Indian biodiesel plants annually produce 140 to 300 million litres of biodiesel [40], which is mostly utilized by the informal sector locally for irrigation, electricity etc., and by automotive companies for experimental projects.

According to recent report by Indian Biofuel Annual report, 2016 [41], demand for diesel for transport is expected to grow from 46.9 billion litres in 2010 to 155.7 billion litres in 2030. Figure 2.3 shows projected biodiesel production and blending share (%) at present

biodiesel estimate as well as Figure 2.4 shows biodiesel demand for the three different blending targets in the near future. Biodiesel demand for 20 % blending targets is expected to grow 19.8 and 31.1 billion litres in 2020 and 2030, respectively.

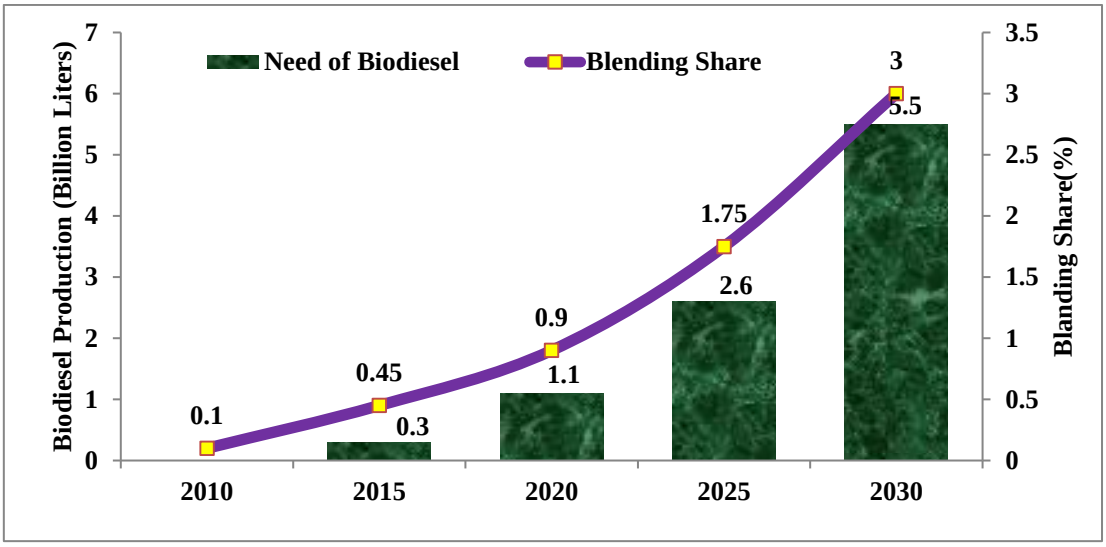

Figure 2.3: Projected biodiesel production and blending share (%)[41].

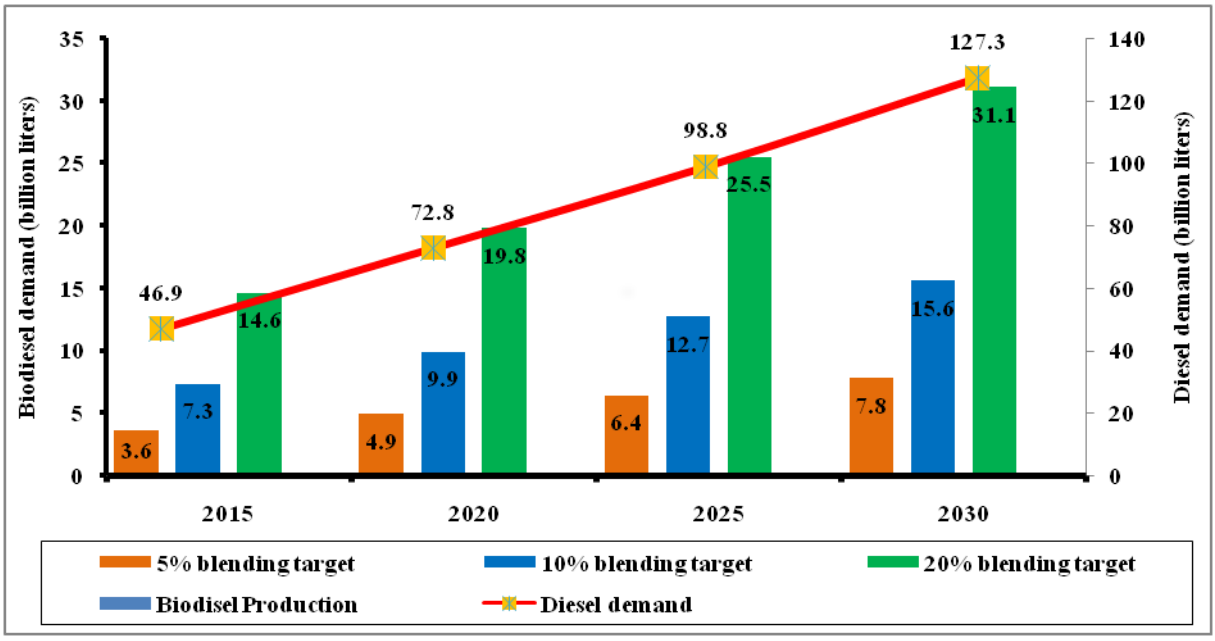

Figure 2.4: Biodiesel demand with blending targets (%) in India [41].

2.3.2 Advantages and limitations of biodiesel

Advantages:

- Biodiesel has 10-11% of oxygen; this makes biodiesel a fuel with good combustion characteristics [42].

- Biodiesel reduces net carbon-dioxide emission by 78% on a lifecycle basis and reduces smoke due to free soot when compared to conventional diesel fuel [42].
- Biodiesel is renewable, non-toxic, non-flammable, portable, readily available, biodegradable, sustainable, eco-friendly, sulphur free and aromatic content, this makes it an ideal fuel for heavily polluted cities. Biodiesel also reduces particular matter content in the ambient air and hence reduces air toxicity. It provides a 90% reduction in cancer risks and neonatal defects due to less polluting combustion [16].
- Biodiesel helps rural development to restore degraded lands over a period. Moreover, it has good potential for rural employment generation [43].
- Biodiesel serves as climatic neutral in view of the climatic change that is presently an important element of energy use and development.
- Biodiesel has higher cetane number (about 55 to 65 depending on the vegetable oil) than petroleum diesel (47 to 53) which reduces the ignition delay [2].
- Production can be raised easily and is less time consuming [44].
- No need for drilling, transportation, or refining like petroleum diesel. Therefore, each country has the ability to produce biodiesel as a locally produced fuel. Moreover, there is no need to pay tariffs or similar taxes to the countries from which oil and petroleum diesel is imported [42].
- Biodiesel has superior lubricity properties. This improves lubrication in fuel pumps and injector units, which decreases engine wear, tear and increases engine efficiency [45].
- Biodiesel is safe for transportation, handling, distribution, utilization and storage due to its higher flash point (above 100-170°C) than petroleum diesel (60-80°C) [44].

- Biodiesel reduces the environmental effect of waste product and can be made out of used cooking oils and lards [2].
- Transesterification process is less expensive (cost of fuel increases), these oils require expensive fatty acid separation or use of less effective (or expensive acid catalysts) [46].

Limitations:

- Biodiesel has 12% lower energy content than diesel, this leads to an increase in fuel consumption of about 2-10%. Moreover, biodiesel has higher cloud point and pour point, higher nitrogen oxide emissions than diesel. It has lower volatilities that cause the formation of deposits in engines due to incomplete combustion characteristics [47].
- Biodiesel causes excessive carbon deposition and gum formation (polymerization) in engines and the oil gets contaminated and suffers from flow problem. It has relatively higher viscosity (11-18 times diesel) and lower volatility than diesel and thus needs higher injector pressure [48].
- Oxidation stability of biodiesel is lower than that of diesel. It can be oxidized into fatty acids in the presence of air and causes corrosion of fuel tank, pipe and injector [49].
- Due to the high oxygen content in biodiesel, advances in fuel injection and timing and earlier start of combustion, biodiesel produces relatively higher NOx levels than diesel in the range of 10-14% during combustion [16].
- Biodiesel can cause corrosion in vehicle material (cooper and brass) such as fuel system blockage, seal failures, filter clogging and deposits at injection pumps [50].

- Use of biodiesel in internal combustion engine may lead to engine durability problems including injector cocking, filter plugging and piston ring sticking etc [51].
- As more than 95% of biodiesel is made from edible oil, there have been many claims that this may give rise to further economic problems. By converting edible oils into biodiesel, food resources are being used as automotive fuels. It is believed that large-scale production of biodiesel from edible oils may bring about a global imbalance in the food supply-and-demand market [2].
- Lower engine speed and power, high price, high engine wear, engine compatibility[52].
- The transesterification has some environmental effects such as waste disposal and water requirement for washing, soap formation, etc [53].

2.4 Biodiesel feedstock: India

Globally, there are more than 350 oil-bearing crops identified as potential sources for biodiesel production. Biodiesel feedstocks are regionally diversified [54]. There are wide range of available feedstocks for biodiesel. The availability of feedstock for producing biodiesel depends on the regional climate, geographical locations, soil conditions and agricultural practices of any country [55,56]. From literature, feedstock alone represents 75% of the overall biodiesel production cost [57,58] as shown in Figure 2.5. Therefore, selecting the low-priced feedstock is vital to ensure low production cost of biodiesel.

In general, biodiesel feedstock can be divided into four main categories [36,57,59] as shown Table 2.1 and potential feedstocks of India which depicted the impact on the literature as shown in Table 2.2.

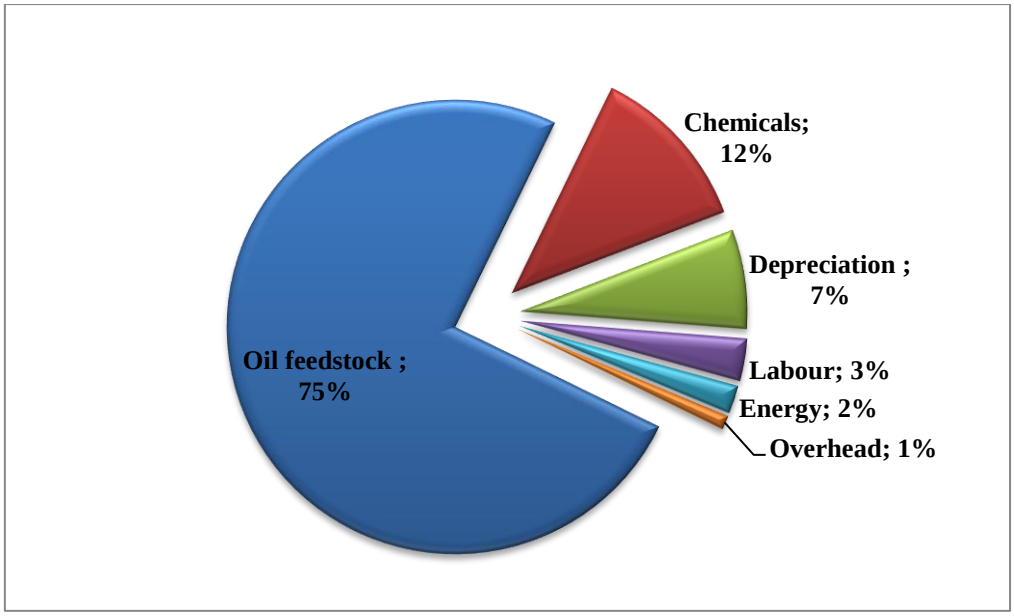

Figure 2.5: General cost breakdown for production of biodiesel [57,58]

Table 2.1: Types of feedstocks of biodiesel production [38]

Edible oils	Non-edible oils	Animal Fats	Other Sources
Soybeans	Jatropha curcas	Pork lard	Bacteria
Rapeseed	Mahua (Madhuca indica)	Beef tallow	Algae (Cyanobacteria)
Safflower	Karanja (Pongamia)	Poultry Fat	Microalgae
Rice bran oil	Kusum	Fish oil	Tarpenes
Barley	Cotton seed	Chicken fat	Poplar
Sesame	Castor		Switchgrass
Groundnut	Polanga (Calophyllum)		Miscanthus
Sorghum	Sal (Shorea robusta)		Latexes
Wheat	Neem		Fungi
Corn	Jojoba		Chlorellavulgaris
Coconut	Rubber seed tree		
Canola	Moringa		
Palm and palm kernel	Waste cooking oil		
Sunflower	Soapnut		

Table 2.2: Potential tree borne non edible feedstocks of India

Tree borne Non-edible vegetable source	Plant part	Oil content		Uses
		Seed (wt%)	Kernel (wt%)	
Jatropha curcas L.	seed, kernel	20-60	40-60	oil-Illuminant (burns without soot), lubricant, biodiesel
Pongamia pinnata (Karanja)	seed, kernel	25-50	30-50	oil-illuminant, timber, firewood, biodiesel
Ricinus communis (Castor)	seed	45-50	-	seed oil-fuel, lubrication and illumination
Madhuca indica (Mahua)	seed, kernel	35-50	50	firewood, biodiesel
Azadirachta indica (Neem)	seed, kernel	20-30	25-45	oil-illuminant, timber, firewood, biodiesel
Shorea robusta (Sal)	seed, kernel	30-35	30-40	oil-illuminant, timber, firewood, soap making, fodder for cattle
Schleichera oleosa (Kusum)	seed	30-40		Lac hosting, hair dressing, firewood
Calophyllum inophyllum L. (Polanga)	seed, kernel	65	22	oil-used for burning, timber
Hevea brasiliensis (Rubber)	seed	40-60	40-50	surface coatings, paints, printing inks, rubber/plastic processing
Aphanamixis piolystachya wall. (Parker)	kernel	-	35	oil-illuminant
Cerbera odollam (Sea mango)	seed, kernel	40-50	45-55	illuminant (release thick smoke)
Guizotia abyssinica L. (Niger)	seed	50-60	-	Commercial oil, biodiesel
Linum usitatissimum (Linseed)	seed	35-45	-	oil for wall paint and floor oil, biodiesel resin, fibre, surface coating

Michela chaampaca (Champa)	seed	40-45	-	oil, biodiesel
Mesua ferrea (Nagkesar)	seed	35-50	-	soaps, lubricants, illumination
Nicotiana tabacum (Tobacco)	seed, kernel	36-41	40-45	oil, ethnomedicinal
Sapium sebifeum L. Roxb (Stillingia)	seed, kernel	13-32	53-64	fatty oil known as strillengia oil, drying oil
Sapindus mukorossi (Soapnut)	seed, kernel	45-50	-	oil, biodiesel

To consider any feedstock as a biodiesel source, the oil percentage and the yield per hectare are important parameters. Edible oil resources such as soybeans, palm oil, sunflower, safflower, rapeseed, coconut and peanut are considered as the first generation of biodiesel feedstock for biodiesel production. However, their use raised many concerns such as food versus fuel crisis and major environmental problems such as destruction of soil resources, deforestation and usage of much of the available arable land. Moreover, in the last ten years the prices of vegetable oil have increased dramatically; which will affect the economic viability of biodiesel industry [60–62]. Furthermore, the use of such edible oils to produce biodiesel is not feasible in the long-term because of the growing gap between demand and supply of such oils in many countries.

In India, the main sources for biodiesel production from non-edible oils are Jatropha (*Jatropha curcas*), Karanja or Honge (*Pongamia pinnata),* Polanga (*Calophyllum inophyllum*), Rubber seed tree (*Hevca brasiliensis*), Rice bran, Sea mango (*Cerbera odollam*), Neem (*Azadirachta indica*), Mahua (*Madhuca indica*), Tobacco seed (*Nicotiana tabacum L.*), Sal (*Shorea robusta*) and Kusum (*Schleichera oleosa*) [2].

Non-edible oils are regarded as the second generation of biodiesel feedstocks. Animal fats such as beef tallow, poultry fat and pork lard, waste oils and grease are also considered

second generation feedstocks [63]. However, it has been reported that second generation feedstocks may not be enough to satisfy the global energy demand. Moreover, biodiesel derived from saturated vegetable oils and animal fats has a relatively poor performance in cold weather [36]. Furthermore, for many animal fats the transesterification process is difficult because they contain high amount of saturated fatty acids. In case of waste cooking oil [64], collection and logistics could be hurdles as the sources are generally scattered [36,57].

Recent comprehensive reviews on biodiesel production from various feedstocks showed the advantages of non-edible oils over edible oils. Production of biodiesel from non-edible oils feedstocks can overcome the problems of food verse fuel, environmental and economic issues related to edible vegetable [65]. Moreover, Non-edible biodiesel crops are expected to use lands that are largely unproductive and those that are located in poverty-stricken areas and in degraded forests. They can also be planted on cultivators' field boundaries, fallow lands, and in public land such as along railways, roads and irrigation canals. Non-edible biodiesel production could become a major poverty alleviation program for the rural poor apart from providing energy security in general and to rural areas in particular and upgrading the rural non-farm sector. Many researchers have concluded that non-edible feedstocks of biodiesel should be considered as sustainable and alternative fuels [30,57].

Non-edible oils plants are well adapted to arid, semi-arid conditions and require low fertility and moisture demand to grow [2]. Moreover they are commonly propagated through seed or cuttings. Since these plants do not compete with food, seed cake after oil expelling may be used as fertilizer for soil enrichment [66]. Several potential tree borne oilseeds (TBOs) and non-edible crop source have been identified as suitable feedstock for biodiesel [67]. In subsequent subsection potential feedstocks of India are discussed.

Jatropha curcas

Jatropha curcas is a small tree or large shrub, up to 5-7m tall, belonging to the Euphorbiaceae family [30,60]. It is a drought-resistant plant capable of surviving in abandoned and fallowed agricultural lands [68–70]. It is a tropical plant that able to thrive in a number of climatic zones with rainfall of 250-1200 mm. It is well adapted in arid and semi-arid conditions and has low fertility and moisture demand.

It can also grow on moderately sodic and saline, degraded and eroded soils [71]. The ideal density of plants per hectare is 2500. It produces seeds after 12 months and reaches its maximum productivity by five years and can live 30 to 50 years. Seed production ranges from 0.1 tone/(hectare year) to more than 8 tone/(hectare year) depending on the soil conditions [66]. Depending on variety, the decorticated seed of *Jatropha* contain 43-59 % oil content [72].

Pongamia pinnata L. (Karanja)

Pongamia pinnata (L.) Pierre, (karanja or honge) an arboreal legume is a medium sized evergreen tree belongs to the family (Legumnosae; Pappilonaceae), more specifically the Millettieae tribe, which grows in Indian subcontinent and south-east Asia. A single tree is said to yield 9-90 kg seeds, indicating a yield potential of 900-9000 kg seed/ha (assuming 100 trees/ha) [73]. It is one of the few nitrogen fixing trees (NFTS) that produce seeds with a significant oil content. The plant is fast growing, drought resistant, moderately frost hardy and highly tolerant of salinity [65]. It can be regenerated through direct sowing, transplanting and root or shoot cutting. Its maturity comes after 4-7 years. Historically, this plant has been used in Indian and neighbouring regions as a source of traditional medicines, animal fodder, green manure, timber, water-paint binder, pesticide, fish poison and fuel [74].

Recently, *Pongamia pinnata* has been recognized as a viable source of oil for the burgeoning biofuel industry. The oil is reddish brown and rich in unsaponifiable matter and

oleic acid [51,74]. Karanja oil mainly contains oleic acid (44.5–71.3%), followed by linoleic (10.8–18.3%) and stearic acids (2.4–8.9%) [75].

Ricinus communis (Castor)

Ricinus communis belongs to the Eurphorbiaceae family and also called castor beans. It is non-edible oilseed crop that is easily grown and resistant to drought [76,77]. The tree is grown in many countries such as United States, India, China, Central Africa, Brazil and Australia with different cultivation cultures [65,78,79]. Its oil is viscous, slightly odour, pale yellow, non-volatile and non-drying oil with a bland taste and is sometimes used as a purgative. On the average, the seeds contain about 46-55% oil [80].

Calophyllum inophyllum L. (Polanga)

Calophyllum inophyllum L. commonly known as Polanga or Honne, is a non-edible oilseed belongs to the Clusiaceae family. The tree supports a dense canopy of glossy, green and lustrous elliptical leaves and branched stem. The tree yields 100–200 fruits/kg. In each fruit, one large brown seed2–4cm (0.8–1.6 in.) in diameter is found. Oil yield per unit land area has been reported at 2000 kg/ha. The seed oil has very high oil content (65–75%) [42,81–83]. It contains mainly unsaturated fatty acids, that is, approximately 34.09– 37.57% oleic acid and 26.33–38.26% linoleic acid. Saturated acids, such as stearic (12.95–19.96%) and palmitic (12.01–14.6%) acids, can also be found in this oil [75].

Madhuca indica (Mahua)

M*adhuca indica* is mainly found in central part of India [84]. It belongs to the Sapotaceae family and grows quickly to approximately 20 m in height, possesses evergreen or semi-evergreen foliage, and is adapted to arid environments [85,86]. M*adhuca indica* is one of the forest based tree-borne non-edible oils with large production potential of about 60 million tons per annum in India. Its seed contains about 35-40% of Madhuca indica [87,88].

Mahua oil contains approximately 41–51% oleic acid. Other fatty acids are also present in the oil, such as stearic (20.0–25.1%), palmitic (16.0– 28.2%), and linoleic acids (8.9–18.3%) [75].

Azadirachta indica (Neem)

Azadirachta indica (Neem) tree belongs to the Meliaceae family. It is native to India. It reaches maximum productivity after 15 years and has a life span of 150-200 years. Planting is usually done at a density of 400 plants per hectare. The productivity of Neem oil mainly varies from 2-4 ton/(ha.year) and a mature Neem tree produces 30-50 kg fruit. The seed of the fruit contains 20-30 wt% oil and kernels contain 40-50% of an acrid green to brown colored oil [66,89,90]. Neem oil has high-unsaturated constituents, such as linoleic acid (6–16%) and oleic (25–54%) acid, and saturated oil like stearic acid (9–24%) [58,91].

Hevea brasiliensis (Rubber seed)

Hevea brasiliensis tree, commonly referred to Rubber tree, belongs to the family Euphorbiaceae. Moreover, the tree's sap-like extract (known as latex) can be collected and used in various applications, growing up to 34 m in height. On an average, a healthy tree can give about 5 kg of useful seeds during a normal year and this works out to an estimated availability of 150 kg of seeds per hectare [92]. Rubber seed oil is non-edible oil, which contain 50-60wt% oil and kernel contain 40-50wt% of brown colour oil. The oil is high in unsaturated constituents such as linoleic (39.6 wt.%), oleic (24.6 wt.%), and linolenic (16.3 wt.%) acids. Other fatty acids found in rubber seed oil include saturated species such as palmitic (10.2 wt.%) and stearic (8.7 wt.%) acids [89,92,93].

Nicotiana tabacum (Tobacco)

Nicotiana tabacum, commonly referred to Tobacco, is a by-product that contains significant amount of oil. The oil extracted from tobacco seed is non-edible with physical, chemical and thermal properties that conferred favorably with other vegetable oils and have the potential to be considered as a interesting feedstock for biodiesel production [94,95].The

seed contains approximately 35–49 w% oil with fatty acid composition of 69.49–75.58% of linoleic acid [75].

Shorea robusta (Sal)

Sal is a tree-borne product available in states like Odisha, Chhatishgarah, Madhya Pradesh, east Maharashtra etc, all in India. The annual estimated production of sal seeds is around 1.5 million tonnes and the sal seed oil or fat production is around 0.18 million tonnes annually. Sal is the source of one of timbers which are used for railway sleeper, beams, dyeing vats, beer, oil casks and tanning materials [96,97]. Sal fruit content 66.4% of kernel and pod, reaming 33.6% is shell and calyx. Sal seeds are processed mainly for its fat or oil [98].

Schleichera oleosa (Kusum)

Schleichera oleosa is belonging to Sapindaceae family and also known as Kusum fruit. It is widely found in the sub-Himalayan region, throughout central and Southern India, Burma, Ceylon, Java and Timor. The oil obtained from Kusum or Macassar, is used for the cure of itch, acne and burns [9,10]. The seeds are brown, irregularly elliptic, slightly compressed, oily, enclosed in a succulent aril. The oil content of the seed is around 59–72% with yellowish green color [99,100].

2.4.1 Advantages of non-edible oils

Preliminary evaluation of several non-edible oilseed crops for their growth, feedstock and adaptability showed that these feedstocks have the following advantages [89,101]:

(1) The adaptability of cultivating non-edible oil feedstocks in marginal land and non-agricultural areas with low fertility and moisture demand [50].

(2) They can be grown in arid zones (20 cm rainfall) as well as in higher rainfall zones and even on land with their soil cover. Moreover, they can be propagated through seed or cuttings.

(3) They have huge potential to restore degraded lands, create rural employment generation and fixing of up to 10 ton/ha/year CO_2 emissions [102].

(4) They do not compete with existing agricultural resources.

(5) They eliminate competition for food and feed. Non-edible oils are not suitable for human food due to the presence of some toxic components in the oils.

(6) They are more efficient and more environmentally friendly than the first generation feedstocks. Conversion of non-edible oil into biodiesel is comparable to conversion of edible oils in terms of production and quality [63].

(7) Less farmland is required and a mixture of crops can be used. Non-edible oil crops can be grown in poor and wastelands that are not suitable for food crops.

(8) Non edible feedstock can produce useful by-products during the conversion process, which can be used in other chemical processes or burned for heat and power generation. For instance, the seed cakes after oil expelling can be used as fertilizers for soil enrichment [103].

(9) The main advantages of non-edible oils are their availability, renewability, higher heat content, lower sulphur content, lower aromatic content and biodegradability [101].

2.4.2 Problems in exploitation of non-edible oils

The use of non-edible oilseed as alternative biodiesel feedstock in the transportation sector is critical towards achieving higher self-reliance energy security. This situation offered challenges as well as opportunities as replacement of fossil fuels with economic and environmental benefits [48,101].

(1) Collection, high dormancy and problems in picking and harvesting in avenue and forest plantations.

(2) Non-availability of quality planting material or seed, limited period of availability, unreliable and improper marketing channels.

(3) Lack of post-harvest technologies and their processing, non-remunerative prices, wide gap between potential and actual production, absence of state incentives promoting bio-diesel as fuel, and economics and cost-benefit ratio.

2.4.3 Fatty acid compositions of potential feedstocks

Fatty acid composition is an important property for any biodiesel feedstock as it determines the efficiency process to produce biodiesel. The percentage and type of fatty acids composition relies mainly on the plant species and their growth conditions [104]. The fatty acids composition of some feedstocks are generally aliphatic compounds with a carboxyl group at the end of a straight-chain. The most common fatty acids are C_{14} to C_{20} acids [105]. However, some feedstocks contain significant amounts of fatty acids other than the typical C_{16} and C_{18} acids [42,106]. Table 2.3 shows the chemical structures of common fatty acids. Table 2.4 shows the fatty acid composition of non-edible feedstocks that were found suitable for production of biodiesel. Moreover, more fatty acid compositions can also be found in references [66,75,101,107,108].

Table 2.3: The chemical structures of common fatty acids [101].

Fatty acid	Structure	Systematic name	Chemical structure
Lauric	(12:0)	Dodecanoic	$CH_3(CH_2)_{10}COOH$
Myristic	(14:0)	Tetradecanoic	$CH_3(CH_2)_{12}COOH$
Palmitic	(16:0)	Hexadecanoic	$CH_3(CH_2)_{14}COOH$
Stearic	(18:0)	Octadecanoic	$CH_3(CH_2)_{16}COOH$
Oleic	(18:1)	cis-9-Octadecenoic	$CH_3(CH_2)_7CH=CH(CH_2)_7COOH$
Linoleic	(18:2)	cis-9-cis-12-Octadecadienoic	$CH_3(CH_2)_4CH=CHCH_2CH=CH(CH_2)_7COOH$
Linolenic	(18:3)	cis-9-cis-12,	$CH_3CH_2CH=CHCH_2CH=CHCH_2CH=CH(CH_2)_7COOH$
Arachidic	(20:0)	Eicosanoic	$CH_3(CH_2)_{18}COOH$
Behenic	(22:0)	Docosanoic	$CH_3(CH_2)_{20}COOH$
Erucic	(22:1)	cis-13-Docosenoic	$CH_3(CH_2)_7CH=CH(CH_2)_{11}COOH$
Lignoceric	(24:0)	Tetracosanoic	$CH_3(CH_2)_{22}COOH$

2.4.4 Challenges and potential solutions of using non edible oils

The direct use of vegetable oils or blends has generally been considered to be impractical for both direct and indirect diesel engines. The high viscosity, low volatility, acid

composition, free fatty acid and moisture content, gum formation due to oxidation and polymerization during storage [53,65]. In addition, poor combustion, poor cold engine start-up, misfire, ignition delay, incomplete combustion, carbon deposition around the nozzle orifice, ring sticking, injector choking in engine and lubricating oil thickening are the major problems of using vegetable oils [35].

In general, the problems associated with using straight vegetable oil in diesel engines are classified into short term and long term. Table 2.5 highlights the problems, probable causes and the potential solutions.

Table 2.4: Fatty acid composition of Indian non-edible feedstocks [101,109]

Fatty acids (%)	**C14:0**	**C16:0**	**C16:1**	**C18:0**	**C18:1**	**C18:2**	**C18:3**	**C20:0**	**C20:1**	**C22:0**	**C24:0**	**Other**
Azadirachta indica (Neem)	0.2	14.9	0.1	20.6	43.9	17.9	0.4	1.6	-	0.3	0.3	
Calophyllum inophyllum L.	0.09	14.6	2.5	19.96	37.57	26.33	0.27	0.94	0.72	-	2.6	
Rubber	2.2	10.2	-	8.7	24.6	39.6	16	-	-	-	-	
Jatropha curcas.	1.4	12.7	0.7	5.5	39.1	41.6	0.2	0.2	-	-	-	
L.usitatissimum (Linseed)	-	4.4	0.3	3.8	20.7	15.9	54.6	0.2	-	0.3	0.1	
Madhuca indica (Mahua)	-	16.0-28.2	-	20.0-25.1	41.0-51.0	8.9-13.7	-	3.3	-	-	-	
Nicotiana T.(tobacco)	0.09	10.96	0.2	3.34	14.54	69.49	0.69	0.25	0.13	0.12	0.4	
Pongamia p. (Karanja)	-	3.7-7.9	-	2.4-8.9	44.5-71.3	10.8-18.3	-	4.1	2.4	5.3	3.5	
Ricinus communis (Castor)	-	1.1	0	3.1	4.9	1.3	0.6	0.7	-	-		90[a]
Shorea robusta (Sal)		4-7		41-47	37-43	0-4		3-9				
Schleichera oleosa (Kusum)		1.6	3.1	10.1	52.5			19.7		4		

[a]Ricinoleic acid ($C_{18}H_{34}O_3$);

Table 2.5: Reported problems, probable cause and potential solutions for using straight vegetable oil in diesel engines [101,110]

Problem	**Probable cause**	**Potential solution**
Short-term		
1. Cold weather starting	• High viscosity, low cetane number and high flash point of vegetable oils.	• Preheat fuel prior to injection.
2. Plugging and gumming of filters, lines and injectors	• Natural gums in vegetable oil. • Other ash.	• Refine the oil partially to remove gums.
3. Engine knocking	• Low cetane numbers. Improper injection timing.	• Adjust injection timing. • Use higher compression engines. Preheat fuel prior to injection and use its ester.
Long term		
4. Cooking of injector on piston and engine head	• High viscosity of vegetable oil. • Incomplete combustion of fuel. • Poor combustion at part loads with vegetable oils.	• Heating fuel prior to injection. • Switch engine to diesel fuel when operating at part loads. • Chemically alter the vegetable oil to an ester.
5. Carbon deposits on piston and head of engine	• High viscosity of vegetable oil. • Incomplete combustion of fuel and poor combustion at	• Heat fuel prior to injection. Switch engine to diesel fuel when operation at part loads.

	part load with vegetable oils.	Chemically alter the vegetable oil to an ester.
6. Excessive engine wear	• High viscosity of vegetable oil, incomplete combustion of fuel. • Poor combustion at part loads and free fatty acids in vegetable oil. • Dilution of engine lubricating oil due to blow-by of vegetable oil.	• Heat fuel prior to injection. • Switch engine to diesel fuel when operation at part loads. • Chemically alter the vegetable oil to an ester. Increase motor oil changes. • Motor oil additives to inhibit oxidation.
7. Failure of engine lubricating oil due to polymerization	• Collection of poly-unsaturated vegetable oil blow-by in crankcase to the point where polymerization occurs.	• Heat fuel prior to injection. • Switch engine to diesel fuel when operation at part loads. • Chemically alter the vegetable oil to an ester. • Motor oil additives to inhibit oxidation.

2.5 Biodiesel Production Technologies

Globally, there are many efforts towards improving vegetable oil properties in order to enhance the properties of diesel fuel. Viscosity is the problem in directly using vegetable oils in conventional diesel engines. These problems can be overcome by four methods; pyrolysis [35], dilution with hydrocarbons blending [48], Micro-emulsion, and transesterification [111] conduct a comparison between different biodiesel production technologies. This comparison is given in Table 2.6.

Table 2.6: Comparison of main biodiesel production technologies [48,111,112].

Technologies	Advantage	Disadvantage
Dilution (direst blending or micro-emulsion	• Simple process	• High viscosity • Poor volatility • Poor stability
Pyrolysis	• Simple process • No-polluting	• High temperature is required • Equipment is expensive • Low purity
Transesterification	• Fuel properties are closer to diesel • High conversion Efficiency • Low cost • It is suitable for industrialized production	• Low free fatty acid and water content are required (for base catalyst) • Waste water is produced because products must be neutralized and washed • Accompanied by side reactions • Difficult reaction products separation
Supercritical methanol	• No catalyst • Short reaction Time • High conversion • Good adaptability	• High temperature and pressure are required • Equipment cost is high • High energy consumption

2.5.1 Pyrolysis (Thermal cracking)

Pyrolysis is the thermal decomposition of the organic matters by heat in the absence of oxygen and in presence of a catalyst. The paralyzed material can be vegetable oils, animal

fats, natural fatty acids or methyl esters of fatty acids. Many investigators have studied the pyrolysis of triglycerides to obtain suitable fuels for diesel engine. Thermal decomposition of triglycerides produces alkanes, alkenes, alkadienes, carboxylic acids, aromatics and small amounts of gaseous products [113].

The liquid fractions of the thermally decomposed vegetable oils are likely to approach diesel fuels. The pyrolyzate had lower viscosity, flash point, and pour point than diesel fuel and equivalent calorific values. However, cetane number of the pyrolyzate was lower compared to diesel fuel[114]. The pyrolyzed vegetable oils contain acceptable amounts of sulphur, water content, copper corrosion values and sediments but unacceptable ash, carbon residual and pour point. It has been observed that pyrolysis process is effective, simple, waste less and pollution free [35,63].

2.5.2 Dilution

Mainly, vegetable oils are diluted with diesel to reduce the viscosity and improve the performance of the engine. This method does not require any chemical process [115]. It has been reported earlier that substitution of 100% vegetable oil for diesel fuel is not practical. Therefore, blending of 10-25% vegetable oil to diesel has been considered to achieve good results for diesel engine [7,61,112,115]. Generally, direct use of vegetable oils and their blends have been considered to be difficult to use in both direct and indirect diesel engines [110,115,116].

2.5.3 Micro-emulsion

A micro-emulsion is defined as a colloidal dispersion of optically isotropic fluid with dimensions ranging into 1–150 nm. It is formed from two immiscible liquids and one and more ionic or more ionic amphiphiles. Vegetable oils micro emulsion can be formed with an ester and dispersant (co solvent), or of vegetable oils, and alcohol such as ethanol, ethanol, butanol, hexanol and a surfactant and a cetane improver, with or without diesel fuels [35]. Micro-emulsion has met the minimum viscosity requirement for diesel fuel. It has been

demonstrated that short-term performances of both ionic and non-ionic micro-emulsions of aqueous ethanol in soybean oil are close to that of No.2 diesel fuel [7,61,112,115,117].

2.5.4 Transesterification

Transesterification is regarded as the best method due to its low cost, high yields and simplicity [35,63,109,118]. Transesterification or alcoholysis is defined as the chemical reaction of alcohol with vegetable oils. One mole of fat or oil are reacts with three moles of a short chain alcohol in the presence of catalyst to produce one mole of glycerine and three moles of alkyl esters [119]. The triglycerides are converted step wise into diglycerides, monoglyceride and finally glycerol which are easily separated by gravity into biodiesel and glycerol layers. Glycerol is an important by-product in the cosmetic industry. In this reaction, methanol and ethanol are the two main light alcohols used in transesterification process due to their relatively low cost. However, propanol, isopropanol, tert-butanol, n-butanol, branched alcohols and octanol could also be employed but their cost is much higher.

Generally, transesterification process includes two main processes; catalytic and non-catalytic methods. The catalyst enhances the solubility of alcohol and thus increases the reaction rate. The most frequently used process is the catalytic transesterification process. Alkaline catalytic method is the fast and economical. An alkaline catalyst proceeds at around 4000 times faster than with the same amount of acid catalyst [101,120]. Moreover, this method can achieve high yield and purity of biodiesel product in a short time (30-60min). The widely reported alkaline catalysts include NaOH, KOH, $NaOCH_3$ and $KOCH_3$. Researchers have reported that both sodium and potassium hydroxide perform equally well. Sodium and potassium methoxides favored high yields than other base catalysts but they are costly.

However, in using alkaline catalysts, free fatty acid (FFA) level should be below a desired limit (ranging from less than 0.5% to less than 3%). Beyond this limit the reaction proceeds with difficulty and challenges such as soap formation and reduced esters yields

[121]. In addition to this, the reaction has several drawbacks; it is energy intensive; recovery of glycerol is difficult; the catalyst has to be removed from the product; alkaline wastewater requires treatment and the level of free fatty acids and water greatly interfere with the reaction [56,109].

Acid catalysts include sulphuric acid, hydrochloric acid, ferric sulphate acid, phosphoric acid, para toluene sulfonic acid (PTSA) and Lewis acids ($AlCl_3$ or $ZnCl_2$). Researchers have shown that acid catalysts are more tolerant than alkaline catalysts for vegetable oils having high FFA and water. Therefore, acid catalyst is used to reduce the free fatty acids contents to a level enough for alkaline transesterification which is preferred over the acid catalyst after the acid value is reduced to the desired limit. It has been reported that acid-catalyzed reaction gives very high yield in esters. However, the reaction is slow (3-48h). It has been reported that the homogeneous transesterification consumes large amount of water for wet washing to remove the excess salt from the neutralization process, and the residual acid or base catalyst [122]. Nevertheless, this technology has relatively low energy use, high conversion efficiency and cost effective reactants and catalyst [56,109].

The catalytic transesterification has some challenges such as; long reaction time, poor catalysts solubility and poor separation of the products. Furthermore, the wastewater generated during biodiesel purification is not environment friendly. To overcome these challenges, other faster methods such as supercritical fluids method have been developed. For example, during supercritical esterification, reaction completes in a very short time (2-4 min) compared to catalytic transesterification.

Further, since no catalyst is used, the purification of biodiesel and the recovery of glycerol are much easier, trouble free and environment friendly [56,112,123]. However, the method has high cost in reactor and operation (due to high pressures and high temperatures) and high methanol consumption (e.g. high methanol/crude-oil molar ratio of 40/1) [124–126].

Transesterification reaction is affected by various parameters depending upon the reaction conditions. The reaction is either incomplete or the yield is reduced to a significant extent if the parameters are not optimized. The most important parameters that affect the transesterification process reported include molar ratio, reaction temperature, reaction time, catalyst concentration and stirring speed [61,109].

2.6 Review on optimization of biodiesel production

The need for process optimization has been emphasized by Gandure et al. [127] reported the importance of process optimization including; development of reaction kinetics, large scaling of production, reactor design, reduced production cost, and predicting yields, among others [128,129]. Researchers optimized the conversion of biodiesel. For example, *Kilic et. al.*[128] investigated the optimization of biodiesel production from castor oil using full factorial design. Effects of temperature, methanol/oil molar ratio and catalyst concentration were optimized according to the 2^4 full factorial central composite designs (CCD). Second order model was obtained to predict biodiesel yield as a function of these variables.

Accordingly, other researchers reported the average yield of more than 90%. The catalyst concentration and its nature play significant roles. For example, *Lee et. al.* [130] employed CaO–MgO mixed oxide catalyst in transesterification of non-edible Jatropha curcas oil into biodiesel. Response surface methodology (RSM) using central composite design (CCD) was employed to statistically evaluate and optimize the biodiesel production process. It was found that the production of biodiesel achieved an optimum level of 93.55% yield at the following reaction conditions: 1) Methanol/oil molar ratio: 38.67; 2) Reaction time: 3.44 h; 3) Catalyst amount: 3.70 wt.%; and 4) Reaction temperature: 115.87 °C.

Economically, transesterification of Jatropha curcas oil using heterogeneous catalyst CaO–MgO mixed oxide required less energy which contributed to high production cost in biodiesel production. *Wu et. al.* [131] carried out an optimization study on the production of

biodiesel from Camelina seed oil using alkaline transesterification. The optimization was based on sixteen well-planned orthogonal experiments. Parameters including methanol ratio, reaction time, temperature and catalyst concentration were investigated. It was found that the order of significant factors for biodiesel production was *reaction temperature > catalyst concentration > methanol to oil ratio > reaction time*. Based on the results of the range analysis and analysis of variance (ANOVA), the maximum biodiesel yield was found at a molar ratio of methanol to oil of 8:1, a reaction time of 70 min, a reaction temperature of 50°C, and a catalyst concentration of 1 wt.%. The product and FAME yields of biodiesel under this optimal conditions reached 95.8% and 98.4%, respectively.

Enzymes as catalysts have also been very effective catalysts in biodiesel production. *Yucel* [132] immobilized microbial lipase from T. lanuginosus supported on poly-glutar aldehyde activated olive Pomace powder. The support was used to produce biodiesel with Pomace oil and methanol. RSM using CCD was used to optimize the biodiesel production parameters. The predicted Pomace oil methyl ester yield was 92.87% under the optimal conditions. Verification experiment yield was 91.81%, confirmed the validity by suggested model. Biodiesel yield reached 93.73% by adding water (1% w/w) in reaction medium under the optimal conditions.

Also, *Uzun et. al.*[128] carried out alkali-catalysed transesterification of waste frying oils (WFO) in various conditions to investigate the effects of catalyst concentration, reaction time, methanol/oil molar ratio, reaction temperature, catalyst type (hydroxides, methoxides and ethoxides), and purification type (such as washing with hot water, purification with silica gel and dowex) on the biodiesel yields. The optimum conditions were 0.5% wt. of NaOH, 30 min reaction time, 50°C reaction temperature, 7.5 methanol to oil ratio and purification with hot distilled water. A 96% biodiesel yield was obtained, and the activation energy was found to be as 11741 J mol^{-1}. The determined specifications of obtained biodiesel according to ASTM D 6751 and EN 14214 standards were in accordance with the required limits.

In the light of the above review, it may be stated that production of biodiesel from sal oil and kusum oil with optimized process parameters and the subsequent compliance with the corresponding international standards may prove the suitability of this vegetable oil as a true alternative to mineral diesel and outline its economic potentials.

2.7 Biodiesel Standards

The quality of biodiesel fuel can be influenced by various factors include: the quality of feedstock, fatty acid composition of the feedstock, type of production and refining process employed and post production parameters. Since biodiesel is produced from quite differently scaled plants of varying origins and qualities, it is necessary to develop standards for fuel quality to guarantee an engine performance without any difficulties.

The establishment of standard for biodiesel depends on country's standards and specifications. It's utilized to protect both consumers and producers as well as to support the development of biodiesel industries. These specifications include the American Standards for Testing Materials (ASTM 6751) or the European Union (EN 14214) Standards [42,55]. However, India has own standard (IS 15607) [133,134]. These standards describe the physical and chemical characteristics including; caloric value (MJ/kg), cetane number, density (kg/m^3), viscosity ($mm^{2/}s$), cloud and pour points ($^{\circ}C$), flash point ($^{\circ}C$), acid value (mg KOH per g-oil), ash content (%), copper corrosion, carbon residue, water content and sediment, sulphur content, glycerine (% m/m), phosphorus (mg/kg) and oxidation stability [42,55]. Table 2.7 gives a summary of some important properties of biodiesel. Table 2.8 gives ASTM 6751, EN 14214 and IS15607 specifications of biodiesel beside ASTM D975 for diesel fuel.

Table 2.7: Summary of some important properties of biodiesel [42,135]

Fuel characteristic	Effects
Cetane number	(i) An ignition quality of diesel fuels (ii) High cetane number implies short ignition delay (iii) Higher molecular weight n-alkanes have high cetane numbers (iv) It influences both gaseous and particulate emissions (v) The cetane index which is very close to cetane number is calculated based on 10, 50, 90% distillation temperatures and specific gravity (vi) The fuels with high auto ignition temperatures are more likely to cause engine knock
Distillation range	(i) It affects fuel performance and safety (ii) It is important to an engine's start and warm up (iii) Presence of high-boiling components affect the degree of formation of solid combustion deposits (iv) It is needed in the estimation of cetane index
Specific gravity	(i) It is required for the conversion of measured volumes to volumes at standard temperature of 15 ˚C (ii) It is used in the calculation of cetane index
Heat of combustion	(i) A measure of energy available in a fuel (ii) A critical property of fuel intended for use in weight-limited vehicles
Flash point	(i) It indicates the presence of highly volatile and flammable materials (ii) To measures the tendency of oil to form a flammable mixture with air (iii) It is used to assess the overall flammability hazard of a material
Viscosity	(i) Proper viscosity of fuel required for proper operation of an engine (ii) Important for flow of oil through pipelines, injector nozzles and orifices (iii) Effective atomization of fuel in the cylinder requires limited range of viscosity of the fuel to avoid excessive pumping pressures

Contamination (water/sediment)	(i) It causes corrosion of equipment (ii) It causes problems in processing (i) It is required to accurately measure net volumes of actual fuel in sales, taxation, exchanges and custody transfer
Copper-strip corrosion	(i) To measure to assess relative degree of corrosively (ii) It is indicates the presence of sulphur compounds
Cloud point, pour point cold-filter plugging point	(i) To measure the performance of fuels under cold temperature conditions (ii) It is used as quality control specification or low temperature handling Indicators for large storage tanks and pipelines at refineries.
Carbon residue	(i) It correlates with the amount of carbonaceous deposits in the combustion chamber (ii) Greater carbon deposits expected for higher values of carbon residue
Particulate matter	(i) It indicates the potential of emission of particulate matter (ii) It contains primarily carbon particles (iii) The Soot (carbonaceous particulates formed from gas-phase processes) particles absorb and carry carcinogenic materials into environment as emission and can cause an ill effect on human health. Excessive soot particles might clog the exhaust valves
Sulphur	(i) It is controlled to minimize corrosion, wear and tear (ii) It causes environmental pollution from their combustion products (iii) It is corrosive in nature and causes physical problems to engine parts
Ash	(i) Results from oil, water-soluble metallic compounds or extraneous solids, such as dirt and rust (ii) It can be used to decide product's suitability for a given application

Table 2.8: Reported ASTM D975 of diesel, and ASTM 6751, EN 14214 and IS 15607 specifications of biodiesel fuels [38].

Property specification (Unit)	**Diesel ASTM D975**		**Biodiesel**					
			ASTM D6751		**EN 14214**		**IS 15607**	
	Test method	Limits	Limits	Test Method	Limits	Test Method	Limits	Test methods
Flash point (°C)	ASTM D975	60 to 80	130 minimum	ASTM D93	101 minimum	EN ISO 3679	120	IS 1448
Cloud point (°C)	ASTM D975	-15 to 5	-3 to -12	ASTM 2500	-	-		IS 1448
Pour point (°C)	ASTM D975	-35 to -15	-15 to -16	ASTM 97	-	-		IS 1448
Cold filter plugging point (°C)	EN 590	-8	Max +5	ASTM D6371	-	EN 14214		
Cetane number	ASTM D4737, EN 590	46	47 minimum	ASTM D613	51 minimum	EN ISO 5165	51	ISO 5156
Density at 15°C (kg/m^3)	ASTM D1298	820-860	880	D1298	860-900	EN ISO 3675/12185	860-900	ISO 3675
Kinematic viscosity at 40°C (mm^2/s)	ASTM D445	2.0 to 4.5	1.9-6.0	ASTM D445	3.5-5.0	EN ISO 3104	2.5-6.0	ISO 3104

Iodine number ($g\ I_2/100\ g$)	-	-	-	-	120	EN 14111	120	EN 14111
Acid number (mg KOH/g)	-	-	0.5 maximum	ASTM D664	0.5 maximum	EN 14104	0.5 maximum	EN 14104
Oxidation stability	ASTM D2274	25 mg/L maximum	-	-	3 hours minimum	EN 14112	3 hours minimum	EN 14112
Carbon residue (% m/m)	ASTM D4530	0.2 maximum	0.050 maximum	ASTM D4530	0.3 maximum	EN ISO 10370		
Copper corrosion	ASTM D130	Class 1 max	No.3 maximum	ASTM D130	class 1	EN ISO 2160	class 1	EN ISO 2160
Distillation temperature (°C)	ASTM D86	370 maximum	360	ASTM D1160	-	-	360	ASTM D1160
Lubricity (HFRR)	IP 450	0.460 mm (max)	520 maximum	ASTM D6079	-	-	520 maximum	ASTM D6079
Sulphated ash content (%mass)	-	-	0.002 maximum	ASTM D874	0.02 maximum	EN ISO 3987		

Water and sediment	ASTM D2709	0.05 maximum	0.005 %v maximum	ASTM D2709	500 mg/kg maximum	EN ISO 12937	0.005 %v maximum	ASTM D2709
Moisture (wt %)	-	-	-	-	0.05 maximum	EN 1412	-	-
Monoglycerides (%mass)	-	-	-	-	0.8 maximum	EN 14105	-	-
Diglycerides (%mass)	-	-	-	-	0.2 maximum	EN 14105	-	-
Triglycerides (%mass)	-	-	-	-	0.2 maximum	EN 14106	-	-
Free glycerine (%mass)	-	-	0.02 maximum	ASTM D6584	0.02 maximum	EN 1405/14016	0.02 maximum	ASTM D6584
Total glycerine (%mass)	-	-	0.24	ASTM D6548	0.25	EN 14105	0.24	ASTM D6548

Phosphorous (%mass)	-	-	0.001 maximum	ASTM D4951	0.001 maximum	EN 14107	0.001 maximum	ASTM D4951
Sulphur (S 15 grade) (ppm)	- ASTM D5453	-10 maximum	150 maximum	ASTM D5453	-	-	150 maximum	ASTM D5453
Sulphur (S 50 grade)	ASTM D5453	50 maximum	-	-	-	-	-	-
Sulphur (S 500 grade)	ASTM D5453	500 maximum	500 maximum	ASTM D5453	-	-	500 maximum	ASTM D5453
Carbon	ASTM D975	87	77	ASTM PS 121	-	-	77	ASTM PS 121
Hydrogen	ASTM D975	13	12	ASTM PS 121	-	-	-	-
Oxygen	ASTM D975	0	11	ASTM PS 121	-	-	-	-
Sodium and potassium	-	-	-	-	5 maximum	EN 14108, EN 14109	-	-

Methanol content	-	-	-	-	0.2 maximum	EN 14110	-	-
Ester content	-	-	-	-	96.5 minimum	EN 14103	-	-
Linolenic acid methyl ester	-	-	-	-	12 maximum	EN 14103	-	-
Polyunsaturated (double bonds) methyl esters	-	-	-	-	1 maximum	EN 14104	-	-
Alkaline metals (Na+ K)	-	-	-	-	5 maximum	EN 14108, EN 14109,	-	-
Alkaline metals (Ca+ Mg)	-	-	-	-	5 maximum	EN 14538	-	-
Total contamination	-	-	24	ASTM D 5452	24	EN 12662	-	-

2.8 Review of Biodiesel Properties

The properties of biodiesel are characterized by physico-chemical properties. Some of these properties include; cetane number, density (kg/m^3), viscosity (mm^2/s), cloud and pour points ($^\circ$C), flash point ($^\circ$C), acid value (mg KOH/g-oil), ash content (%), copper corrosion, carbon residue, water content and sediment, sulphur content, glycerine (% m/m), phosphorus (mg/kg) and oxidation stability. The physical and chemical fuel properties of biodiesel basically depend on the type of feedstock and their fatty acids composition [42,55,136]. A summary of physicochemical properties of biodiesel produced from different feedstock, ASTM 6751-3 and EN 14214 specifications are shown in Table 2.9. The following section gives explanations of some general properties of biodiesel.

2.8.1 Kinematic viscosity/ Viscosity index

Viscosity is defined as the resistance of liquid to flow. It therefore affects the operation of fuel injection equipment, particularly at low temperatures when an increase in viscosity affects the fluidity of the fuel [112]. In some cases; at low temperatures biodiesel becomes viscous or even solidified. Some literature thought that, higher viscosity of biodiesel can affect the volume flow and injection spray characteristics in the engine [137]. At low temperature it may even compromise the mechanical integrity of the injection pump drive systems. The maximum limit according to ASTM D445 ranges are (1.9-6.0 mm^{2}s^{-1}) and (3.5-5.0 mm^{2}s^{-1}) in EN ISO 3104 [60,61].

The viscosity index is an arbitrary number indicating the effect of change of temperature on the kinematic viscosity of oil. A high viscosity index signifies a relatively small change in kinematic viscosity with temperature. The viscosity index of oil is calculated from its viscosities at 40 and 100°C. The procedure for the calculation is given in ASTM Method D 2270-74 for calculating viscosity Index from Kinematic Viscosity.

Table 2.9: Physico-chemical properties of selected biodiesel

Fuel Properties	**Jatropha Biodiesel [69]**	**Calophyllum Biodiesel [42]**	**Mahua Biodiesel [86]**	**Karanja Biodiesel [74]**	**Neem Biodiesel [138]**	**Tobacco Biodiesel [75]**
Density 15°C (kg/m^3)	879.5	888.6	874	931	868	888.5
Viscosity at 40°C (cSt)	4.8[g]	7.724	3.98	6.13	5.213 [g]	4.23[g]
Cetane number	51.6	51.9	65	55	-	51.6
Iodine number (mg equ./g)	104	85	-	-	-	136
Calorific value (MJ/kg)	39.23	-	36.8	43.42	39.81	-
Acid value (mg KOH/g)	0.4	0.76	0.41	0.42	0.649	0.3
Pour point (°C)	2	-	6	3	2	-
Flash point (°C)	135	151	208	95	76	165.4
Cloud point (°C)	2.7	38	-	7	9	-
CFPP (°C)	0	1	4	-1	11	-5
Copper strip corrosion (3h at 50℃)	1a	1b	1b	1b	1b	1a
Water and sediment content (%vol)	<0.005	<0.005	<0.005	<0.005	< 0.005	354.09[b]
Ash content % (m/m,)	0.012	0.026	0.01	0.001	-	-
Sulphur % (m/m)	1.2[a]	16[a]	164.8[a]	50[a]	473.8[a]	-
Sulphated ash % (m/m)	0.009	-	-	-	<0.005	0.0004

Phosphorus content	<0.1	0.223[a]	-	-	<0.1[a]	4[b]
Free glycerin % (m/m)	0.006	-	-	0.015	0	0.002
Total glycerin % (m/m)	0.1	0.232	-	0.0797	0.158	0.23
Monoglyceride % (m/m)	0.291	-	-	-	0.338	0.54
Diglyceride % (m/m)	0.104	-	-	-	0.474	0.13
Triglyceride % (m/m)	0.022	-	-	-	0	0.17
CCR 100% (% mass)	0.025	0.434	0.02	0.781	0.105	0.29
Oxidation stability (hrs, 110°C)	2.3	1.1	2.6	3.6	7.1	0.8

2.8.2 Density/ Specific gravity/API gravity

Density (g/cm^3 or kg/m^3) is important because it gives an indication of the delay between the injection (ignition quality) and combustion (specific energy) of the fuel in a diesel engine. This can influence the efficiency of the fuel atomization for airless combustion systems [42,139]. The ASTM D1298 and EN ISO 3675/12185 Standard test methods are used to measure the density of the biodiesel. According to these standards, density should be tested at the temperature reference of 15°C [140]. Specific gravity which is nothing more than the ratio of its density to that of water (density of the oil/density of water). API gravity inverted scale for denoting the 'lightness' or 'heaviness' of crude oils and other liquid hydrocarbons. Calibrated in API degrees (or degrees API), it is used universally to expresses a crude's relative density in an inverse measure lighter the crude, higher the API gravity, and vice versa. The American

Petroleum Institute gravity, or API gravity, is a measure of how heavy or light petroleum liquid is compared to water:

$$\textit{API Gravity} = \frac{141.5}{\text{Specific Gravity}} - 131.5 \qquad 2.1$$

2.8.3 Flash point

Flash point is the temperature at which fuel will ignite when exposed to a flame or a spark. Flash point varies inversely with the fuel's volatility [141]. The flash point of biodiesel is higher than the prescribed limit of diesel fossil fuel, which is safe for transport, handling and storage purpose [55,136,140]. Usually biodiesel has a flash point more than 120°C, while conventional diesel fuel has a flash point of 55-66°C [42]. Demirbas [112] stated that the flash point values of fatty acid methyl esters are significantly lower than those of vegetable oils. The limit of flash point ranges in ASTM D93 is 93°C and EN ISO 3679 is 120°C.

2.8.4 Cetane number

The cetane number (CN) is one of the most important parameters which are considered during the selection of biodiesel. It is the indication of ignition characteristics or ability of fuel to auto-ignite quickly after being injected. Cetane number provides information on ignition delay (ID) time when injected into the combustion chamber. Better ignition quality of the fuel is always associated with higher CN value [60,142]. Cetane number increases with increasing chain length of fatty acids and increasing saturation. A higher CN indicates shorter time between ignition and initiation into the combustion chamber [143]. Fuels with low CN tend to cause diesel knocking and showed increased gaseous and particulate exhaust emissions due to incomplete combustion [60]. CN is based on two compounds which are hexadecane with a CN of 100 and hepta-methylnonane with a CN of 15 [112,144,145]. Generally, biodiesel has higher CN than conventional diesel fuel, which results in higher combustion efficiency [145]. The CN of diesel, specified by ASTM D613 is 47 (minimum) and EN ISO 5165 is 51.0 (minimum).

2.8.5 Acid number

The acid number is a measure of the amount of carboxylic acid groups in a chemical compound, such as a fatty acid, or in a mixture of compounds [66]. The FFA defines the saturated or unsaturated mono-carboxylic acids that occur in fats, oils or greases glycerol backbones. Fatty acids contained carbon chain length and number of unsaturated bonds (double bonds). The structures of common fatty acids are given in Table 2.4. Higher amount of free fatty acids leads to higher acid value. Higher acid content causes severe corrosion in fuel supply system of an engine. The acid value is determined using the ASTM D664 and EN 14104. Both standards approved a maximum acid value for biodiesel of 0.50 mg KOH/g [35,109].

2.8.6 Free glycerol/Total glycerol

Free glycerol refers to the amount of glycerol that is left in the biodiesel. The content of free glycerol in biodiesel depends on the production process. The high yield of glycerol in biodiesel may be resulted from insufficient separation during ester washing. Glycerol is essentially insoluble in biodiesel so almost all of the glycerol is easily removed by settling or centrifugation. Free glycerol may remain either as suspended droplets or as the very small amount that is dissolved in the biodiesel. High free glycerol causes injector coking and damage to the fuel injection [146]. The ASTM specification required that the total glycerol be less than 0.24% of the final biodiesel product as measured using a gas chromatographic method described in ASTM D6584 and EN 14105/14106 has limit Max. 0.02% [147].

Total glycerine is a measurement of how much triglyceride remains unconverted into methyl esters. Total glycerine is calculated from the amount of free glycerine, monoglycerides, diglycerides, and triglycerides [129,148]. The reaction is presented below:

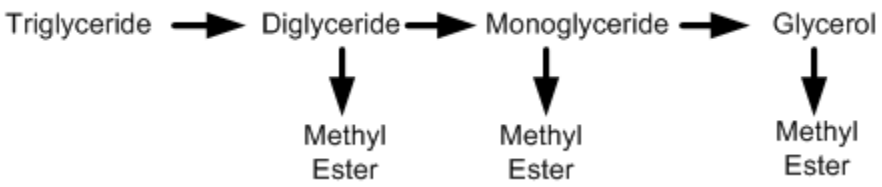

If the reaction is incomplete, then there will be triglycerides, diglycerides, and monoglycerides left in the reaction mixture. Each contains glycerol molecule that has not been released. The glycerol portion of these compounds is referred to as bound glycerol. When the bound glycerol is added to the free glycerol, the sum is known as the total glycerol. The ASTM specification requires that the total glycerol be less than 0.24% of the final biodiesel product as measured using a gas chromatographic method described in ASTM D 6584 and 0.25% in EN 14105. Fuels that do not meet these specifications are prone to coking; thus, may cause the formation of deposits on the injector nozzles, pistons and valves [149].

2.8.7 Water content and sediment

Water and sediment contamination are basically storage issues for biodiesel. Water exists in either dissolved water or suspended water droplets. While biodiesel is generally considered to be insoluble in water, it actually takes up considerably more water than diesel fuel [150]. Water droplets in the fuel cause corrosion of fuel pumps, injector pumps, fuel tubes, etc. Water become acidic with time, resulting acid corrosion on fuel storage tanks, contribute to microbial growth and filter plugging [151]. Moreover, high water content contributes to hydrolysis reaction that converts biodiesel to free fatty acids which is also linked to fuel filter blockage.

Sediment consist of suspended rust and dirt particles or may originate from the fuel as insoluble compounds formed during fuel oxidation [149,150]. If the water and sediment level is below 0.005 % volume, the result is reported as <0.005 % volume [152]. The standard of water content and sediment for biodiesel in ASTM D2709 and EN ISO 12937 specifications is 0.05 (%v) max [152,153].

2.8.8 Sulphur content

Combustion of fuel containing sulphur causes emissions of sulphur oxides. In spite of the fact that; vegetable oils and animal fat-based biodiesel have low levels of sulphur contents, specifying this parameter is important for engine operability [55,61,63].

2.8.9 Carbon residue

Carbon residue test is used to indicate the extent of deposits resulting from the combustion of fuel. Carbon residue which is formed by decomposition and subsequent pyrolysis of the fuel components clogs the fuel injectors due to presence of free fatty acids, glycerides, soaps, polymers, higher unsaturated fatty acids and inorganic impurities [55,151,154]. Although this residue is not solely composed of carbon, the term carbon residue is found in all standards because it has long been commonly used. The range of limit standard ASTM D4530 is Max 0.050% (m/m) and EN ISO10370 is Max. 0.30% (m/m) [55,61,63].

2.8.10 Copper strip corrosion

The copper corrosion test measures the corrosion tendency of fuel when used with copper, brass, or bronze parts. A copper strip is heated to 50°C in a fuel bath for three hours followed by comparison with a standard strips to determine the degree of corrosion. Corrosion resulting from biodiesel might be induced by some sulphur in acids; hence this parameter is correlated with acid number. The ASTM D130 standard mentions that the samples can have class 3 and EN ISO 2160 [55,61,63].

2.8.11 Phosphorous, calcium and magnesium content

Phosphorous, calcium, and magnesium are minor components typically associated with phospholipids and gums that may act as emulsifiers or cause sediment, lowering yields during the transesterification process [123]. The specification from ASTM D6751 states that phosphorous content in biodiesel must be less than 10 ppm, and calcium and magnesium

combined must be less than 5 ppm. Phosphorous is determined using ASTM D4951 and EN14107, Calcium and Magnesium are determined using EN Standard 14538 [155].

2.8.12 Iodine number

The iodine number is an index of the number of double bonds in biodiesel which determines the unsaturation degree of the biodiesel. This property influences the oxidation stability and polymerization of glycerides, leading to the formation of deposits in diesel engines injectors. Iodine value is directly correlated to biodiesel viscosity, cetane number and cold flow characteristics (cold filter plugging point). The iodine number is set to a maximum value of 120 mgI_2/g according to EN 14111 [66,156].

2.8.13 Saponification number

Saponification number expressed by potassium hydroxide in milligrams required to saponify one gram of fat or oil. It depends on the type of fatty acid contained in the oil. Fatty acid alkyl esters saponification is an undesired reaction during alkali-catalysed transesterification, as it hinders the separation process, reduces yield and reduces the quality of the raw biodiesel product [157]. Vegetable oils and fats may contain small amounts of water and free fatty acids (FFA). For an alkali-catalyzed transesterification, the alkali catalyst that is used will react with the FFA to form soap. Eqn. (2.2) shows the saponification reaction of the catalyst (sodium hydroxide) and the FFA (R_1-COOH), forming soap (R_1-COONa) and water. In addition, it binds with the catalyst meaning that more catalyst will be needed and hence the process will involve a higher cost [53].

$$R_1 - COOH + NaOH \rightarrow R_1COONa + H_2O \qquad 2.2$$

2.9 Biodiesel Storage Stability/Oxidation Stability

The oxidative stability of the fatty acids in biodiesel under various storage conditions were evaluated by Leung et al. [158], who found that oxidative instability increases the kinematic viscosity, peroxide value, and acid value of biodiesel. However, no long-term

evaluations of the influence of oxidative variables on the burning characteristics of biodiesel have been reported in the literature.

Oxidation stability is an indication of the degree of oxidation, potential reactivity with air. Oxidation occurs due to the presence of unsaturated fatty acid double bond(s) in the parent molecule, which immediately react with the oxygen as soon as it is being exposed to air [55,159]. The chemical composition of biodiesel fuels make it more susceptible to oxidative degradation than fossil diesel fuel. The Rancimat method (EN ISO 14112) is listed as the oxidative stability specification in ASTM D6751 and EN 14214. A minimum IP (110 °C) of 3 h is required for ASTM D6751, whereas a more stringent limit of 6 hours or greater is specified in EN 14214 [160–162].

Oxidation produces hydroperoxides, aldehydes, ketones and acids that change the fuel's properties. As biodiesel oxidizes, it becomes more viscous. The hydroperoxide induced polymerization and form insoluble gums and sediments [151]. Oxidation and formation of sediments and gum can cause fuel filter plugging. In the presence of oxygen, chain reactions occur simultaneously. Oxidative reactions occur in a series of initiation, propagation, and termination steps as shown in Figure 2.6.

Initiation:

$$\mathrm{RH} \rightarrow R^{-} + \mathrm{H}^{+}$$

Propagation:

$$R^{-} + \mathrm{O}_2 \rightarrow \mathrm{ROO}^{-}$$

$$\mathrm{ROO}^{-} + \mathrm{RH} \rightarrow \mathrm{ROOH} + R^{-}$$

Termination:

$$R^{-} + R^{-} \rightarrow \mathrm{R} - \mathrm{R}$$

$$\mathrm{ROO}^{-} + \mathrm{ROO}^{-} \rightarrow \text{Stable Product}$$

Figure 2.6: Scheme for chain reaction mechanism of oxidation [163]

The initial step involves an abstraction of hydrogen from unsaturated fatty acid to form free radical ($R^{\cdot}$) followed by an attack of molecular oxygen to these locations to form peroxide radicals ($ROO^{\cdot}$). The propagation phase involves intermolecular interactions, whereby the peroxide radical abstracts hydrogen from an adjacent molecule, which gives rise to hydroperoxides (ROOH) and a new free radical. C-H bond dissociation energies of fatty acid are lowest at bisallylic followed by allylic positions as shown in Figure 2.7.

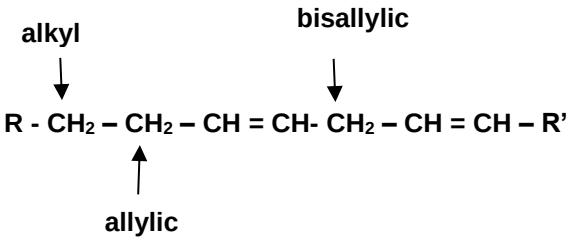

Figure 2.7: Carbon hydrogen bond position in fatty acids [164]

It is reported that lower bond energies for bisallylic and allylic hydrogens are 75 and 88 kcal/mol, respectively while those of methylene hydrogens are 100 kcal/mol [165–167]. Once formed, hydroperoxides tend to proceed toward further oxidation degradation leading to secondary oxidation derivatives such as aldehydes, acids, and other oxygenates [164].

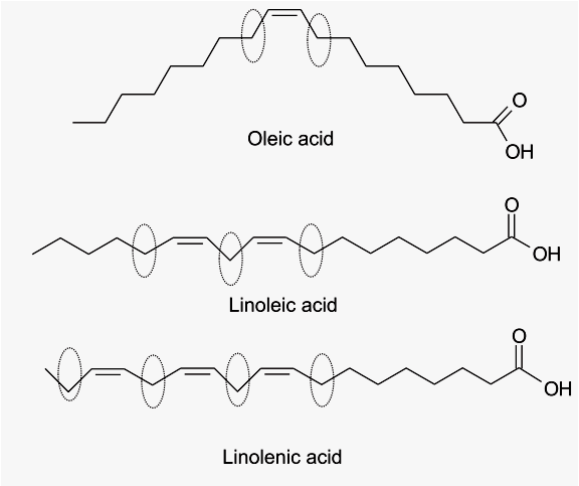

Figure 2.8: Common fatty acid methyl ester molecules[168]

When compared to diesel fuel, the unsaturation accounts for biodiesel instability. As the unsaturation in the fatty acid chain portion increases, the biodiesel becomes more unstable.

In Figure 2.8, the positions in the oleic acid, linoleic acid and linolenic acid (most common unsaturated acids present in the oils or fats and thus in the biodiesel) that are vulnerable to oxidation are highlighted by a circle. The allylic and bisallylic methylene moieties are the most susceptible to oxidation as a result of the radical chain reaction [168]. Other fuel properties are also reported to be increasing with storage time.

Accordingly, Canacki et al [169] reported increasing peroxide value, acid number and viscosity of oxidized biodiesel without anti-oxidants. Similarly, Wang et al. [170] reported increase in peroxide value, acid value, density, viscosity for stored rapeseed methyl and ethyl esters over a storage period of two years. However, they concluded that decrease in calorific value of biodiesel with storage time.

Bondioli et al. [171] investigated long term storage behaviour of 11 biodiesel samples for 1 year. The peroxide value and kinematic viscosity of all the biodiesel samples were found to be increasing with storage time. Since biodiesel physico-chemical properties change with storage period, it is expected that the performance and emission characteristics of such deteriorated biodiesel would change [172]. Agarwal et al.[163] investigated the effect of oxidized biodiesel on engine performance and emission parameters; such biodiesel produced 15 and 16 % lower exhaust carbon monoxide and hydrocarbons respectively and reported decrease in Smoke, HC and CO emission levels with oxidized biodiesel as compared to base line diesel results.

Conventionally, using anti-oxidants such as tert-butylhydroquinone (TBHQ), ECOTIVE, 2,5-Di-*tert*-butylhydroquinone (DTBHQ), butylated hydroxyanisole (BHA), butylated hydroxytoluene (BHT), propyl gallate (PrG) , Ionox 75 (2,6-di-*tert*-butylphenol 75%) and tocopherol have been reported by various researchers to reduce the impact of biodiesel degradation and improved oxidation stability [120-121].

2.10 Cold Flow Property of Biodiesel

The behaviour of biodiesel at low temperature is an important quality criterion. This is because partial or full solidification of the fuel may cause blockage of the fuel lines and filters, starting problems, and engine damage. The cloud point (CP) and pour point (PP) are important for low-temperature applications for fuel. The cloud point is the temperature at which wax crystals first becomes visible when the fuel is cooled under controlled conditions during a standard test. Pour point is the temperature at which the amount of wax out of solution is sufficient to gel the fuel, thus it is the lowest temperature at which the fuel can flow [42,112,173]. Cloud and pour points are measured using ASTM D2500 EN ISO 23015 and D97 procedures [141].

Cold filter plugging point (CFFP) is used as indicator of low temperature operability of fuels. It refers to the temperature at which the test filter starts to plug due to fuel components that have started to gel or crystallize [151]. CFPP defines the fuels limit of filterability, having a better correlation than cloud point for biodiesel as well as petro diesel. CFPP is measured using ASTM D6371 [136,174]. Crystallization of the saturated fatty acid methyl ester increase with decreasing temperature and the pour point is the lowest temperature at which it will cease to flow defined the cloud point and pour point of biodiesel [151,175]. Several approaches exist to improving biodiesel CFPP including the use of additive, esters of other seed oils, and winterization [151,176]. Inherent genetic modification of the fatty acid profile offers the best possibility of addressing several or all fuel property issues simultaneously.

2.11 Engine Performance, Emissions and Combustion Characteristics of Potential Feedstocks of the India

2.11.1 Jatropha curcas biodiesel

Chauhan et al. [177] evaluated the performance and exhaust emissions using Jatropha biodiesel blends with diesel fuel on an unmodified diesel engine. In case of all fuel blends,

brake thermal efficiency, HC, CO, CO_2 and smoke density were lower while BSFC and NO_x were higher than that of diesel. Other similar studies *Rashed et al*. [178], *Nalgundwar et al.* [179] and *Huang et al.* [180] showed similar results for Jatropha biodiesel. According to the *Bari et al.* [181] combustion characteristics of 20% jatropha biodiesel (B20) blend and D100 were also found to be very similar with B20 having 4.8°CA more combustion duration than D100 due to low volatility and presence of heavier molecules in biodiesel. The authors concluded that biodiesel derived from Jatropha and its blends could be used in a conventional diesel engine without any modification up to B20.

Similarly, *Ganapathy et al*. [182] conducted experiments using full factorial design consisting of (33) with 27 runs for each fuel, diesel and Jatropha biodiesel. The effect of variation of above three parameters on brake specific fuel consumption (BSFC), brake thermal efficiency (BTE), peak cylinder pressure (P_{max}), maximum heat release rate (HRR_{max}), CO, HC, NO emissions and smoke density were investigated. It has been observed that advance in injection timing caused reduction in BSFC, CO, HC and smoke levels and increase in BTE, P_{max}, HRR_{max} and NO emission with Jatropha biodiesel operation. Increase in volume fraction showed increase in BTE, P_{max}, HRR_{max} and NO emission at this injection timing, load and speed were 5.3%, 1.8%, 26% and 20% respectively.

Mofijur et al. [183] studied the feasibility of Jatropha as a potential biodiesel feedstock in Malaysia. Interestingly, only B10 and B20 have been used to evaluate engine performance and emission and compared to B0, the average reduction in brake power (BP) is 4.67% for B10 and 8.86% for B20. It was observed that BSFC increased as the percentage of biodiesel increase. In comparison to B0 (D100), reduction in hydrocarbon (HC) emission of 3.84% and 10.25% and carbon monoxide (CO) emission of 16% and 25% was reported using B10 and B20. However, the blends give higher nitrogen oxides (NOx) emission of 3% and 6% using B10 and B20. As a conclusion, B10 and B20 can be used in a diesel engine without any modifications.

2.11.2 Karanja biodiesel

Dhar et al. [184] investigated performance, emissions and combustion characteristics of Karanja biodiesel and its blends on engine with varying engine speed and load. Maximum torque attained by 10% and 20% biodiesel blends were higher than diesel, while higher biodiesel blends produced slightly lower torque. BSFC of biodiesel blends was comparable to diesel however BSFC increased for higher biodiesel blends.

The CO, HC and smoke emissions of Karanja biodiesel blends were lower than mineral diesel but NOx emissions were slightly higher. Comparative investigation of performance, emissions and combustion characteristics of Karanja biodiesel blends and mineral diesel showed that up to 20% Karanja biodiesel blend can be utilized in an unmodified diesel engine. Similar outcomes found by *Raheman et al*. [185]. *Nabi et al.* [74] produced karanja methyl ester (KME), engine result showed reduced engine emissions including carbon monoxide (CO), smoke and engine noise, but increased oxides of nitrogen (NOx). Compared to DF, B100 reduced CO, and smoke emissions by 50 and 43%, while a 15% increase in NOx emission was observed with the B100.

Chauhan et. al.[186] conducted transesterification Karanja oil and found the properties within acceptable limits of relevant standards. The performance studied included brake thermal efficiency of Karanja biodiesel with different compositions at 5%, 10%, 20%, 30% and 100% with diesel. BTE was about 3-5% lower with Karanja biodiesel and its blends with respect to diesel. Also, emissions parameters revealed UBHC, CO, CO_2 and smoke were lower with Karanja biodiesel fuel. However, NO_x emissions of Karanja biodiesel and its blend were higher than diesel. The peak cylinder pressure and heat release rate was lower for Karanja biodiesel. The results suggested that biodiesel from Karanja and its blends with diesel could be a potential fuel for diesel engine and play a vital role in the near future especially for small and medium energy production.

2.11.3 Polanga (*Calophyllum inophyllum*) biodiesel

Sahoo et al. [187]evaluated the performance and emission of Polanga oil methyl ester (POME) blends (0-100%) in a single cylinder diesel engine at different loads (0-100%). Findings demonstrated that the performance of biodiesel-fuelled engine was improved than diesel-fuelled engine regarding thermal efficiency, brake specific energy consumption (BSEC), smoke opacity, and exhaust emissions including NO_x emission for the entire range of operations. The 100% biodiesel was found to be the best, which improved the thermal efficiency of the engine by 0.1%. Similar trend was shown by the BSEC and the exhaust emissions which were reduced. Smoke emissions also reduced by 35% for B_{60} as compared to neat petro-diesel. Decrease in the exhaust temperature of biodiesel-fuelled engine led to approximately 4% decrease in NO_x emissions for B_{100} biodiesel at full load. However long term endurance test and other tribological studies need to be carried out before suggesting long term application of polanga oil based biodiesel.

Sahoo et al. [188] tested the applications of biodiesel in a single cylinder diesel engine and discovered that; neat biodiesel from Jatropha, Karanja and Polanga; and their blends (20 and 50 by v%) were used for conducting combustion tests at varying loads (0, 50 and 100%). The engine combustion parameters such as peak pressure and its occurrence time, heat release rate and ignition delay were computed. Combustion analysis revealed that B20 Polanga biodiesel had maximum peak cylinder pressure. The ignition delays were consistently shorter for neat Jatropha biodiesel, varying between 5.9° and 4.2° crank angles lower than diesel with the difference increasing with the load. Similarly, ignition delays were shorter for neat Karanja and Polanga biodiesel when compared with diesel.

2.11.4 Mahua (Madhuca Indica) biodiesel

Raheman et al. [85] reported the performance of biodiesel obtained from Mahua biodiesel and its blend. The tested properties were found to be comparable to diesel and within

standards. Engine performance (BSFC, BTE and exhaust gas temperature) got reduced in exhaust emissions and BSFC with increase brake power, BTE was impressive when B20 was used. Equally, emissions (CO, smoke density and NO_x) reduced. *Godiganur et. al.* [189] assessed the performance of methyl ester of mahua oil biodiesel and its blends at constant speed of 1500 rpm under variable load conditions. The volumetric blending ratios of biodiesel with conventional diesel fuel were set at 0, 20, 40, 60, and 100. Engine performance and emissions evaluated indicated the increasing biodiesel in the blends CO, HC got reduced significantly, fuel consumption and NO_x emission of biodiesel increased slightly compared with diesel. BSEC decreased and thermal efficiency of engine slightly increased when operating on 20% biodiesel than that operating on diesel.

Puhan et al. [87] performed analysis of Mahua methyl ester with diesel fuel in a single cylinder direct injection CI engine and showed decrease (13%) in thermal efficiency. In the continuing the work, *Puhan et al*. [190] tested Mahua oil ethyl ester and showed the comparable thermal efficiency with diesel fuel. According to *Puhan et al* [87,190], exhaust emissions of CO, HC, NOx and smoke number were reduced around 58%, 63%, 12% and 70% respectively in case of MOEE and 30, 35, 4 and 11% respectively, compared to diesel. The amount of NOx produced for neat biodiesel of Mahua oil was 50 ppm. Similarly, its biodiesel performance tests showed that power loss was around 13% combined with 20% increase and emissions such as CO and HC were lower for MO biodiesel compared to diesel by 26% and 20% respectively. However, it was observed that NOx emission was lesser by 4% for MO biodiesel compared to diesel was tested on a single cylinder CI engine by *Saravanan et al.* [191].

2.11.5 Neem biodiesel

Dhar et al.[138] evaluated neem oil biodiesel regarding its performance, emission and combustion characteristics and its various blends with diesel were compared with baseline data. The BSFC for biodiesel and its blends was higher than diesel and brake thermal efficiency of

all biodiesel blends was found to be higher than diesel. CO and HC emissions were lower than diesel but NOx emissions were higher for biodiesel blends.

Detailed combustion characterization revealed that combustion started earlier for higher biodiesel blends but was slightly delayed for lower blends of biodiesel in comparison with diesel. Rate of heat release remained unchanged. Combustion duration for biodiesel blends was found to be shorter than diesel; suggesting that neem oil biodiesel was marginally inferior compared to diesel.

2.11.6 Sal (Shorea robusta) biodiesel

Hajra et al, [192] produce biodiesel from Sal oil (Shorea robusta) using the transesterification. The studies sal biodiesel emissions such as CO, HC and NOx are reduced by 25%, 45% and 12%, respectively compared to diesel without significant difference in thermal efficiency. Based on this study it is concluded that the SME can be used as fuel without any modifications in the engine and hence this biodiesel can be a potential substitute to standard diesel fuel. *Chhibber et al*. [193] carried out engine trials for 25% sal biodiesel and results exhibited comparable performance and lowered emissions.

2.11.7 Kusum (Schleichera oleosa) biodiesel

Sharma et al. [100] produced biodiesel using Kusum (Schleichera triguga), and found various physical and chemical parameters of the fatty acid methyl esters derived have confirm its suitability as a biodiesel fuel. One another study *Silitonga et al*. [99] found that *Schleichera oleosa* possesses the potential as a feedstock for biodiesel production.

2.11.8 Waste cooking oil biodiesel

Muralidharan et al. [194] carried out experiments to estimate the performance, emission and combustion characteristics of a single cylinder; four stroke variable compression ratio multi fuel engine fuelled with waste cooking oil methyl ester and its blends with diesel. Tests has been conducted using 20%, 40%, 60% and 80% biodiesel blends, with an engine

speed of 1500 rpm, fixed compression ratio 21 and at different loading conditions. The performance parameters elucidated included brake thermal efficiency, specific fuel consumption, brake power, indicated mean effective pressure, mechanical efficiency and exhaust gas temperature. The exhaust gas emission was found to contain carbon monoxide, hydrocarbon, nitrogen oxides and carbon dioxide. The results of the experiment was compared and analyzed with diesel and it confirmed considerable improvement in the performance parameters as well as exhaust emissions. The blends when used as fuel results in the reduction of carbon monoxide, hydrocarbon, carbon dioxide at the expense of nitrogen oxides emissions. It has deduced that the combustion characteristics of waste cooking oil methyl ester and its diesel blends closely followed diesel.

2.12 Outcomes of Literature Review

As an outcome of the elaborative review of existing technical literatures regarding the engine trial results of biodiesels derived from a wide range of vegetable oil feedstocks and its blends, the following conclusions are made.

An exhaustive literature review has been carried out to study the biodiesel production and its utilization in diesel engine. As an outcome of review of literature, the following major findings can be made;

1. The vegetable oils are promising as diesel engine fuel, however, there are many difficulties associated with its use which include; poor atomization, incomplete combustion, ring sticking, fuel system clogging, polymerization and carbon deposits. High viscosity of vegetable oils contributes these difficulties which can be addressed by transesterification, pyrolysis and catalytic cracking, preparation of emulsions and dilution with diesel fuel. However, transesterification is the most preferred for reduction of viscosity of vegetable oils.

2. With some exceptions, most of the non-edible oils have high free fatty acid contents leading to a two stage process (esterification followed by transesterification) to produce biodiesel [107,138,195–198].
3. The energy consumption in two stage transesterification is higher. Therefore, optimization of process parameters is required in high FFA non-edible oil seeds for commercial scale production [165,199,200].
4. Response surface methodology using central composite design method had been used by many researchers as an effective process optimization technique during biodiesel production from a wide range of feedstocks [130,201–203].
5. In some of the literature, the biodiesel sample produced did not fulfil the designated standards of ASTM/EN/IS etc. [121,204,205] resulting in further addition of additives and post-processing [117,133,163,168,173,176,206,207].
6. Depending upon the feedstocks, some of the biodiesel samples showed improved brake thermal efficiency and reduced BSEC with increased biodiesel volume fraction in the test fuel [208–212] whereas some others exhibited exactly opposite trend [213–215]. Therefore, engine performance using biodiesel directly depends upon the property of the corresponding feedstock [42,45,103,209,216] and the efficiency of the conversion process [61,92,199,217].
7. Most of the literature agreed on the common denominator that emissions of carbon monoxide and total hydrocarbons reduced with increasing biodiesel blending [218–221], whereas oxides of nitrogen increased [138,218]. However, even reduction in oxides of nitrogen was reported in many cases, [7,222–224].
8. Literature indicated increased in-cylinder pressure for lower volume fraction of biodiesel in the test fuels irrespective of the feedstocks. This led to shorter combustion duration, increased in-cylinder temperature and lower exhausts temperatures in many

cases. However, with higher volume fractions of biodiesel, some literatures indicated reduction in peak in-cylinder pressure where some indicated minimal changes in the peak in-cylinder pressure. Therefore, the combustion phenomena using biodiesel is highly sensitive to the nature of the feedstock and transesterification process which actually determines the fuel properties [15,194,225,226].

9. With an increase in volume fraction of biodiesel, the reduction in combustion heat release was reported in most cases [227]. However, in few cases a marginal increase was reported at lower blends [182,228].
10. Increased heat release in the diffusion phase, smoother engine operation etc. are some of the findings in most of the literature [45,229,230].

2.13 Research Gap Analysis

On the strength of exhaustive review of literature, the following research gaps were identified.

1. So far, the biodiesel policy of India focuses on Jatropha curcas and this has lead to mono-culture. There is an urgent need to explore other non-edible crops especially TBO as the sustainability of feed stocks remains an issue. No single feedstock can fulfil the demand of 20% blending as proposed by biofuel policy of India.
2. The land availability issues for Jatropha Cultivation cannot be ignored while the use of existing feedstocks like Sal and Kusum is not fully explored.
3. The performance and emission tests have suggested either increase or decrease in BTE with reduction in CO, HC emissions. NO_x has been found to increase in most cases; however, it is reducing in some of the cases. There is a need to explore performance and emission characteristics with the two species selected for the present study.

4. The performance and emission characteristics in respect of different biodiesel suggest that composition of feedstock have a important role to play. These characteristics are not adequately studied for Sal and Kusum biodiesel.
5. Low temperature behaviour along with oxidation stability of biodiesel derived from Sal and Kusum not studied.
6. Exhaustive research work is available on diesel/biodiesel blends however, combustion analysis of biodiesel in the diesel engine is new thrust area.
7. Combustion characteristics based on the heat release models and mass fraction burned model yet to be explored for Sal and Kusum biodiesel.

2.14 Problem Statement

It may be inferred that comprehensive engine trials to evaluate performance, emissions and combustion studies on diesel engines fuelled with **Sal and Kusum biodiesel** are unexplored in the literature.

In the light of the exhaustive literature review and the research gap analysis, it is clear that the most widely used method for vegetable oil usage in diesel engine is the conversion to methyl esters or biodiesel to address the high viscosity issues of vegetable oils. As reported in the preceding section, the primary focus for biodiesel production in India has been on Jatropha oil seed, which is available only during a particular season in a year. Other potential TBOs such as Kusum and Sal have not been studied adequately. Present research explore the production of biodiesel from Sal and Kusum tree borne oils and optimize of process parameters using response surface methodology. Enhancement of cold flow property and long term storage stability due to addition of additives has been carried out. Then, exhaustive engine trials has been carried out using Sal methyl ester and Kusum methyl ester blend with diesel up to 40%. In the subsequent analysis, it may provide a clear picture regarding the suitability of these methyl esters blends as alternative fuels to diesel fuel.

2.15 Objectives

The following objectives were envisaged for the present research work.

1. To produce biodiesel using Sal oil and Kusum oil through transesterification process.
2. To optimize production process parameters using response surface methodology for maximizing yield.
3. To determine various physico-chemical properties of biodiesels and different blends as per the appropriate International standards like ASTM.
4. To evaluate the effects of additives on oxidation stability and cold flow properties of test fuels.
5. To study the storage stability of biodiesel for a period of one year with and without additives.
6. To develop experimental set up for the engine trials.
7. To conduct the combustion, performance and emission tests on the single cylinder Diesel engine with diesel in order to generate baseline data for reference in all subsequent tests, and to carry out the same trials for biodiesel/diesel under similar conditions as well.

CHAPTER 3

SYSTEM DEVELOPMENT AND METHODOLOGY

3.1 Introduction

This chapter explains how the whole research was conducted with the systematic execution of steps followed and as mentioned in the problem statement section. Figure 3.1 gives a brief summary of the implemented flow chart of this research.

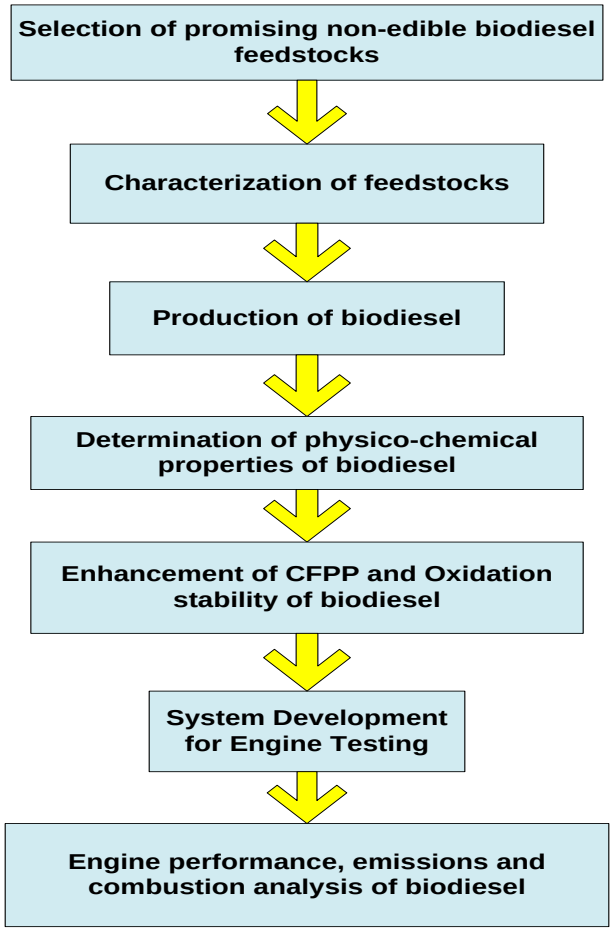

Figure 3.1: Flow chart of research methodology

It includes the production of biodiesel from Sal oil and Kusum oil and its optimization using response surface methodology, comprehensive physico-chemical characterization, improvement in some desired properties (such as oxidation stability and cold flow property).

The preparation of various blends of Sal methyl ester (SME) and Kusum methyl ester (KME) with diesel, and development of engine test rig for the engine trials have been described in details. The chapter also described the procedures for the calculations of heat release rate, mass friction burnt, and the exhaustive engine trials. Finally, the accuracy and uncertainties of measurements are also reported in this chapter.

3.2 Sal (Shorea robusta)

Sal is a large sub deciduous tree named as *Shorea robusta* [193]. It is up to 50 meter high. It has large leathery leaves and yellowish flowers. The oil from seed is known as Sal butter. It is spread across 10 million hactares in India, covering approximately 14% of the total forest area of the country [231]. Also it plays an important role in the economics of some Indian states *i.e*. Orissa, Jharkhand, Chhattisgarh and Madhya Pradesh; with Sal forest area covering about 45% of their total forest area. About 20-30 million forest dwellers, depend on Sal seeds, leaves and resigns as source of their livelihood. At present about 1.50 million metric tons of Sal seeds are produced per year in India, which generates around 1.32 million metric tons of de-oiled cake after oil extraction [231].

Sal seed is light brown in color, contains calyx and wings. The de-shelled seeds contain a thin seed coat and seed pod as shown in Figure 3.2. The kernel has five segments covering the embryo. Strong wind or storm helps in bumper fall towards [96,232]. The quality of the Sal fat depends on kernels collection and stored. Sal seed contains high moisture content which in turns increases the FFA level, making it non-edible. Some important properties of pure Sal oil and Kusum oil are shown in Table 3.1.

Table 3.1: Properties of the Sal oil and Kusum oil [98,99].

S.No.	Properties	Sal oil	Kusum
1	Appearance	White or Light yellow fat	Pale brown oil
2	Iodine Value (wijs)	28 – 42	45-65
3	Saponication value	230- 280	170-190
4	% FFA	1-3	7-11
5	Melting Point (^{0}C)	33- 38	-1
6	Total saturated	61%	31%
7	Total monounsaturated	39%	62%
8	Total polyunsaturated	-	7%

Figure 3.2: Various parts of Sal (Shorea robusta) tree

Footnote: A: Tree; B: Flower canopy; C: Fruit; D: Seed

3.3 Kusum (Schleichera oleosa)

The botanical name of Kusum is *Schleichera oleosa* and the annual production potential is around 66,000 tonnes in India, out of which 4000 to 5000 tonnes are actually collected [233]. It is a medium to large sized, evergreen, dense tree with 35 to 50 feet height as shown in Figure 3.3. It mainly nurtures sub-Himalayan tracts in the north and central parts of eastern India. Seeds are mostly globular with 1.5 cm in diameter and weighing between 0.5 and 1.0 g. The brown seed coat is brittle and breaks at a slight pressure to expose a 'U' shape kernel as shown Figure 3.3. The leaflets are 2 to 4 pairs, elliptic or elliptic-oblong, margins entire and apex rounded. It is host tree for best grade lac insects [100].

Figure 3.3: Kusum (Schleichera oleosa); A: Tree; B: Fruits; C: Seeds

Kusum oil is non-edible. In India, the oil is used generally for soap making. It is traditionally used as medicine for the cure of itch, acne, burns, other skin troubles, rheumatism (external massage), hair dressing and promoting hair growth. Oil is also used for culinary, lighting purposes and lubrication.

3.4 Physico-chemical Properties of Sal oil and Kusum oil

In this research, the important physico- chemical properties of the crude oils and their respective methyl esters were tested according to ASTM D 6751 standard. These properties include: viscosity, density, flash point, cold filter plugging point (CFPP), Carbon residue, calorific value (heating value), oxidation stability, moisture content, copper strip corrosion, cetane number and so on. These properties are discussed further in consequent section 3.11. Table 3.2 shows the equipment used to analyse these properties, their manufacturers and the standards used to measure these properties. All these equipment were located in Centre for Advanced Studies and Research in Automotive Engineering (CASRAE), Delhi Technological University, Delhi.

Table 3.2: List of equipments

	Property	**Equipment**	**Manufacturer**	**ASTM D6751**
1	Kinematic viscosity	Petrotest viscometer	(Anton Paar, UK)	ASTM D7042/D445
2	Flash Point	Pensky-martens flash point - automatic	(Baveno, Italy)	D 93
3	Oxidation stability	873 Rancimat	(Metrohm, Switzerland)	D 675
4	Cloud and Pour point	Cloud and Pour point tester - automatic NTE 450	(Normalab, France)	D 2500 and D 97
5	CCR	Micro Carbone Residue Tester - automatic Alcor	Alcor Petroleum Instruments, USA	D 4530
6	Density	Density meter DMA-450	(Anton Paar, UK)	D 1298
7	CFPP	Cold filter plugging point – automatic NTL 450	(Normalab, France)	D 6371
8	Caloric value	Bomb calorimeter Parr 6100	(IKA, UK)	D 5865
9	Acid Value	Potentiometer titrator	Metrohm	D 664
10	Peroxide value	Potentiometer titrator	Metrohm	D 664
11	Saponification value	Potentiometer titrator	Metrohm	D.664

12	Iodine value	Potentiometer titrator	Metrohm	D 664
13	Fatty acid profile	GCMS Auto sampler AOC 20i	Shimaddzu corporation	-
14	Functional Group	FTIR-8400 S	Shimaddzu corporation	-
15	Water content	Karl Fischer's Moisture Titrator	Metrohm	D 2709

3.4.1 Determination of acid value

Acid value is defined as the number of milligrams of potassium or sodium hydroxide necessary to neutralize the free acid in 1g of sample. The procedure conducted in this research to measure the acid values of non-edible crude oils such as Sal oil and Kusum oil. To determine acid value potentiometer titrator is used as shown in Plate 3.1. It is universal titrator which provides acid value, peroxide value, saponification number and iodine number of the test fuel/sample.

Acid number determines the acidic constituents in a fuel. For biodiesel, the acid number is an indicator of the quality of the product. Specifically, it detects the presence of any un-reacted fatty acids still in the fuel, or any acids that were used in biodiesel processing. This is also an indication of the condition of the stability of the fuel, because the acid number increases as the fuel ages. The acid number was determined by Potentiometric titration method in accordance with ASTM D-664.

The equipment used for the determination of total acid number is the Potentiometric Titrator and is shown in the Plate 3.1. During the test, the sample is dissolved in a mixture of toluene and iso-propanol that contains a small amount of water. The sample is titrated potentiometrically with alcoholic potassium hydroxide. The meter readings are plotted against the respective volumes of titrating solution and the end points are taken at well-defined inflections in the resulting curve. The titration commences with adding the base

(NaOH solution) with a known normality (0.1N) from the burette drop by drop to the mixture until the indicator changes its color at the endpoint. The volume of reactant consumed was measured and used to calculate the acid value of the sample by using the following equation 3.1.

$$\mathbf{AV} = \frac{\mathbf{MW} \times \mathbf{N} \times \mathbf{V}}{\mathbf{W}} \qquad (3.1)$$

Where: MW ≡ Molecular weight of sodium hydroxide; N≡ Normality of sodium hydroxide solution (0.1 N); V≡ Volume of sodium hydroxide solution used in titration; W ≡ Weight of oil sample.

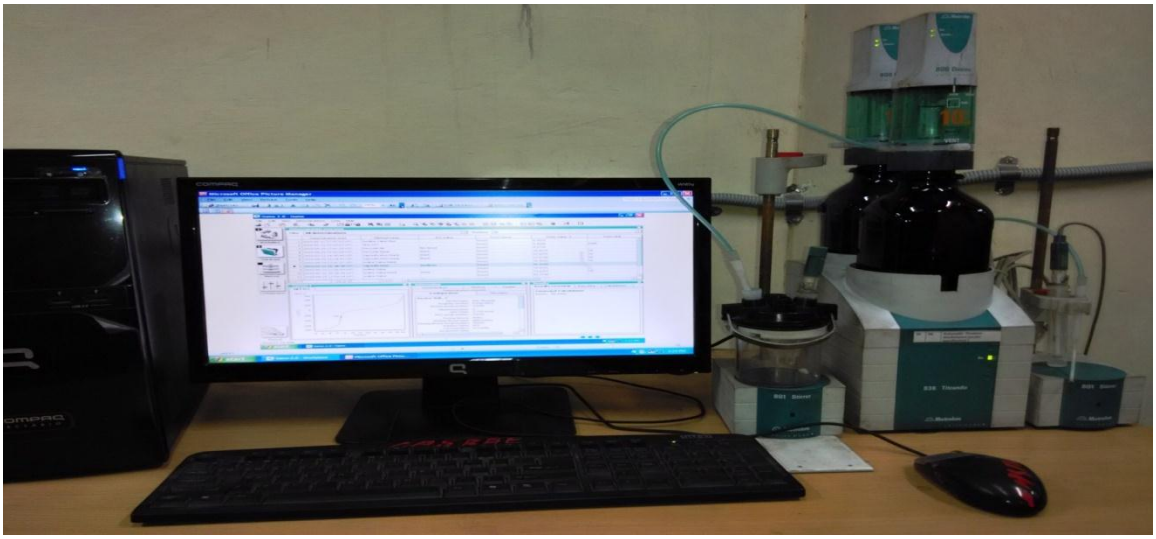

Plate 3.1: Potentiometer titrator/petrochemical

3.5 Biodiesel Production

Biodiesel was produced using transesterification process as discussed elsewhere [234]. FFA content of the Sal seed oil was less than 2%, so single stage transesterification process was used to produce Sal methyl ester. The transesterification was conducted using optimized process parameters. However Kusum oil has high free fatty acid (8 to 11%) contents leading to two stage process to produce biodiesel. In the first stage (esterification) the FFA is reacted with the alcohol in presence of acid catalyst and when the FFA is reduced below 2%, then it is transesterified in presence of alkaline catalyst.

Normally sulphuric acid and PTSA is considered as the suitable catalyst for esterification. The FFA can react with alcohol to form ester (biodiesel) by an acid-catalyzed esterification reaction [235]. The reaction for reducing FFA, as shown in the equation 3.2;

$$R_1 - COOH + ROH \xleftrightarrow{H^+} R - O - CO - R_1 + H_2O \qquad (3.2)$$

(FFA) (Alcohol) (Fatty acid ester) (Water)

The general scheme of the transesterification reaction is presented in Figure 3.4, where R is a mixture of fatty acid chains.

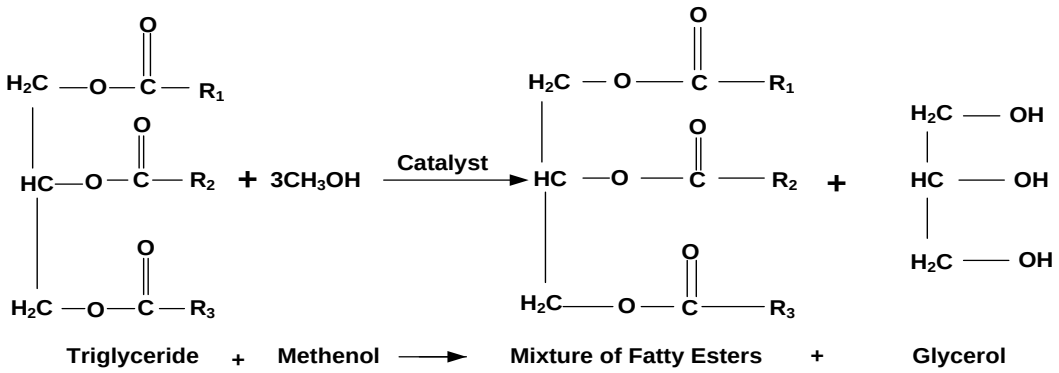

Figure 3.4: Scheme for transesterification reaction

Typical biodiesel production stages are shown in Figure 3.5 whereas in the present study optimised process parameters were used for esterification and transesterification using Response Surface Methodology (RSM). All the chemicals used were analytical reagent grade: methanol (CH_3OH), potassium hydroxide (KOH), PTSA (para toluene sulphonic acid), 2-Propanol (iso-propyl alcohol), potassium hydroxide solution (0.1N), phenolphthalein as indicator and glassware & filter paper of 125mm size were used.

Experimental arrangement is shown in Plate 3.2. RSM, based on the combination of statistical and mathematical tools, is considered to be a valuable technique for the development, modification and optimization of various processes.

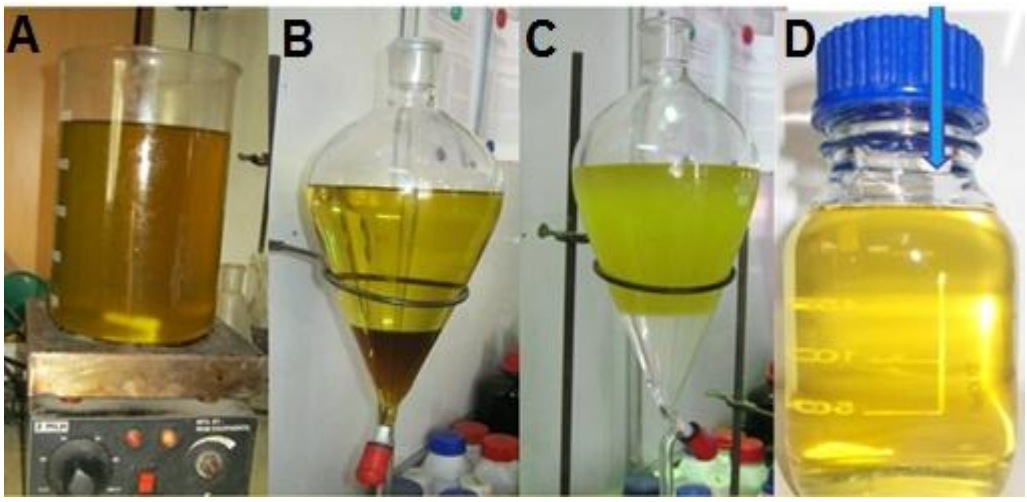

Figure 3.5: Various steps in biodiesel production

Footnote: A – Transesterification (Alcoholics); B – Gravity settling; C – Water washing; D – Fatty acid methyl ester (Biodiesel)

RSM is proved to be useful tool for the analysis of problems during which a certain response of concern is usually influenced by different process variables with the purpose to optimizing defined response of interest [236]. Plate 3.3 and Plate 3.4 represents the post processing of Sal oil and Kusum oil after the transesterification process.

Plate.3.2: Experimental run as per RSM test matrix

Plate 3.3: Post processing for Sal biodiesel

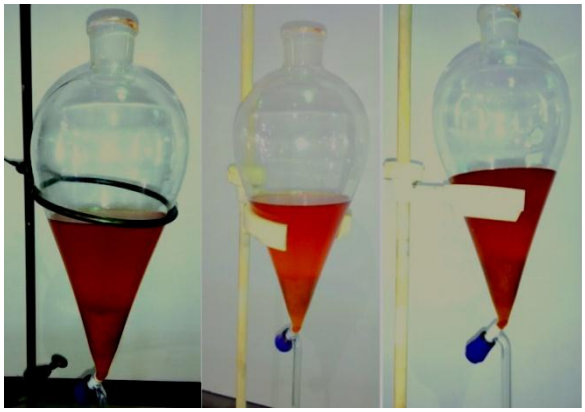

Plate 3.4: Post processing for Kusum biodiesel

The same process parameters used to produce large quantity of biodiesel in the 10 L capacity reactor as presented in Plate 3.5. Arrangement is also provided to control the heating rate. Stirring of the reactants is carried with the help of a blade agitator mounted on alternating current geared motor. Digital display of temperature and stir speed (rpm) is provided. A heat exchanger (condenser) with appropriate cooling arrangement through water is provided to condense the methanol during transesterification reaction.

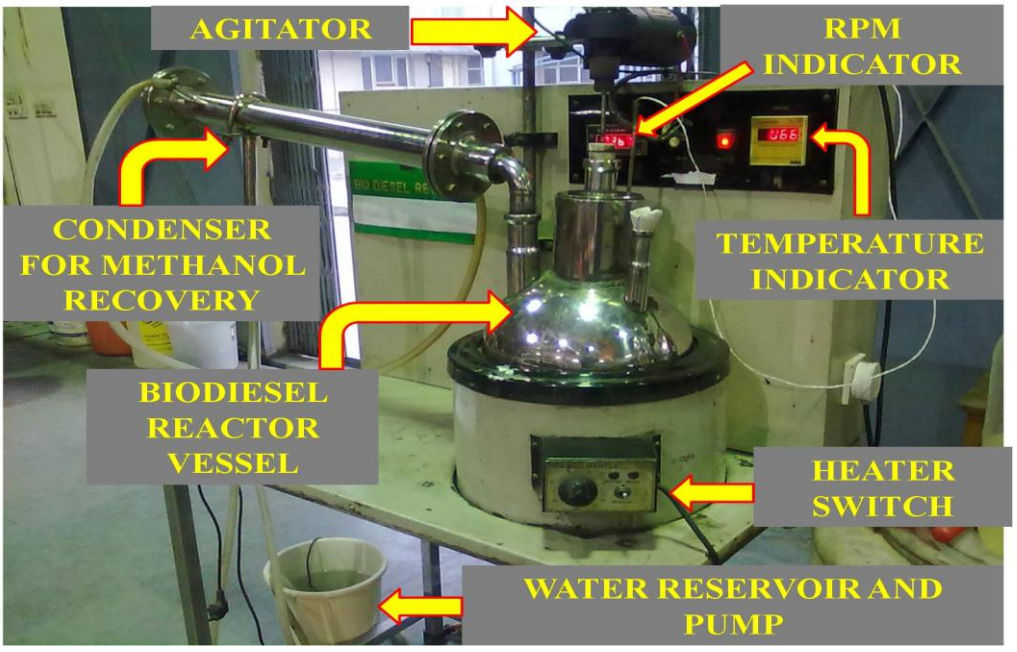

Plate 3.5: 10 Liter Capacity Biodiesel Reactor

3.6 Optimization of Biodiesel Production Using RSM

The energy consumption of production biodiesel is integral part for biodiesel costing (economics). Therefore, optimization of process parameters of esterification and transesterification is required of non-edible oil seeds for commercial scale production.

RSM in experimental design has increasingly attracted the attention of many researchers [97,200,237,238]. The most widely used model was Central Composite Design (CCD) of Response Surface Methodology (RSM) as found from the literature review. CCD was employed to determine the optimal reaction conditions. It is a second order experimental model which composed of factorial design, set of central points, and axial points equidistant to the center point. The factorial design component of CCD is of the class 2^k factorial, where k represents the number of appropriate factors or variables. Each of the variables is chosen at two levels meaning that each variable has a low (coded numeric value of -1) and high numeric value (coded numeric value of +1). A spherical design is obtained in the reason that there is an equal variance from the center to all the points in the sphere. Steps involved in Central Composite Design are given in Figure 3.6.

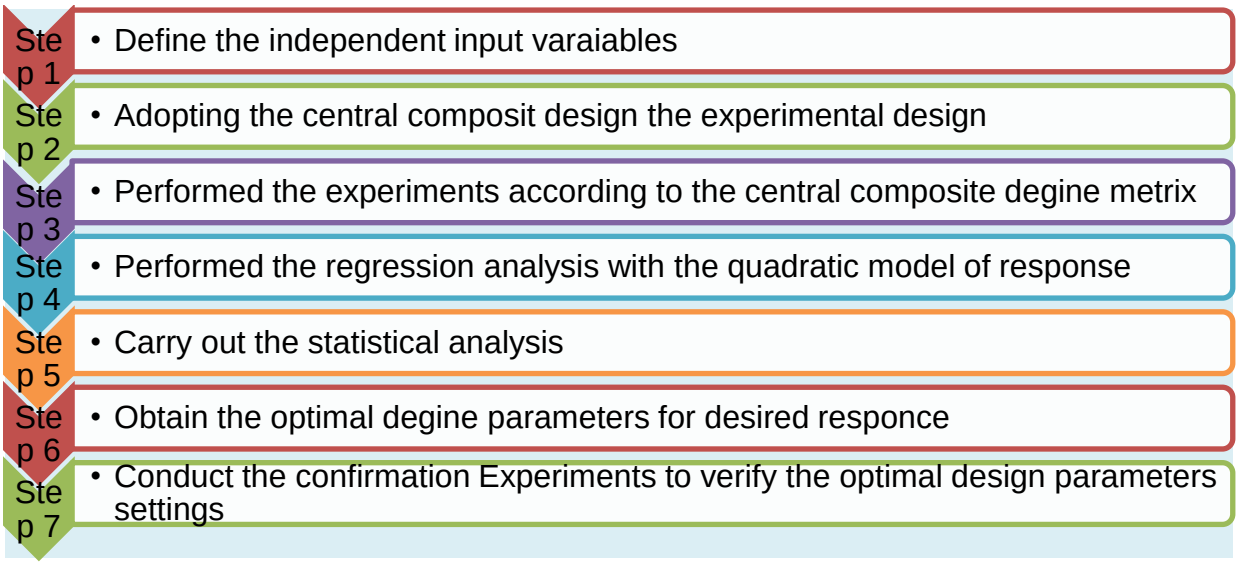

Figure 3.6: Steps involved in Central Composite Design

Aim of the present work is to focus on the second strategy: statistical modeling to build up an suitable approximating model between the response y and independent variables, $£_1, £_2, \ldots\ldots, £_k$

In general, the relationship is,

$$y = f(£_1, £_2, \ldots\ldots, £_{k)} + \varepsilon \qquad (3.3)$$

Where, variables $£_1, £_2, \ldots\ldots, £_k$ are usually the natural variables and ε is intercept. Than the terms of the coded variables, the response function (Eqn. 3.3) will be written as,

$$E(y) = f(X_1, X_2 \ldots\ldots\ldots X_k) \qquad (3.4)$$

3.6.1 Selection of process parameters for esterification

Optimization of the transesterification process was conducted via 4-factor experiment to examine the effects of catalyst concentration (A), Reaction temperature (B), Reaction time (C) and methanol/oil molar ratio (D) of methyl esters using central composite design (CCD). A total of 30 experimental-sets including factorial points, axial points and central points were developed. Number of experimental set was calculated from the standard design of experiments formula given in equation 3.5.

$$N = 2^k + 2k + N_o \qquad (3.5)$$

Where k is the number of independent variables = 4; N_o is the number of repetition of experiments at the central point for the design to be rotatable = 6.

The test matrix based on Table 3.3 was generated for esterification using a design of experiment software 10.0.3.0 and the subsequent experiments were carried out at the laboratory facility.

Number of experiments was conducted for the selection of esterification process parameters for FFA reduction. In the pilot run, arbitrarily the catalyst concentration (w/w %) of 0.1 % was chosen and others process parameters were kept constant. Process parameters with their ranges on the basis of pilot run investigation are shown in Table 3.3. When process parameters values were taken beyond the range, FFA and yield of biodiesel production significantly diminished.

Table 3.3: Process Parameters with their Ranges for esterification of Kusum oil

Name	**Factor**	**Units**	**Low Level**	**High Level**
Catalyst concentration	A	% (w/w)	0.25	1.75
Reaction temperature	B	℃	40	70
Reaction Time	C	Minutes	30	90
Molar Ratio	D	Methanol/oil	3	9

Table 3.4: Design matrix for esterification of Kusum oil

Run	**A: Catalyst concentration (w/w %)**	**B: Temperature (^{0}C)**	**C: Time (min)**	**D: Molar Ratio**	**Response (Y): FFA (%)**
1	1.5	45	120	3	5.6
2	2	57.5	80	6	6.15
3	1.5	70	120	3	4.7
4	1	57.5	80	6	1.7
5	1	57.5	80	6	2
6	0.5	70	120	3	4.5
7	1.5	45	40	3	6.85
8	1	57.5	5	6	5.5
9	1	57.5	160	6	3.35
10	1	57.5	80	6	2.2
11	0.5	45	120	9	3.8
12	1.5	70	40	3	5.2
13	0.5	45	40	3	8.1
14	0.5	70	120	9	4.2
15	0.5	70	40	9	4.5
16	1	82.5	80	6	4.8

17	1.5	70	40	9	4.6
18	1	57.5	80	6	1.6
19	1	57.5	80	0	6.9
20	0.5	45	120	3	6.2
21	0.5	70	40	3	6.9
22	1	57.5	80	12	3.5
23	1	57.5	80	6	1.8
24	1	57.5	80	6	1.7
25	0.5	45	40	9	3.6
26	1.5	70	120	9	5.5
27	1.5	45	120	9	3.5
28	1.5	45	40	9	3.7
29	0	57.5	80	6	7.5
30	1	32.5	80	6	4.5

The experimental data presented in Table 3.4 was analyzed using response surface regression (RSREG) procedure in the statistic analysis system (SAS) that fits a full second-order polynomial model as shown in eqn. 3.6. Confirmatory experiments were carried out to validate the model using combinations of independent variables according to the predicted points by experimental design.

$$Y = \beta_0 + \sum_{i=1}^{3} \beta_i x_i + \sum_{i=1}^{3} \beta_{ii} x_i^2 + \sum \sum_{i<j=1}^{3} \beta_{ij} x_i x_j \qquad (3.6)$$

Where x_i and x_j are the uncoded independent variables, β_o is the intercept, β_i, β_{ii} and β_{ij} represent the linear, quadratic and interaction constant coefficients respectively, while Y is the response (FFA or yield).

Esterification process parameters of Kusum oil were selected randomly as per design matrix shown in Table 3.4. Corresponding measured response i.e. FFA of Kusum oil under different runs is shown in same table.

3.6.2 Selection of process parameters for transesterification

To maximize the yield of fatty acid methyl ester (SME or KME) using the transesterification process was conducted via 4-factor experiment to examine the effects of catalyst concentration (A), reaction temperature (B), reaction time (C) and methanol/oil molar ratio (D) using CCD. Process parameters with their ranges on the basis of pilot run investigation are shown in Table 3.5.

Table 3.5: Process Parameters with their Ranges for transesterification

Name	Factor	Units	Low Level	High Level
Catalyst Concentration	A	% (w/w)	0.25	1.25
Reaction Temperature	B	^{0}C	30	70
Reaction Time	C	Minutes	30	90
Molar Ratio	D	Methanol/oil	3	9

To optimize the process parameters of the transesterification were selected randomly as per design matrix shown in Table 3.6. Corresponding measured response i.e. yield (w/w %) of both biodiesel (SME and KME) under different runs are shown in Table 3.6.

Table 3.6: Design matrix for transesterification

Std. Run	Run	A: Catalyst concentration (w/w %)	B: Temperature (^{0}C)	C: Time (Minutes)	D: Molar Ratio (methanol/oil)	Response (Y): Yield (%)
27	1	0.75	55	60	6	92.7
22	2	0.75	55	120	6	82
17	3	0	55	60	6	63
20	4	0.75	75	60	6	68
4	5	1.25	65	30	3	32
30	6	0.75	55	60	6	92.5
15	7	0.25	65	90	9	89
16	8	1.25	65	90	9	85
26	9	0.75	55	60	6	92.5
7	10	0.25	65	90	3	65

12	11	1.25	65	30	9	69
18	12	1.75	55	60	6	65
29	13	0.75	55	60	6	93.7
6	14	1.25	45	90	3	67
10	15	1.25	45	30	9	88
5	16	0.25	45	90	3	62
21	17	0.75	55	0	6	56
8	18	1.25	65	90	3	52
9	19	0.25	45	30	9	74
11	20	0.25	65	30	9	75
13	21	0.25	45	90	9	80
24	22	0.75	55	60	12	89
14	23	1.25	45	90	9	94
23	24	0.75	55	60	0	35
28	25	0.75	55	60	6	93.5
25	26	0.75	55	60	6	93
2	27	1.25	45	30	3	59
19	28	0.75	35	60	6	84
3	29	0.25	65	30	3	45
1	30	0.25	45	30	3	52

3.7 Sal Biodiesel Production

The FFA of Sal was measured to be less than 2 % of oil. Before the biodiesel production pre-treatment is required. In this process oil was heated to remove moisture for 1 h at 110°C under agitated condition with 450 rpm stir speed. Sal used single stage transesterification process and various stages are shown in Figure 3.7.

After the transesterification process, post-treatment process is required such as separating, washing and heating. A particular measured quality of the Sal oil (100 g has been used for all the experiments) was heated up to a specific temperature. The reaction started when a defined amount of methanol pre-mixed with the potassium hydroxide catalyst was added to the reactor containing the oil at the reaction temperature. The reactor was always

kept under vigorous magnetic mixing. At the end of the reaction, products were left to settle in a separating funnel overnight (12-15 h) for separation between biodiesel and glycerol. The lower layer which contained impurities and glycerol was drawn off.

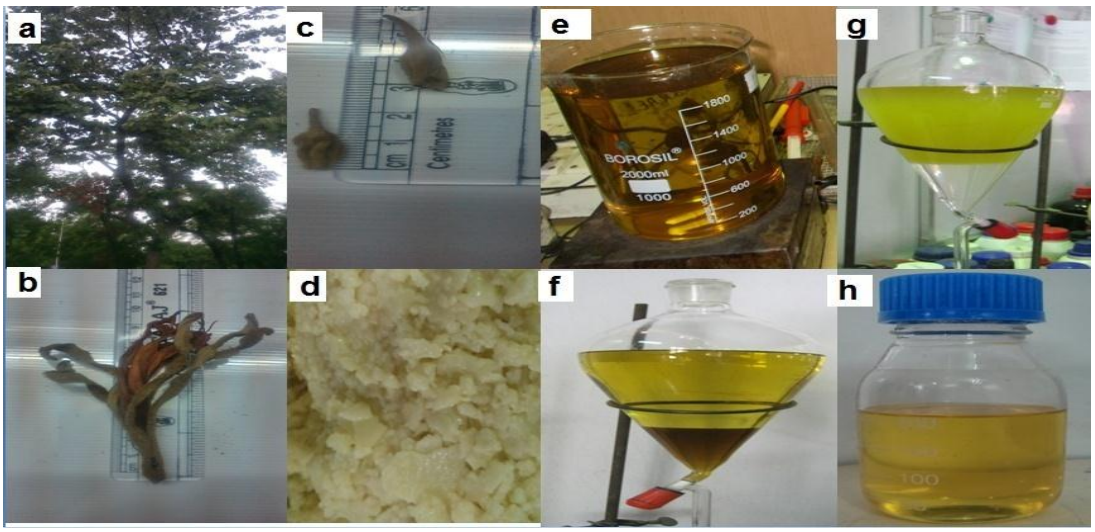

Figure 3.7: Various steps of Sal Biodiesel Production

Footnote- (a)- Sal tree; (b)- Flower; (c)- Seed; (d)- Sal butter; (e)- Sal oil.; (f)- Glycerol separation; (g)- Water washing; (h)- Sal biodiesel.

In post treatment process, 50% (v/v) of distilled water at 60°C was mixed into ester and shacked gently. This process was repeated several times until the p^H of the distilled water became neutral. The lower layer was discarded and upper layer was entered into a flask and dried using Na_2SO_4 and then further dried using rotary evaporator to make sure that biodiesel is free from methanol and moisture. Finally a good quality Sal methyl ester or Sal biodiesel (SME) was produced.

3.8 Kusum Biodiesel Production

The acid value of crude Kusum oil was measured to be 16.2 mg KOH/g. Therefore two stage transesterification (acid catalyzed esterification followed by base catalyzed transesterification) is required.

In the esterification process Kusum oil reacts with methanol in presence of acid catalyst (PTSA). In this stage, an optimal FFA of 1.8 % was achieved for using optimized process parameters achieved ramp function graph. On completion of this reaction, the products were separated from excess alcohol, PTSA and impurities presented in the upper layer. The lower layer was separated and entered into a rotary evaporator and heated at 95°C under vacuum conditions for 1 h to remove methanol and water from the esterified oil. Similarly, in the transesterification stage, it produced the optimum yield of 96.5%. Different stages of Kusum biodiesel production shown in Figure 3.8. Based on this result, bulk quantity of Kusum biodiesel was prepared in a large capacity biodiesel reactor as shown in the Plate 3.5.

Figure 3.8: Various stages of Kusum biodiesel production

3.9 Determination of Fatty Acid Composition

Gas chromatography–mass spectrometry (GC-MS) was used to determine the fatty acid composition and molecular weight of biodiesel. The gas chromatograph utilizes a capillary column which depends on the column's dimensions (length, diameter, film thickness) as well as the phase properties. The fatty acid composition and free glycerin in the fuel is determined by Gas Chromatograph as per ASTM D-6584 test method. In a gas liquid

chromatography, an inert carrier gas (Helium or Nitrogen) acts as the mobile phase. This carries the components of analyte (a substance whose chemical constituents are being identified and measured) mixture and elutes through the column.

The column usually contains an immobilized stationary phase. In mass spectrometer, gas is converted into ions in mass spectrometer. Gas chromatography–mass spectrometry (GC-MS) equipment was used in present study as shown in Plate 3.6.

3.10 Preparation of Test Fuels (Blends)

The biodiesel so obtained was completely miscible with mineral diesel. To check the miscibility, various proportions of biodiesel was added to mineral diesel and monitored for 60 days. Test fuels were regularly checked for phase separation and homogeneity, No signs of separation were observed.

Plate 3.6: Gas chromatography–mass spectrometry (GC-MS) Equipment

In this context, the present study considered 10%, 20%, 30% and 40% blends of SME and KME in diesel. The test fuel samples were prepared by volume wise substitution of Sal and Kusum biodiesel in the diesel. Blending was done using rigorous agitation at a high rpm

hand by blender. Therefore, the test fuels for engine trial comprised of SME10, SME20, and SME30, SME40 for Sal biodiesel and KME10, KME20, KME30, KME40 for Kusum biodiesel along with the neat diesel. All test fuels are shown in Table 3.7 and Plate 3.7 depicts SME, KME and neat diesel.

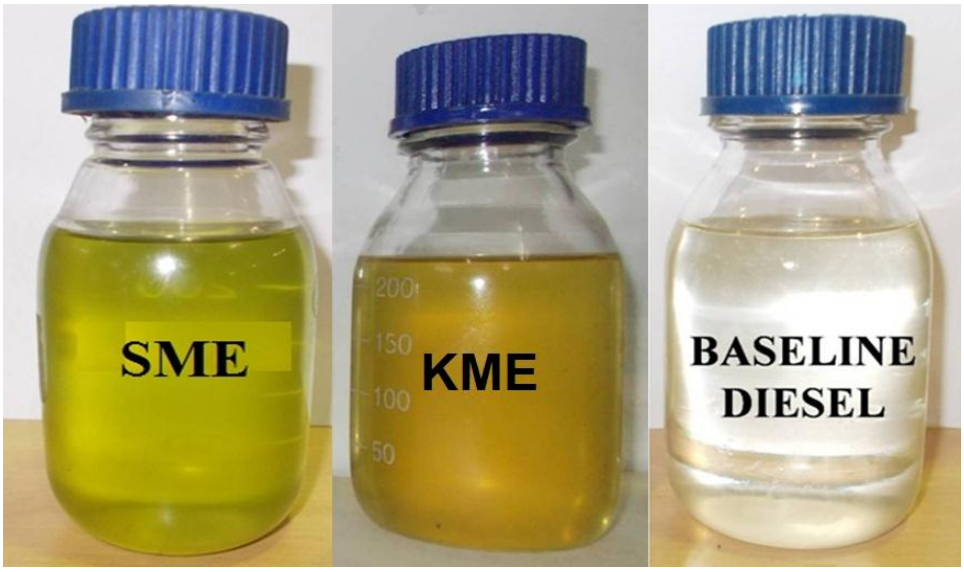

Plate 3.7: Sample of Sal biodiesel, Kusum Biodiesel and Diesel

Table 3.7: Nomenclature and composition of various test fuels

S. No.	Test Fuel's composition	Nomenclature
1.	100% Diesel or Baseline Diesel	D100
2.	100% Sal Methyl Ester or Sal Biodiesel	SME
3.	100% Kusum Methyl Ester or Kusum Biodiesel	KME
4.	10% Sal Methyl Ester and 90% Diesel	SME10
5.	20% Sal Methyl Ester and 80% Diesel	SME20
6.	30% Sal Methyl Ester and 700% Diesel	SME30
7.	40% Sal Methyl Ester and 60% Diesel	SME40
8.	10% Kusum Methyl Ester and 90% Diesel	KME10
9.	20% Kusum Methyl Ester and 80% Diesel	KME20
10.	30% Kusum Methyl Ester and 70% Diesel	KME30
11.	40% Kusum Methyl Ester and 60% Diesel	KME40

3.11 Test Methods for Physico-Chemical Properties

Determination of various physico-chemical fuel properties of the Sal methyl ester and Kusum methyl ester as well as their blends are essential in engine trials. Therefore, 11 test fuel samples of 500 ml each were prepared comprising of neat diesel (baseline).

3.11.1 Density

The equipment used was "Antan Par Density Meter, Model DMA 4500 shown in Plate 3.8. In the present investigation the specific gravity of the test fuel samples was measured at a temperature of 15^0C in accordance with ASTM D-4052. The procedure for measurement of density and specific gravity was trouble-free. Then the test fuel pipeline was rinsed by injecting 10 ml of toluene through the sample injection port. Subsequently 10 ml of actual sample was fed to the injection port. The repeatability was checked thrice and found satisfactory. Moreover, the average of the three measurements was taken as the final value for each sample.

3.11.2 Kinematic viscosity

Plate 3.9 shows the viscometer taken for the measurement of kinematic viscosity. The determination of viscosity and the effect of temperature on viscosity can provide a better understanding of Sal and Kusum biodiesel as a fuel cum lubricant. Viscosity measurements were conducted for different test fuels under consideration. Kinematic viscosity of liquid fuel samples were measured at 40^0C as per ASTM D-445. The equipment used was "Petrotest Viscometer. A measured quantity of sample was allowed to free flow through the capillary tube. Time was noted in passing of the fluid from the capillary tube having an upper level and lower level mark. Subsequently, kinematic viscosity was calculated by multiplying the

capillary constant with the time measured in seconds (Equ. 3.7). The final value was obtained in mm^2/s or cSt.

$$\nu = k^* t \qquad (3.7)$$

Where; ν = Kinematic viscosity, mm^2/sec; k = Constant; mm^2/sec^2 (k= 0.005675 mm^2/sec^2); t = Time, in second

Plate 3.8: Density meter

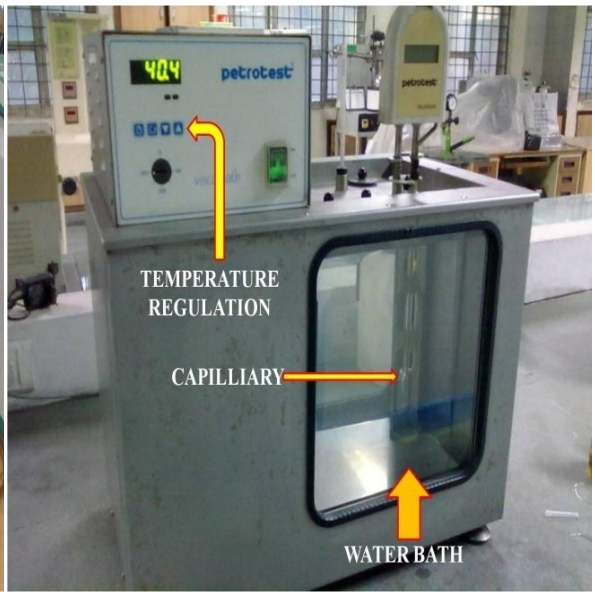

Plate 3.9: Viscometer

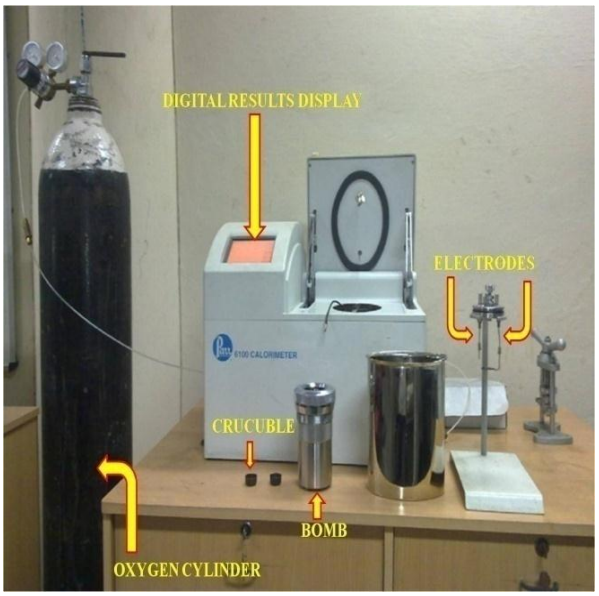

Plate 3.10: Bomb Calorimeter

Plate 3.11: Flash Point Apparatus

3.11.3 Calorific value

The calorific value is the amount of heat released by the combustion of unit quantity of fuel in the presence of oxygen in a bomb calorimeter. The calorific value of the fuel was determined with the Isothermal Bomb Calorimeter as per the specifications given in ASTM D240 standard. The calorimeter model used was Parr 6100 Oxygen Bomb Calorimeter. Electrodes were used to burn the sample of fuel in the bomb calorimeter. Bomb calorimeter is shown in Plate 3.10.

3.11.4 Flash point

Flash point is the minimum temperature at which the oil vapour, which when mixed with air forms an ignitable mixture and gives a momentary flash on application of a small pilot flame [239]. The flash and fire point of the test fuels were measured as per the standard of ASTM D 93 by Pensky Martens Automatic Flash Point Apparatus as shown in Plate 3.11. The sample was heated in a test cup before small pilot flame was directed into the cup through the opening provided at the top cover at the regular intervals. The IS-15607, EN-14214 and ASTM D-6751 specify the minimum value of flash point as 120°C and 130°C respectively.

3.11.5 Peroxide Value

The peroxide value is a measure of the peroxides contained in a vegetable oil derived sample as milli-equivalents (meq.) of peroxide per 1000 grams of sample. One of the most commonly used methods to determine peroxide value utilizes the ability of peroxides to liberate iodine from potassium iodide (KI) as shown eqe.3.8. The lipid is dissolved in a suitable organic solvent and an excess of KI is added:

$$ROOH + KI_{excess} = ROH + KOH + I_2 \qquad (3.8)$$

Once the reaction got completed, the amount of ROOH that has reacted can be determined by measuring the amount of iodine formed. This was done by titration with sodium thiosulphate ($Na_2S_2O_3$) and a starch indicator as shown in eqe. 3.9.

$$I_2 + \text{starch} + 2Na_2S_2O_3\,(\text{blue}) = 2NaI + \text{starch} + Na_2S_4O_6\,(\text{colorless}) \qquad (3.9)$$

The amount of sodium thiosulphate required to titrate the reaction is related to the concentration of peroxides in the original sample. This test was conducted on Potentiometer titrator as shown Plate 3.1.

3.11.6 Saponification value

The saponification value or saponification number is a measure of the average molecular weight of the triglyceride in a sample, such that fatty acids by treatment with alkali as shown in eqn. 3.10.

Triglyceride + 3 KOH = Glycerol + 3 Fatty acid Salts of potassium (3.10)

Saponification value is a measure of the free fatty acid and saponifiable ester groups. It is expressed as the number of milligrams of potassium hydroxide required to neutralize the free acids and saponify the esters contained in one gram of the material. It is calculated as the difference between the saponification value and the acid value.

The lipid is dissolved in an ethanol solution which contains a known excess of KOH. This solution is then heated so that the reaction goes to completion. The un-reacted KOH is then determined by adding an indicator and titrating the sample with HCl. The saponification number is then calculated from the amount of KOH which reacted. The Potentiometer titrator is shown in Plate 3.1.

3.11.7 Iodine Value

The iodine value is the measure of the unsaturation (or amount of double bonds) of fats and oils, expressed in terms of number of grams of iodine absorbed per 100g of sample of oil. Firstly, sample fat is dissolved in carbon tetrachloride, and Hanus reagent is added and left in a dark room for reaction. Then, potassium iodide is added for titration with 0.1mol/L sodium thiosulfate. The iodine value of fatty sample is calculated from titration volume of sodium thiosulfate.

3.11.8 Cetane Number

Cetane number (CN) is a measure of ignition quality of a diesel fuel. One of the ways of solving the problem of CN determination is to develop models to predict the CN when saponification value and iodine value are known of the biodiesel. The predicated CN of biodiesel is comparable to that of the actual CN of the biodiesel, and it has been concluded that the CN of biodiesel can be predicted based on thermal properties using the empirical equation (eqn. 3.11) for predicting the CN of biodiesel.

$$Cetane\ Number = 46.3 + \frac{5458}{Saponification\ value} - (0.225 * Iodine\ value) \qquad (3.11)$$

3.11.9 Water Content

Water content was determined by Karl Fischer titrator as shown in Plate 4.12 as per ASTM D-1744 standard. Karl Fisher test measures water by titration and is reported in either ppm (parts per million) or % by volume. This reagent is a mixture of iodine, sulphur dioxide, pyridine, and methanol. When excess iodine exists, electric current can pass between two platinum electrodes or plates.

The water in the sample reacts with the iodine. When the water is no longer free to react with iodine, an excess of iodine depolarizes the electrodes, signalling the end of the test.

3.11.10 Carbon Residue:

Carbon Residue is determined by the equipment shown in Plate 3.13 as per carbon residue micro test method (ASTM D-4530). The sample is first distilled (D-86) until 90% of the sample has been recovered. The residue is weighed into a special glass bulb and heated in a furnace to 1022°F (550°C). Most of the sample evaporates or decomposes under these conditions. The bulb is cooled and the residue is weighed.

3.11.11 Lubricity

The lubrication of the pump is not provided by viscosity alone but also by the lubricity property of the fuel. Even with 2% biodiesel mixed in diesel fuel, the WSD values comes down to around 325 micron and is sufficient to meet the lubricity requirements of the fuel injection pump (460 micron max.). B100 performs still better, with a WSD of about 314 micron. With further reduction of sulfur content is diesel for Euro II and Euro IV fuels; the lubricity loss due to sulfur removal can easily be compensated by the addition of appropriate amount of biodiesel in diesel fuel. A 2% inclusion into any conventional diesel fuel is sufficient to address the lubricity problem.

3.11.12 Copper Strip Corrosion

This test gives an indication of the corrosiveness of the fuel to the metallic parts of the system in which the product is used, whether during transportation or actual use in engine. This property is determined by Copper Strip Corrosion Test apparatus as shown in Plate 3.14, as per ASTM D-130. This property is determined by copper strip tarnish test. A polished copper strip is immersed in the specified volume of the samples and maintained at the

specified temperature for the specified length of time. The strip is then compared with ASTM copper strip corrosion standard colour code after cleaning with sulphur free petroleum spirit. The rating of copper corrosion should not be worse than No.1 specification (rating scale for visual assessment of corrosion).

Plate 3.12: Karl Fischer's Moisture Titrator

Plate 3.13: Carbon Residue Apparatus

Plate 3.14: Copper Strip Corrosion Test Apparatus

Plate 3.15 Element Analyzer

3.11.13 Elemental analysis

Elemental analyser as shown in Plate 3.15 provide a means for the rapid determination of carbon, hydrogen, nitrogen and sulphur inorganic matrices and other types of materials. In this technique, the substance under study is combusted under oxygen stream in a furnace at high temperatures. These gases are then separated and carried to the detector using inert gases like helium or argon. It is one of the few analytical techniques that give a clear quantitative measurement of the carbon, hydrogen and nitrogen contents. In this combustion process is take place at 1000 ^{0}C, carbon is converted to carbon dioxide; hydrogen to water; nitrogen to nitrogen gas/ oxides of nitrogen and sulphur to sulphur dioxide.

3.11.14 Fourier Transform Infra-Red (FTIR) Spectroscopy

FT-IR stands for Fourier Transform Infra-Red, the preferred method of infrared spectroscopy. The resulting spectrum represents the molecular absorption and transmission, creating a molecular fingerprint of the sample. This makes infrared spectroscopy useful for several types of analysis. Apparatus used for present study is shown in Plate 3.16.

Plate 3.16: FTIR 8400S

Infrared spectroscopy is the study of interactions between matter and electromagnetic fields in the IR region. The probability of a particular IR frequency being absorbed depends on the actual interaction between this frequency and the molecule. In general, a frequency will be strongly absorbed if its photon energy coincides with the vibrational energy levels of the molecule. IR spectroscopy is therefore a very powerful technique which provides fingerprint information on the chemical composition of the sample.

3.11.15 Cold Flow Plugging Point

Cold Filter Plugging Point (CFPP) is defined as the minimum temperature at which the fuel filter does not allow the fuel to pass through it. The sample was cooled in bath fixed at –34℃ and vacuum is maintained for suction of fuel in the capillary provided for every degree fall in temperature, the temperature at which the fuel fails to come up or fall down within 60 seconds through the filter of 10 micron is observed as the cold filter plugging point of fuel.

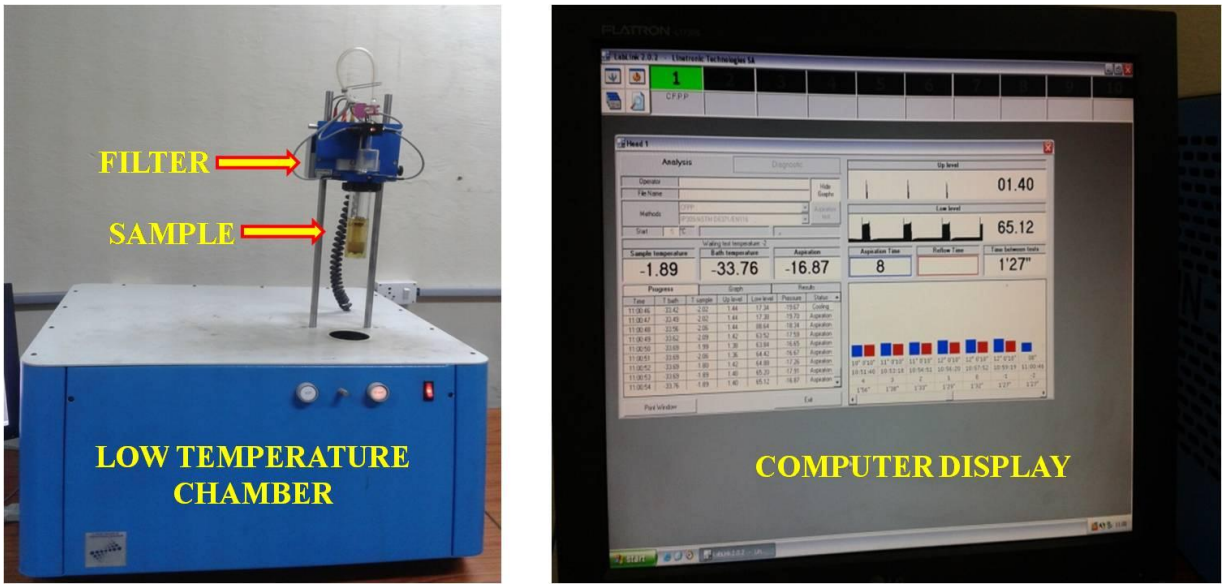

Plate 3.17: Cold flow plugging point apparatus

Cold filter plugging point of biodiesel reflects its cold weather performance. It defines the fuel's limit of filterability. The apparatus for CFPP measurement is shown in Plate 3.17. The measurements were carried out as per the ASTM D6371 05 (2010) standards. All the test samples of SME and KME were subjected to the CFPP test to evaluate the effect with or without pour point depressants. Results were calculated by CFPP apparatus. The cold flow properties may be improved with use of different pour point depressants as shown in Table 3.8.

Table 3.8: Test fuels for CFPP measurement

Biodiesel	**Additives (vol. %)**	**Test Fuel**
SME	-	SME (B100)
	Kerosene	SME + 5% Kerosene
		SME + 10% Kerosene
	EVA	SME + 1% EVA
		SME + 2% EVA
	Lubrizol 7671	SME + 1% Lubrizol 7671
		SME + 2% Lubrizol 7671
	CRISTOL BIO	SME + 1% CRISTOL BIO
		SME + 2% CRISTOL BIO
KME	-	KME (B100)
	Kerosene	KME + 5% Kerosene
		KME + 10% Kerosene
	EVA	KME + 1% EVA
		KME + 2% EVA
	Lubrizol 7671	KME + 1% Lubrizol 7671
		KME + 2% Lubrizol 7671
	CRISTOL Bio	KME + 1% CRISTOL BIO
		KME + 2% CRISTOL BIO

The cold flow properties of biodiesel can be improved using various strategies. Studies related to two common strategies, dilution and addition of polymer additives are presented below. Dilution lowers the freezing point of biodiesel constituents. It is noted that freezing point is visually observed as the onset of crystal formation, which was distinct from the pour point. The purpose of the solvent evaluation is to outline which aspects of dilution are the most relevant.

In the present work four additives are used as viscosity modifier and pour point depressants to improve CFPP of both biodiesels. Therefore kerosene, EVA, Lubrizol and CRISTOL were used as pour point depressants and 18 test samples were prepared for investigation as shown in Table 3.8. Kerosene used as extender 5% and 10% whereas other PPDs were used 1% and 2% as additive.

3.11.16 Oxidation Stability

Oxygen in the surrounding atmosphere causes a chemical reaction to take place within fuels overtime. During autoxidation, unsaturated fatty acids undergo radical reactions in which decomposition products are formed such as peroxides as the primary oxidation products and alcohols, carboxylic acids, and aldehydes as the secondary oxidation products. In the present investigation, the oxidation stability index (hours) was measured by the induction period of the sample due to electric conductance of the peroxides formed by bubbling oxygen from the water source system flowing at 10L/hour in the biodiesel Rancimat 873 shown in the Plate 3.18. The standard for the measurement was EN14112.

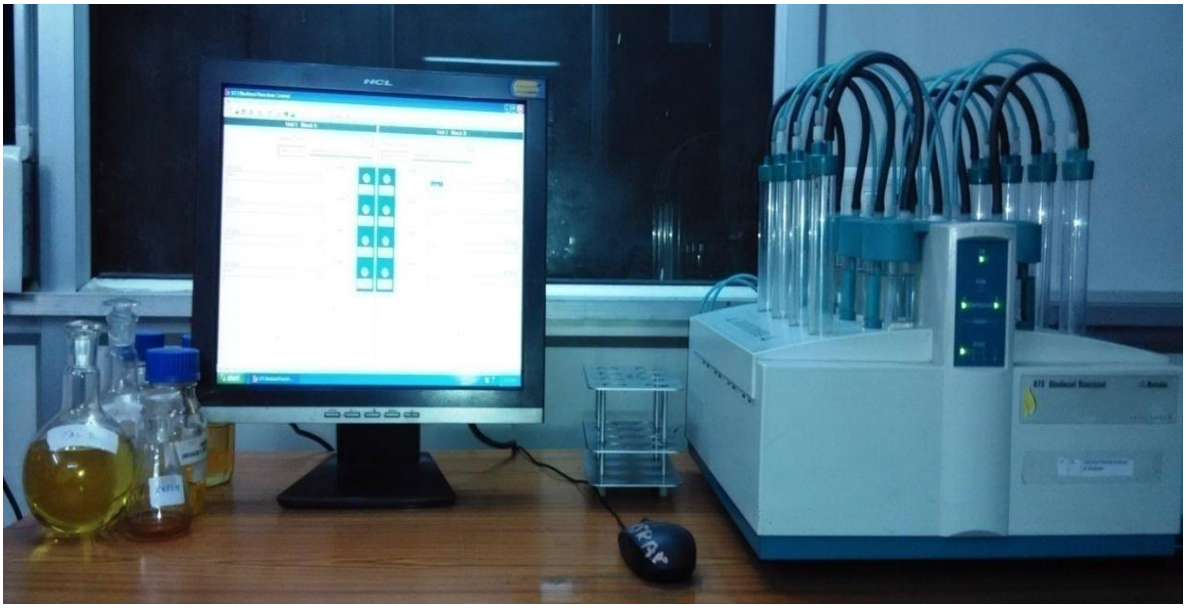

Plate 3.18: Biodiesel Rancimat

3.12 Long Term Storage Stability Test

In the present study two additives (ECOTIVE and TBHQ) were used to access the long term storage stability of biodiesel on physico chemical properties. Both biodiesels were doped with 0.1% and 0.5% (by weight) concentration of ECOTIVE and TBHQ and 10 test samples (Table 3.9) were prepared.

Table 3.9: Test fuels for long term storage stability study

Biodiesel	**Additives (wt. %)**	**Test Fuel**
SME		SME
	ECOTIVE	SME + 0.1% ECOTIVE
		SME + 0.5% ECOTIVE
	TBHQ	SME + 0.1% TBHQ
		SME + 0.5% TBHQ
KME		KME
	ECOTIVE	KME + 0.1% ECOTIVE
		KME + 0.5% ECOTIVE
	TBHQ	KME + 0.1% TBHQ
		KME + 0.5% TBHQ

Plate 3.19 SME and KME fuel samples for storage stability test

For experimental accuracy, each sample was placed in three air-tight glass bottles and considered the mean value for observation and analysis. Therefore 30 test samples (air-tight glass bottles) were used to investigate the biodiesel for a period 1 year. All SME and KME samples (with and without additive) were periodically evaluated on monthly basis for peroxide value, density, acid number, viscosity and calorific value for a storage period of one year. Test samples of long term storage stability are shown in Table 3.9 and Plate 3.19.

3.13 Selection of Diesel Engine

As indicated earlier, single cylinder and light duty diesel engine was chosen for experimental trials because of a number of reasons. Firstly, such engines used anywhere, are an integral part of rural agrarian economy of India and thirdly are actively running across the country. A single cylinder, four stroke, vertical, light duty, water cooled, diesel engine of Kirloskar make was chosen for the present engine trials. Plate 3.24 shows the engine.

The cylinder was made of cast iron and fitted with a hardened high-phosphorus cast iron liner. The lubrication system used in this engine was wet sump type and oil was delivered

to the crankshaft. The inlet and exhaust valves were operated by an overhead camshaft driven from the crankshaft through two pairs of bevel gears. The fuel pump was driven from the end of camshaft. The detailed specification of the engine is provided in Table 3.8.

Plate 3.20: Test Engine

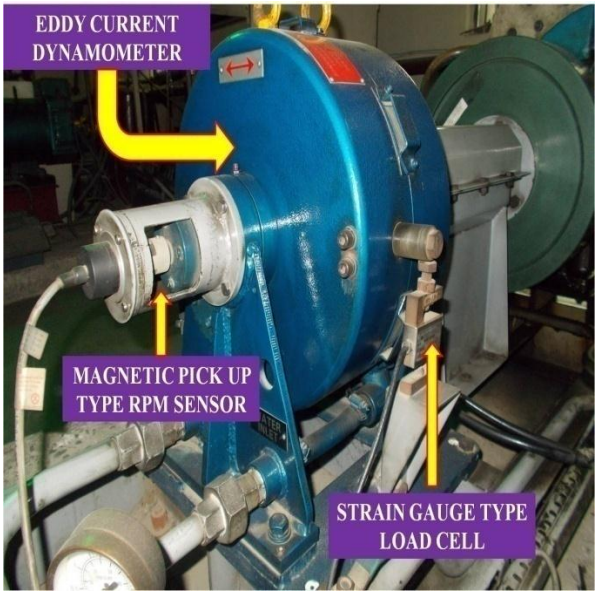

Plate 3.21: The eddy current dynamometer with load and rpm sensor

Table.3.10 Test Engine Specification

Make	**Kirloskar**
No. of cylinder	1
Strokes	4
Rated Power	3.5 kW@1500rpm
Cylinder diameter	87.5mm
Stroke length	110mm
Connecting rod length	234mm
Compression ratio	17.5:1
Orifice diameter	20mm
Dynamometer arm length	185mm
Inlet Valve Opening	4.5°BTDC
Inlet Valve Closing	35.5°ABDC

Exhaust Valve Opening	35.5°BBDC
Exhaust Valve Closing	4.5°ATDC
Fuel injection timing	23^0BTDC
No. of injector holes	3
Nozzle diameter	0.148 mm
Spray orientation angle	55°CA
Injection duration	18°CA

A high precision stain gauge type load cell was attached to the dynamometer to accurately transmit the engine loading. A magnetic pick up type rpm sensor was attached at the end of the dynamometer to measure rpm. The eddy current type dynamometer, the magnetic pick up type rpm sensor and the strain gauge type load cell are shown in Plate 3.21. The cooling water flow for the engine was 350 Liters/hour and that of the dynamometer was 120 Liters/hour. The flow of the cooling water was controlled by two numbers of rotameters, one for the engine and other for the dynamometer.

Two fuel tanks for diesel and the other tank are meant for the biodiesel/diesel blends were provided. The cyclic variation of combustion pressure and the corresponding crank angle was recorded using a "Kubeler" piezoelectric transducer, with low noise cable, mounted into the engine head. The pressure transmitter contained piezoelectric sensor and charge amplifier. The maximum resolution of the pressure sensor was 1°CA. For exhaust gas temperature measurement, Chrome-Alumel K-Type thermocouples were employed close to the engine exhaust manifold. Air flow rate was measured using a mass airflow sensor.

Fuel consumption rate was measured by 20cc burette and stop watch with level sensors. Fuel flow rate, air flow rate, load, rpm, pressure crank angle history and temperature data were fed to a centralized data acquisition system NI USB-6210, 16-bit. Various measuring sensors of engine test rig like data acquisition system, air sensor, fuel pump, pressure transducer and thermocouple are shown in Plate 3.22. A personal computer with a

software package "Enginesoft" was connected to the data acquisition system for online and subsequent offline analysis.

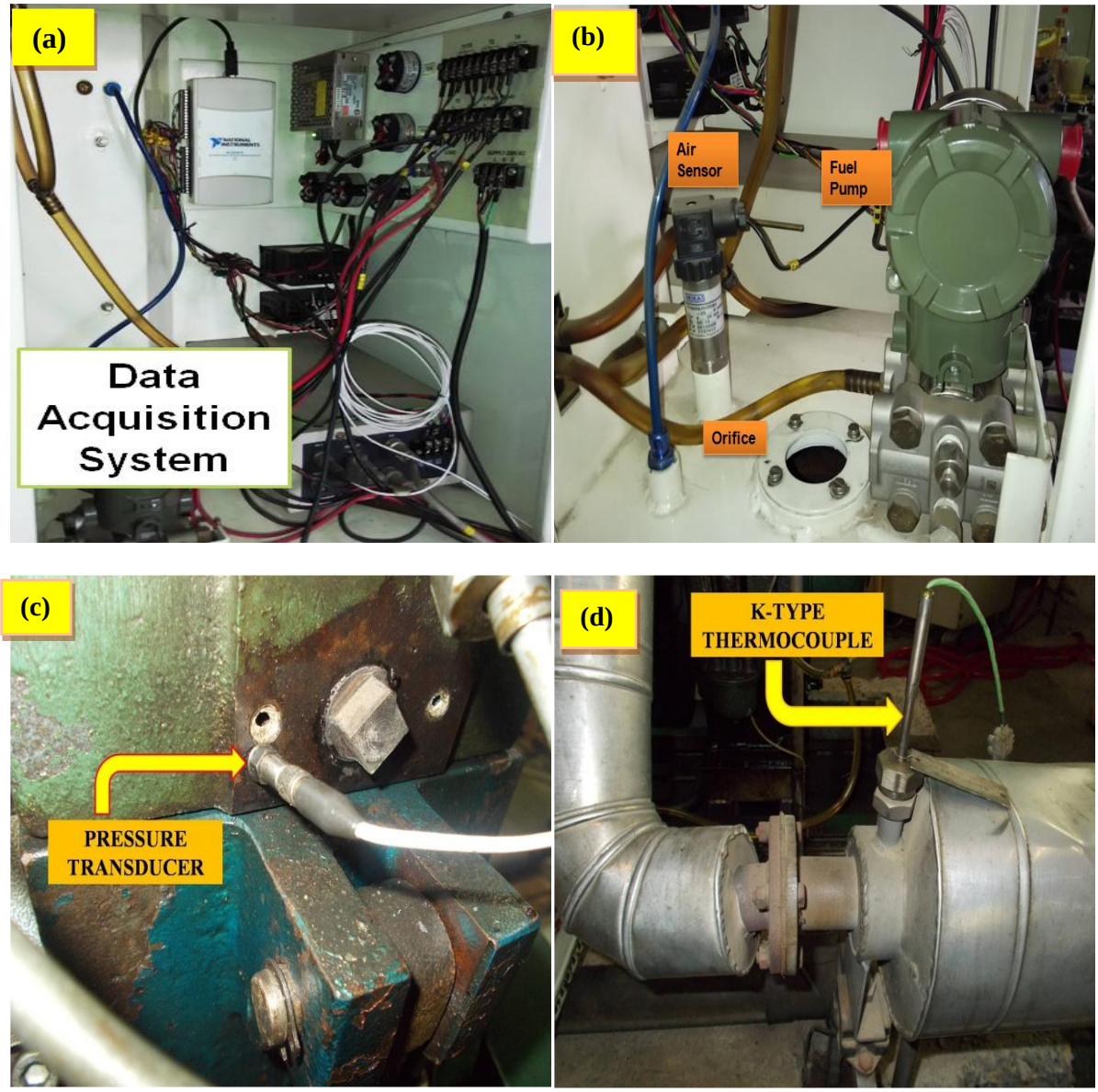

Plate 3.22: Various measuring sensors of engine test rig

Footnote: (a) - Data acquisition system; (b) - Air sensor and Fuel pump; (c) - Pressure transducer and (d) - 'K'-type thermocouple

The control panel (Plate 3.23) of the engine test rig comprised of the data acquisition system, burette for fuel measurement, "U" tube manometer for air measurement, sensor indicator for manual data access, load variation switch etc.

The control panel was used for loading and unloading the engine. Besides, the air and fuel consumption data of the sensor was verified from the manual measurements. The data acquisition system inside the control panel received the signals and transmitted them to the computer.

The major pollutants in exhaust of a diesel engine are the oxides of nitrogen, smoke opacity, unburnt hydrocarbons, carbon monoxide, carbon dioxide, etc. For measuring the smoke opacity, AVL 437 smoke meter was utilized as shown in Plate 3.24 and technical specifications are shown in Appendix I.

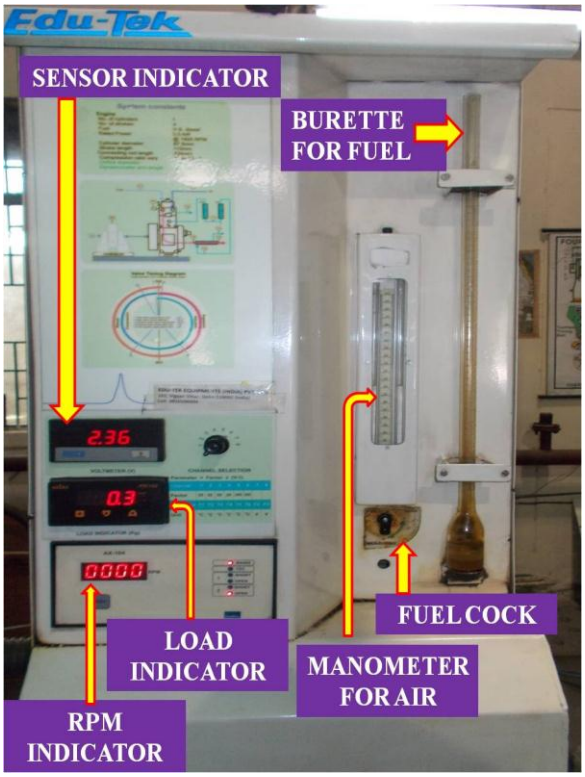

Plate 3.23: The Control Panel

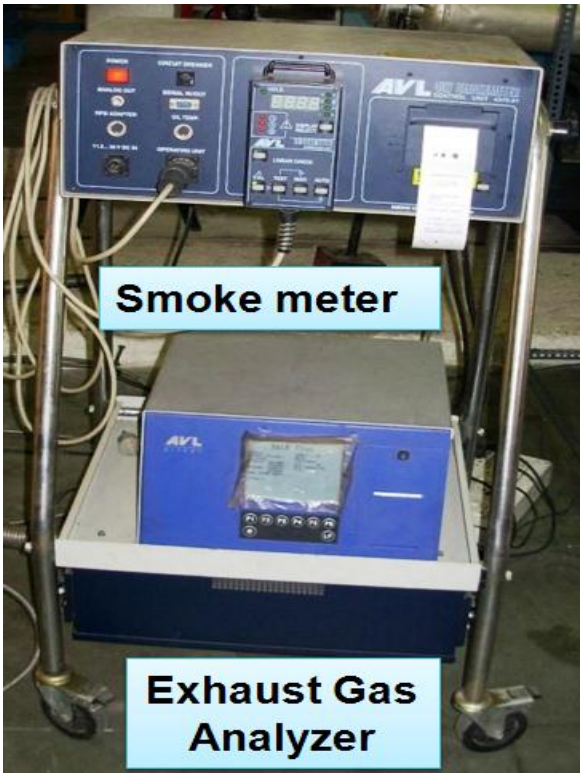

Plate 3.24 Exhaust gas analyzer and smoke meter

A light beam projected across a flowing stream of exhaust gases, a certain portion of light is absorbed or scattered by the suspended soot particles in the exhaust. The remaining portion of the light falls on a photocell, generating a photoelectric current, which is a measure of smoke density. The technical detailed specifications have been given in Appendix II. AVL

4000 Light Di-Gas Analyzer (Plate 3.24) was used for measurement of exhaust emissions like total hydrocarbon, carbon monoxide, carbon dioxide and oxides of nitrogen. The gas analyzer was connected to the engine exhaust by means of probes and the smoke meter was extension pipe.

Plate 3.25: Actual engine test rig

The final experimental test setup consisted of the CI engine, engine cooling water system, the fuel supply and measurement system, air supply and measurement system, load variation and measurement system, rpm measurement system, in-cylinder pressure measurement system, emission measurement system, digital data acquisition system and

computer. Plate 3.25 shows actual engine test rig and Figure 3.9 shows the schematic engine test rig lay out comprising of individual components and their inter-connectivity.

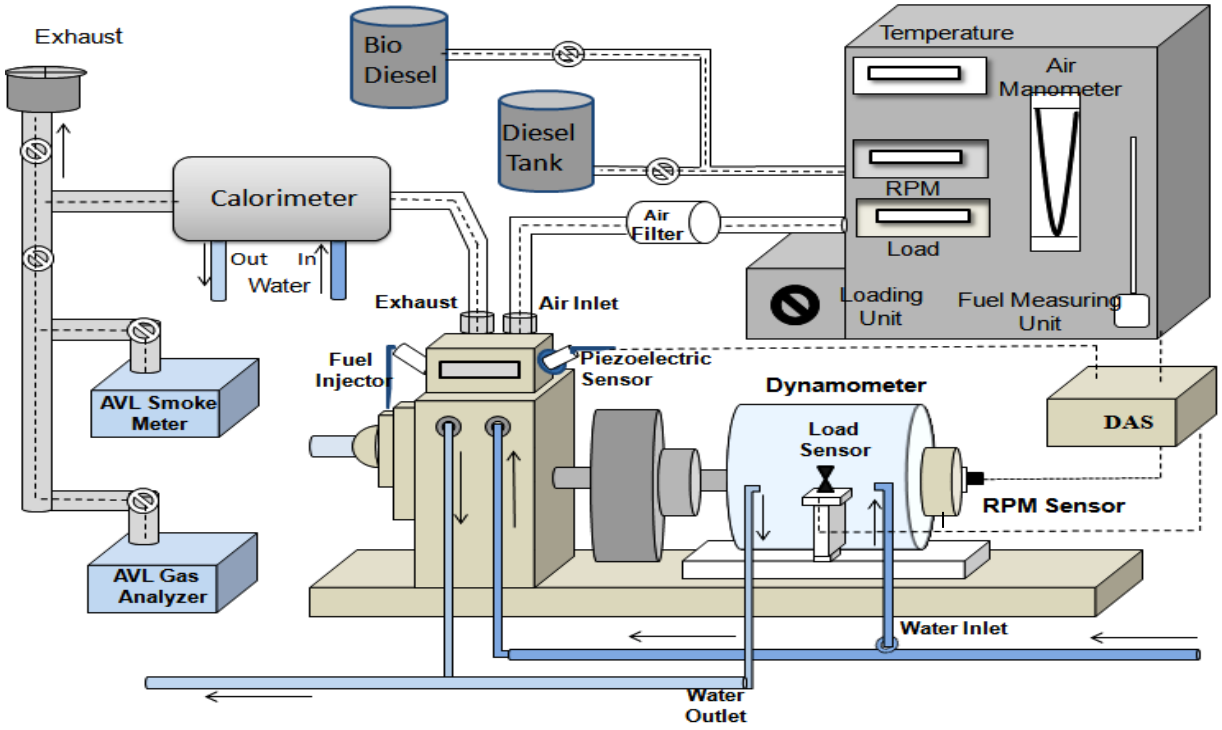

Figure 3.9: Layout of engine test rig

3.14 Selection of Engine Test Parameters

The selections of appropriate test parameters are vital part of engine research. The engine test was done as specified by IS: 10000. The main parameters desired from the engine were selected. Various engine parameters are observed and the calculated parameters.

Observed parameters are enlisted below.

1. Engine load.
2. Engine speed.
3. Fuel consumption rate.
4. Air flow rate.
5. In-cylinder pressure.

6. Emissions of CO, CO_2, NO_x, THC.
7. Exhaust temperature.
8. Smoke opacity.

Calculated parameters are given below.

1. Brake mean effective pressure (BMEP).
2. Brake thermal efficiency (BTE).
3. Brake specific energy consumption (BSEC).
4. Mass fraction burnt rate (MFB).
5. Pressure rise rate (PRR).
6. Heat release rate (HRR).

3.15 Measurement Methods and Calculations

As already elaborated, the main components of the experimental setup are two fuel tanks (Diesel and Biodiesel), fuel consumption measuring unit, air flow rate measuring unit, eddy current dynamometer for loading arrangement, RPM meter, temperature indicator, in-cylinder pressure sensor and emissions measurement equipments. While carrying out the experiment the engine was always started with diesel and allowed to run for 30 minutes for warm up. For baseline diesel data, the observations were taken only after the prescribed 30 minutes were complete. For biodiesel blends the fuel line was swapped, after the warm up period with neat diesel, allowing the biodiesel tank to connect to the engine for taking observations. The load on the engine shaft was varied using the eddy current dynamometer.

3.15.1 Measurement of brake power and brake mean effective pressure

The brake power (BP) at the engine shaft was calculated by the formula in equation 3.12.

$$\text{BP (kW)} = \frac{2\ X\ \pi\ X\ rpm\ X\ Load\ (Kg) X\ 9.81\ X\ Dynamometer\ arm\ length\ (m)}{60\ X\ 1000} \quad (3.12)$$

Similarly the brake mean effective pressure (BMEP) was calculated using the formula in equation.3.13.

$$\text{BMEP (bar)} = \frac{120\ X\ BP\ (kW)}{L\ X\ A\ X\ N\ X\ 101.325} \quad (3.13)$$

Where L = Stroke length in meter; A = Piston area in m^2; N = Engine rpm.

The rated power of the engine was 3.5 kW. However, after re-calibration it was found that the engine hardware was able to operate smoothly up to 4.7 kW at 1500 rpm. With the dynamometer arm length of 0.185 meter, it was calculated that 17.3 Kg corresponded to 100% of the engine load and 0.3Kg was equivalent to the zero load. Therefore, various loads applied to the engine were 0.3Kg, 3.7Kg, 7.1Kg, 10.8Kg, 14.5Kg and 17.3Kg corresponding to the loads of 0%, 20%, 40%, 60%, 80% and 100% of the calibrated load. All performance, emission and combustion data were recorded at each load for various test fuels.

On the basis of the above calculation, the brake power at 0%, 20%, 40%, 60%, 80% and 100% loads were 0.087kW, 1.056kW, 1.99kW, 3.01kW, 3.99kW and 4.71kW respectively where as the BMEP were calculated to be 0.13 bar, .53 bar, 2.88 bar, 4.36 bar, 5.77 bar and 6.82 bar in the same order.

3.15.2 Measurement of fuel flow

The fuel consumption of an engine is measured by determining the time required for consumption of a given volume of fuel. The mass of fuel consumed can be determined by multiplication of the volumetric fuel consumption to its density. In the present set up volumetric fuel consumption was measured using a fuel flow sensor inserted inside the control panel. The sensor signal was fed to the data acquisition system. The sensor data in

many cases was validated by manually taking the time for 20cc fuel consumptions in the burette by blocking the fuel cock. However, it was observed that the fuel sensor data was more precise.

Two important engine performance parameters i.e. BTE and BSEC were determined from the rate of fuel flow as shown below. BTE is the ratio of brake power to the product of mass flow rate of fuel and its heating value. The BTE is calculated by the formula mentioned in equation 3.14.

$$\text{BTE (\%)} = \frac{\text{BP (kW)}}{m^* \text{ x Qcv}} \qquad (3.14)$$

Where m* = Mass flow rate of fuel in (Kg/s); Qcv = Calorific value of fuel (kJ/Kg)

Brake specific energy consumption is the amount of fuel energy consumed in order to generate one unit of shaft power. It is calculated by the formula mentioned in equation 3.15.

$$\text{BSEC (MJ/kWh)} = \frac{\mathbf{m^* X Qcv X 3600}}{\mathbf{BP(kW)}} \qquad (3.15)$$

3.15.3 Measurement of RPM

A magnetic pick up type rpm sensor was attached to the end of the dynamometer shaft which was toothed. This type of sensor consists of a permanent magnet, yoke, and coil. This sensor was mounted close to a toothed gear. As each tooth moved by the sensor, an AC voltage pulse was induced in the coil. Each tooth produced a pulse. As the gear rotated faster more pulses were produced. These impulse signals were fed digitally to the data acquisition system. The engine control module of the data acquisition system calculated the engine rpm which was subsequently displayed both in the control panel and the enginesoft database in the computer. The rpm sensor is already shown in Plate 3.21.

3.15.4 Exhaust temperature and emission measurement

Chromel-Alumel K-type thermocouples (Plate 3.22 (d)) were connected to a six-channel digital panel meter to measure temperatures of exhaust gas. The meter was calibrated by a millivolt source up to 800^{o} C. The sensor was placed close to the exhaust manifold of the engine. The temperature data was observed both at the sensor indicator in the control panel as well as the engine-soft database.

As discussed above the gaseous pollutant emissions were measured using the gas analyzer and the smoke meter. The emission data was collected manually from the printed results of the analyzers as well as the engine-soft database from the computer.

3.15.5 Measurement of air flow

The air flow was measured using air sensor (turbine type flow meter) installed inside the control panel. Plate 3.22 (b) shows the sensor in the previous sections. In principle, the turbine flow meters use the mechanical energy of the fluid to rotate a “pinwheel” (rotor) in the flow stream. Blades on the rotor are angled to transform energy from the flow stream into rotational energy. The rotor shaft spins on bearings. When the fluid moves faster, the rotor spins proportionally faster. Blade movement is often detected magnetically, with each blade or embedded piece of metal generating a pulse. The transmitter processes the pulse signal to the data acquisition system that determines the flow of the fluid. The air flow data was available in the sensor indicator of the control panel and the enginesoft database. Moreover, there was another method available to validate the sensor data. It was based on the orifice and the air box method.

The differential pressure across the orifice inserted in the air flow channel provides the air flow rate using the formula in equation 3.16.

$$\text{Mass of air (m)} = C_d \text{ X A X } \sqrt{(2gh_w\rho_w\rho_a)} \qquad (3.16)$$

Where C_d = Co-efficient of discharge of orifice (0.6 in the present case); A = Orifice area; g = Acceleration due to gravity; h_w = Height of water column; ρ_w/ρ_a = Density of water/air

3.15.6 In-cylinder pressure measurement

As discussed in the earlier sections, the "Kubeler" piezoelectric transducer was used for in-cylinder pressure measurement. Plate 3.22 (c) shows the pressure transducer. The signals from the charge amplifier were fed to the data acquisition system where the engine control module converted the signals into digital data. The in-cylinder pressure data in terms of pressure – crank angle history was only obtained in the enginesoft database. In the present study the average of 91 cycles were considered for analysis of in-cylinder pressure crank angle data.

3.16 Characterization of Heat Release Rate

Evaluation of cyclic heat release is very much significant for combustion study. Various heat release models have been proposed by researchers for determining critical combustion parameters like heat release rate, pressure rise rate etc. In the present investigation, the heat release calculations described by Rakopoulos [240] was referred. Although combustion in a CI, DI (compression-ignition, direct-injection) engine is quite heterogeneous, the contents of the combustion chamber are assumed to be homogeneous in the method suggested by Sorenson [241]. This type of heat release model is generally termed as zero-dimensional model in the literature. In the light of the above fact, the zero dimensional model proposed by Sorenson was considered for combustion characterization.

The Sorenson's model [242,243] is a thermodynamic model based upon energy conservation principle. Neglecting the heat loss through piston rings [244] the energy balance inside the engine may be written as (eqn.3.17):

$$\frac{dQ}{d\theta}-\frac{dQw}{d\theta} = \frac{d(\text{mu})}{d\theta} + P\frac{dV}{d\theta} = mC_v\frac{dT}{d\theta} + P\frac{dV}{d\theta} \quad (3.17)$$

Where: $dQ/d\theta$ = Rate of net heat release inside the engine cylinder (J/°CA); $dQ_w/d\theta$ = Rate of heat transfer from the wall (J/°CA); m = Mass flow of the gas (Kg); u = Internal energy of the gas (J/Kg); P = Cylinder pressure (bar); V = Gas volume (m^3); θ = Crank angle (°); T = Gas temperature (°K); C_v = Specific heat at constant volume (J/Kg°K)

Now the ideal gas equation is given by $PV = mRT$ (3.18)

Where R = Universal gas constant

The derivative of univerSal gas equation with respect to crank angle is given by

$$P\frac{dV}{d\theta} + V\frac{dP}{d\theta} = mR\frac{dT}{d\theta} \quad (3.19)$$

Putting equation (3.19) in equation (3.17), the heat release rate is derived as follows.

$$\frac{dQ}{d\theta} = P\frac{Cp}{R}\frac{dV}{d\theta} + V.\frac{Cv}{R}\frac{dP}{d\theta} + mT\frac{dCv}{d\theta} + \frac{dQw}{d\theta} \quad (3.20)$$

Where C_p = Specific heat at constant pressure (J/Kg°K)

Equation (3.20) is further simplified for actual heat release calculation and is given below.

$$\frac{dQ}{d\theta} = \frac{1}{\gamma-1}\left(V\frac{dP}{d\theta} + \gamma P\frac{dV}{d\theta}\right) - \frac{dQw}{d\theta} \quad (3.21)$$

Where γ = ratio of specific heats

In a four-stroke engine, crank angles are typically given with zero values at the TDC, (top dead center) between the intake and exhaust strokes. However, the important heat release events occur between SOI (start of injection, typically about 337°) and EVO (exhaust valve opening, typically about 500°).

The trigonometric functions require their arguments in radians that are essential for gas volume calculations. The formula for calculating the arguments for the trigonometric functions, equation 3.22 was used.

$$\theta_{rad} = \frac{\pi(\theta - 360 + Phase)}{180} \qquad (3.22)$$

Where: θ_{rad} = argument of trigonometric functions (radians); Phase = phase shift angle (°CA)

The piston displacement was needed in calculating the gas volume. It is provided in equation 3.23.

$$\frac{S}{R} = [1 - \cos(\theta_{rad})] + \frac{L}{R}\{1 - [\sqrt{1 - \frac{\sin(\theta rad)}{L/R}}]^2\} \qquad (3.23)$$

Where: S = piston displacement from TDC (m); R = radius to crank pin (m); L = connecting rod length (m)

Then the gas volume was calculated as in the equation 3.24

$$V = V_{cl} + S\,A_p \qquad (3.24)$$

Where: A_p = top area of piston (m^2) = $\pi(bore)^2/4$; bore = cylinder bore (m); V_{cl} = clearance volume (m^3); r = compression ratio; Stroke = piston stroke (m)

The combustion chamber wall area, needed for heat transfer calculations, was given in the equation 3.25.

$$A_{wall} = 2A_p + \pi\,(bore)\,S \qquad (3.25)$$

Equation 3.25 ignores the area associated with the piston cup, but the approximation has little effect on the heat release results.

The heat release equation (3.21) requires the calculation of $dP/d\theta$. It can be shown that the slope at the j^{th} point of the curve defined by n sequential points is as shown in equation 3.25.

$$\frac{dPj}{d\theta} = \frac{n\Sigma(Pi\theta i) - \Sigma Pi\ \Sigma\theta i}{n\Sigma(\theta i)2 - (\Sigma\theta i)2} \qquad (3.26)$$

Where n is an odd number and each summation is from [j – (n – 1)/2] to [j + (n – 1)/2].

When a shaft encoder is used to trigger pressure measurements, the points are equally spaced along the θ axis at spacing Δθ. The choice of n is a compromise; a larger n helps to combat noise in the pressure data, but may also obscure real changes in the heat release curve. In the present case with Δθ = 1°, choice of n = 7 was found to fit the equation 3.15 over 4° of the pressure trace and was a suitable compromise. Equation 3.27shows the pressure smoothing technique applied to the noise in pressure data.

$$P_{j+1} = P_j + \frac{dPj}{d\theta}\Delta\theta \qquad (3.27)$$

Calculation of dV/dθ was accomplished as per the equation 3.28.

$$\frac{dVj}{d\theta} = V_j - V_{j-1} \qquad (3.28)$$

In-cylinder gas temperature varies rapidly throughout the cycle. Consequently the value of γ varies with temperature. The ideal gas law was used to calculate the spatially averaged temperature in the combustion chamber as mentioned in the equation 3.29.

$$T_j = \frac{PjVj}{MRg} \qquad (3.29)$$

Where: T_j = bulk gas temperature at point j (°K); R_g = idea gas constant = 8.314/29 = 0.287; M = mass of charge, g = (1 + AF) mf; AF = air/fuel ratio of engine; m_f = mass of fuel injected into each engine cycle (g)

3.17 Calculation of Mass Fraction Burnt

Mass fraction burned (MFB) in each individual engine cycle is a normalized quantity with a scale of 0 to 1, describing the process of chemical energy release as a function of crank angle. The determination of MBF is commonly based on burn rate analysis – a procedure developed by Rassweiler and Withrow [243]. It is still widely used because of its relative simplicity and computational efficiency, despite the approximate nature of this method [245].

The Rassweiler and Withrow procedure is based on the assumption that, during engine combustion, the pressure rise Δp_j (at crank angle increment) consists of two parts: pressure rise due combustion (Δpc_j) and pressure change due to volume change (Δpv_j).

$$\text{Therefore, } \Delta p_j = \Delta pc_j + \Delta pv_j \qquad (3.30)$$

Assuming that the pressure rise Δpc_j is proportional to the heat added to the in-cylinder medium during the crank angle interval, the mass fraction burned at the end of the considered j^{th} interval may be calculated as [245].

$$\text{MFB} = \frac{mb\ (i)}{mb\ (total)} = \frac{\Sigma_0^i \Delta Pc}{\Sigma_0^N \Delta Pc} \qquad (3.31)$$

Where N is the total number of crank angles in the in-cylinder pressure ~ crank angle data

The cumulative heat release was calculated by summing up the heat release per crank angle data throughout the cycle. The pressure rise rate for various test fuels were calculated from the spread sheet data base using equation (3.27) and (3.28). The mass fraction burnt was calculated from equation (3.31). Ignition delay for the test fuels were calculated as the difference between the fuel injection angle and the crank angle corresponding to the MFB of 0.05. Similarly the total combustion duration for the test fuels was calculated as the difference between the crank angles corresponding to MFB of 0.10 to MFB of 0.95.

3.18 Procedures for Engine Trial

The engine was started at no load by pressing the exhaust valve with decompression lever and it was released suddenly when the engine was hand cranked at sufficient speed. After feed control was adjusted so that engine attained rated speed and was allowed to run (about 30 minutes) till the steady state condition was reached and the exhaust gas temperature corresponding to that load stabilized. The enginesoft software was connected to the data acquisition system and allowed to run. Automatic data entry system was activated and the

resolutions of various sensors were set. All the sensors were allowed to perform at their minimum resolutions. For pressure crank angle history the average of 91 cycles were chosen for each load where as for performance and emission studies the average of 10 consecutive data was chosen to minimize error.

To validate the sensors, and the electronic gadgets, the time for 20 cc fuel consumption and the manometric readings of air consumption were taken repeatedly and averaged several times. The manual data so obtained was compared with the "enginesoft" data and found very close to each other. Similarly, data in the printed copies of emission analyzers were often compared with the emission data of the enginesoft database and found all most identical.

All the performance, emission and combustion parameters were evaluated at each load thoroughly. Many times the trial was repeated to avoid any discrepancy in results. As mentioned earlier, for baseline data, diesel tank was used and thereafter for blends the biodiesel tank was used by swapping the fuel line by the rotary valve. Every time the engine was started with diesel and stopped after running at least 20 minutes on diesel.

3.19 Accuracies and Uncertainties of Measurements

Table 3.9 shows the accuracies and uncertainties associated with various measurements. It may be observed that all of the measurements exhibited higher accuracy. The repeatability of all measurements were checked throughout the experimental trial and found sufficiently close.

It may be noted that the various measured properties like kinematic viscosity, density, calorific value, oxidative stability, flash point, acid value, peroxide value, fatty acid profile, elemental analysis etc. observed thrice and consider the average value for analysis. Observed values were identical because equipment had high precision and regularly calibrated.

Therefore, the % uncertainties in these equipments were very low. For viscosity, density, calorific value and cold flow plugging point the % uncertainty was less than 0.1%. The repeatability of these equipments were checked and found highly satisfactory.

Table.3.9: Accuracies and uncertainties of measurements

S.N.	Measurements	Measurement Principle	Range	Accuracy
1	Engine load	Strain gauge type load cell	0-25 Kg	±0.1Kg
2	Speed	Magnetic pick up type	0-2000 rpm	±20 rpm
3	Time	Stop watch	--	±0.5%
4	Exhaust Temperature	K-type thermocouple	0-1000°C	$\pm 1^0$C
5	Carbon monoxide	Non-dispersive infrared	0-10% vol.	±0.2%
6	Carbon dioxide	Non-dispersive infrared	0-20% vol.	±0.2%
7	Total hydrocarbons	Non-dispersive infrared	0-20,000 ppm	±2 ppm
8	Oxides of nitrogen	Electrochemical	0-4000 ppm	±15ppm
9	Smoke	Photochemical	0-100%	± 2%
10	Crank angle encoder	Optical	0-720 °CA	$\pm 0.2^0$CA
11	Pressure	Piezoelectric	0-200 bar	± 1 bar
	Calculated results			**Uncertainty**
12	Engine power	--	0-8 kW	±1.0%
13	Fuel consumption	Level sensor	--	±2.0%
14	Air consumption	Turbine flow type	--	±1.0%
15	BTE	--	--	±1.0%
16	BSEC	--	--	±1.5%
17	Heat release	Sorenson model	--	±5.0%
18	In-cylinder temp.	Ideal gas equation	Up to 3000°K	±5.0%

CHAPTER 4

RESULTS AND DISCUSSION

This chapter discusses the results of investigations. Firstly, the chapter focused on physico chemical properties of pure Sal and Kusum oils. Further it describes the biodiesel production and optimized the process parameters using the RSM. Furthermore, the results of physico chemical properties of both biodiesel SME and KME are analyzed. Subsequently, this chapter discusses the effects of additives on long term storage stability and CFPP. Chapter also enlightens engine trials of the SME and KME with diesel blends. Detailed discussion on engine trials have been carried out to evaluate engine performance, emission and combustion characteristics of biodiesel-diesel and compare with baseline diesel. A single cylinder four stroke diesel engine (Kirloskar- TV1) is used for current research.

4.1. Analysis of Straight Vegetable Oils (Sal and Kusum)

Vegetable oils are water insoluble, hydrophobic substances of plant and animal origin, which are primarily composed of the fatty esters of glycerol, i.e. triglycerides. Furthermore, composition of vegetable oil greatly change (fatty acid profile) because of the storage conditions and local climatic conditions [246]. Hydrocarbon chain of fatty acids is different in chain length and number of double bonds. Free fatty acids play vital role during the biodiesel production process which lead to formation of soap and water [188]. Results indicated that the FFA content of the vegetable oils increased with duration of storage of seeds/oils and led to degeneration of the quality of vegetable oils, having an adverse impact on the properties of the vegetable oils and biodiesel. To deal with these parameters, there is the need to produce biodiesel from low or medium quality vegetable oils, which have high FFA content [247].

The main findings of physico-chemical properties and fatty acid composition of sal, Kusum and Jatropha oil have been illustrated in Table 4.1 and Table 4.2 respectively. These properties have been compared with Jatropha oil. Jatropha oil is the main feedstock for biodiesel production by National Biodiesel Mission of Government of India.

Table 4.1- Physico chemical properties of Sal oil, Kusum oil and Jatropha oil.

S. No.	**Property**	**Saloil**	**Kusum oil**	**Jatropha oil**
1	Kinematic viscosity (mm^2/s) at 40°C	52.6	40.97	48.09
2	Kinematic viscosity (mm^2/s) at 100°C	10.36	10.32	9.10
3	Dynamic viscosity (mpa.s) at 40°C	46.81	37.76	43.55
4	Viscosity Index (VI)	191.00	254.00	174.10
5	Flash Point (°C)	225.50	185.50	258.50
6	Density (g/cm^3) at 15°C	0.89	0.92	0.91
7	Acid Value (mg KOH/g)	3.36	16.20	17.63
8	Cold filter plugging point (°C)	38.00	15.00	21.00
9	Calorific value (MJ/kg)	39.18	38.47	38.98
10	Copper strip corrosion (3h at 50°C)	1a	1a	1a
11	Oxidation stability (h at 110°C)	4.15	0.16	0.32
12	p^H at 26°C	6.14	4.12	4.83

Physico chemical properties of the Sal oil and Kusum oil are similar to Jatropha oil. Sal oil has less acid value (3.36 mg KOH/g), good calorific value (39.18 MJ/kg) and oxidation stability (4.15 hours). From the fatty acid composition, Sal oil had 61% total saturated and 39% unsaturated fatty acids; whereas Kusum oil and Jatropha oil had 31% total saturated and 69% unsaturated fatty acids. Saturation and unsaturation of the oils have significant impacts on the final biodiesel produced from such oils [160,248,249].

Sal oil is typically composed of mainly C-16 to C-20, where 61% saturated and 39% unsaturated of the total mixture. The promising existence of Arachidic acid (C-20) and Stearic

acid (C-18) improved its cetane number and ignition quality as well as these monosaturated compounds made it highly susceptible to cold flow property [250,251]. The major composition of Kusum oil was unsaturated acids like oleic acid (49.29%) and Eicosenoic acid (18.19%). So it exhibited low CFPP (15 ^{o}C) and flash point (185.5 ^{o}C) with better viscosity index but poor oxidation stability (0.16 hours).

Table 4.2- Fatty acid composition of Sal, Kusum and Jatropha oils

Fatty Acid	**Chemical formula**	**C:H Ratio**	**Fatty Acid Methyl Ester**	**Chemical formula**	**Sal Biodiesel**	**Kusum Biodiesel**	**Jatropha Biodiesel**
Myristic acid	$C_{14}H_{28}O_2$	C14	Myristic acid methyl ester	$C_{15}H_{30}O_2$	8.764	-	-
Palmitic acid	$C_{16}H_{32}O_2$	C16	Hexadecanoic acid methyl ester	$C_{17}H_{34}O_2$	6.86	9.89	19.15
Palmitoleic acid	$C_{16}H_{30}O_2$	C17:1	9-Hexadecenoic acid methyl ester	$C_{17}H_{32}O_2$	-	-	1.99
Stearic acid	$C_{18}H_{36}O_2$	C18	Octadecanoic acid methyl ester	$C_{19}H_{38}O_2$	28.33	3.63	10.16
Oleic acid	$C_{18}H_{34}O_2$	C18:1	cis-9-Octadecenoic acid methyl ester	$C_{19}H_{36}O_2$	30.19	49.29	68.26
Linoleic acid	$C_{18}H_{32}O_2$	C18:2	cis-9-cis-12-Octadecadienoic acid methyl ester	$C_{19}H_{34}O_2$	8.78	1.8	-
Arachidic acid	$C_{20}H_{40}O_2$	C20	Eicosanoic acid methyl ester	$C_{21}H_{42}O_2$	16.77	15.27	-
Eicosenoic acid	$C_{20}H_{38}O_2$	C20:1	cis-11 Eicosenoic acid methyl ester	$C_{21}H_{40}O_2$	-	18.19	-
Behenic acid	$C_{22}H_{44}O_2$	C22	Docosanoic acid methyl ester	$C_{23}H_{46}O_2$	-	1.82	-

Convincingly, the oxidative stability and cold flow properties are normally inversely related: geometrical factors that improved oxidative stability. Ester group was the only exception to this relationship, as larger ester tend to improve both cold flow properties and oxidative stability [250]. Table 4.2 depicts fatty acids and their resulting fatty acid methyl esters.

4.2 Optimization of Biodiesel Production

A 2^4 full-factorial CCD for four independent variables at three levels was employed and the total 30 experiments were conducted. Twenty-four experiments were augmented with six replications as the center points to evaluate the pure error [199]. The Design Expert 10.0.3.0 software (academic version) was used for regression and graphical analyses of the data was obtained. The minimum value of the FFA and maximum values of the yield were taken as the responses of the experimental design.

Analysis of variance (ANOVA) was performed on the model to evaluate its fitness. It was observed that optimization of various process parameters for biodiesel production through acid catalyzed esterification followed by base catalyzed transesterification route and was dependent upon the effects of different operating parameters. The parameters which affected the esterification and transesterification are methanol/oil molar ratio, catalyst concentration, reaction time and reaction temperature. The Kusum oil which have higher acid value or FFA (greater than 2) required pre-treatment or two stage process (esterification followed by transesterification); while Sal oil with low required single stage base catalyzed transesterification to produce the biodiesel.

4.2.1 Optimization of acid catalysed esterification

Kusum oil was having FFA of 8% suggesting two stage process to produce biodiesel. In the first stage vegetable oil is reacted with the alcohol (methanol) in presence of acid catalyst (PTSA), till the FFA is reduced below 2%, then it is transesterified in presence of base catalyst (KOH). Methanol was used as alcohol in both steps of the transesterification process.

The model that fitted to the response as suggested by the software was the quadratic model, due to its highest order polynomial with additional terms and the model was not aliased. A total of 30 experiments were performed as indicated by the design matrix (Table 3.4) generated from the software. The results obtained for the analysis of variance (ANOVA) is shown Table 4.3. As discussed in the previous section, concentration of catalyst (A), reaction temperature (B), reaction time (C) and methanol/oil molar ratio (D) were considered as the factors and the % FFA as the response in the esterification stage.

From the results good correlations were obtained with the reduced quadratic model. It may be observed that the p-value was less than 0.0001 while the model F-value of 257.10 was obtained. Since only 0.01% chance that an F-value could occur due to noise. The values of "Prob> F" less than 0.0500 indicated model terms are significant. In this case A, B, C, D, AB, BC, BD, CD, A^2, B^2, C^2, D^2 are significant model terms. The "Lack of Fit F-value" of 0.36 implies the Lack of Fit was not significant relative to the pure error. Insignificant lack of fit suggests model accuracy [252]. All these information outlined the model was statistically significant. On simpler term, the quadratic model could effectively predict, with minimal error, the actual % FFA during large scale esterification of the oil [97].

The predicted R-Squared value was 0.98 and was in reasonable agreement with the "Adj R-Squared" of 0.99. "Adeq Precision" measures the signal to noise ratio. A ratio greater than 4 was desirable. The ratio of 51.97 indicates an adequate signal and can be employed on the response surface to be navigated. The analysis of Variance for esterification is shown in the Table 4.3.

Table 4.3: Analysis of Variance for esterification

Source	**Sum of Squares**	**Degree of freedom**	**Mean Square**	**F Value**	**p-value Prob> F**	
Model	57.99	14	4.14	257.10	< 0.0001	Significant
A-Catalyst Concentration	*3.57*	*1*	*3.57*	*221.78*	*< 0.0001*	
B-Reaction Temperature	*11.07*	*1*	*11.07*	*687.18*	*< 0.0001*	
C-Reaction Time	*1.71*	*1*	*1.71*	*105.94*	*< 0.0001*	
D-Molar Ratio	*1.93*	*1*	*1.93*	*119.59*	*< 0.0001*	
AB	*0.75*	*1*	*0.75*	*46.44*	*< 0.0001*	
AC	*6.400E-003*	*1*	*0.006*	*0.40*	*0.5380*	
AD	*0.011*	*1*	*0.011*	*0.68*	*0.4211*	
BC	*0.25*	*1*	*0.25*	*15.52*	*0.0013*	
BD	*0.80*	*1*	*0.80*	*49.72*	*< 0.0001*	
CD	*0.81*	*1*	*0.81*	*50.28*	*< 0.0001*	
A^2	*19.12*	*1*	*19.12*	*1187.08*	*< 0.0001*	
B^2	*7.20*	*1*	*7.20*	*447.19*	*< 0.0001*	
C^2	*3.51*	*1*	*3.51*	*217.60*	*< 0.0001*	
D^2	*19.88*	*1*	*19.88*	*1233.74*	*< 0.0001*	
Residual	0.24	15	0.016			
Lack of Fit	*0.10*	*10*	*0.010*	*0.36*	*0.9200*	*not significant*
Pure Error	*0.14*	*5*	*0.028*			
Cor Total	58.23	29				
Std. Dev.	0.13	R-Squared	0.9958			
Mean	4.01	Adj R-Squared	0.9920			
C.V. %	3.17	Pred R-Squared	0.9865			
PRESS	0.79	Adeq Precision	51.978			

In summary, the model was a good model because the fitness and accuracy of a model depend on the degree of freedom, the lack of fitness must be non-significance; showing R-squared value closer to unity.

The main factors (catalyst concentration, reaction time, reaction temperature and molar ratio) showed significant effect on yield, while the effects of the combination of factors equally showed cumulative effects as first term, second term, third term and so on. According to the results, binomial terms A^2, B^2 and C^2 showed statistically significant contribution on the response. Other factorial combinations also showed degree of significance in the model terms. Final equation in terms of coded factors is provided as eqn. (4.1), where Y is the response is the FFA (%).

FFA = +1.96 – 0.39A – 068B -0.27C -0.28D + 0.22AB – 0.020AC – 0.026AD – 0.13BC + 0.22BD + 0.22CD +0.83A^2 + 0.51B^2 + 0.36C^2 + 0.85D^2 (4.1)

The equation in terms of coded factors was employed in making predictions about the response for given levels of each factor. By default, the high levels of the factors are coded as +1 and the low levels of the factors are coded as -1. The coded equation was useful for identifying the relative impact of the factors by comparing the factor coefficients.

Final equation in terms of actual factors is provided as eqn. (4.2)

FFA = +21.83583 – 4.41722 * Catalyst Concentration - 0.32822* Reaction Temperature - 0.055389* Reaction Time - 1.64125* Molar Ratio+0.019222* Catalyst Concentration * Reaction Temperature-8.88889E-004* Catalyst Concentration * Reaction Time+4.97222E-003* Reaction Temperature * Molar Ratio+2.50000E-003* Reaction Time * Molar Ratio+1.48444* Catalyst Concentration^2+2.27778E-003* Reaction Temperature^2+3.97222E-004* Reaction Time^2+ 0.094583* Molar Ratio^2 (4.2)

The equation in terms of actual factors was useful in predicting the response for given levels of each factor. Here, the levels should be specified in the original units for each factor.

The probability of finding the optimal point of the actual and the predicted FFA is represented by the normal probability plots of residuals [112].

In this study, the normal plot of the residuals indicated the uniform normal distribution of error within the limits of the experiments showing the close linearity of the plots. It was observed from the Figure 4.1 that there occurred partial groupings of the experiments concentrating along the range on the normal probability against internally studentized residuals plot possible due to presence of the central point around this region.

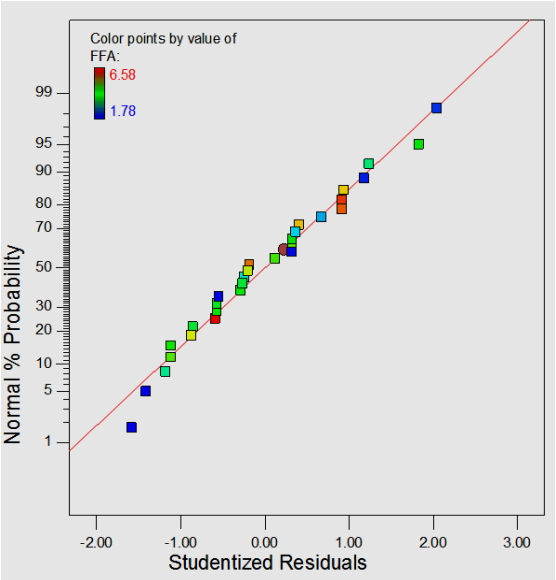

Figure 4.1: Normal % probability vs. residuals plot

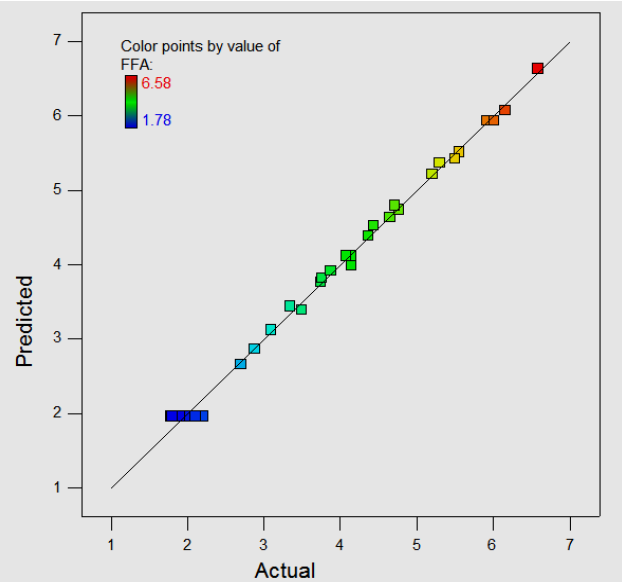

Figure 4.2: Predicted vs. Actualplot for FFA

The graph between the predicted and actual FFA values given in Figure 4.2, showing that the predicted values are quite close to the experimental values, thus, validating the credibility of the model developed for establishing correlation between the process variables and the FFA content. It may be observed that, the predicted and the observed %FFA were very close in all the cases; validating the previous assumption that the model was a good fit one. It may be clearly seen that the predicted and the observed values are grouped close to each other and concentrating around a medium range.

In the light of the earlier discussions, it may be stated that the model could effectively predict the % FFA for large sized esterification with minimal error.

4.2.1.1 Effects of process parameter on FFA

The response graphs represent the main and interactive effects of the factors on the response (% FFA). The main factor plot is shown in Figure 4.3 and three dimensional surface interaction plots are shown in Figure 4.4 to Figure 4.9. The main factor graphs for catalyst concentration, reaction temperature and molar ratio were significant for the model with p-values of less than 0.05. The positive main factor for catalyst (A) and molar ratio (D) coefficients indicates a favorable effect on FFA reduction.

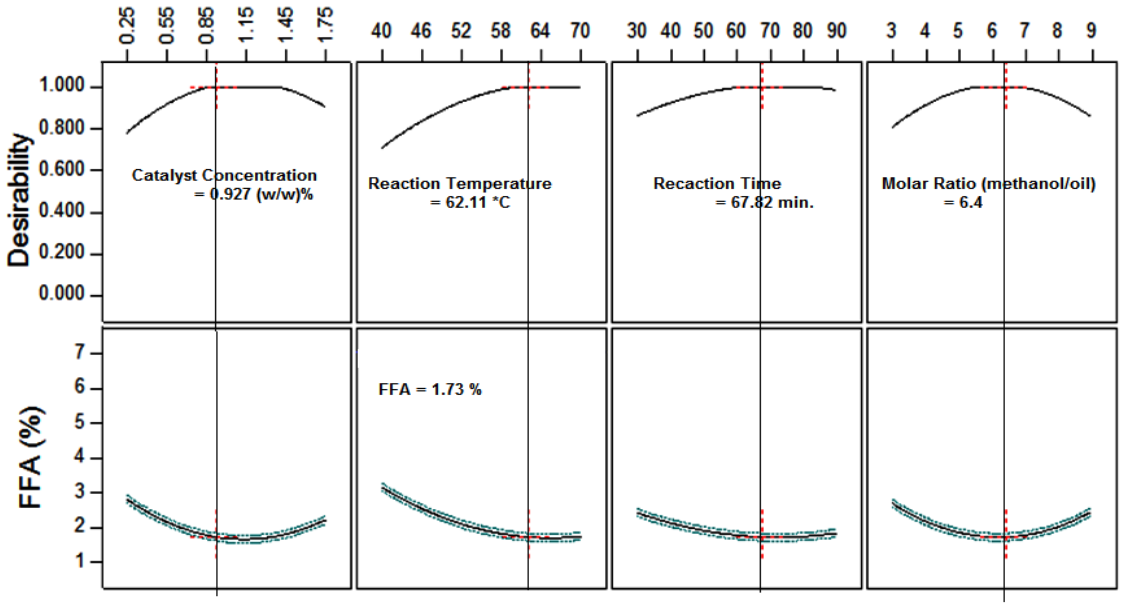

Figure 4.3: Effect of one factor on optimum FFA

Figure 4.3 shows the effects of main factor on FFA. It represents catalyst concentration showed improvement in results up to 0.927 (%wt/wt). Further increase in catalyst concentration showed negative effect. Similarly, reaction temperature and reaction time showed in reduction in FFA up to 62.11 ^{0}C and 67.82 min respectively. Similarly molar ratio showed improvement till 6.4.

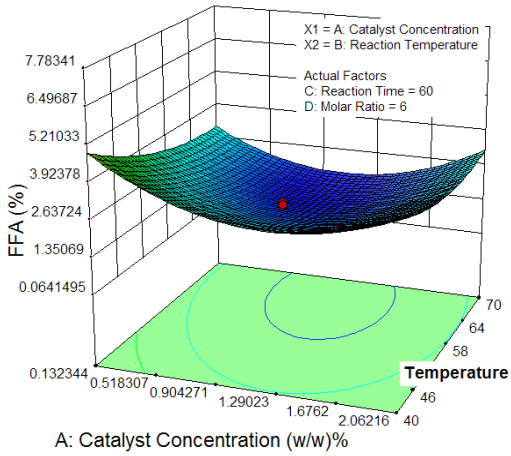

Figure 4.4: Interaction effect of catalyst concentration and reaction temprature on FFA

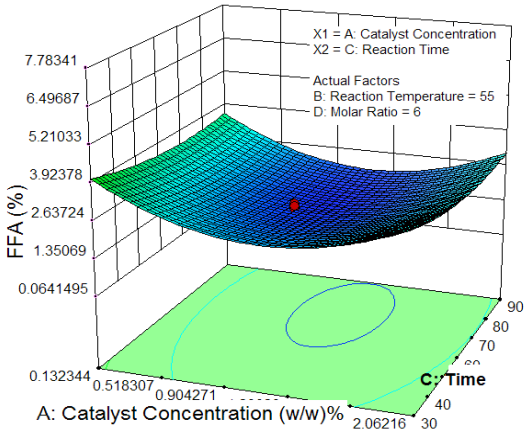

Figure 4.5: Interaction effect of catalyst concentration and reaction time on FFA

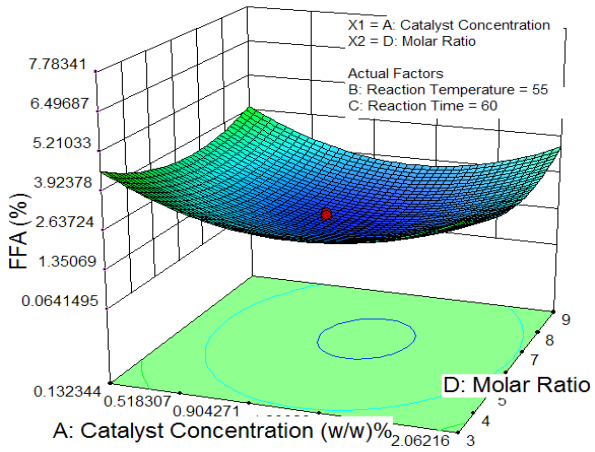

Figure 4.6: Interaction effect of catalyst concentration and molar ratio on FFA

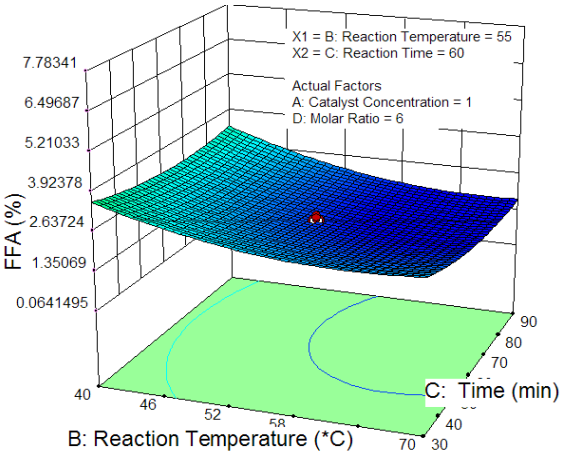

Figure 4.7: Interaction effect of reaction temperature and reaction time on FFA

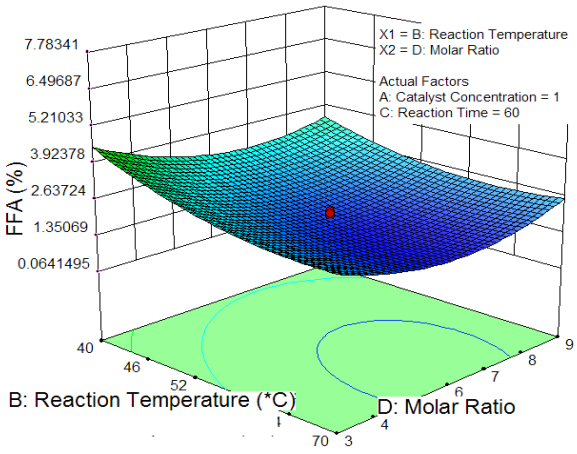

Figure 4.8: Interaction effect of reaction temprature and molar ratio on FFA

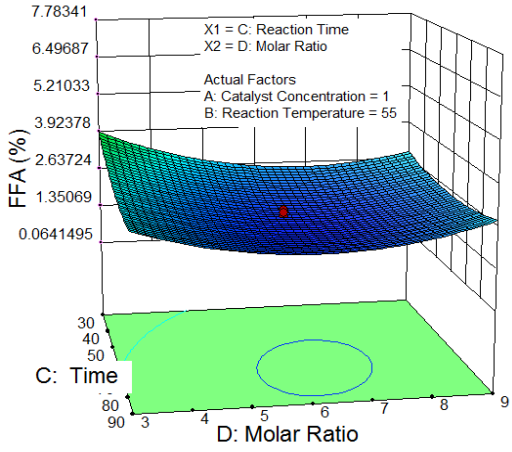

Figure 4.9: Interaction effect of reaction time and molar ratio on FFA

Figure 4.4 showed the interaction effect of catalyst concentration and reaction temprature on FFA. This surface graph showed significant change in FFA with respect to catalyst concentration and reaction temprature. Interaction effect of catalyst concentration and reaction time on FFA is shown in Figure 4.5. Catalyst concentration showed significant change in compare to the reaction time.

Interaction effects of catalyst concentration and molar ratio on FFA is shown in Figure 4.6. It clearly dipicts design points for minimum FFA (red dot in graph) at catalyst concentraton 0.927 (% w/w) and molar ratio 6.4. Figure 4.7 shows the interaction effects of reaction temperature and reaction time on FFA. This surface graph shows change in reaction temprature but reation time was not affected more on response (FFA). Figure 4.8 shows the surface graph of reaction temprature and molar ratio on FFA. Interaction effect of reaction time and molar ratio on FFA is shown in Figure 4.9. This surface graph represents that reaction time is affect more on response.

4.2.1.2 Ramp fuction graph for esterification

The ramp function is a basic unary real function, easily calculable as the mean of its independent variable and its absolute value [253,254]. It presents the value of parameters to obtain minimum value of %FFA for different process parameters as shown Figure 4.10. The desirability value of 1.73153 corresponded to the minimum value of %FFA in the given range of process parameters of acid catalyzed esterification process.

4.2.1.3 Confirmation experiment

The diminishing FFA of the Kusum oil under esterification, the average possible predicted response (FFA) was found to be 1.73 %, as illustrated in Table 4.4. The F-values ranked the significance of process parameters in Table 4.3. It can be concluded that

temperature is influencing more. It is followed by catalyst concentration and molar ratio. The optimum FFA (1.86 %) from the experiments corresponding to these parameters (catalyst concentration is 0.92 (% w/w), reaction temperature is 62.11°C, reaction time is 67.82 minutes and methanol to oil molar ratio (6.4) was found. The error between the experimental and modelled results was 7.51%. Therefore, the model can be successfully used to predict the surface of FFA for these process parameters.

Table 4.4: Optimized results of acid catalyzed esterification of Kusum oil

Response	**Optimized value of input process parameters**				**Predicted Value (%)**	**Experimental Value (%)**
	A	**B**	**C**	**D**		
FFA (%)	0.927	62.11	67.82	6.4	1.73	1.86

Footnote: A: Catalyst concentration (%w/w); B: Reaction temperature (°C); C: Reaction time (minutes); D: Molar ratio (methanol/oil)

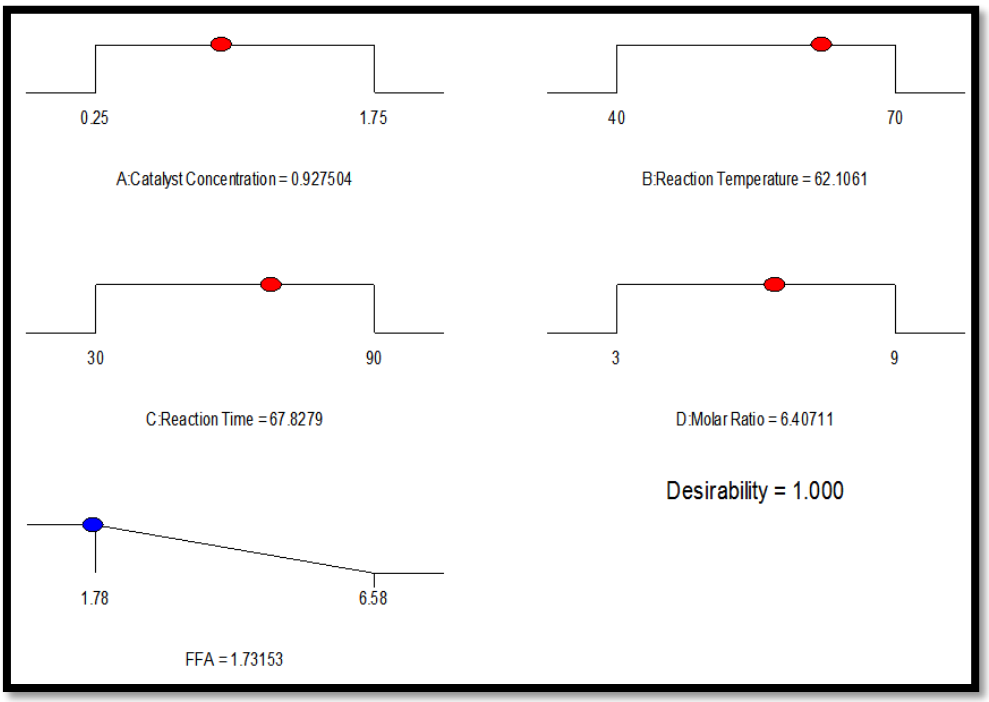

Figure 4.10: Ramp function graph for optimum FFA.

4.2.2 Optimization of transesterification

Biodiesel was produced using transesterification process in which, the triglyceride was reacted with an alcohol in presence of a catalyst. As discussed earlier, the production of

Sal biodiesel (SME) was carried out in a single stage transesterification process and Kusum biodiesel (KME) was carried out in a two stage process (Esterification followed by transesterification). The free fatty acid (FFA) content of Sal oil was 1.68% and Kusum oil was 1.86 % (after esterification). Transesterification process was carried out monitoring; catalyst concentration (A), reaction temperature (B), reaction time (C) and methanol to oil molar ratio (D) at constant stirring speed at 450 rpm to determine corresponding optimum conditions using RSM (shown in Table 3.5). These results are similar to the results reported for waste rapeseed oil [199], cotton seed oil [255] and used frying oil [256]. Characterization of SME and KME samples produced in the transesterification is an integral part of biodiesel quality control.

Similar to the esterification discussed earlier, the model F-value of 1257.12 implied the model is significant for the transesterification as well. There is only 0.01% chance that an F-value this large could occur due to noise. Values of "Prob> F" less than 0.0500 indicated model terms are significant. In this case A, B, C, D, AB, AC, BD, CD, A^2, B^2, C^2, $D^2$are significant model terms as shown Table 4.5.

Values greater than 0.10 indicate the model terms are not significant. The "Lack of Fit F-value" of 0.23 implied the Lack of Fit was not significant relative to the pure error. There is 97.55% chance that a "Lack of Fit F-value" this large could occur due to noise. Non-significant lack of fit was required to validate the model.

The "Predicted R^2=0.99 was in reasonable agreement with the "Adj R^2=0.99. Moreover, the Adeq Precision" measured the signal to noise ratio. The ratio of 114.68 indicated an adequate signal. The coefficient of determination (R^2 = 0.99) found, implied that the accuracy of the predictive model was adequate. This model could be used to navigate the design space.

Table 4.5*:* ANOVA for Response Surface Quadratic model for transesterification

Source	**Sum of Squares**	**Degree of freedom**	**Mean Square**	**F Value**	**p-value Prob> F**	
Model	6893.20	14	492.37	1257.12	< 0.0001	Significant
A-Catalyst Concentration	*425.04*	*1*	*425.04*	*1085.21*	*< 0.0001*	
B-Reaction Temperature	*1666.67*	*1*	*1666.67*	*4255.32*	*< 0.0001*	
C-Reaction Time	*273.38*	*1*	*273.38*	*697.98*	*< 0.0001*	
D-Molar Ratio	*1472.67*	*1*	*1472.67*	*3760.00*	*< 0.0001*	
AB	*20.25*	*1*	*20.25*	*51.70*	*< 0.0001*	
AC	*68.06*	*1*	*68.06*	*173.78*	*< 0.0001*	
AD	*1.00*	*1*	*1.00*	*2.55*	*0.1309*	
BC	*0.56*	*1*	*0.56*	*1.44*	*0.2494*	
BD	*9.00*	*1*	*9.00*	*22.98*	*0.0002*	
CD	*10.56*	*1*	*10.56*	*26.97*	*0.0001*	
A^2	*801.67*	*1*	*801.67*	*2046.82*	*< 0.0001*	
B^2	*1687.53*	*1*	*1687.53*	*4308.58*	*< 0.0001*	
C^2	*820.31*	*1*	*820.31*	*2094.41*	*< 0.0001*	
D^2	*820.31*	*1*	*820.31*	*2094.41*	*< 0.0001*	
Residual	5.87	15	0.39			
Lack of Fit	*1.87*	*10*	*0.19*	*0.23*	*0.9755*	*not significant*
Pure Error	*4.00*	*5*	*0.80*			
Cor Total	6899.08	29				
Std. Dev.	0.63	R-Squared	0.9991			
Mean	75.15	Adj R-Squared	0.9984			
C.V. %	0.83	Pred R-Squared	0.9976			
PRESS	16.56	Adeq Precision	114.681			

The final equation for the yield and the effects of the individual as well as the interactive effects of the factors on the yield is given as eqn. (4.3).

$$Yield = +94.5 + 4.21A + 8.33B + 3.37C + 7.83D - 1.13AB - 2.06AC + 0.25AD + 0.19BC + 0.75BD - 0.81CD - 5.41A^2 - 7.84B^2 - 5.47C^2 - 5.47D^2 \quad (4.3)$$

As discussed previously, the coded equation is useful for identifying the relative impact of the factors by comparing the factor coefficients. Final equation in terms of actual factors for maximum (optimum) yield is provided as eqn. (4.4)

Yield = -280.90625 + 60.47917 * Catalyst Concentration + 9.44271* Reaction Temperature + 0.96458 * Reaction Time + 8.94444 * Molar Ratio - 0.2250 * Catalyst Concentration * Reaction Temperature - 0.13750 * Catalyst Concentration * Reaction Time + 0.16667 * Catalyst Concentration * Molar Ratio + 0.000625 * Reaction Temperature * Reaction Time + 0.025000 * Reaction Temperature * Molar Ratio - 0.0090277 * Reaction Time * Molar Ratio - 21.62500 * Catalyst Concentration^2 - 0.078437 * Reaction Temperature^2 - 6.07639E-003 * Reaction Time^2 -0.60764 * Molar Ratio^2 (4.4)

The equation in terms of actual factors can be used to make predictions about the response for given levels of each factor. These levels should be specified in the original units for each factor [254]. The predicted and actual values were correlated by the graph, showing the precision as well as the normal distribution of the data as a function of the percentage yields for both actual and predicted. The plots between the normal % probabilities vs. residuals is shown in Figure 4.11 and predicetd vs. the actual values are provided in Figure 4.12. The one factor plot is shown in Figure 4.13 and three dimensional response surface plot for the tranesterification stage is provided in the Figure 4.14 to Figure 4.19.

The graph between the predicted and actual methyl ester yield (%) given in Figure 4.12 shows that the predicted values are quite close to the experimental values, thereby,

validating the reliability of the model developed for establishing a correlation between the process variables and the methyl ester yield.

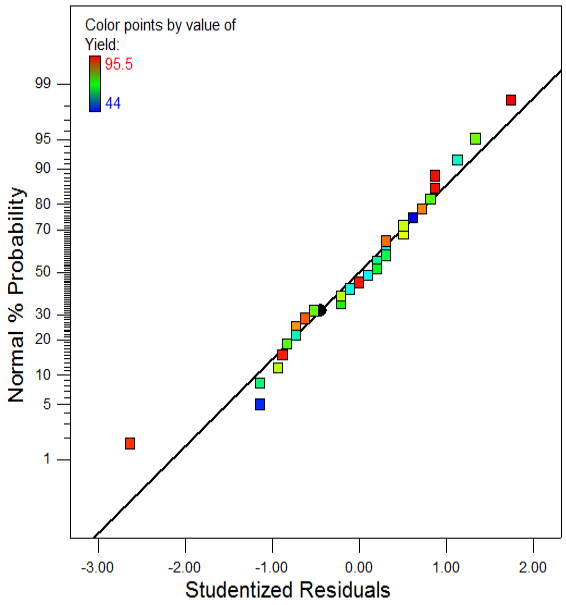

Figure 4.11: Normal % probability vs. residuals for transesterification

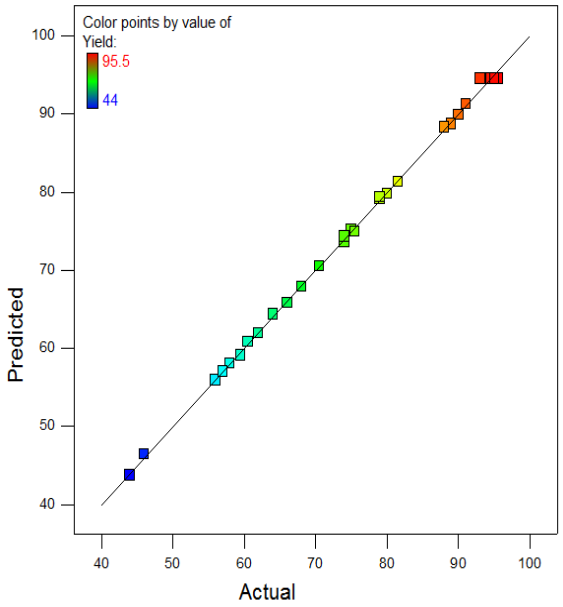

Figure. 4.12: Predicted vs. actual yield for transesterification

4.2.2.1 Effect of process parameters on yield

Figure 4.13 indicates the synegistic effects of the independent variables as can be clearly seen on the graph. The increasing catalyst concentration showed improvement in results up to 1.13 (% wt/w). Further increase in catalyst concentration beyond this concentration showed reduction in yield. Similarly reaction temperature and reaction time showed in improvement in yield up to 63.18 ^{0}C and 79.2 minutes respectively. Similarly molar ratio showed improvement till 8.16.

The response surface graph in the Figure 4.14 shows the effects of the reaction temperature and the catalyst concentration as it affected the yield. Low catalyst concentration and low reaction temperature negatively affected the yield, while the increase in temperature increased the yield to a point closer to the boiling point of methanol before slight decrease in

the yield was observed. The increase in biodiesel yield at higher temperature was due to the fact that viscosity of oils decreases at high temperature and results in an increased reaction rate and shortened reaction time, thereby, increasing the biodiesel yield [255,257].

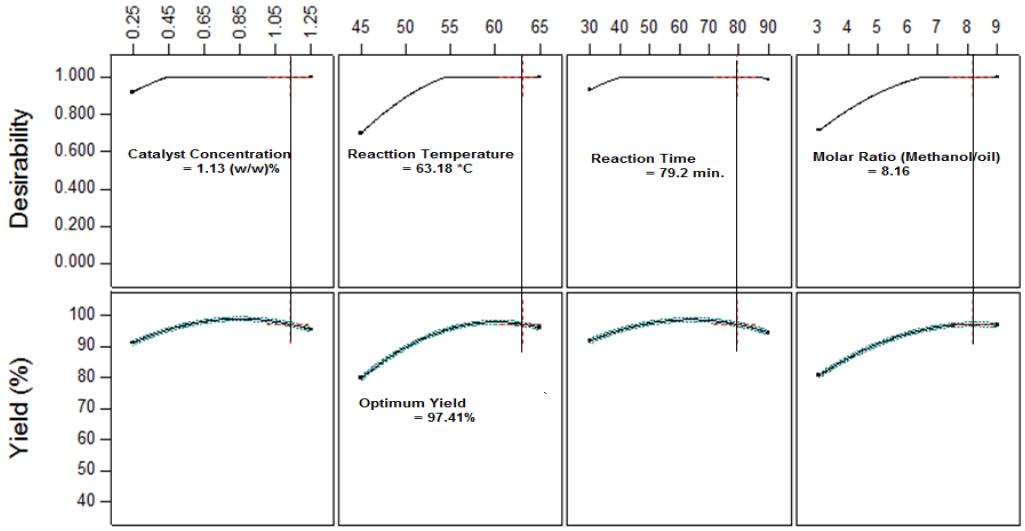

Figure 4.13: Effect of single factor on optimum yield

It also increases with increasing reaction time at low catalyst concentration [199]. Interaction effects of catalyst concentration and reaction time on yield is shown in Figure 4.15. Catalyst concentration showed significant changes in compare to the reaction time. Low catalyst concentration and low reaction time showed low yield.

Interaction effects of catalyst concentration and molar ratio on yield are shown in Figure 4.16. Figure clearly dipicts design point for optimum yield at catalyst concentraton 1.13 (w/w)% and molar ratio 8.16.

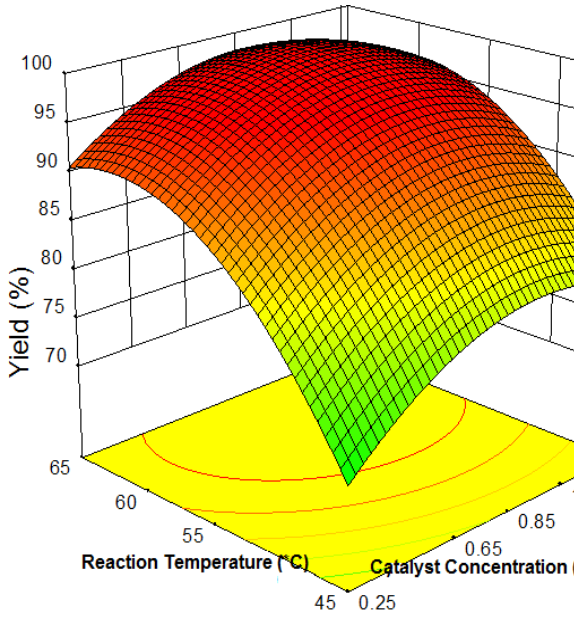

Figure 4.14: Interaction effect of catalyst concentration and reaction temprature on yield

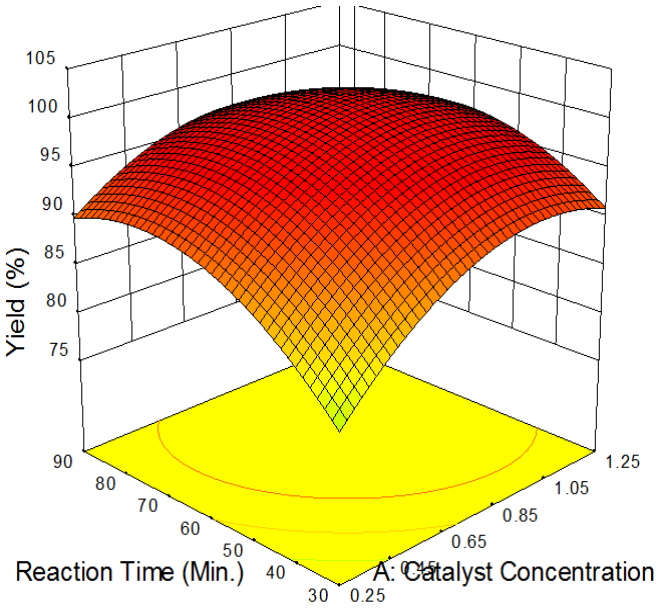

Figure 4.15: Interaction effect of catalyst concentration and reaction time on yield

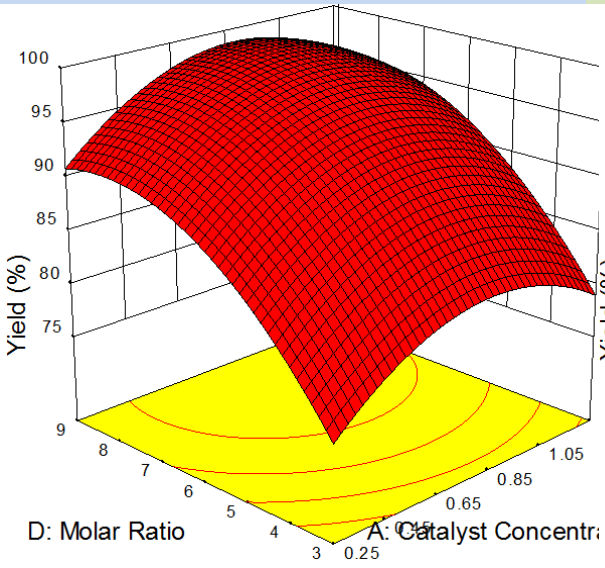

Figure 4.16: Interaction effect of catalyst concentration and molar ratio on yield

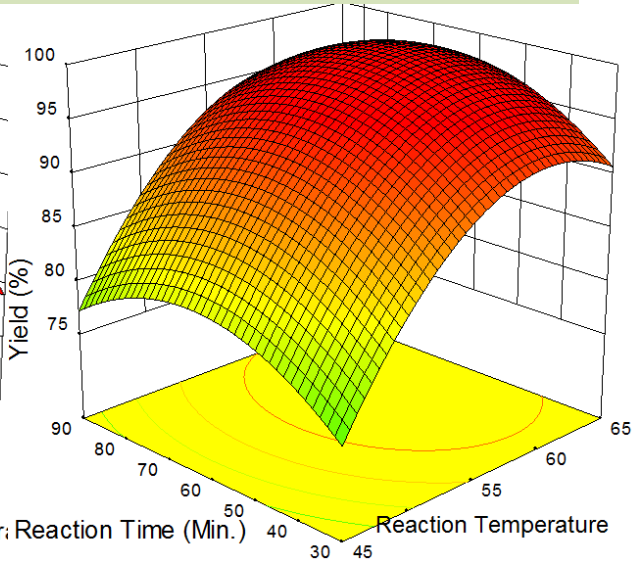

Figure 4.17: Interaction effect of reaction temperature and rection time on yield

Figure 4.17 shows the interaction effects of reaction temperature and reaction time on yield. This surface graph shows significant change in reaction temprature but reaton time was not affected more on yield. Figure 4.18 shows the surface graph of reaction temprature and

molar ratio on yield. Interaction effect of reaction time and molar ratio on yield is shown in Figure 4.19. This surface graph represents that reaction time is affect more on response.

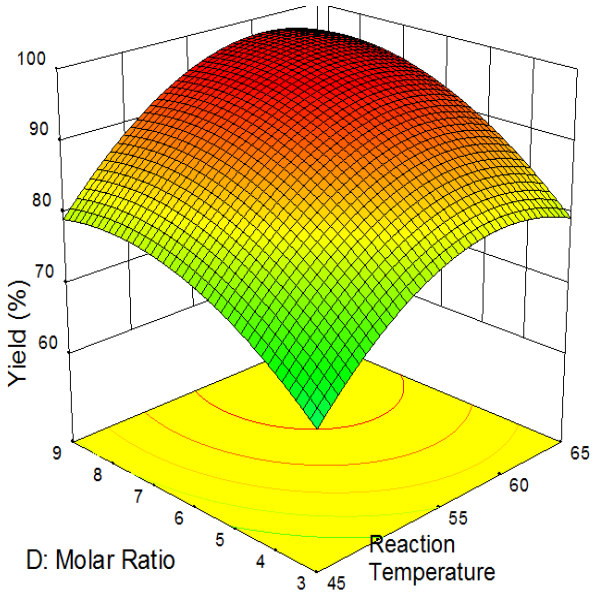

Figure 4.18: Interaction effect of reaction temperature and molar ratio on yield

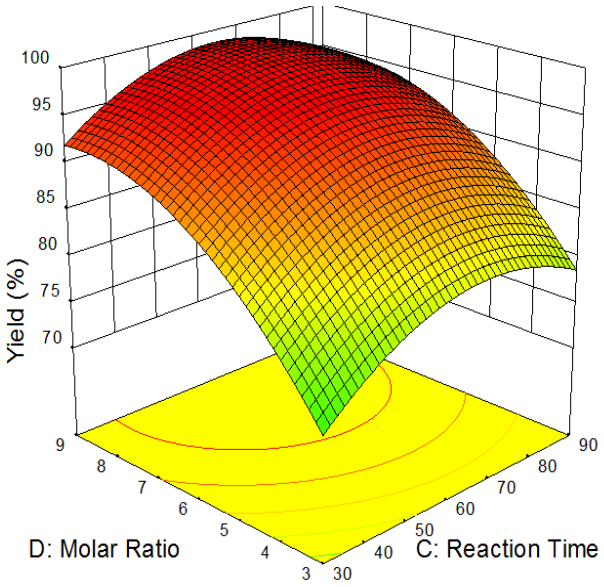

Figure 4.19: Interaction effect of reaction time and molar ratio on yield

From surface graphs and F values; the model ranked the significance of process parameters in Table 4.6. It can be concluded that the influence of the parameters as follows Reaction temperature > Molar ratio > Catalyst concentration > Reaction time. The same trend was observed for catalyst concentration as the increase in the catalyst resulted in the increase in the yield but was also found to decrease slightly with the highest catalyst concentration. This was discussed in details by Hassan and Vinjamur, [258]. This could be attributed to the formation of much glycerol that results in persistant washing. For the transesterification of the biodiesel, the optimal yield was predicted as 97.43% under the reaction conditions of 1.13% catalyst (KOH) concentration react at temperature of 63.18℃ for the reaction time of 79.2 minutes and methanol to oil molar ratio of 8.16 with constant 450 rpm stirring speed.

4.2.2.2 Ramp fuction graph for tranesesterification

The ramp function is the basic unary real function. The desirability value of 97.43% corresponded to the maximum value of yield (%) in the given range of process parameters of base catalyzed transesterification process as shown in Figure 4.20.

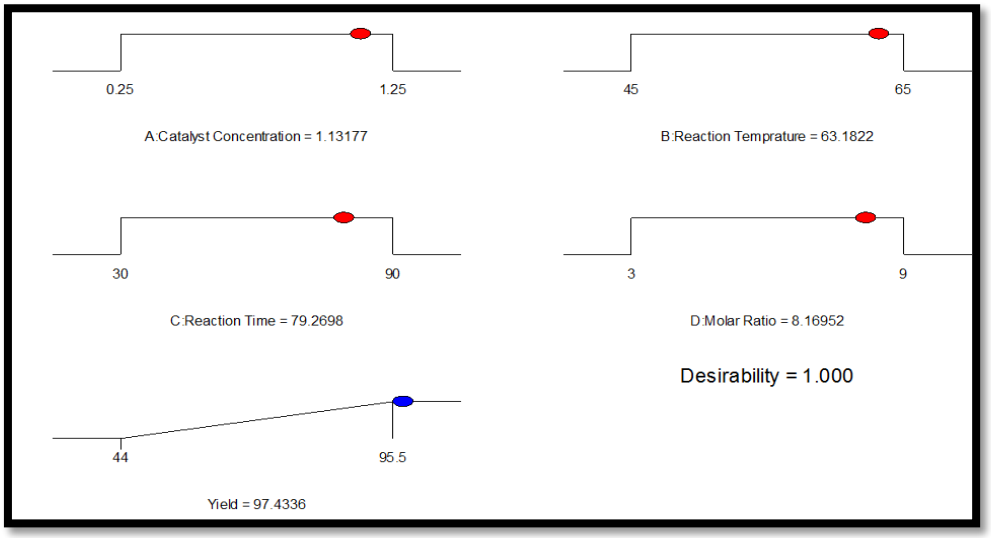

Figure 4.20: Ramp function graph for optimum yield of biodiesel

4.2.2.3 Confirmation experiment

Once the optimal value of the design parameters has been selected, the final step was to predict and verify the improvement of the quality characteristic using the optimum level of the design parameters. By evaluating the yield under transesterification, the average possible predicted yield is found to be 97.41%, as illustrated in the Table 4.6.

Table 4.6: Optimized Process Parameters for Sal biodiesel and Kusum biodiesel

Response	Optimized value of input process parameters				Predicted Value	Experimental Value
	A	B	C	D		
SME yield (%)	1.13	63.18	79.2	8.16	97.41	96.92
KME yield (%)	1.13	63.18	79.2	8.16	97.41	96.5

Footnote: A: Catalyst concentration (%w/w); B: Reaction temperature (°C); C: Reaction time (minutes); D: Molar ratio (methanol/oil)

The product yield from five experiments corresponding to these parameters (catalyst concentration is 1.13 w/w%, methanol to oil molar ratio is 8.16 reaction temperature is 63.18 °Cand reaction time 79.2 minutes) is found to be 96.92 ± 0.48 % for SME and 96.5 ± 0.72 % for KME. The error between the experimental and modelled results was 0.5% for SME and 0.9% for KME. Therefore, the model can be successfully used to predict the surface of yield (%) for this parameter.

4.3 Results of Physico-Chemical Characterization

4.3.1 Fatty acid composition of Sal biodiesel

The physico-chemical properties were determined according to standard methods. Table 4.7 presents the average values of triplicate analysis. Figure 4.21 shows the fatty acid profile obtained from GCMS.

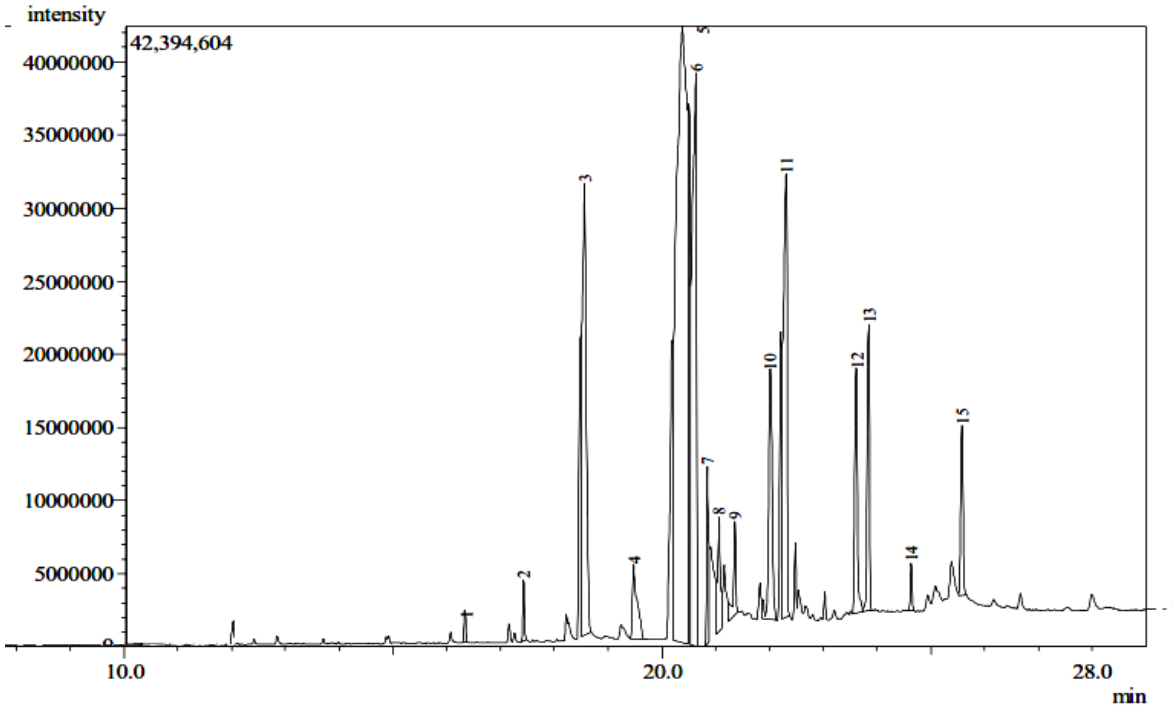

Figure 4.21: Fatty acid profile Sal methyl ester using GCMS

Table 4.7: Fatty acid profile for methyl esters Sal and Kusum

S. No.	Fatty Acid Methyl Ester	Chemical Formula	Molecular Weight	Density (kg/m^3)	Flash Point (℃)	Enthalpy (MJ/kg)	Boiling Point (℃)	SME	KME
1.	Myristic acid methyl ester or Methyl myristate	$C_{15}H_{30}O_2$	242	862	124	53.9	289	8.76	--
2.	Hexadecanoic acid methyl ester	$C_{17}H_{34}O_2$	470	853	152	57.5	351	6.86	9.89
3.	Octadecanoic acid methyl ester/Methyl stearate	$C_{19}H_{38}O_2$	298	910	169	62	355	28.3	3.63
4.	cis-9-Octadecenoic acid methyl ester	$C_{19}H_{36}O_2$	296	895	102	59.6	360	30.1	49.29
5.	cis-9-cis-12-Octadecadienoic acid methyl ester	$C_{19}H_{34}O_2$	294	900	303	118	230	8.78	1.8
6.	Eicosanoic acid methyl ester	$C_{21}H_{42}O_2$	326	824	169	65.3	328	16.7	15.27
7.	cis-11 Eicosenoic acid methyl ester	$C_{21}H_{40}O_2$	324	900	209	78	402	--	18.19
8.	Docosanoic acid methyl ester	$C_{23}H_{46}O_2$	354	920	176	67	391	--	1.82

From the results, the major constituents are saturated fatty acid methyl ester (Myristic acid methyl ester (8.76%), Hexadecanoic acid methyl ester (6.86%), Octadecanoic acid methyl ester (28.33%) and Ecosanoic acid methyl ester (16.77)), and unsaturated fatty acid methyl (cis-9-Octadecenioc acid methyl ester (30.19%) and cis-9-cis-15- Octadecadienioc acid methyl ester (8.78%)) are also identified.

4.3.2 Fatty acid composition of Kusum biodiesel

Figure 4.22 shows the fatty acid profile of KME obtained from GCMS. The major constituents are saturated fatty acid methyl ester (Hexadecanoic acid methyl ester (9.89%) and Eicosanoic acid methyl ester (18.19%), and unsaturated fatty acid methyl (cis-9-Octadecenoic acid methyl ester (49.29%) and cis-11 Eicosenoic acid methyl ester (18.19%) are also available.

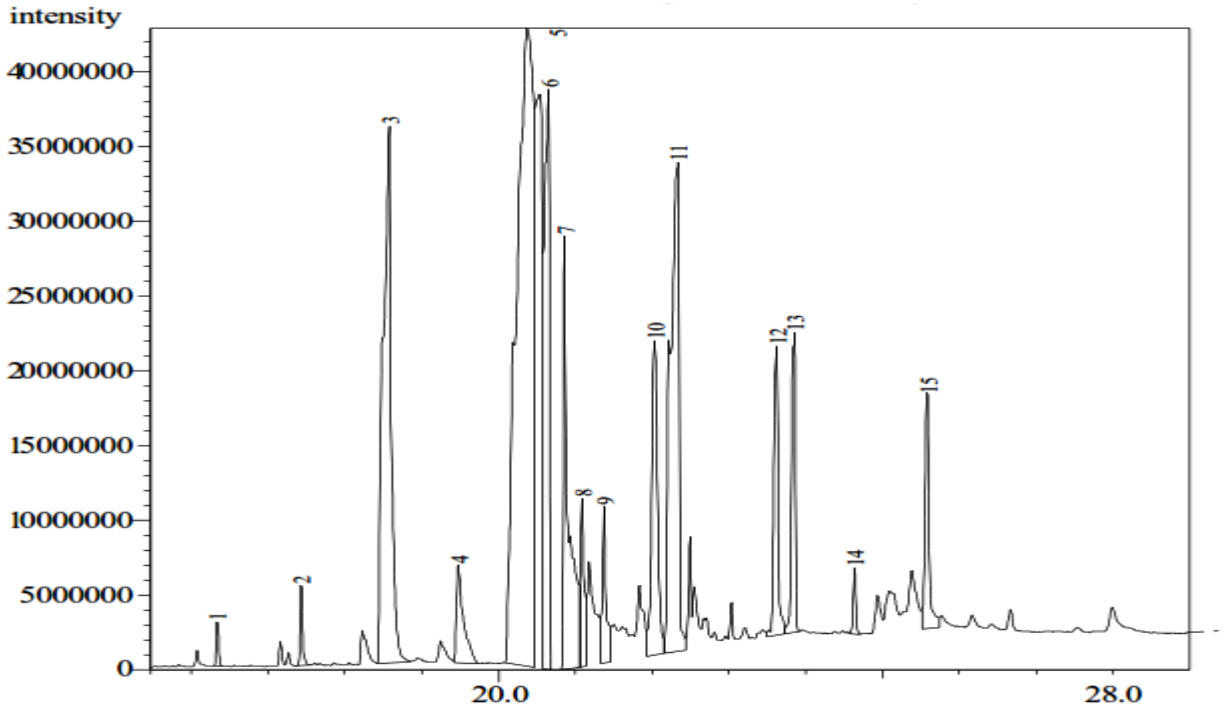

Figure 4.22: Fatty acid profile of Kusum methyl ester using GCMS

4.3.3 Infrared spectroscopy

The infrared (IR) analysis of SME and KME were carried out to detect the possible functional group similarities and are shown in Figures 4.23 and Figure 4.24 respectively. The following wave numbers have been observed to be distinct in case of SME and KME. The instrument recorded spectra from an upper limit of around 4500 $cm^{-1}$to 350 cm^{-1}; however

relevant spectra is lies between 4000 $cm^{-1}$to 700 cm^{-1}. IR correlation table is shown in Appendix-III.

Table 4.8: Infra-red absorption frequencies of SME and KME

S. No.	Functional group	Frequency (cm^{-1}) wavenumber	SME wavenumber	KME wavenumber
1.	—O—H stretching (alcohol)	3300-3400	3474	3471
2.	=C—H stretching (alkene)	3265-3335	2862	2860
3.	—C—H stretching (alkanes)	2850-3000	2926	2925
4.	—C—H stretching (aliphatic)	4200-4600	4254	4258
5.	—C= O stretching(ester)	1730-1750	1736	1744
6.	—C=C Alkyne	1600-1680	1611	1625
8.	—CH_3 bending	1450-1375	1471	1451
9.	O=C-O-C aliphatic (ester)	1160-1210	1177	1164
10.	—C— O stretching (ester)	1000-1300	1023	1013
11.	Alcohols free	3600-3650	3865	3853
12.	Alcohols H- bonded	3200-3500	3474	3471
13.	Out of plane bend	>1000	713	720

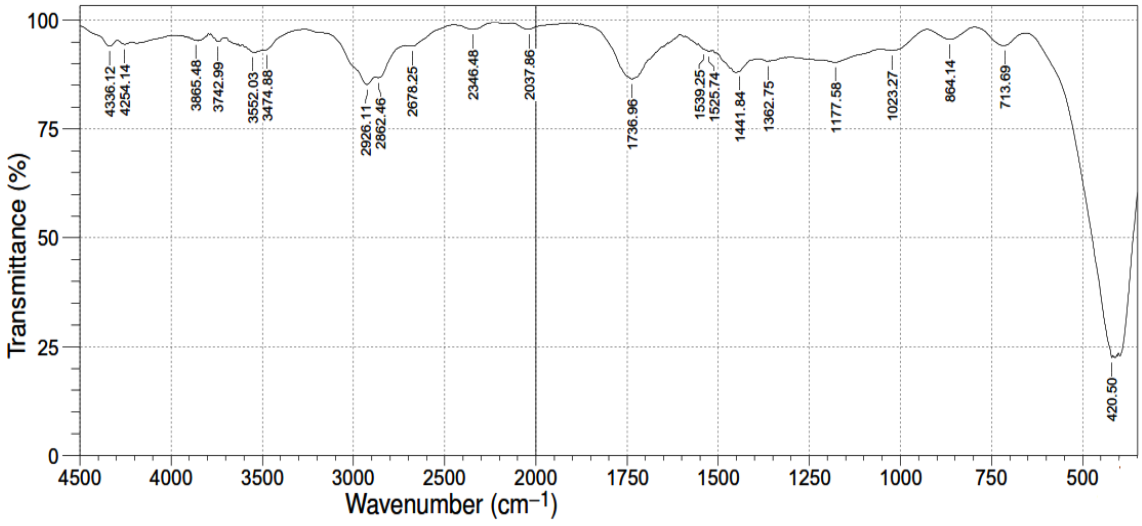

Figure 4.23: FTIR of Sal biodiesel (SME)

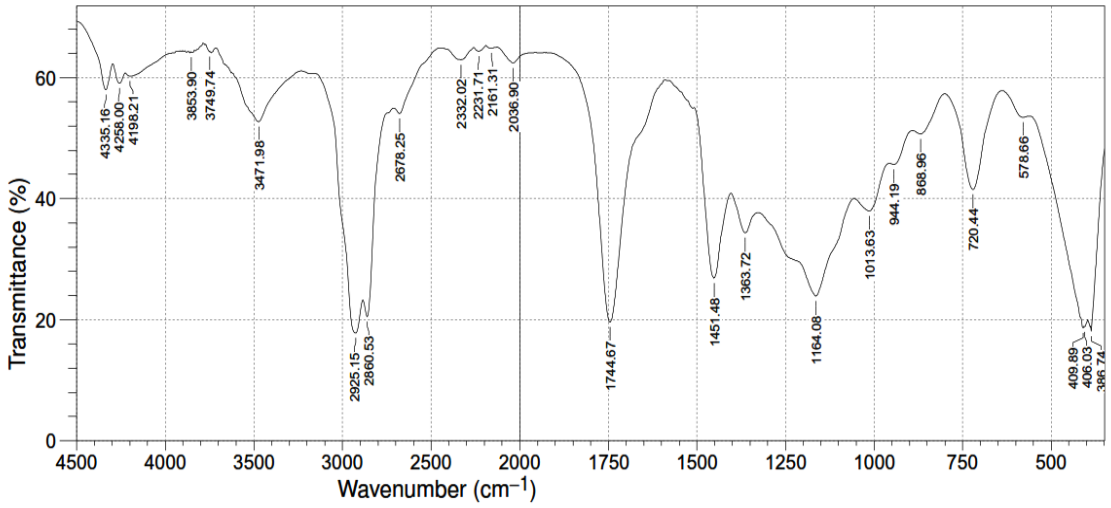

Figure 4.24: FTIR of Kusum biodiesel (KME)

After production of SME and KME, they were blended with diesel fuel in several proportions and studies were made for the homogeneity of all biodiesel-diesel fuel blends. Some samples were kept in open atmospheric conditions and some were kept in closed atmospheric conditions but all fuel blends have been found to be homogeneous even after 12 months. There was no sign of phase separation in any of the fuel blends.

4.3.4 Kinematic viscosity

Kinematic viscosity is the most important property of any fuels since it affects the operation of fuel injection equipment and spray atomization, particularly at low temperatures when an increase in viscosity affects the fluidity of the fuel [149,257] and engine combustion. Moreover, high viscosity may lead to the formation of soot and engine deposits due to insufficient fuel atomization.

It can be seen that; both vegetable oils have very high viscosity. This is attributed to their large molecular masses and large chemical structures which indicated that these oils have good lubrication properties in CI engine [104]. From Table 4.1, it could be seen that Sal oil presented highest kinematic viscosity of 52.6 (mm^2/s) and 10.36 (mm^2/s) at 40°C and

100°C, respectively. Dynamic viscosity of 43.62 (mpa.s) at 40°C, which was nearly equal to the Jatropha oil. Kusum oil possessed lower kinematic viscosity of 40.97 (mm^2/s) at 40°C. It was also found that Kusum oil owned the highest viscosity index of 189. A high viscosity index signified relatively small change of kinematic viscosity with temperature.

The kinematic viscosities of the methyl esters were found to be lower than those presented by their respective vegetable oils as could be seen in Table 4.9. Since, biodiesel molecules are single, long chain fatty esters, than triglyceride molecules [21]. It could be observed that all results are in agreement with the standard specified by ASTM D6751. Figure 4.25 showed the variation of viscosity of SME blends and KME blends at 40℃. KME exhibited kinematic viscosity of 5.91 cSt and SME 5.79 cSt; which are lower than the ASTM 6751 limit of 6 cSt. Therefore, the viscosities of both biodiesel were within the ASTM standard limit.

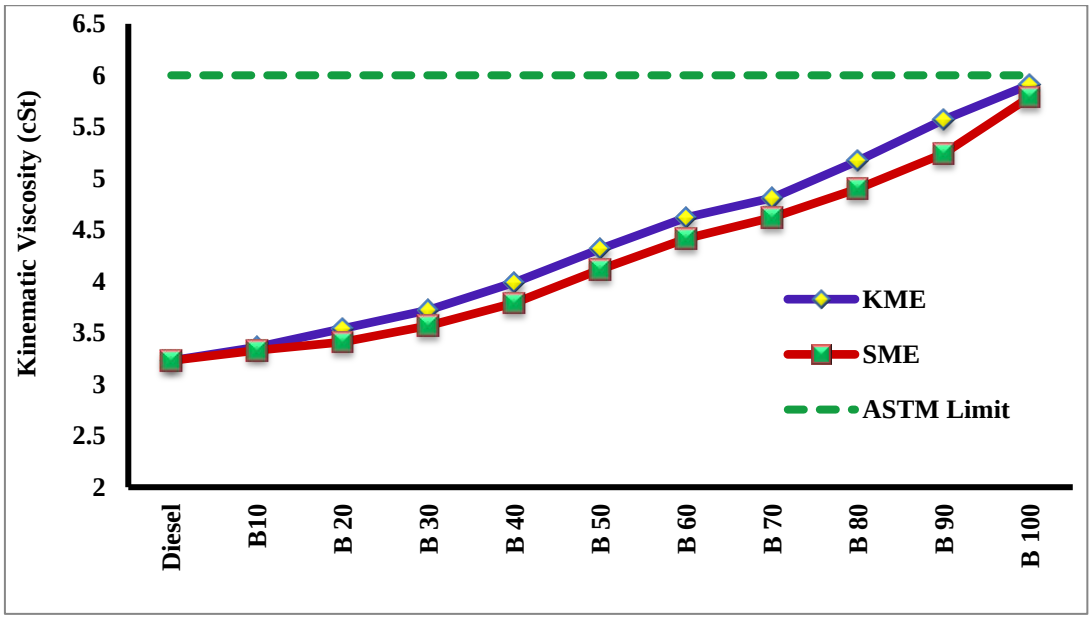

Figure 4.25: Variation of viscosity for various test fuels

Table 4.9- Physico-chemical properties of the test fuels

Test Fuel	Density (g/cm^3)	API Gravity	Viscosity (cSt)	Calorific Value (MJ/kg)	Flash Point (℃)	CFPP (℃)
D100	0.832	38.572	3.23	44.7	65	-15
SME	0.8765	29.938	5.79	39.65	172	10
KME	0.8967	26.301	5.91	39.11	148	-1
SME10	0.8333	38.307	3.33	44.51	67	-2
SME20	0.8396	37.033	3.41	43.95	72	2
SME30	0.845	35.956	3.57	43.75	79	3
SME40	0.8507	34.834	3.79	42.85	88	4
KME10	0.838	37.354	3.36	44.15	67	-13
KME20	0.844	36.154	3.54	43.56	70	-11
KME30	0.851	34.775	3.72	43.11	73	-9
KME40	0.858	33.418	3.99	42.65	78	-7

4.3.5 Density / API gravity

Density was measured using an oscillating "U" tube density meter as elaborately discussed in the earlier section. It is also a key fuel property, with potential to directly influence the engine performance, emission and combustion behavior. Many important characteristics, such as cetane rating and heating value, are related to the density [113]. Fuel density influences engine output power; due to difficulty in fuel mass injection [114]. The conversion of Sal and Kusum oils into its mono-esters brings about significant change in the density of vegetable oil.

In the present investigation, the density of Sal and Kusum oils are 0.89 g/cm^3 and 0.92 g/cm^3 respectively. The density of vegetable oil, SME, KME and its blends were determined at temperatures 15°C. At this temperature, SME and KME exhibited densities of 0.8765 (g/cm^3) and 0.89 (g/cm^3), respectively as compared to 0.83 (g/cm^3) showed by the neat diesel.

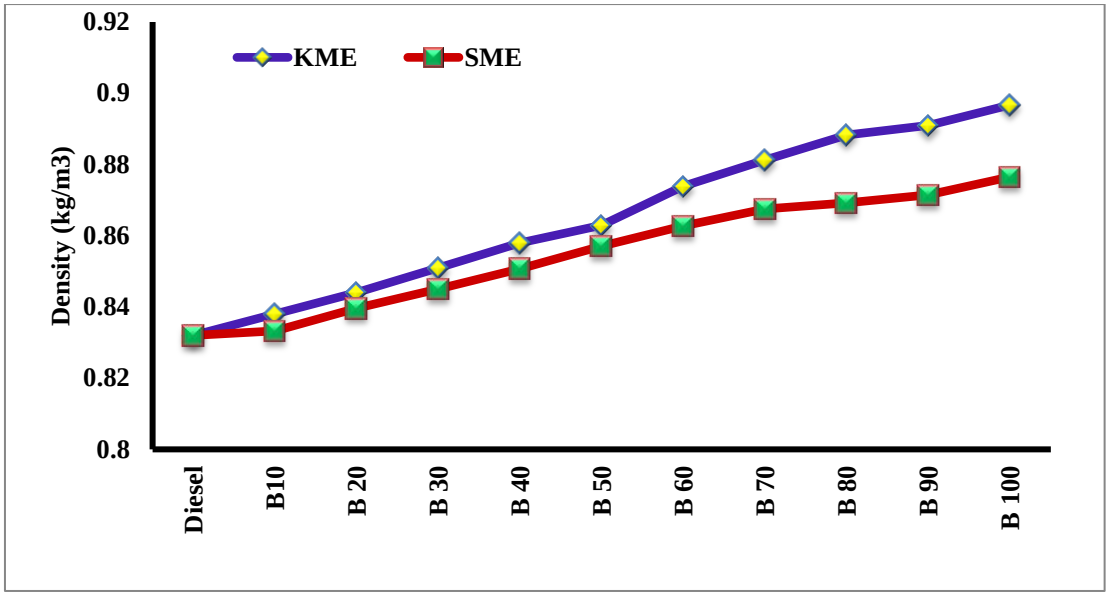

Figure 4.26: Variation of density for various test fuels

In either of the cases, the density was within prescribed limits of 0.86-0.9. ASTM specification does not specify the range of density for biodiesel.

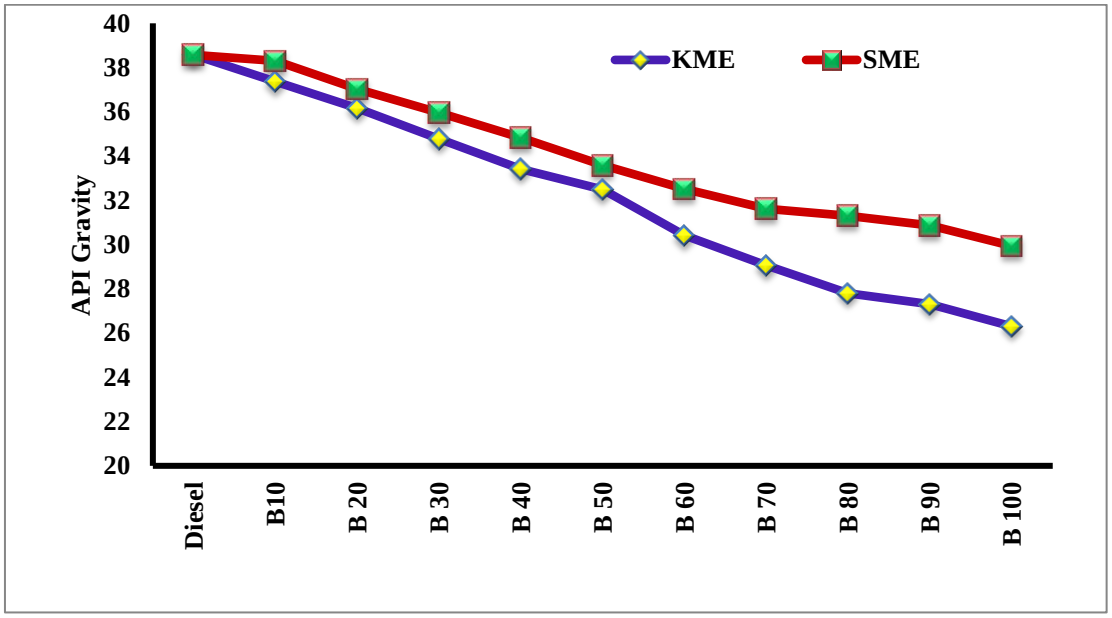

Figure 4.27: Variation of API Gravity for various test fuels

As the concentration of the biodiesel in diesel increased, the density of the blend also increased. This was reflected in the graphs both for SME and KME as shown in Figure 4.26 and Table 4.9. The API gravity decreased with increasing concentration of both the biodiesel

in diesel as shown in Figure 4.27. This is reflected in the graphs both for SME and KME. The API gravity of KME (26.3) has been found to be lower than SME (29.94).

4.3.6 Calorific value

Calorific value is an important parameter in the selection of a fuel. The caloric value of vegetable oils and biodiesel is generally lower than of diesel because of its higher oxygen content [92]. This is proved in Table 4.1 as the calorific values of all vegetable oils are lower than diesel fuel. It may be observed that SME and KME were having calorific value of 39.65 (MJ/kg) and 39.11 (MJ/kg) as compared to 44.7 (MJ/kg) in case of diesel.

Calorific value of various blends of SME and KME with diesel is shown in Figure 4.28 and Table 4.9. A bomb calorimeter was used to determine the calorific value of the test fuels as discussed briefly in the earlier sections.

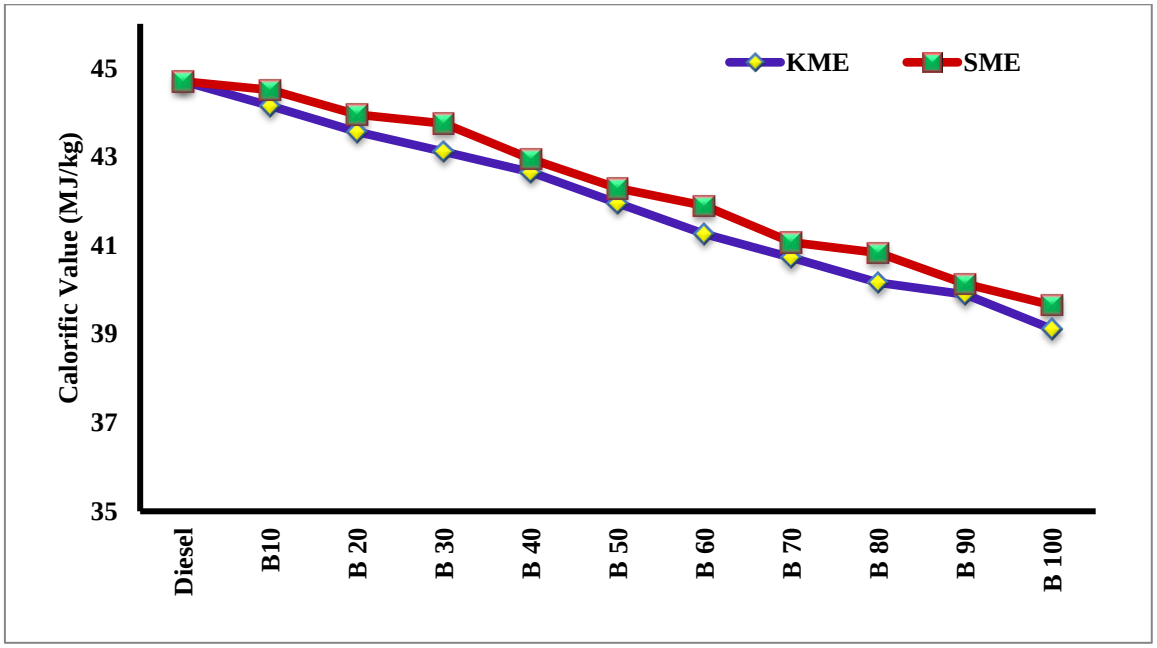

Figure 4.28: Variation of calorific value for various test fuels

4.3.7 Flash point

Flash point is another important property for any fuel. Generally, vegetable oils and biodiesel have higher flash point compared to diesel which is usually more than 120°C, while generally conventional diesel fuel has a flash point of 55-66°C. So biodiesel is safe for transport, handling and storage purpose [140,259]. The results of flash point of test fuels are shown in Figure 4.29. The results from Table 4.1 showed that Jatropha oil possessed the highest flash point of 258°C followed by Sal oil with 225°C; while Kusum oil has the lowest flash point of 185.5°C.

The flash point of diesel fuel has been found to be 65ºC, whereas for SME and KME, its values were 172°C and 148°C, respectively. The IS-15607, EN-14214 and D-6751 specified the minimum value of flash point as 120°C, 120°C and 130°C respectively.

Therefore it can be seen that flash point of both the biodiesel was above the minimum limit of all the three specifications. Blending of biodiesel in diesel increased flash point of test fuels.

4.3.8 Cold filter plugging point

Cold filter plugging point (CFPP) is the temperature at which the test filter starts to plug due to fuel components that have started to gel or crystallize. It is commonly used as indicator of low temperature operability of fuels and reflects their cold weather performance [97]. From Table 4.1, it can be seen that Sal oil acquired the higher CFPP point of 39°C whereas Kusum oil has 11°C.

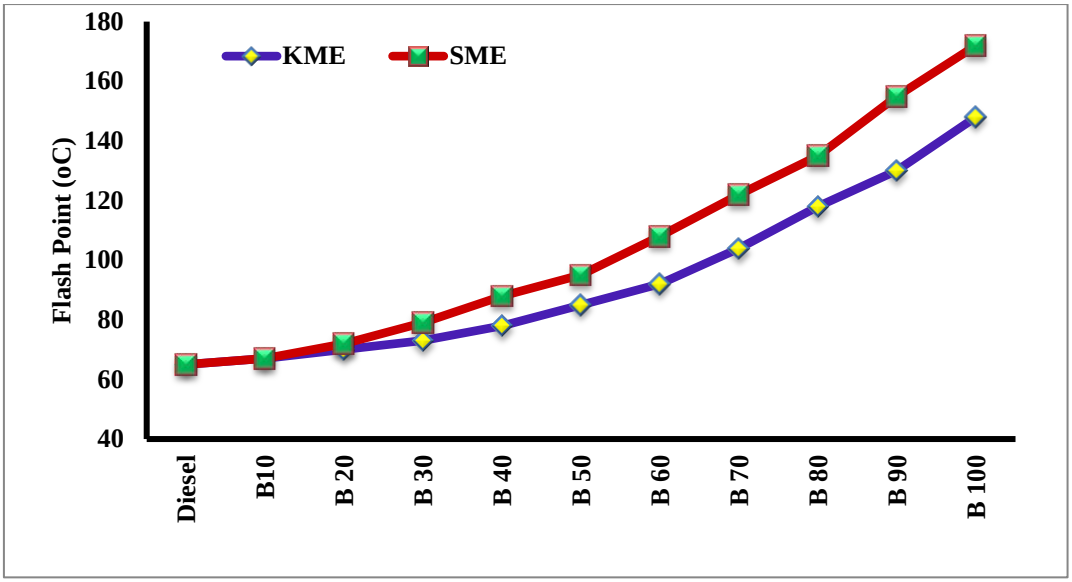

Figure 4.29: Variation of flash point for various test fuels

Variation in CFPP for the test fuels is shown in Figure 4.30 and Table 4.9. It may be observed that neat diesel exhibited CFPP of -15°C; whereas SME and KME showed CFPP of 10°C and -1°C, respectively. The flow properties of SME were poor and KME were mediocre to cold climate region. As India is mostly a tropical country, -1°C CFPP of KME may be acceptable for diesel engine application in India. Moreover, the variation of CFPP with increasing volume fraction of SME and KME in the test fuels was not linear.

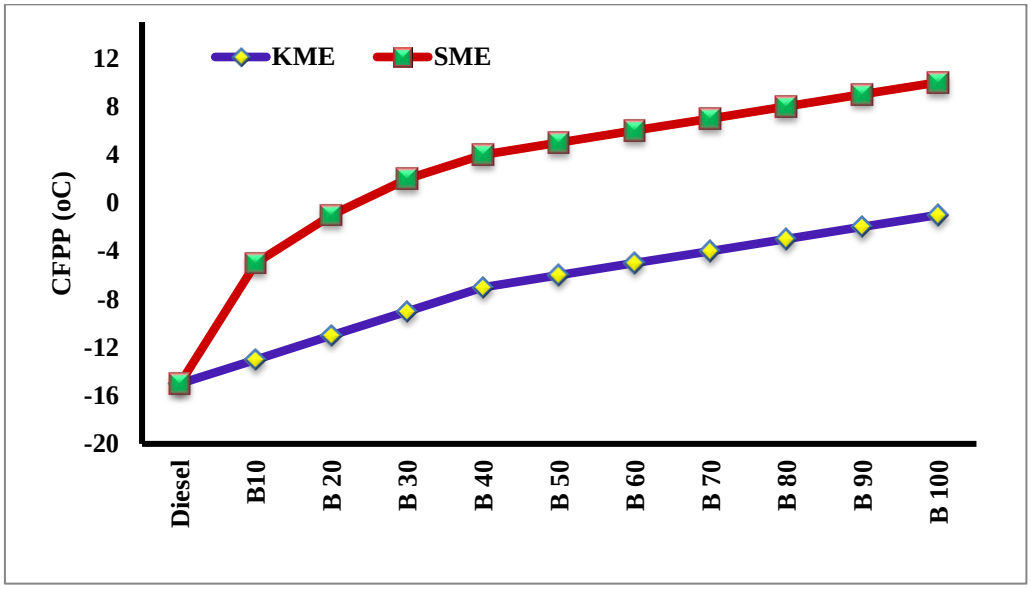

Figure 4.30: CFPP for various test fuels

4.3.9 Oxidation stability

Oxidation stability is one of the most important properties of fatty-acid methyl esters and affects biodiesel primarily during extended storage. As describe earlier, the biodiesel Rancimat method was used for oxidation stability study. The EN14112 standard was followed with 10 L/h air flow and 110 °C bath temperature. The total induction time showed by the SME sample was 6.17 hours as against the standard of six hours. Therefore, the oxidation stability of SME was found to be within the limits of European biodiesel standard. However, the oxidation stability of the Kusum biodiesel was poor i.e. only 1 hour (Figure 4.31), which was lower than prescribed limit. Therefore, addition of antioxidant improved the oxidation stability. To enhance the oxidation stability, antioxidants were employed to prolong the stabilized time of biodiesel. Figure 4.32 shows the conductivity and induction time curve for KME with 0.1% TBHQ of oxidation stability study using Rancimat.

Table 4.2 suggests that KME was rich in double bonds and poly-unsaturated fatty acids such as Oleic (18:1), Linoleic (18:2) and Eicosenoic (20:1) acids. It may be observed that 69% composition by weight of KME contained unsaturated fatty acids and only 31% saturated fatty acids. Due to excess availability of double bonds, KME tends to have higher inclination to react with oxygen. This is consistent with the previous observation of comparatively inferior oxidation stability of KME.

However, availability of unsaturated fatty acids also has some advantages. Due to high reaction tendency, the KME when injected in to the diesel engine suddenly broke in to lighter compounds reducing the ignition delay [260].

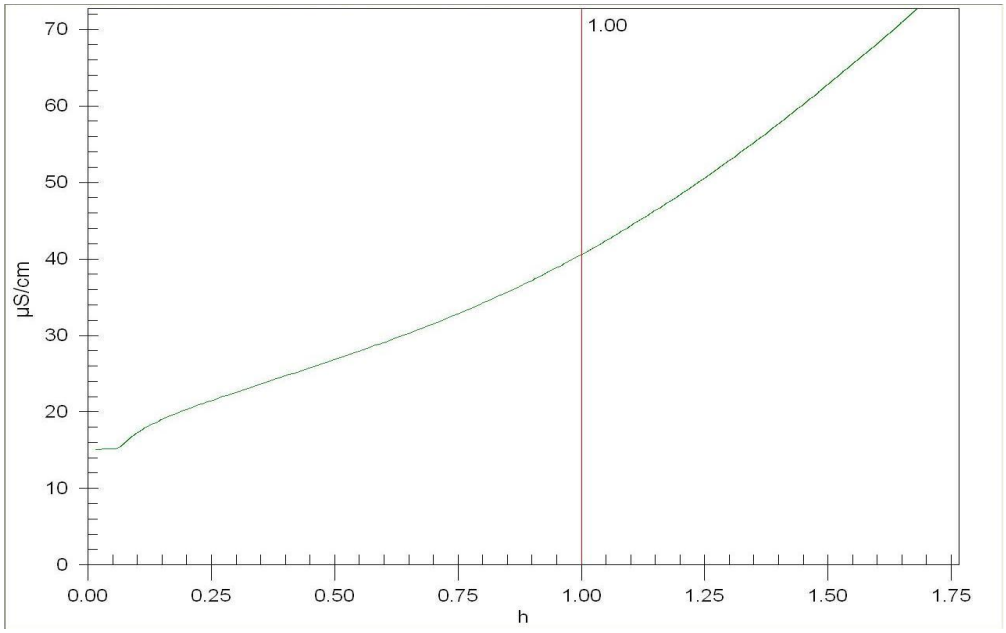

Figure 4.31: Oxidation stability of Kusum biodiesel

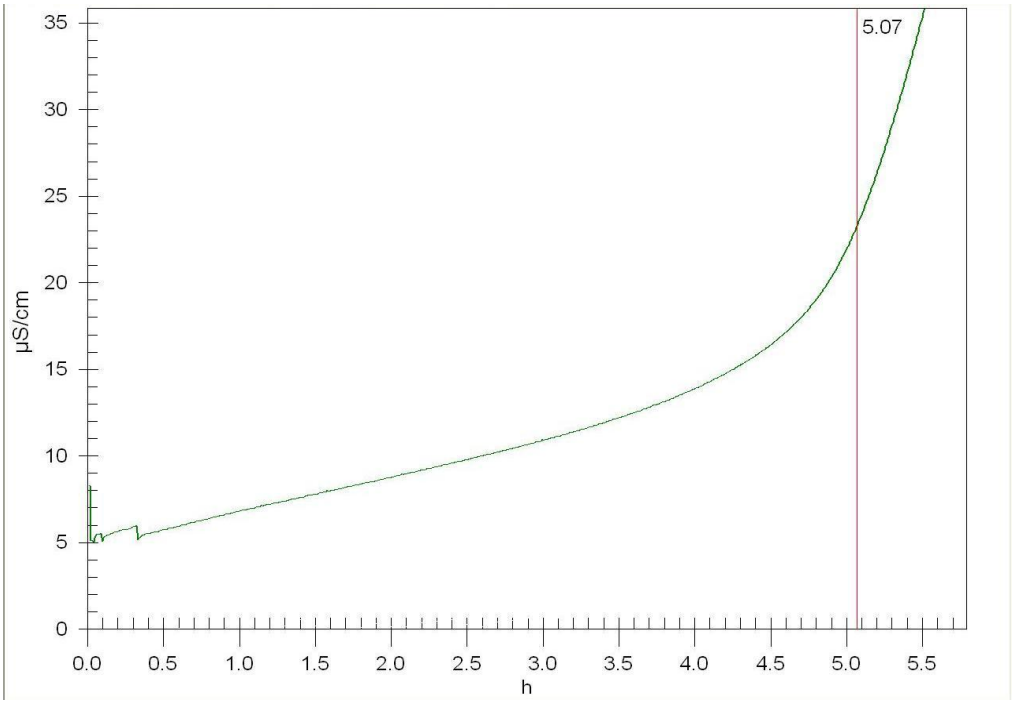

Figure 4.32: Oxidation stability of KME with 0.1% TBHQ

On the basis of the previous discussion, it may be concluded that SME and KME were within the limits of international biodiesel standards except the cold flow properties and oxidation stability for KME. Its various critical physico-chemical characteristics closely

matched with the methyl ester of Jatropha curcas recognized by Government of India as the best oil seed for biodiesel production.

4.3.10 Other physico chemical properties

Physico-chemical properties like specific gravity, water content, dynamic viscosity, carbon residue, pour point, cloud point, lubricity, acid value, iodine value, saponification value and peroxide value were estimated and shown in Table 4.10. The cetane number (CN) of methyl ester was calculated based on the estimated SV and IV using the equation 3.11. Cetane number (CN) defines the ability of fuel to ignite quickly after being injected. Better ignition quality of the fuel is always associated with higher CN value. This is one of the important parameter, which is considered during the selection of methyl esters for use as biodiesel.

Table 4.10- Various physico-chemical properties of SME and KME

Fuel property	**Unit**	**Limits**	**Standard**	**Diesel**	**SME**	**KME**
Density at 15℃	g/cm^3	0.85-0.89	D1298	0.8327	0.8765	0.8967
Specific gravity at 15℃		-	-	0.8335	0.8773	0.8971
API Gravity		-	-	38.572	29.93	26.301
Kinematic viscosity at 40℃	mm^2/s	1.9 – 6.0	D445	3.23	5.79	5.91
Dynamic viscosity at 40℃	Mpa.s	-	-	2.687	5.074	5.299
Viscosity index at 40℃		-	D2270	1070	200.5	185.7
Calorific value	MJ/kg			44.7	39.65	39.11
Flash point	℃	130 min.)	D93	65	172	148
Cloud point	℃		D 2500	-16	17	2
Pour point	℃		D 97	-20	12	0
CFPP	℃		D6371	-15	10	-1
Copper strip corrosion	Rating	No.3	D130	1a	1a	1a
Carbon residue	% m/m	0.050	D189	-	0.025	0.042

Oxidation stability at 110℃	Hours	3 (min.)	EN 14112	-	6.17	1
Acid value	mgKOH/g	0.5 max.	D664	-	0.16	0.13
Iodine value	g I_2/100g	120 max.	EN14111	-	29	52
Saponification value	mgKOH/g		D94	-	255	179
Cetane number		47 (min.)	D613	49	61	65
Peroxide value	meq/kg			-	16.8	20.1
Lubricity	µm	520 max	D6079	441	266	289
Free glycerin	% mass		D6584	-	0.023	0.027
Ester content	% mass		EN14105	-	96.92	96.5

4.4 Effect of Additives on Storage Stability

Poor stability of biodiesel vis-a-vis diesel is because of the double bonds and certain functional groups present in the molecules of biodiesel (as per FTIR and GCMS results). It is therefore essential to evaluate the storage stability of biodiesel. Chemically, biodiesel is an ester molecule and more prone to be hydrolyzed to alcohol and acid in the presence of air or oxygen [261]. Presence of alcohol will lead to reduction in flash point and presence of acid will increase acid number. A comprehensive storage stability study of biodiesel was carried out to assess the degradation of biodiesel during storage and evaluate the effect of additive to improve the storage stability. It was seen that KME did failed the oxidative stability specification EN 14112. In order to enhance the oxidation stability, synthetic antioxidants were used. Antioxidant inhibits the formation of free radicals or interrupts the propagation of free radical and hence contributes to the stabilization of the lipid sample. In this study, two antioxidant namely tert-butyl hydroquinone (TBHQ) and Ecotive were used to study its effect on SME and KME. The antioxidant was added 0.1 % and 0.5 % by weight of oil in the biodiesel sample as discussed earlier in Table 3.9. Application of additive 0.5 % (by weight) passed the minimum limit of Rancimat Induction Period (RIP) of 6 hrs.

So the results of 0.5% doped samples were investigated at every month to observe physico chemical properties of SME and KME. The results are presented in subsequent section. In order to study the storage stability of biodiesel, samples of SME and KME was tested for peroxide value, density, acid number, viscosity and calorific value for a storage period of one year with and without additive. All these parameters were periodically evaluated on monthly basis.

4.4.1 Peroxide value

Figure 4.33 and Figure 4.34 show the variations in peroxide values of SME and KME with and without additive over a storage period of 12 months. The peroxide values have been found to be increasing with storage period both for SME and KME fuels. The additive has slowed the change in peroxide value of both the biodiesel. The peroxide value in case of KME at 0 month was 20.1 meq/kg. It increased by 9.7 times at the end of the test. The peroxide value in case of SME at 0 month was 16.8 meq/kg and it was 7.86 times at the end of 12^{th} month. Also, SME (39% unsaturated) has been found to be more stable as compared to KME (69% unsaturated) as far as oxidation is concerned.

It has been observed that the additive TBHQ has exhibited better results than ECOTIVE. Both antioxidants slowed down the oxidation of SME and KME significantly. The increase in peroxide value was lowered at the end of test for SME and KME with the addition of this additive.

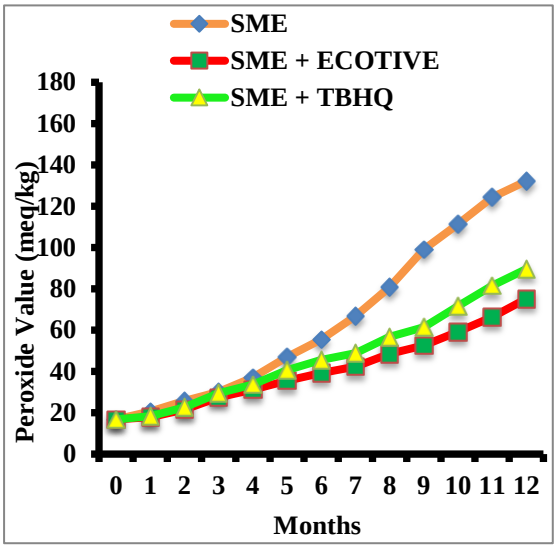

Figure 4.33: Effects of antioxidants on peroxide value of SME

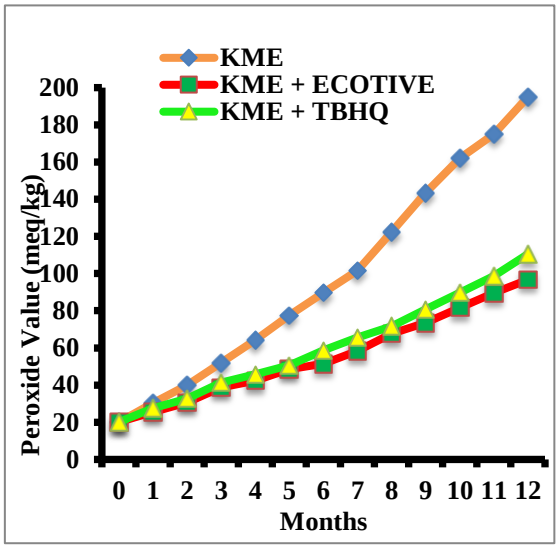

Figure 4.34: Effects of antioxidants on peroxide value of KME

4.4.2 Density

Figure 4.35 and Figure 4.36 represents the variation of density of SME and KME with and without additive over a storage period of 12 months. The densities have been found to be increasing with storage period both for SME and KME fuels. The rate of increase was found to be more for KME than for SME. The density in case of SME and KME at 0 months was 0.8765 and 0.8967 g/cm^3 which increased to 0.8816 g/cm^3 and 0.9037 g/cm^3 at end of the test. A similar trend of increase in density for SME and KME with additive TBHQ and ECOTIVE have also been observed. However, the both additives marginally affected densities of KME and SME. Partial increase in densities of both the biodiesel was observed with or without additive. Anti-oxidant TBHQ showed better performance than ECOTIVE.

4.4.3 Kinematic viscosity

The variation of kinematic viscosity of SME and KME with and without additives over a storage period of 12 months is represented in Figure 4.37 and Figure 4.38 respectively. The values of viscosity have been found marginal increase with storage period up to first 6 months for SME and KME fuels. The rate of increase was found to be more for KME than

SME. The viscosities in case of SME and KME at 0 month were 5.79 and 5.91 cSt, respectively i.e. close to ASTM limit.

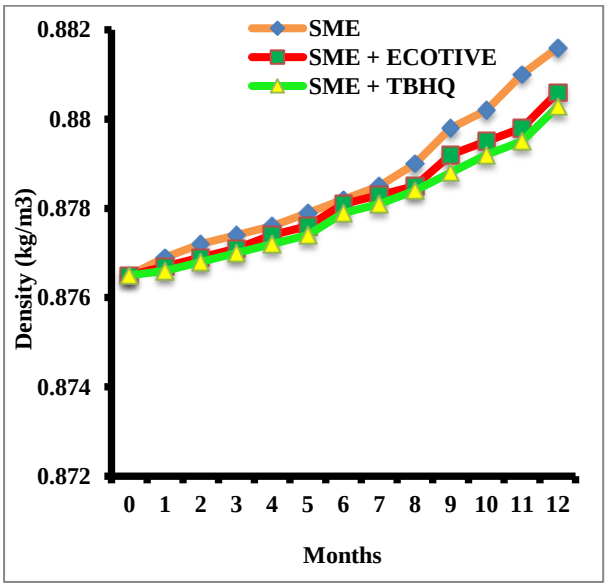

Figure 4.35: Effects of antioxidants on Density of SME

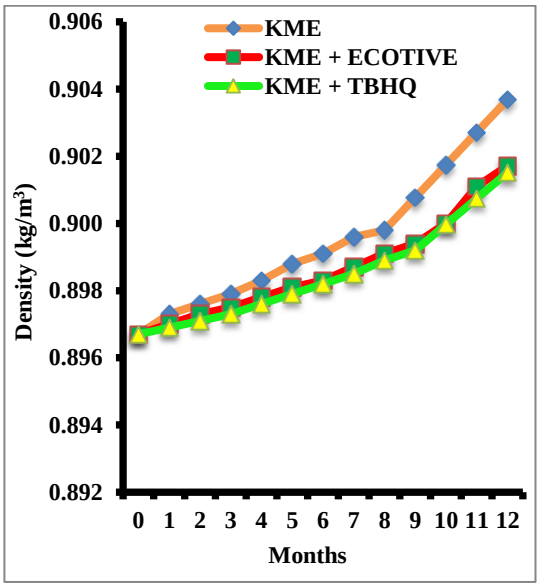

Figure 4.36: Effects of antioxidants on Density of KME

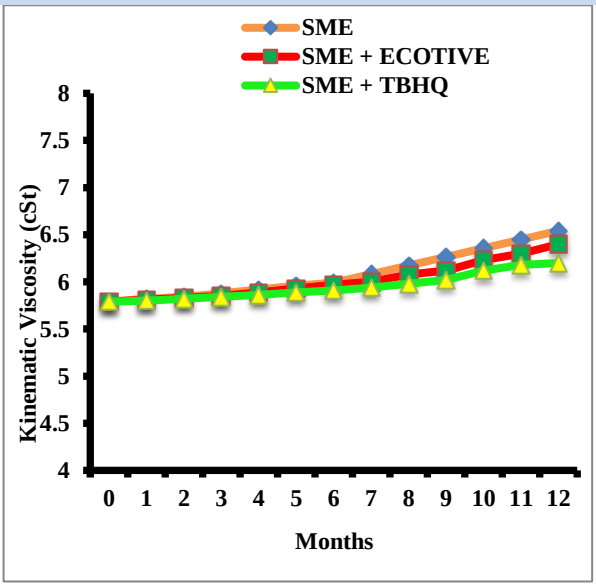

Figure 4.37: Effects of antioxidants on kinematic viscosity of SME

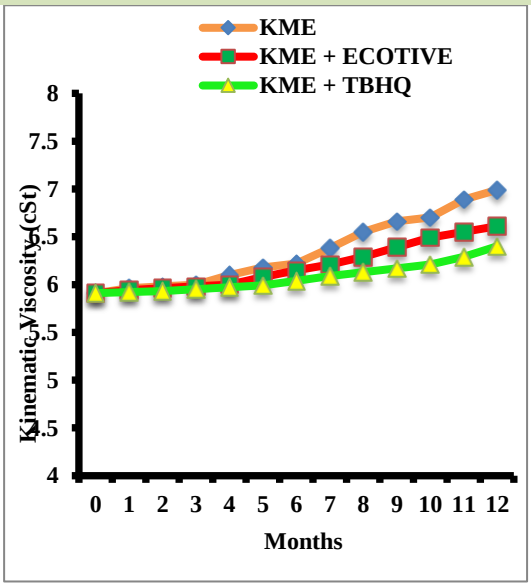

Figure 4.38: Effects of antioxidants on kinematic viscosity of KME

The SME reached to the value of 6.04 cSt in the 8th month and became off specification, whereas KME reached the value of 6.02 in 5th month and became off

specification. At end of the test, the viscosities for SME and KME were 6.54 and 6.99 cSt respectively, indicating an increase of around 13% and 18% from 0 month.

TBHQ showed better performance from ECOTIVE. In fact with the use of TBHQ, SME become off specification even after 10 months whereas KME became off specification on the seventh month.

4.4.4 Acid number

Figure 4.39 and Figure 4.40 represent the variation of acid number (AN) of SME and KME with and without additive over a storage period of 12 months. The Acid number has been found to be partially increased up to six months for both test fuels. The rate of increase was found to be more for KME than for SME. The AN in case of SME and KME at 0 months were 0.16 and 0.13.

The SME reached to the AN value of 0.49 in the 10^{th} month and became off specification, whereas KME reached to the AN value of 0.52 in 9^{th} month and became off specification. At end of the test, AN for SME and KME were 0.78 and 0.82 respectively almost 5 and 7 times increase from 0 month. It showed the tendency of increasing acidity in biodiesel with storage.

The additives have slowed the increase in AN for both the biodiesel. ECOTIVE showed better results than TBHQ. In fact with the use of ECOTIVE, SME become off specification even after 12 months whereas KME became off specification in 10 months.

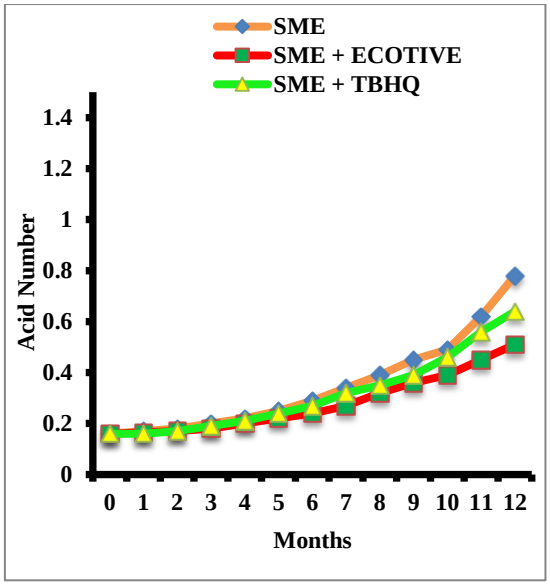

Figure 4.39: Effects of antioxidants on acid number of SME

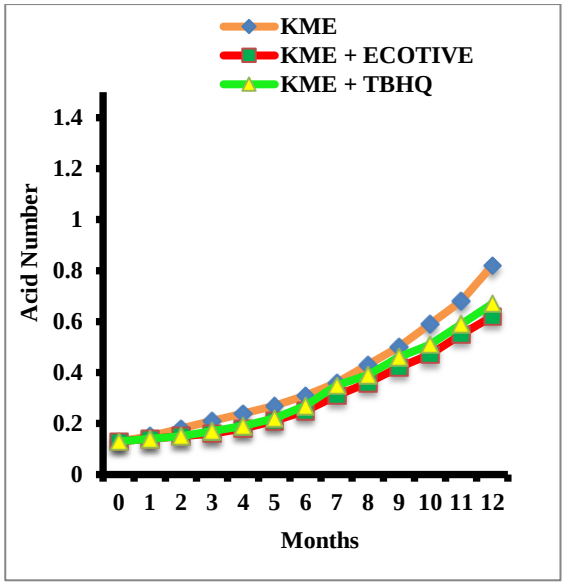

Figure 4.40: Effects of antioxidants on acid number of KME

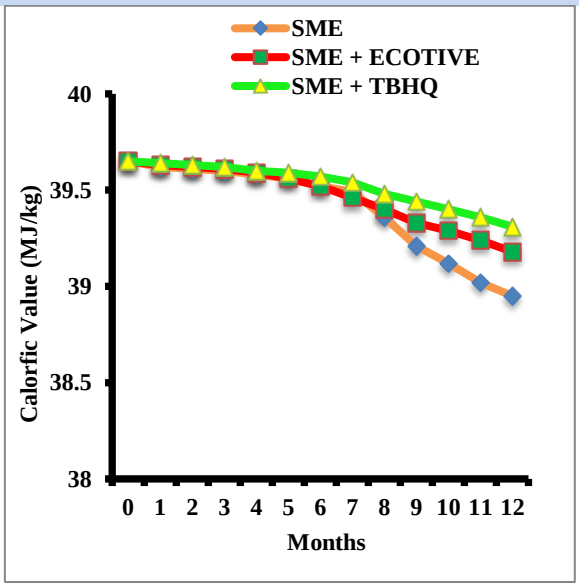

Figure 4.41: Effects of antioxidants on calorific value of SME

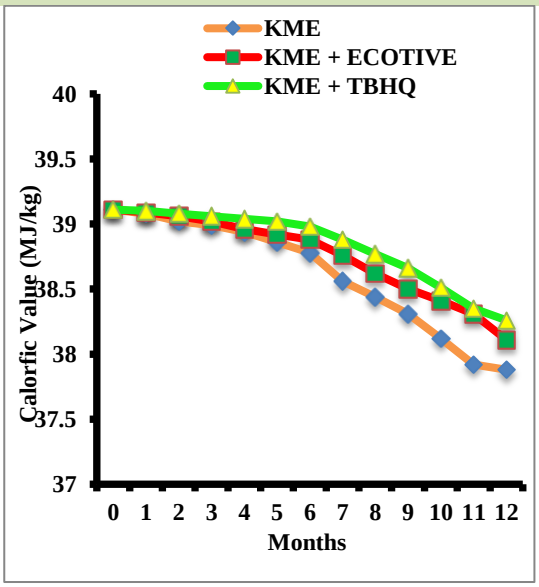

Figure 4.42: Effects of antioxidants on calorific value of KME

4.4.5 Calorific value

The variation in calorific value of SME and KME fuels was insignificant for first 6 months with and without additives as shown in Figure 4.41 and Figure 4.42 respectively. However, calorific values have been found to be diminishing with storage period both for SME and KME fuels. The rate of decrease was found to be more for KME than for SME. The calorific values in case of SME and KME at 0 months were 39.65 and 39.11 (MJ/kg),

respectively. At the end of the test, calorific values for SME and KME were 38.95 and 37.88 MJ/kg respectively.

Both additives inhibited degradation of biodiesel, thus the calorific value for both the biodiesel TBHQ showed improved calorific value to the ECOTIVE.

4.4.6 Flash point

Figure 4.43 and Figure 4.44 represents the variation of flash point of SME and KME with and without additive over a storage period of 12 months.

The values of flash point have been found to be decreasing with storage period both for SME and KME biodiesels. The flash point in case of SME and KME at 12 month was 111 and 98 °C respectively.

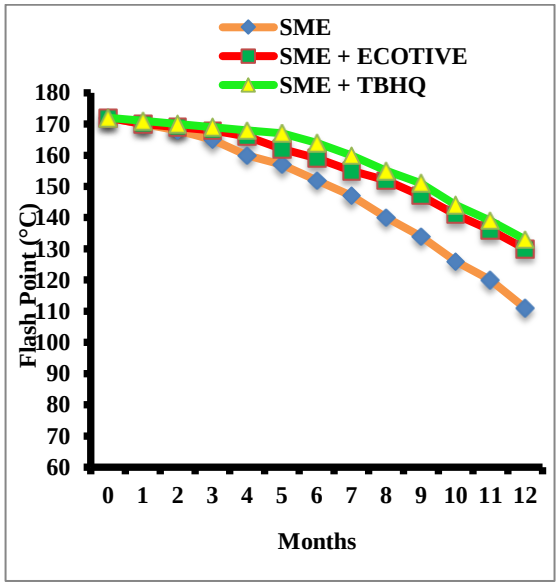

Figure 4.43: Effects of antioxidants on flash point of SME

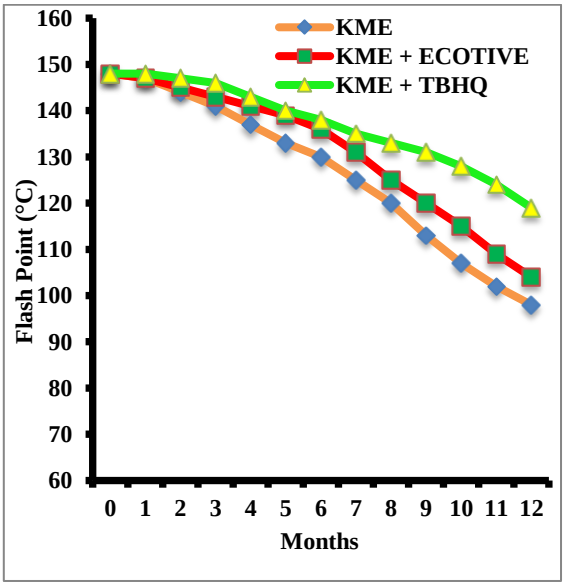

Figure 4.44: Effects of antioxidants on flash point of KME

The both additives have slowed down the decrease in flash point of both the biodiesel and with the additives. The additives have slowed down the decrease in flash point of both the biodiesel and TBHQ showed better performance to ECOTIVE. SME did not become off

specification even after the entire test of 12 months whereas KME became off specification in the 10^{th} month for TBHQ.

4.5 Effect of Additives on CFPP of Biodiesel

An inherent problem with biodiesel is its tendency to solidify at cold temperatures. This risk of solidification often limits the extensive use of biodiesel. The biodiesel fuels derived from fats or oils with significant amounts of saturated fatty compounds will exhibit higher cloud points and pour points. Crystallization of the saturated fatty acid methyl ester components of biodiesel during cold seasons causes fuel starvation and operability problems as solidified material clog fuel lines and filters.

With decreasing temperature more solids form and material approaches the pour point, the lowest temperature at which it will cease to flow [175].

In addition, several polymer additives are evaluated based on their ability to lower the pour point (PP) and cold flow plugging point (CFPP) of biodiesel [262]. Pour point (PP) and cold filter plugging point (CFPP) are important indices related to low-temperature operability of diesel fuels. The pour point is the temperature at which a fuel can no longer be poured due to gel formation, while the cold filter plugging point is the temperature at which a fuel jams the filter due to the formation of agglomerates of crystals [207].

Various dispersing agents often referred to as pour point depressants (PPD), have been proposed. Most PPDs have been designed to prevent growth of wax crystals in fuel. Major classes of diesel PPDs are poly (malefic-anhydride) copolymers , poly(vinyl acetate) copolymers and so on [263]. In the present work kerosene, EVA, Lubrizol and CRISTOL were used as pour point depressants. Kerosene used as extender 5% and 10% whereas other PPDs were used 1% and 2% as additive.

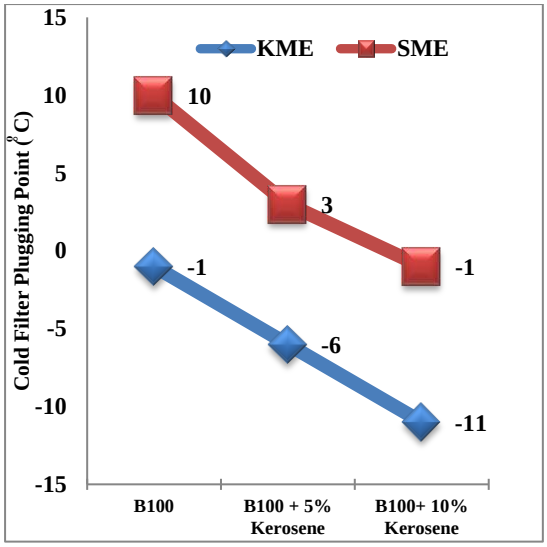

Figure 4.45:Blending with Kerosene

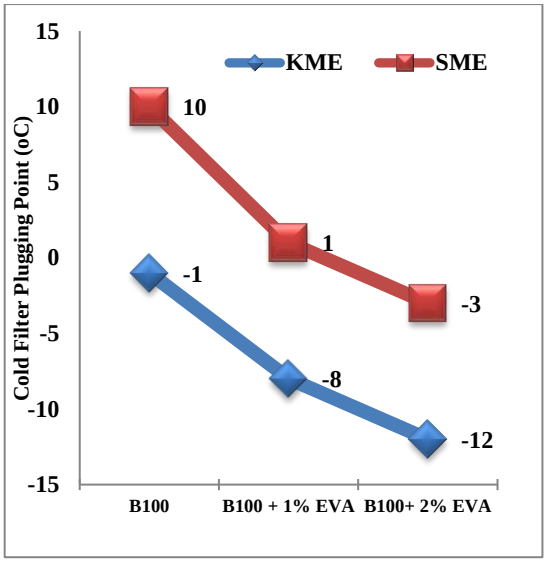

Figure 4.46: Blending with Ethyl Vinyl Acetate (EVA)

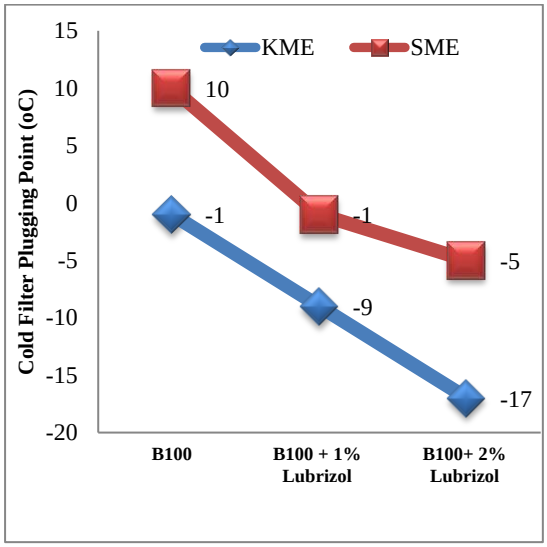

Figure 4.47*:* Blending with Lubrizol 7671

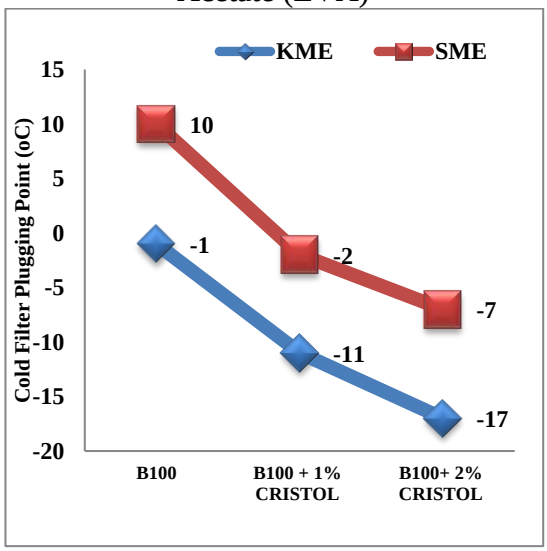

Figure 4.48: Blending with CRISTOL BIO

The cold filter plugging point (CFPP) was measured at a specified rate by drawing the liquid under vacuum through a wire mesh filter screen. The CFPP may be defined as the lowest temperature at which a fixed volume of sample safely passes through the filter within 60 s. In addition, the uncertainties were calculated to confirm that each instrument meets the limits of accuracy as set by the specifications of the standard method. Figure 4.45 shows the effect of the kerosene oil on SME and KME. Kerosene oil was used as blending stock 5% and 10% substitution by volume. Results showed 10% blend of kerosene improved the CFPP

of SME were -1℃ and KME were -11℃. Figure 4.46, Figure 4.47 and Figure 4.48 were confirmed the effects of Ethyl Vinyl Acetate (EVA), Lubrizol 7671 and CRISTOL BIO respectively.

All these pour point depressants showed improved CFPP with increased vol. % of additive. Lubrizol and CRISTOL BIO showed the significant reduction in CFPP. Among all three additives CRISTOL BIO proved the best results.

4.6 Engine Performance Results

The impact of Sal and Kusum biodiesel/diesel blend (up to 40%) fuel was compared baseline diesel. Engine performance at partial to full load conditions was studied regarding brake thermal efficiency (BTE), brake mean effective pressure (BMEP), brake specific energy consumption (BSEC) and exhaust gas temperature (EGT).

4.6.1 Brake thermal efficiency

The brake thermal efficiency (BTE) is a vital engine performance parameter. It is a parameter to represent how efficiently an engine transforms the chemical energy of the fuel into useful work. This is the ratio determined by brake power in the output shaft divided by the amount of energy delivered to the engine [264]. It was observed that with increasing load, BTE of the engine was increased for all test fuels. This was attributed to the fact that at higher loads more power was generated and heat loss was reduced [40,177,187].

For all the fuels, BTE has the tendency to increase with increase in applied load. This is due to the reduction in heat loss and increase in power developed with increase in load. According to the engine mapping (calibration) 0% (no load), 20%, 40%, 60%, 80% and 100% are approximately identical to the BMEP 0.127 bar, 1.534bar, 2.883 bar, 4.320 bar, 5.785bar

and 6.816 bar respectively. So the results are presented with respect to the BMEP. Variation of BTE with BMEP for the SME test fuels is shown in Figure 4.49, while KME test is shown in Figure 4.50.

BMEP is a mean pressure; which, if imposed on the pistons uniformly from the top to the bottom of each power stroke, would produce the measured (**brake**) power output. It then reflects the product of volumetric efficiency, fuel/air ratio and fuel conversion efficiency.

It is more useful relative to performance, which is obtained by dividing the work per cycle by cylinder volume displacement per cycle. Figures 4.49 and Figure 4.50 depict BTE versus BMEP for all selected SME and KME fuel blends respectively.

Both the figures showed slight improvement in BTE with biodiesel addition up to 20 % and decreasing trend beyond 20% substitution level.

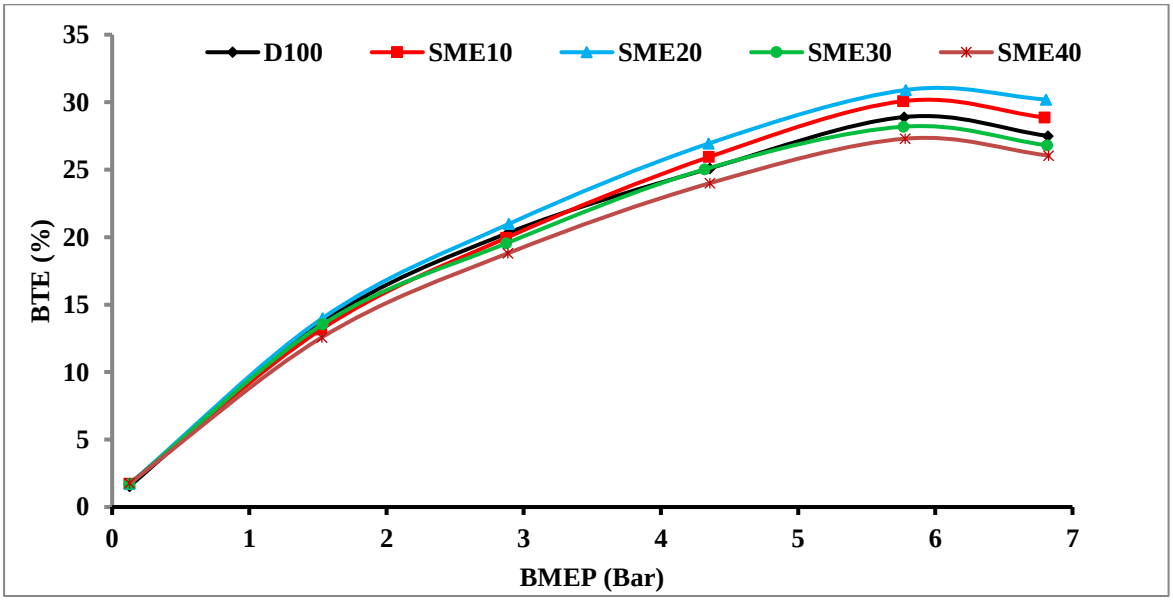

Figure 4.49: BTE *vs* BMEP for SME fuel blends

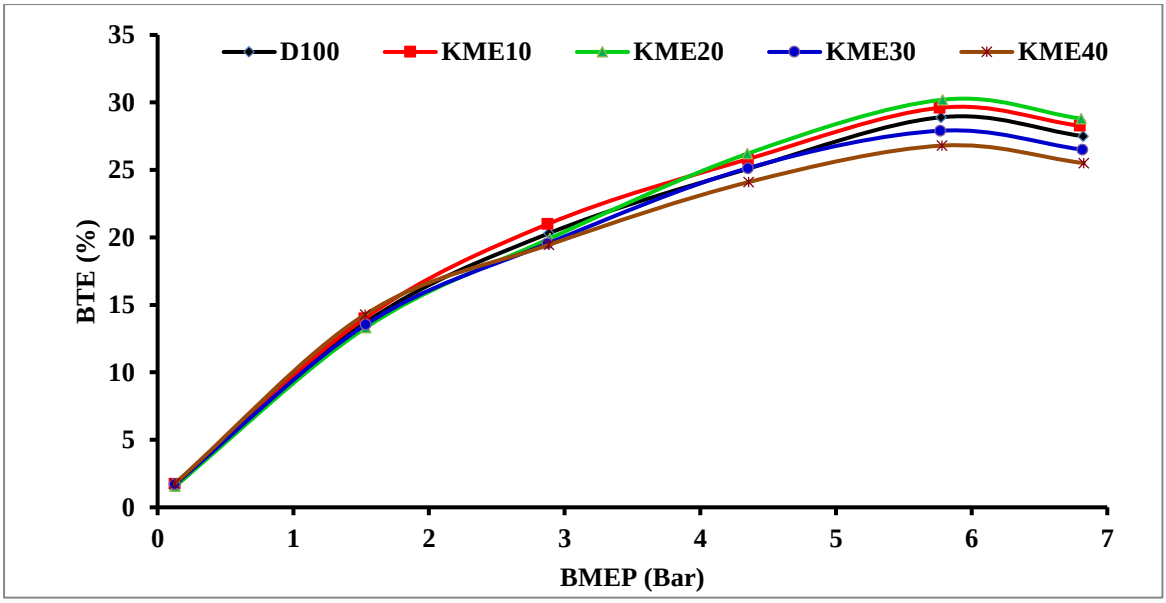

Figure 4.50: BTE *vs* BMEP for KME fuel blends

The biodiesel contain some amount of oxygen, which takes part in the combustion process. It is observed that after a certain limit with respect to biodiesel blends, the thermal efficiency trend was reverted and it started decreasing as a function of the concentration of biodiesel blend. This may be due to improved combustion with lower percentage substitution of biodiesel in diesel and this effect being offset at higher substitution due to lower calorific value [35].

The maximum thermal efficiency has been observed at 20% substitution of both SME and KME in diesel. However, it was found to be higher for SME20 as compared to KME20. The lower BTE obtained for SME40 and KME40 could be due to the reduction in calorific value and increasing fuel consumption as compared to lower concentration biodiesel-diesel blends. This indicates that the thermal efficiency is a more representative reflection of the fuel economy by using the diesel equivalent BSFC or energy consumption rate when operated on oxygenated fuels like biodiesel. The above results are in agreement with the results reported by Ramadhas et al., [92]; Karnwal et al., [265] and Pali et al., [257] on different tree borne biodiesels.

The variation of BTE of all the test fuels at full load is shown in Figure 4.51. It was observed that SME20 and KME20 exhibited 30.2% and 28.8% full load BTE, respectively as compared to 27.5% illustrated by diesel baseline. On the other hand, SME30 and KME30 showed 26.8% and 26.5% full load BTE respectively, lying close to the baseline. However, the usage of B40 in the engine trial demonstrated 25.5% full load BTE. In a nutshell, it may be stated that thermal efficiency of the diesel engine was increased with increasing volume fraction of biodiesel up to 20%. As an oxygenated fuel as it was, biodiesel, led to complete combustion even at lower equivalence ratio zones [85]. Secondly, the lower flame temperature of the blends than diesel led to reduction in heat loss [154]. Engine operated at 30% substitution of biodiesel was found to be the inflexion point, beyond which; the reductions in higher load thermal efficiency as compared to neat diesel operation were significant. This reduction in thermal efficiency was observed due to lower calorific value, higher viscosity and density, poor atomization/vaporization, increase in fuel consumption *etc.* starts negating the gain [177,186,266].

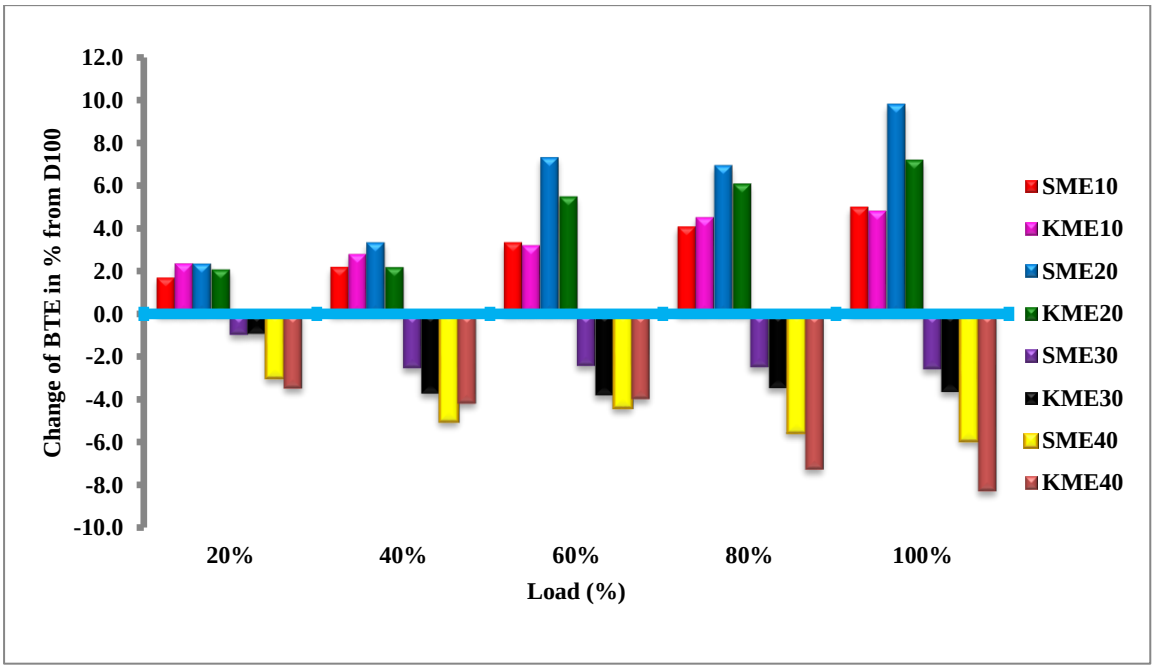

Figure 4.51: % change in BTE from diesel baseline at various loads

Figure 4.51 shows the variation in BTE of various test fuels compared to the baseline data at all loading conditions. It is significant to note that up to 20% blending of SME and KME exhibited higher BTE than the baseline diesel. This may be attributed to the fact that, the higher A/F ratio at 40% load coupled with the oxygenated nature of biodiesel led to improved combustion even at higher volume fractions. SME10, KME10, SME20 and KME20 illustrated higher BTE at all loads compared to the baseline data.

In the light of the above results, it may be concluded that the engine performance in terms of BTE was improved with biodiesel blends up to 20% substitution. Beyond B30, it resulted in reduction of thermal efficiency as compared to the diesel baseline. Similar results were obtained by several researchers using on biodiesel derived from Apricot oil, Karanja oil, Mahua oil, Polanga, Waste cooking oil, Rape seed oil etc [85,187,189,194,267–269].

4.6.2 Brake specific energy consumption

Comparative assessment of volumetric consumption of fuel is an important parameter in explain the engine performance of different test fuels. In this context, BSFC; which is a ratio between mass flow rates of fuel to the brake power has been used as a conventional parameter. However, BSFC has not been considered as a reliable parameter when the calorific values and densities of test fuels vary considerably [189]. In this case, SME exhibited 5.35% and KME exhibited 7.77% higher density and 11.25% and 12.5% less calorific value respectively than diesel. Therefore, BSEC was considered as more reliable assessment method for comparison of volumetric fuel consumption.

Variation of BSEC with BMEP for the test fuels under designated conditions of load is shown in Figure 4.53 and Figure 4.54. It may be observed that SME10, SME20, SME30 and SME40 pursued full load BSEC of 13.31 MJ/kWh, 13.01 MJ/kWh, 14.45 MJ/kWh and

14.77 MJ/kWh respectively as compared to 13.62 MJ/kWh illustrated by the baseline diesel operation. Conversely, KME10, KME20, KME30 and KME40 exhibited 12.99 MJ/kWh, 13.3 MJ/kWh, 14.22 MJ/kWh and 14.77 MJ/kWh respectively.

Therefore, it may be concluded that up to 20% volume fraction of SME and KME in the diesel, full load BSEC was found to get reduced whereas, beyond 30% substitution of diesel by biodiesel led to increased full load BSEC compared to the neat diesel operation. The reduction in BSEC at lower volume fractions of SME and KME may be attributed to the enhanced combustion as discussed earlier. However, the increase in BSEC beyond 30% substitution of biodiesel in the fuel was mainly due to the combined effects of the relative fuel density, viscosity and heating value of the blends. The higher density of Sal and Kusum biodiesel has led to more discharge of fuel for the same displacement of the plunger in the fuel injection pump, thereby increasing the specific energy consumption [186,189].

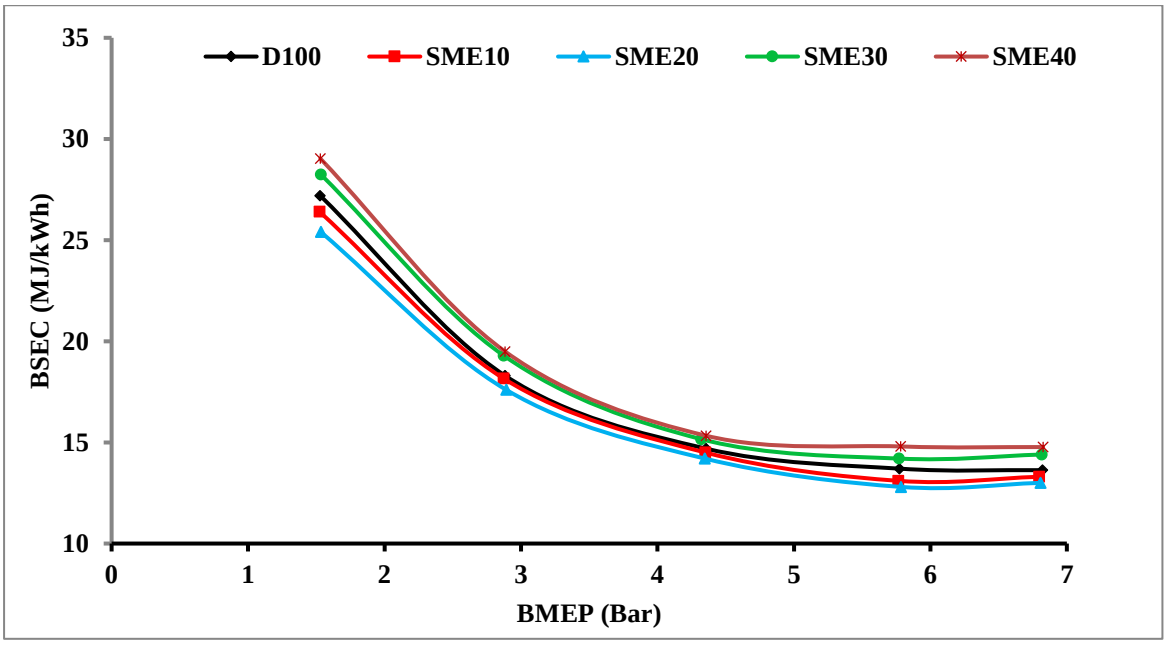

Figure 4.52: BSEC *vs* BMEP for SME fuel blends

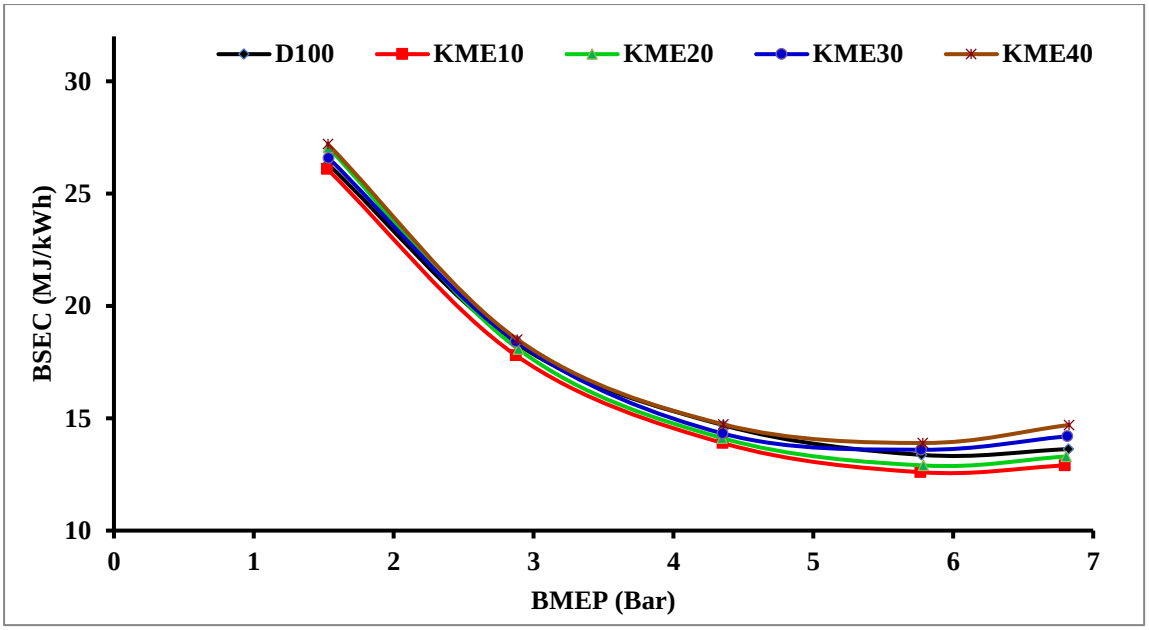

Figure 4.53: BSEC *vs* BMEP for KME fuel blends

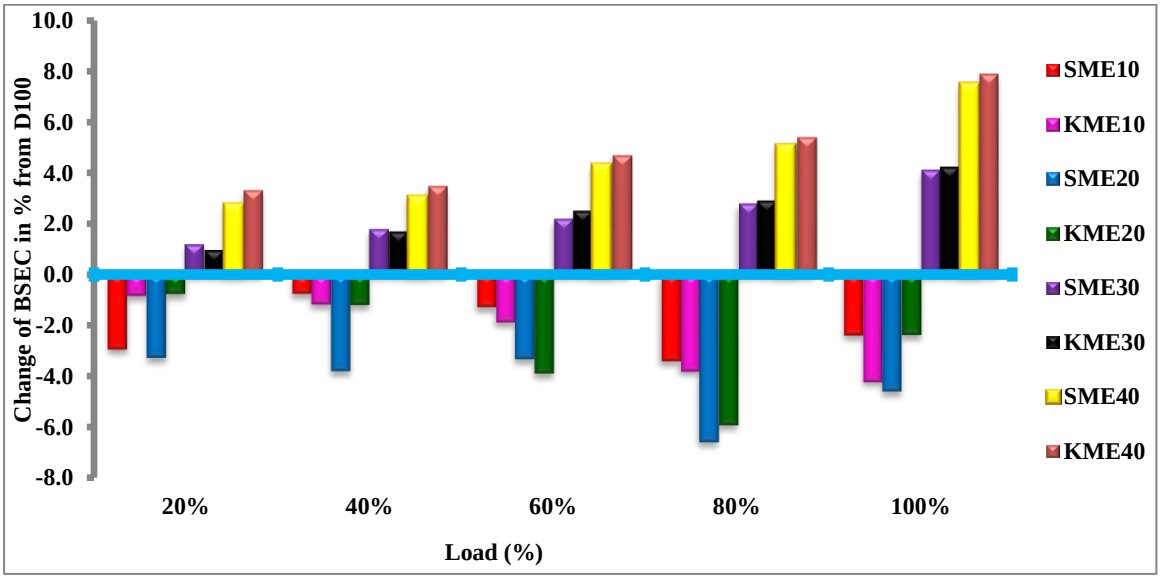

Figure 4.54: % change in BSEC from diesel baseline at various loads

Figure 4.54 shows the variation in BSEC from diesel baseline for various test fuels under the designated loading conditions. It was observed that BSEC was found to get reduced with increasing volume fraction of biodiesels up to 20%. Various reductions shown by the test fuels compared to the baseline data were 2.41%, 4.19%, 4.61%, and 2.39% for SME10, KME10, SME20 and KME20 respectively. It may be observed that SME20 and KME10 exhibited better reduction in BSEC compared to the baseline data at higher loading

conditions. On the contrary SME30, KME30, SME40 and KME40 illustrated higher BSEC than neat diesel data at all loading conditions. Similar type of results were obtained by several researchers [49,270–273].

4.6.3 Exhaust gas temperature

The variation of exhaust gas temperature (EGT) with BMEP is shown in the Figure 4.55 and Figure 4.56. It may be observed that temperature of the engine exhaust gases varies linearly with load for all test fuels. Temperature in the baseline diesel increased from 159°C at no load to 550°C at full load with an almost linear rise with applied load on the engine shaft. This similar pattern was observed with other test fuels with different temperature rise rate with loads. The increase in exhaust temperature with loads may be due to increased amount of fuel burnt inside the engine at higher loads to generate the requisite BMEP [274,275]. SME and KME blends exhibited lower EGT pattern to the baseline data of diesel.

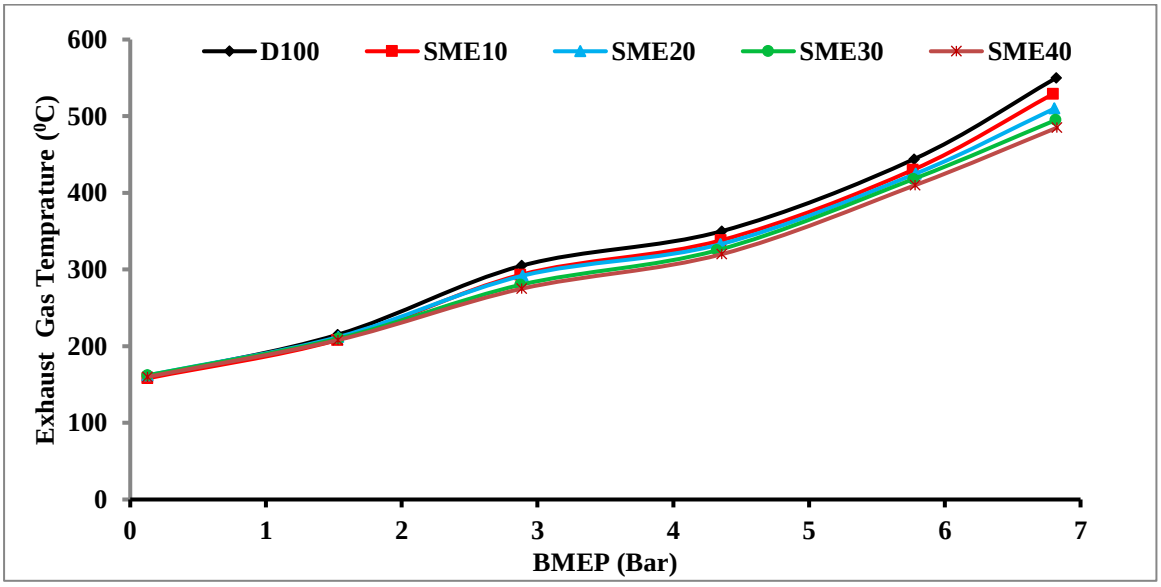

Figure 4.55: Exhaust gas temperature *vs* BMEP for SME fuel blends

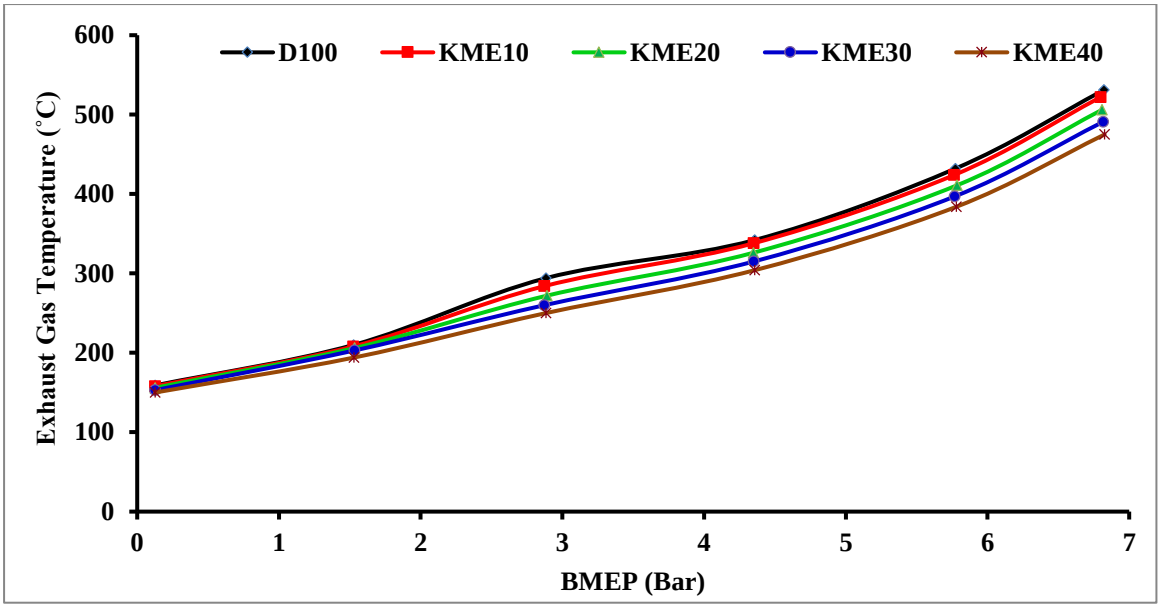

Figure 4.56: Exhaust gas temperature*vs* BMEP for KME fuel blends

Percentage variation of EGT from the baseline data of diesel at various loads is shown in Figure 4.57. All test fuel SME10, SME20, SME30, SME40, KME10, KME20, KME30 and KME40 showed 2.4%, 4.6%, 4.1%, 7.5%, 1.7%, 4.7%, 7.5% and 10.5% reduction in EGT at full load to the baseline data of diesel.

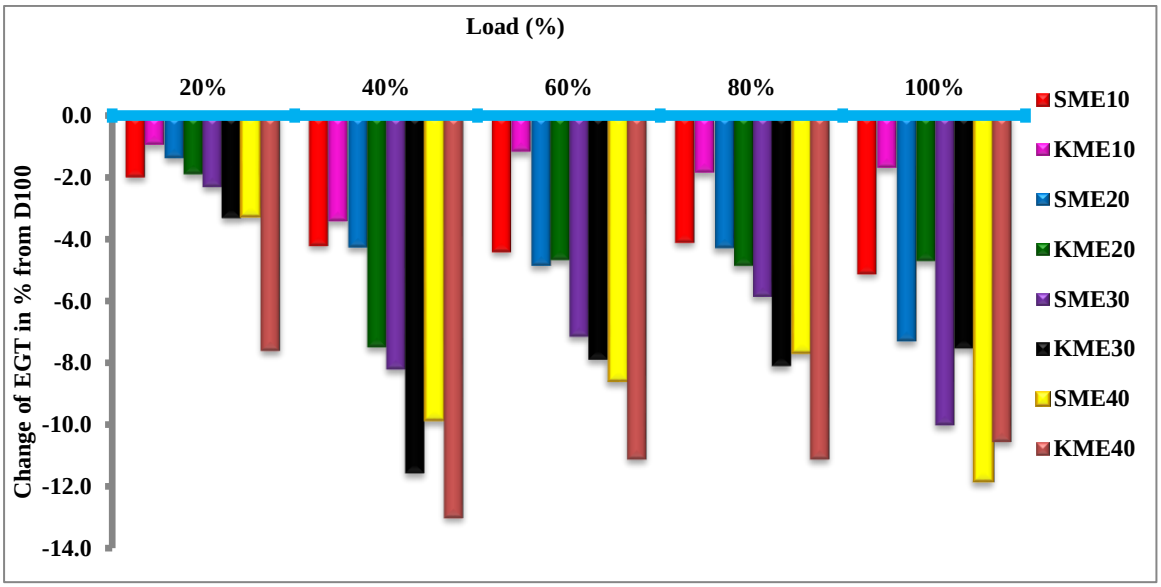

Figure 4.57: % Variation of exhaust gas temperature from diesel baseline at various loads

The lower exhaust temperature is an indicator of earlier combustion and a lower heating value of the biodiesel fuel; thus, the earlier combustion allows more time and crank angle for the expansion process of these fuels so that most of the increased heat release was converted into useful work resulting in reduced exhaust temperature [247,276]. Results are consistent with the present experiment and were reported by various researchers [68,78,133,134] working on a variety of vegetable oil esters.

4.7 Engine Emissions Results

In this section, engine emissions of Sal and Kusum biodiesel/diesel blend (up to 40%) fuel were compared baseline diesel. Results are analyzed from partial to full load conditions was studied based on the emissions of carbon monoxides (CO), carbon dioxides (CO_2), total hydrocarbons (THC), oxides of nitrogen (NO_x) and smoke opacity.

4.7.1 Carbon monoxide emission

Carbon monoxide is considered as a major diesel engine pollutant. The formation of CO during combustion in diesel engines is primarily attributed to lower fuel-air equivalence ratios of combustible mixtures [277]. However, factors like combustion chamber design, atomization rate, start of injection timing, fuel injection pressure, engine load, speed etc. may affect formation of CO at varied influences [15,278]. The emission of CO with BMEP for various test fuels are shown in Figure 4.58 and Figure 4.59 for SME and KME blends respectively.

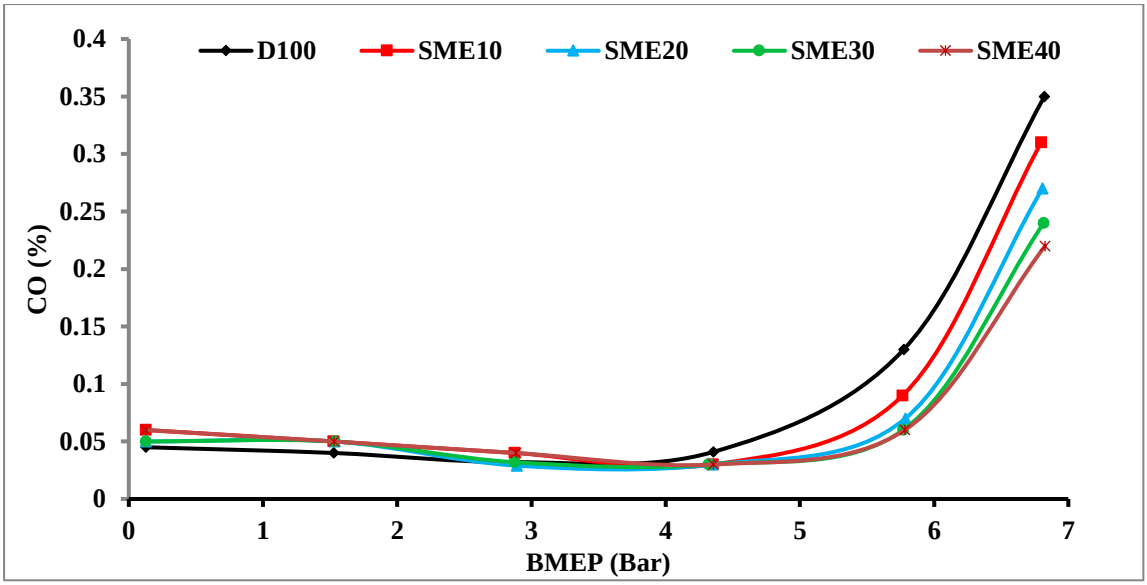

Figure 4.58: Carbon monoxide emissions *vs* BMEP for SME Fuel Blends

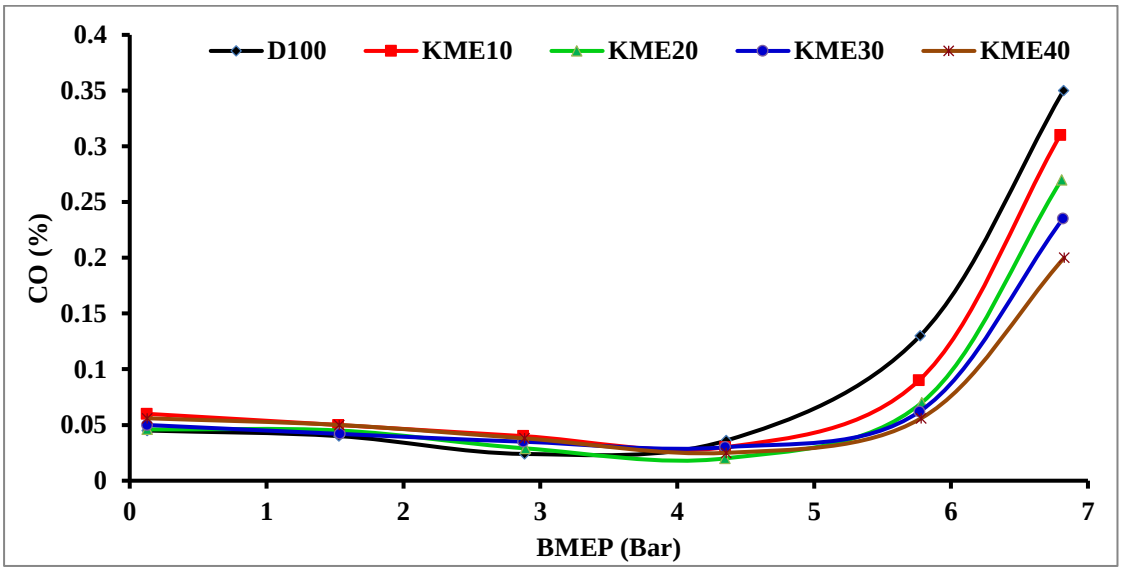

Figure 4.59: Carbon monoxide emissions *vs* BMEP for KME Fuel Blends

It may be noted that initially the emissions of CO were lower for all test fuels. However, after 60% load a steep hike in CO emission was observed irrespective of test fuels. This is attributed to the fact that at no load condition, in-cylinder temperatures are fairly low led to incomplete combustion; however, with increase in load, temperature got elevated due to burning of more fuel injected in to the cylinder. At higher temperatures improved burning of the fuel reduces CO emissions [81,279,280].

Interestingly beyond 60%load, higher amount of fuel injection into the engine leads to incomplete combustion and steep increase in CO emissions. A load specific analysis of variation of CO emissions from various blends of SME and KME were compared to the baseline data is shown in Figure 4.58 and Figure 4.59 respectively. It was observed in the engine trial that; up to 40% engine load, biodiesel and its blends illustrated higher CO emissions than the diesel baseline as indicated in the Figure 4.60.

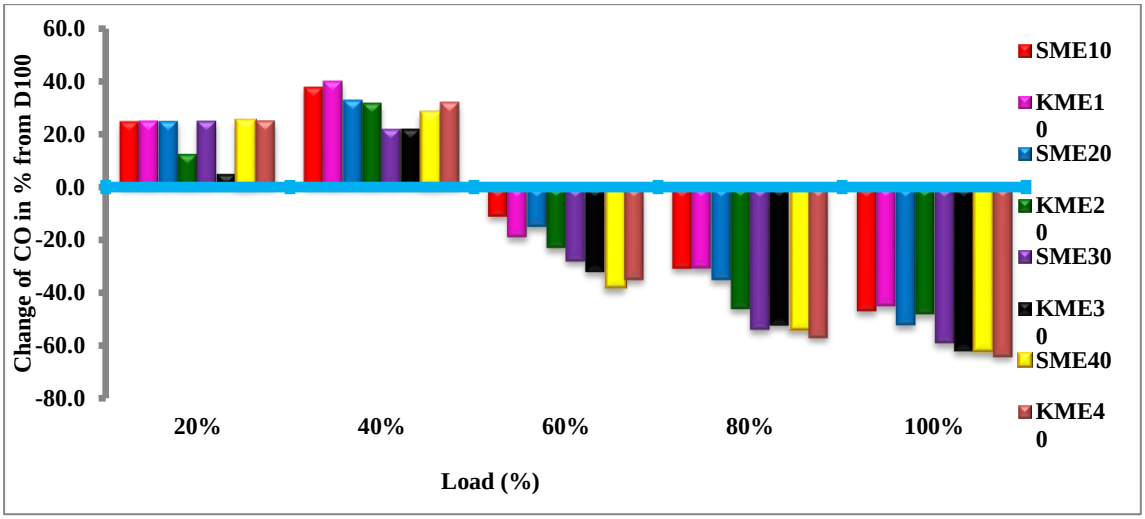

Figure 4.60: %Variation of CO emission from diesel baseline at various loads

This may be attributed to the theory that the air–fuel mixing process was affected by the difficulty in atomization of biodiesel due to its higher viscosity resulting in locally rich mixtures of biodiesel and consequent higher CO emissions [12]. This also can be explained in terms of the premixed lean combustion in presence of excess air in these loads that makes the effect of biodiesel on CO emission reductions less tangible.

At full load 47.14%, 45.05%, 52.13%, 48.25%, 59.36%, 61.89%,61.23% and 63.77% reductions in carbon monoxide emissions were observed for SME10, KME10, SME20, KME20, SME30, KME30, SME40 and KME40 test fuels respectively as compared to the full load neat diesel operation.

Reduction in emissions of CO for SME and KME blends were observed at higher loads (<60%) may be attributed by the fact that biodiesel is an oxygenated fuel with lesser C/H ratio than diesel resulting in enhanced combustion [281]. One significant observation in the experiment reiterates that the reduction in CO emissions are not a function of SME or KME volume fraction in the test fuel i.e. reductions in CO emissions are evident with increase in volume fractions biodiesel in the test fuel, but the trend is not linear. Similar observations were reported by Panichelli et al., [282]; Rashed et al., [283] and Lapuerta et al., [264].

4.7.2 Total hydrocarbon emissions

Emissions of total hydrocarbons (THC) with BMEP are shown in Figure 4.61 and Figure 4.62 for SME and KME blends respectively. The detail mechanism of formation of hydrocarbons inside engine cylinder during combustion and its theoretical study is still at infancy and elusive [284]. However, certain factors like in engine cylinder crevices, engine configuration, fuel structure, combustion temperature, oxygen availability, residence time etc. are presumed to affect the hydrocarbon emissions in compression ignition engines [285–287].

In the present study reduction in emissions of hydrocarbons was reported with increase in SME and KME volume fractions, however, the trend was not linear. At partial loads, there was no significant variation in THC emissions between diesel and the blends. However, at higher and full load both biodiesel blends were exhibited significantly lower emission as compared the baseline data of diesel**.** Variation in hydrocarbon emissions exhibited by various test fuels at the designated conditions of load is shown in Figure 4.63.

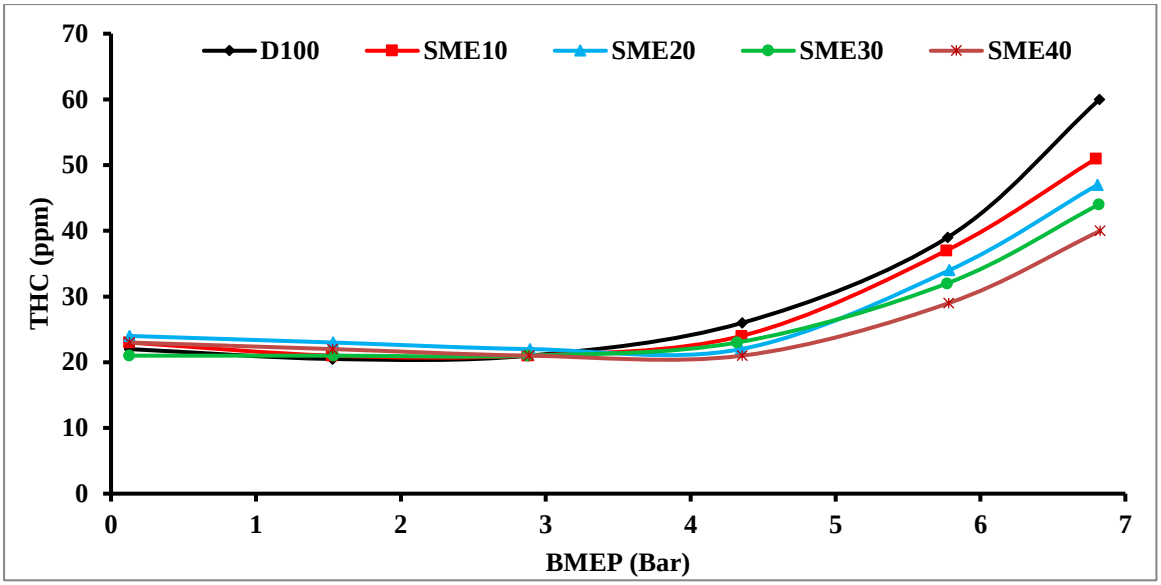

Figure 4.61: Total hydrocarbon emissions *vs* BMEP for SME Fuel Blends

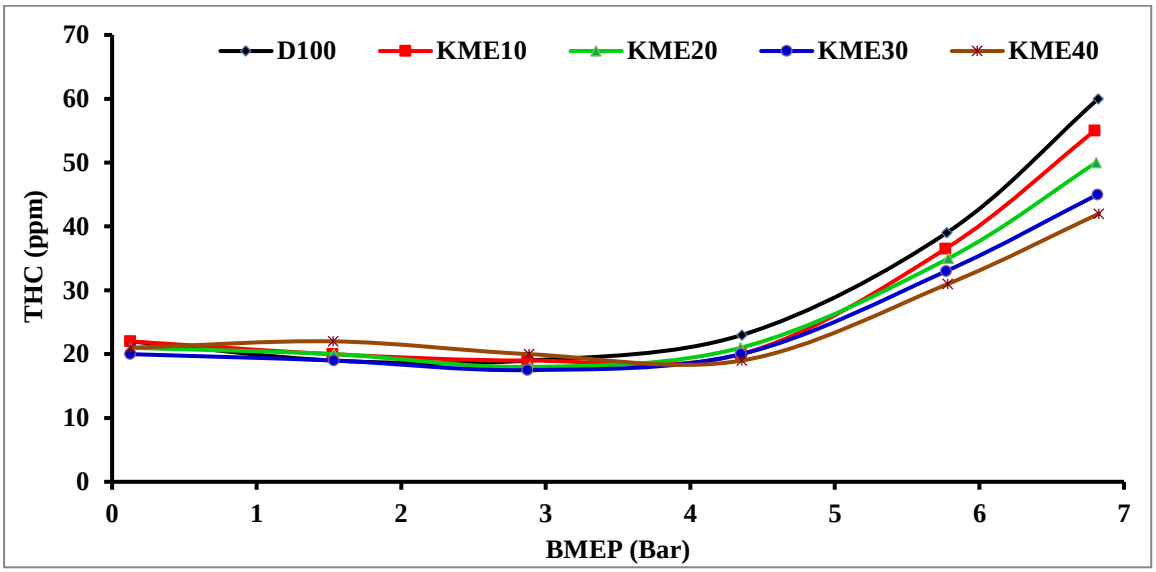

Figure 4.62: Total hydrocarbon emissions *vs* BMEP for KME Fuel Blends

It may be observed in the Figure 4.63 that all most all the test fuels at higher loads demonstrated reductions in THC emissions as compared to the baseline data of diesel. At full load 18.31%, 15.24%, 24.52%, 21.72%, 29.17%, 26.72%, 33.39% and 31.74% reductions in emissions of THC was reported for SME10, KME10, SME20, KME20, SME30, KME30, SME40 and KME40 test fuels respectively.

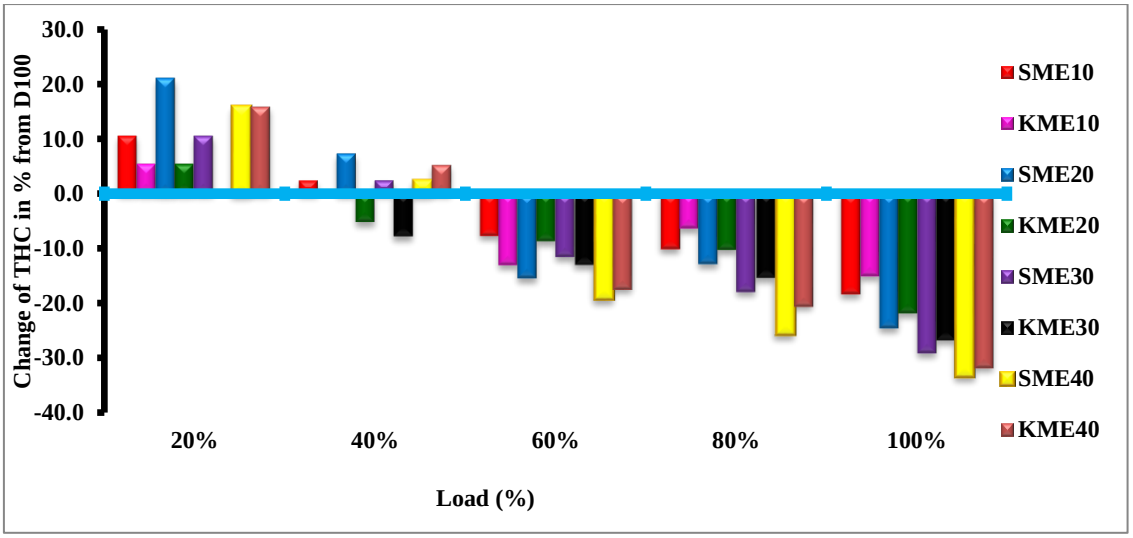

Figure 4.63: % Variation of THC emissions from diesel baseline at various loads

There are two basic explanations may be suitable to describe the reductions in THC emissions with increased fractions of SME and KME in the test fuels. Firstly, up to lower blend of SME and KME in diesel, higher in-cylinder pressures and bulk gas temperature was reported compared to the neat diesel operation that prevented the condensation of heaviest hydrocarbons at the sampling line. Secondly, these test fuels had higher cetane rating and lower ignition delay than diesel. Therefore, a combined effect of higher in-cylinder temperature, higher cetane rating and reduced ignition delay resulted in reduced emissions of THC by SME and KME blends compared to the baseline data of diesel [218,288,289].

4.7.3. Oxides of nitrogen emissions

Oxides of nitrogen commonly referred as NO_x are the critical diesel engine emissions of major concern. It comprises of nitric oxide (NO) and nitrogen dioxide (NO_2), formed by "Zeldovich Mechanism". Combustion flame temperature, availability of oxygen and time for oxygen-nitrogen reaction are the major factors controlling NO_x formation in diesel engines [12,222,290–292]. Figure 4.64 and Figure 4.65 show the volumetric emissions of NO_x demonstrated by various test fuels SME and KME blends under the designated operating loads.

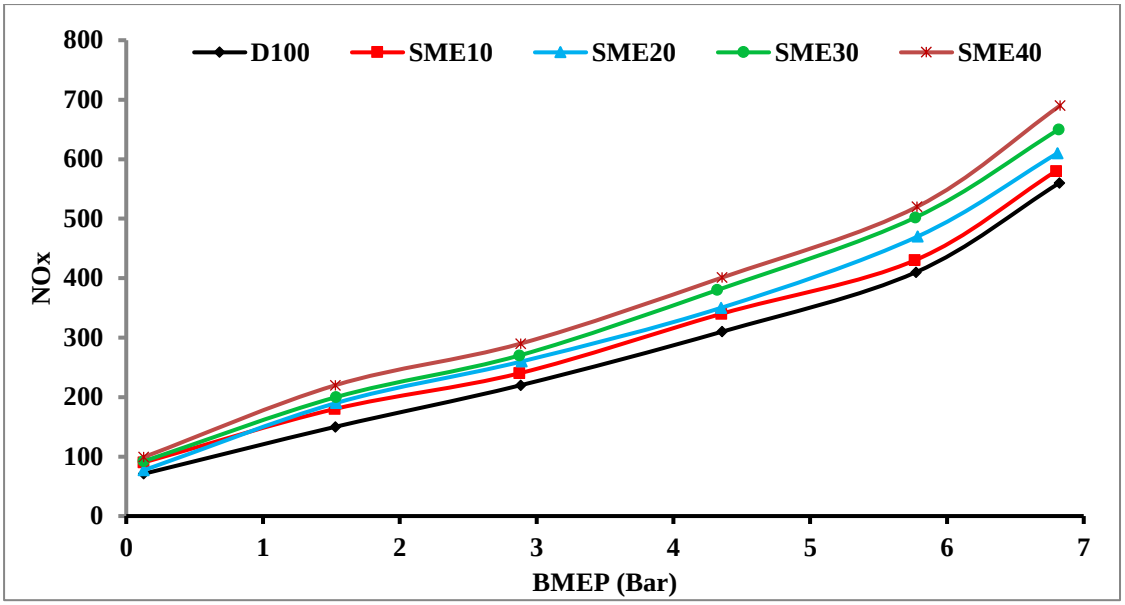

Figure 4.64: Oxides of nitrogen emissions *vs* BMEP for SME Fuel Blends

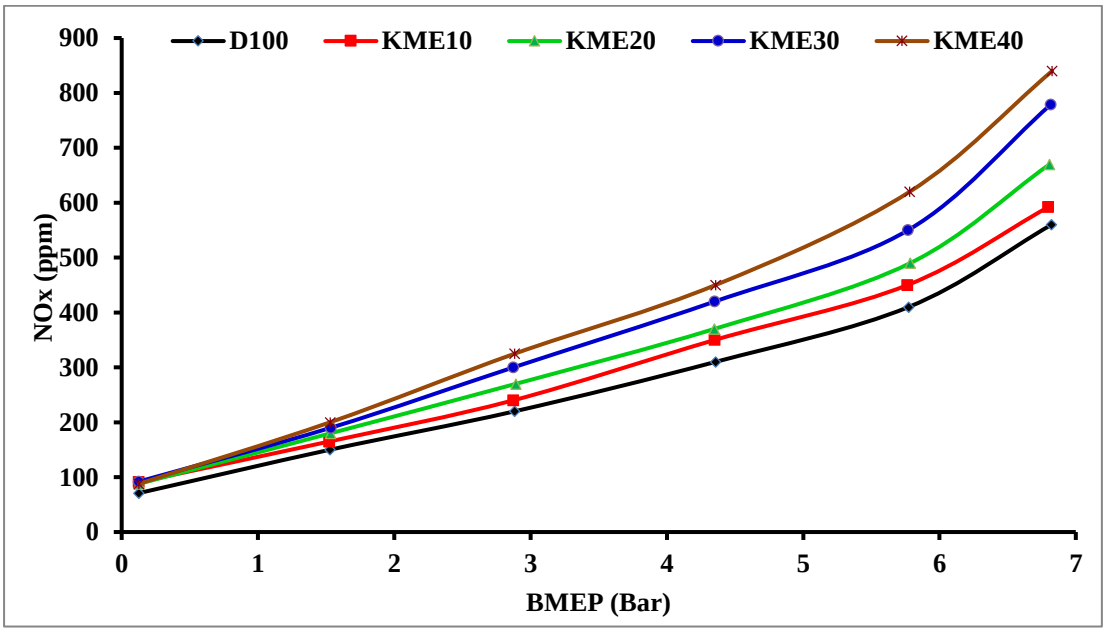

Figure 4.65: Oxides of nitrogen emissions *vs* BMEP for KME Fuel Blends

It was observed that NO_x emissions increased with increasing engine load for all test fuels. This was attributed to the fact that increase in engine loading led to increase in in-cylinder pressure and bulk gas temperature. NO_x formations are highly temperature dependent phenomena, hence, a closely linear increase in the formation of NO_x was observed with loading for all test fuels [187].

The results suggested that SME10, SME20, SME30 and SME40 exhibited 580, 610, 650 and 690 ppm volumetric emissions of NO_x at full load which was higher than 560 ppm showed by the baseline data of diesel in Figure 4.64 whereas KME10, KME20, KME30 and KME40 depicted 592, 670, 779 and 840 ppm shown in Figure 4.65. SME test fuels showed less NOx emission in compare to the KME test fuels. It means the fatty acids (unsaturated fatty acids) exaggerated the NOx formation. Load specific variations in NOx emissions for various test fuels as that of the baseline data is shown in Figure 4.66.

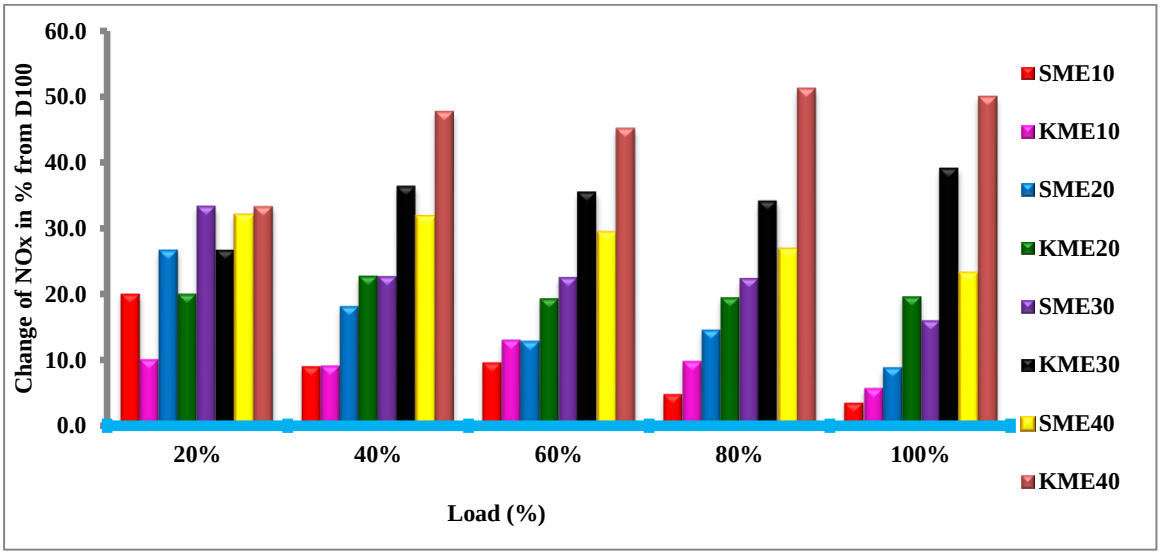

Figure 4.66: % Variation of NO_x emissions from diesel baseline at various loads

It may be observed that SME and KME blends deomnstrated higher emissions of NO_x compared to the baseline data for all loads. This may be attributed to the fact that biodiesl blends are an oxygenated fuel and the adiabatic flame temperature was higher than neat diesel operation. So therefore, higher combustion temepratures and excess avaialbility of oxygen were the predominant factor for increased NOx emissions all test fuels in compare to the baseline diesel. On the contrary a marginal drop in NOx emisisons for SME blends compared to the KME blends may be due to fatty acid composition. Similar results were reported by Hess et al., [291];İleri et al., [293]; Hoekman et al., [294] and Lanjekar et al., [295].

The theory suggested by Zheng et al., [296] which states higher cetan rating fuels emits higher NOx as well as the biodiesel with equal cetane rating with diesel produces more NOx. However, biodiesel with higher cetane rating than diesel leads to comparable NOx emissions with the baseline data as higher cetane rating causes reduced ignition delay and less exposure of the fuel at high tempearture premixed burning phase. As explained earlier, KME has higher cetane rating than SME hence, its NOx emissions were higher.

4.7.4 Smoke opacity

The particulate matter is essentially composed of soot, though some hydrocarbons, generally referred to as a soluble organic fraction (SOF) of the particulate emissions, are also adsorbed on the particle surface or simply emitted as liquid droplets. Among the particulate matter components, soot is recognized as the main substance which is responsible for the smoke opacity. Smoke opacity formation occurs at the extreme air deficiency. It increased as the air/fuel ratio decreases. Soot is produced by oxygen deficient thermal cracking of long-chain molecules [297].

Figure 4.67 shows the variation of smoke opacity of SME test fuels and Figure 4.68 shows variation of smoke opacity of KME test fuels with respect to BMEP and compared with baseline diesel (D100). It could be seen from Figure 4.67 and Figure 4.68, smoke level increased with increase in load for all fuels tested. It was mainly due to the decreased air–fuel ratio at such higher loads when larger quantities of fuel are injected in to the combustion chamber, much of which goes unburnt into the exhaust [228,269,272,297].

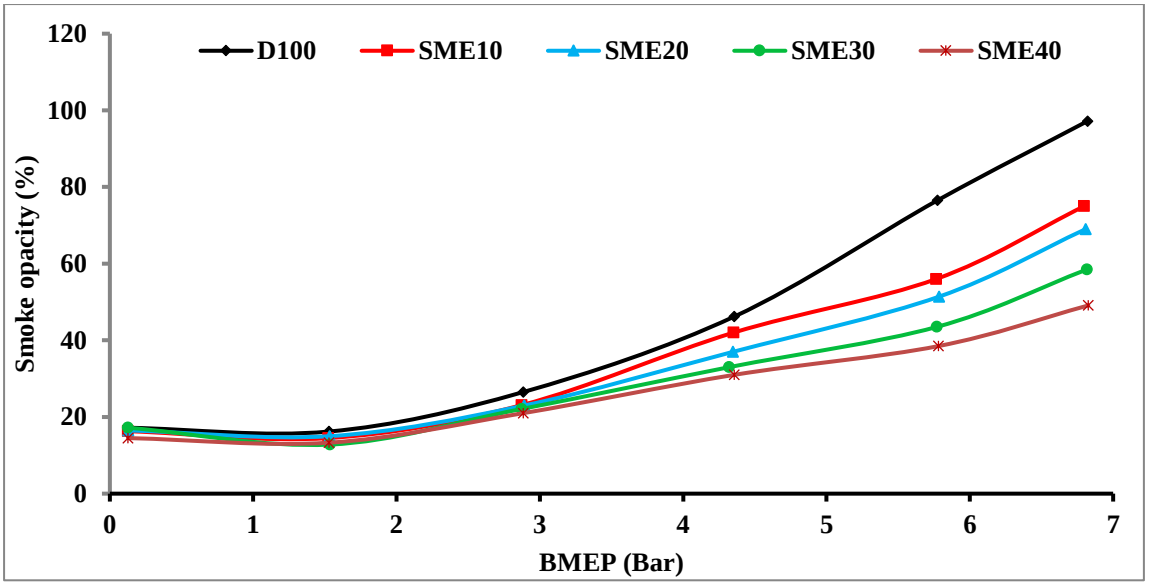

Figure 4.67: Smoke opacity *vs* BMEP for SME Fuel Blends

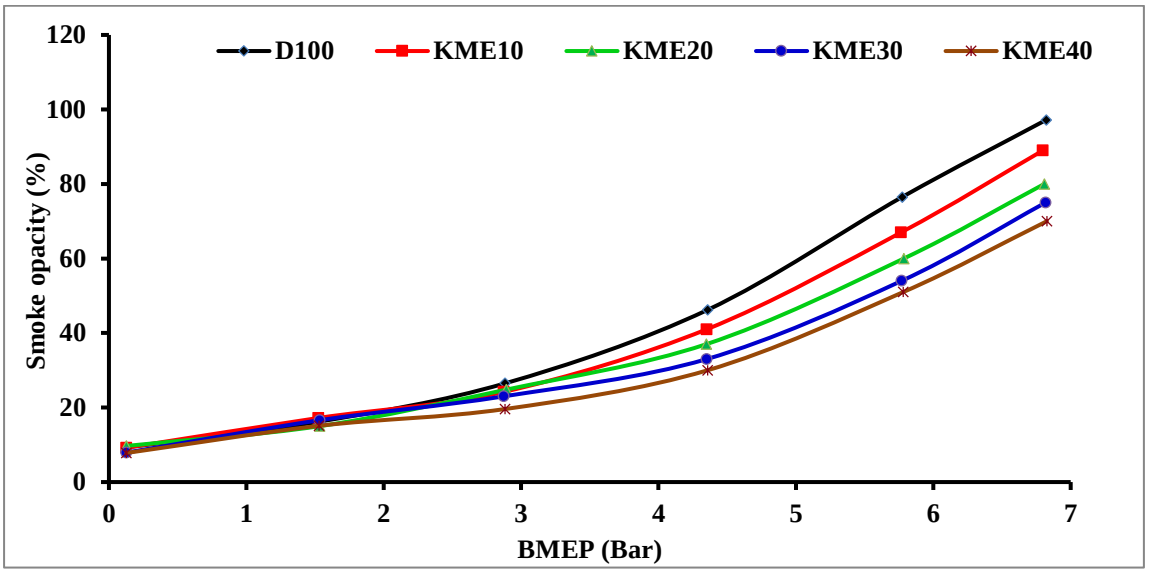

Figure 4.68: Smoke opacity *vs* BMEP for KME Fuel Blends

It may be observed that SME and KME blends demonstrated reduced smoke at higher loads. At full load SME10, SME20, SME30, SME40, KME10, KME20, KME30, and KME40 showed smoke opacities of 75%, 69%, 58%, 49%, 89%, 80%, 75% and 70% as compared to 97% shown by baseline diesel at full load. The reduced smoke opacity was attributed to higher oxygen content in methyl esters that contributes towards complete fuel oxidation even at locally rich zones [264,289], lower C/H ratio and absence of aromatic compounds [297]. Higher number of carbon atoms in a fuel molecule leads towards higher

smoke and soot formations where as higher number oxygen and hydrogen atoms leads to lower smoke and soot [298,299].

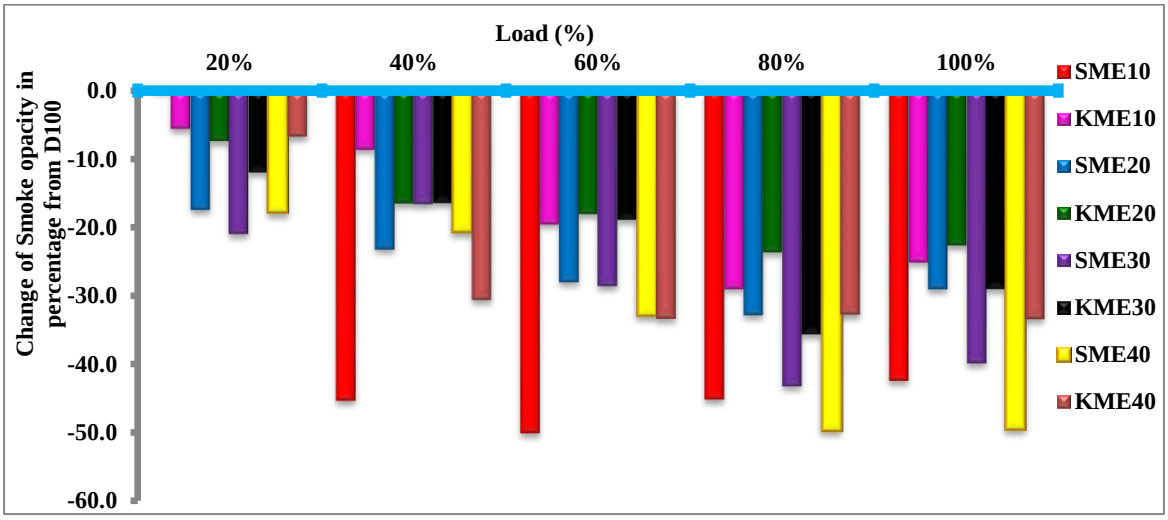

Figure 4.69: % Variation of smoke opacity from diesel baseline at various loads

It may be observed that at entire range loads SME and KME blends exhibited lower smoke opacities than the baseline. Variation in smoke opacities exhibited by SME and KME blends with the baseline data of diesel at various loads is shown in Figure 4.69.

They concluded that the effect of the composition and structure on smoke opacity is negligible as compared to the oxygen content, which was acknowledged as the main factor causing smoke reductions [264].

4.7.5 Carbon dioxide emissions

The carbon dioxide is a major emission from diesel engines, which can contribute to serious public health problems and play a major role in ozone formation. On the other hand carbon dioxide in the exhaust gases is an indication of complete combustion. The variation in emissions of carbon dioxide with BMEP at various loads for SME and KME blends are shown in Figure 4.70 and Figure 4.71 respectively. It was noted that biodiesel blends exhibited

higher CO_2 emissions as compared to the neat diesel operation at all loads.

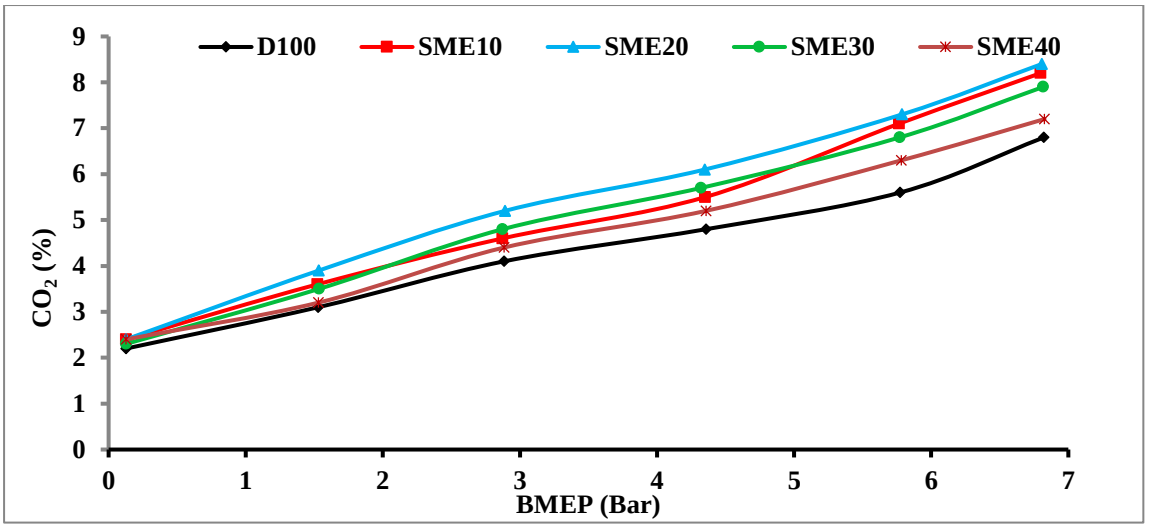

Figure 4.70: Carbon dioxide *vs* BMEP for SME Fuel Blends

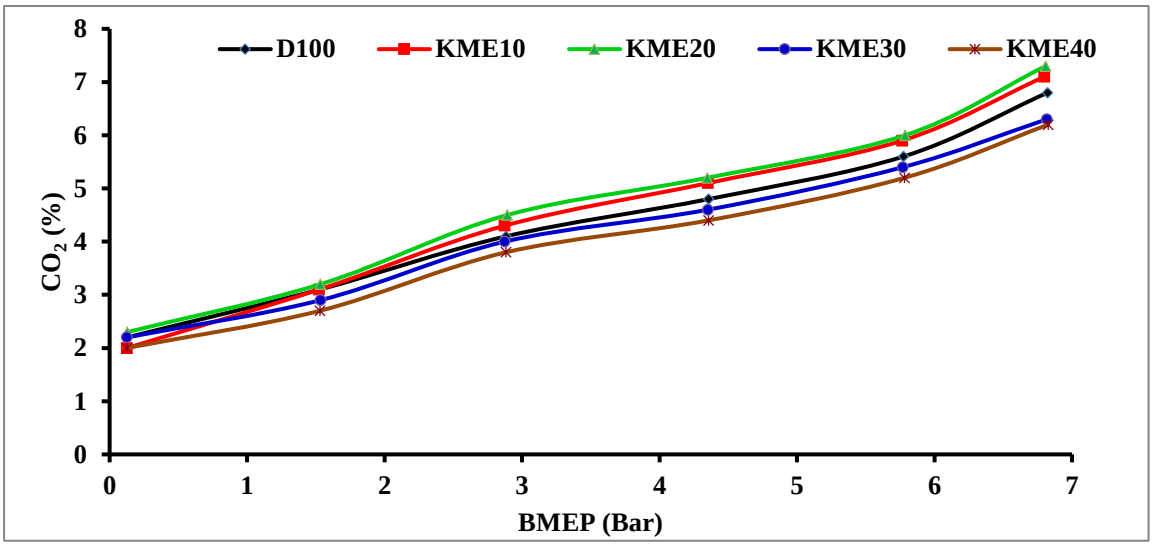

Figure 4.71: Carbon dioxide *vs* BMEP for KME Fuel Blends

This indicates complete combustion and higher heat release for test fuels. The same was evident from higher BTE and lower BSEC indicated by theses test fuels in the earlier sections. SME10 and SME20 have higher CO_2 emissions as compared to the other test fuel and baseline data as shown in Figure 4.72. Higher percentage of biodiesel blends emits relatively lower amount of CO_2 emissions as a consequence of higher viscosity, poor atomization and incomplete combustion. Fuel spray cone angle, in which air entrainment

depends, decreases with increased fuel viscosity. Decrease in cone angle results in reduction of amount of air entrainment in the spray. Lack of enough air in the fuel spray impedes completion of combustion and decreases formation of CO_2 emissions for higher volume of biodiesel [269].

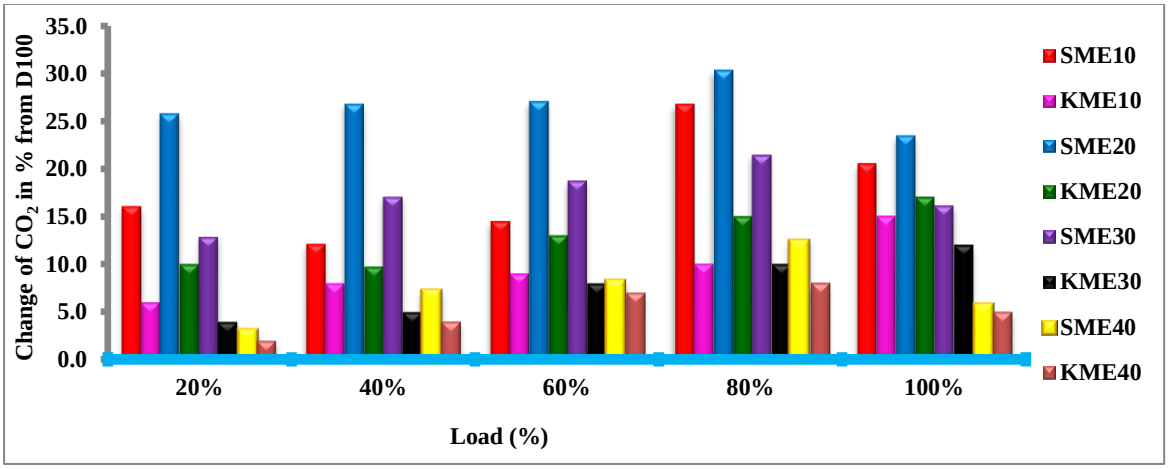

Figure 4.72: % Variation CO_2 emission from diesel baseline at various loads

4.8 Engine Combustion Results

Combustion of fuels is one of the most important processes which affect the performance and emission characteristics as well as the engine durability [300]. The important parameters that signify the combustion process effectiveness are in-cylinder pressure, ignition delay, combustion duration, heat release and cumulative heat release rate [301,302]. In-cylinder pressure can be measured directly from the engine and the other combustion parameters can be calculated from the in-cylinder pressure. The heat release rate is estimated from the first law of thermodynamics using the in-cylinder pressure and the geometry of crank and connecting rod [300]. The other important combustion parameters can be easily estimated from the heat release rate variation over an engine cycle.

In the subsequent section combustion results of Sal and Kusum biodiesel/diesel blend (up to 40%) fuel was compared baseline diesel. Engine combustion characteristics at full load

conditions were studied based on In-cylinder pressure, maximum pressure rise rate, heat release rate (HRR), cumulative heat release rate (CHRR), mass fraction burnt (MFB). These results were investigated with different blend percentages of both biodiesel at full load.

4.8.1 In-cylinder pressure

The in-cylinder pressure measurement is considered to be a very valuable source of information during the development and calibration stages of the engine. The in-cylinder pressure signal can provide vital information such as peak pressure, indicated mean effective pressure, fuel supply effective pressure, heat release rate, combustion duration, ignition delay and so on [300].

In present study Compared with Sal and Kusum biodiesel with diesel fuel gives almost the same level of maximum pressure at low and medium engine loads, but higher maximum pressure at the high engine load. Biodiesel vaporizes more slowly than neat diesel and contributes to less air/fuel mixture prepared for combustion in the premixed phase [11]. Moreover, the higher bulk modulus of compressibility of methyl esters led to advanced injection timing with in-line pump and nozzle fuel injection system [303]. The earlier injection timing of biodiesel contributed to the advance of the peak cylinder pressure and the maximum heat release rate [266].

The variation of full load in-cylinder pressure with crank angle of SME blends is shown in Figure 4.73 and KME blends is shown in Figure 4.74. For the purpose of clarity, the pressure data between 335°CA and 400°CA was taken for in-cylinder pressure. It may be observed that at full load neat diesel exhibited 63.8 bar pressure corresponding to 375°CA. SME10 and SME20 showed full load peak pressure of 66.72 bar and 65.63 bar respectively corresponding to 374°CA and 373°CA.

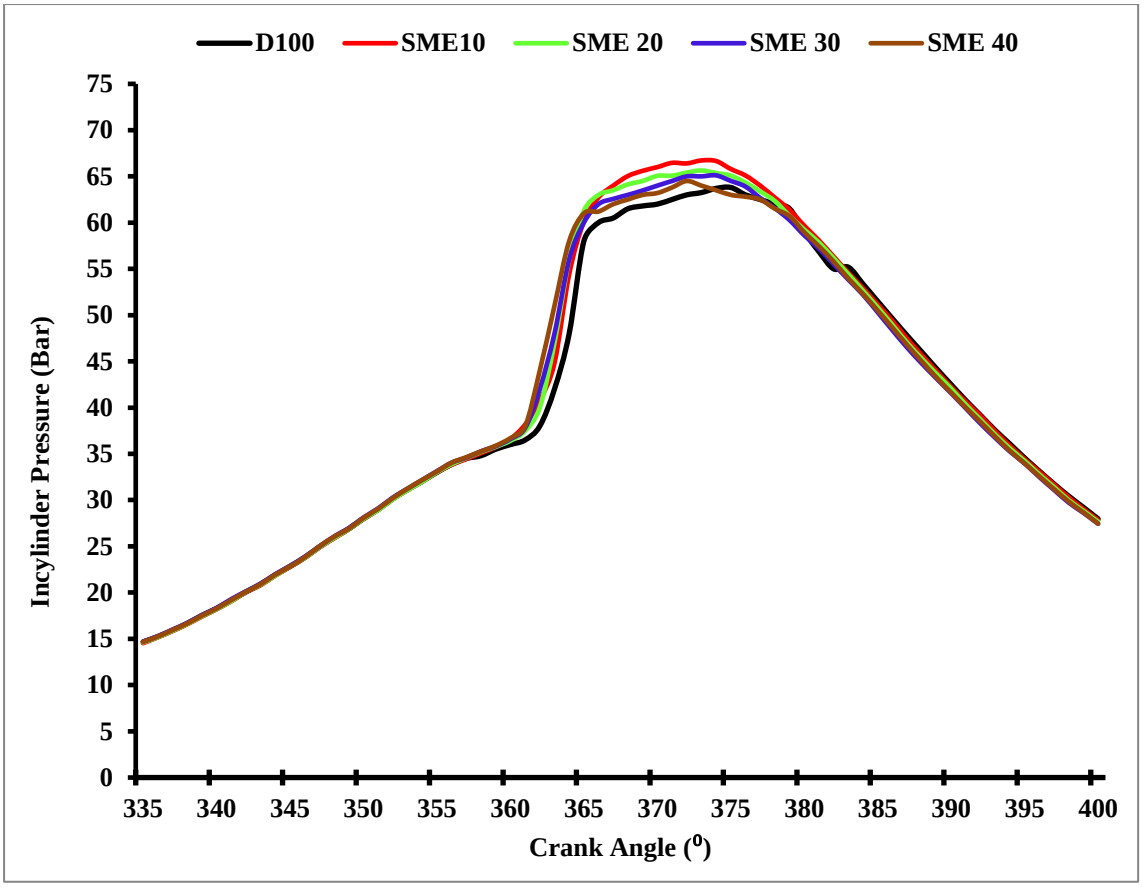

Figure 4.73: Variation In-cylinder pressure for SME fuel blends

The higher and earlier peak pressure observed for SME10 and SME20 compared to the baseline data of diesel may be explained by the fact that at lower fractions of SME in the blend, the fuel became more oxygenated due to SME and the higher viscosity of SME was not felt due to lower proportions. Moreover, the higher cetane rating of SME compared to neat diesel led to improved combustion. This may be validated by the fact that that SME10 and SME20 exhibited higher full load BTE and lower exhaust temperature compared to the baseline data. However, SME30 and SME40 showed peak in-cylinder pressure of 65.1 bar and 64.5 bar corresponding to 372°CA. The lower in-cylinder pressure exhibited by the blends of SME beyond 20% substitution may be due to the reduced heating value of the fuel and increasing difficulty in atomization and vaporization [35].

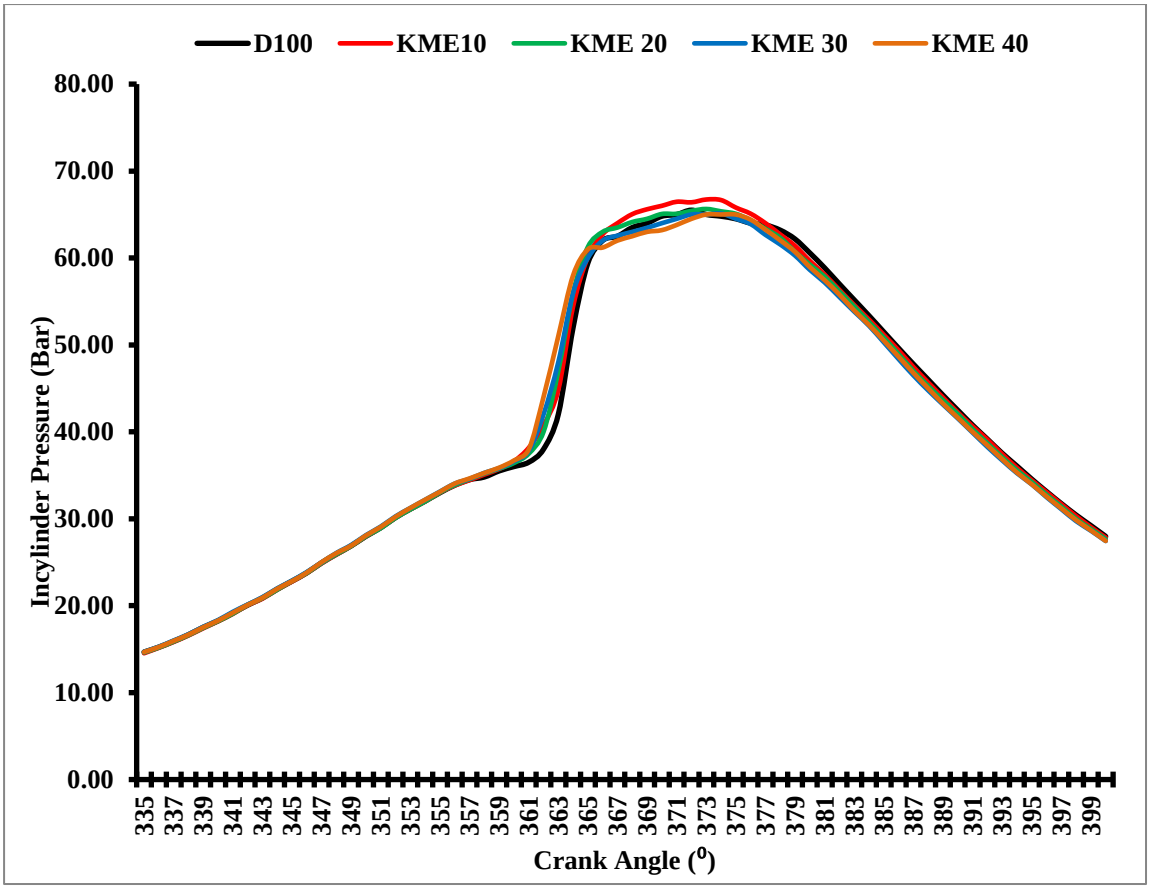

Figure 4.74: Variation In-cylinder pressure for KME fuel blends

Similarly in Figure 4.74 KME10 and KME20 showed full load peak pressure of 69.06 bar and 68.12 bar respectively corresponding to 373°CA same for both case. The higher and earlier peak pressure observed for KME10 and KME20 compared to the baseline data of diesel may be explained by the fact that at lower fractions of KME in the blend, the fuel became more oxygenated due to KME and the higher viscosity of KME was not felt due to lower proportions. Moreover, the higher cetane rating of KME compared to neat diesel led to improved combustion. This may be validated by the fact that that KME10 and KME20 exhibited higher full load BTE and lower exhaust temperature compared to the baseline data. However, KME30 and KME40 showed peak in-cylinder pressure of 65.81 bar and 65.1 bar corresponding to 372°CA. The lower in-cylinder pressure exhibited by the blends of KME

beyond 20% substitution may be due to the reduced heating value of the fuel and increasing difficulty in atomization and vaporization.

4.8.2 Pressure rise rate

The rate of pressure rise defines the load that is imposed during the combustion process on the cylinder head and other components. The rate of pressure rise depends on the amount of heat released in the initial stages of combustion and the fuel quality. The higher the rate of pressure rise, the higher the load on the piston and other components, which may lead to severe damage of the parts [276]. The rate of pressure rise for diesel is the highest compared to those of SME and KME blends, as a result of longer ignition delay and shorter combustion duration of diesel. High peak pressure and maximum rate of pressure rise corresponded to the large amount of fuel burned in premixed combustion stage. The cylinder pressure crank angle history is obtained at different loads for diesel and biodiesel blends. Peak pressure and maximum rate of pressure rise are obtained at different loads from these measurements.

It may be observed that the rate of pressure rise was lower for biodiesel blends with respect to baseline diesel. The variation of full load pressure rise rate with crank angle of SME blends is shown in Figure 4.75 and KME blends is shown in Figure 4.76. Maximum pressure rise rate for SME10, SME20, SME30, SME40, KME10, KME20, KME30 and KME40 were 4.9 bar/°C, 4.51 bar/°C, 4.45 bar/°C, 4.32 bar/°C, 4.28 bar/°C, 4.62 bar/°C, 4.58 bar/°C, 4.32 bar/°C and 4.35 bar/°C whereas D100 was higher pressure rise rate 4.95 bar/°C. The lower pressure rise rate of SME and KME fuels was evident from the smooth engine operation when running on these test fuels. It also provided clear picture of the start of combustion and ignition delay. Similar results were obtained by Sahoo et.al. [304]and Sivalakshmi et.al. [305].

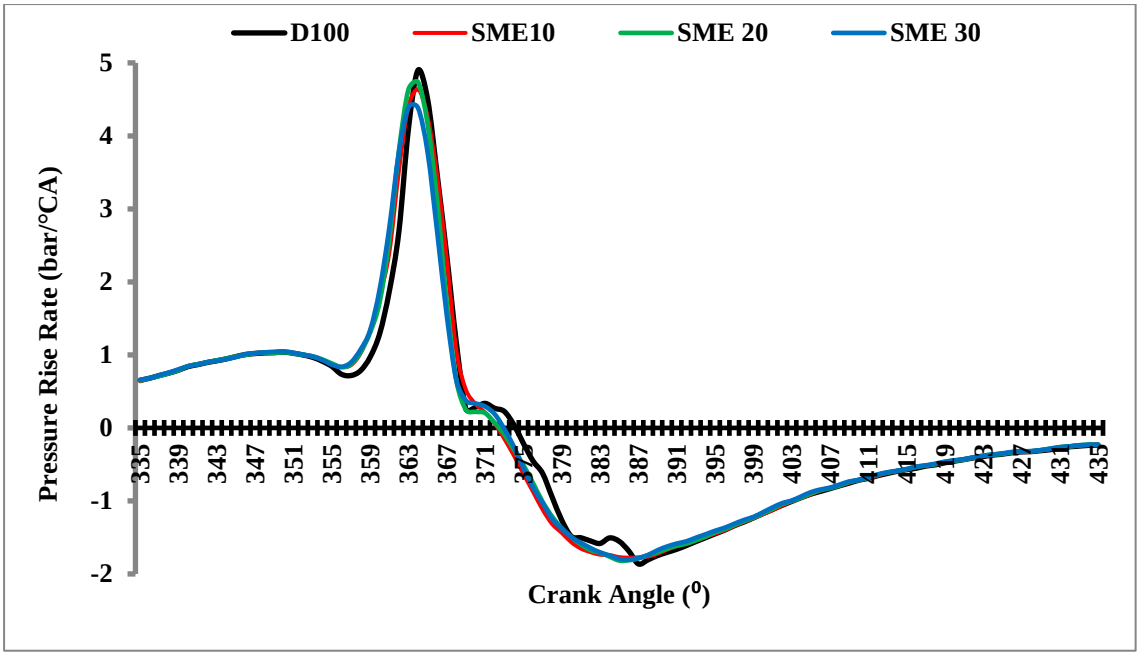

Figure 4.75: Pressure rise rate for SME fuel blends

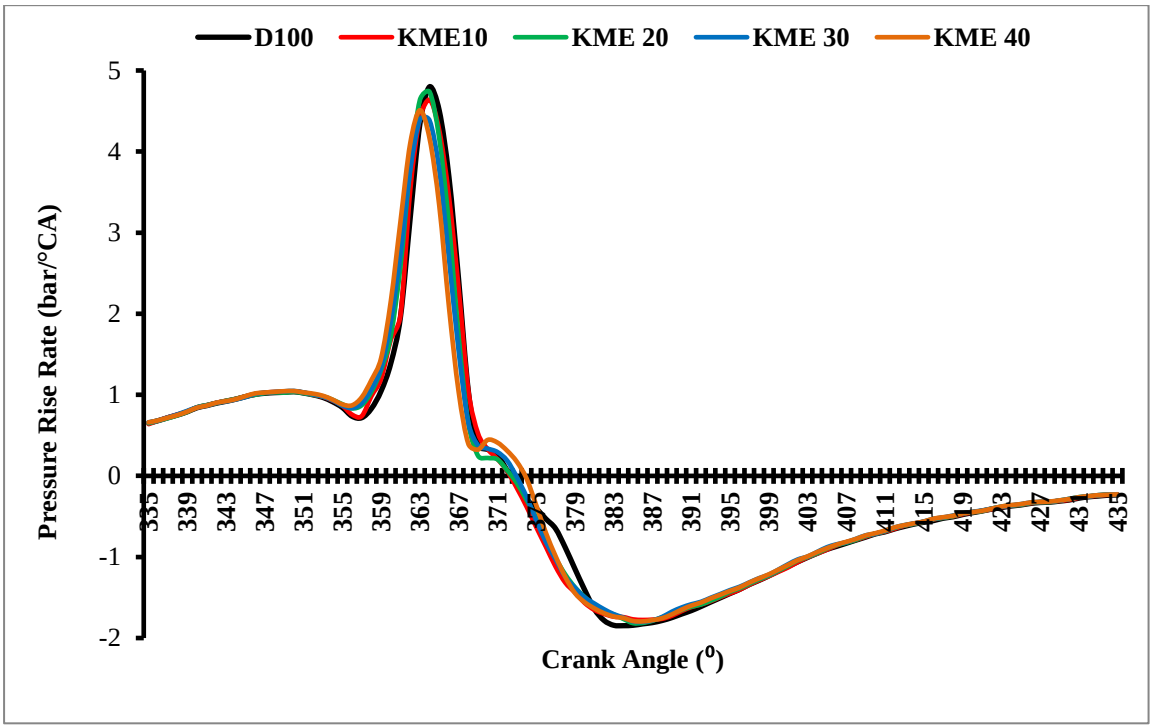

Figure 4.76: Pressure rise rate for KME fuel blends

Biodiesel blends (SME and KME) showed lower pressure rise rate as compared to diesel fuel due to lower ignition delay (ID) and premixed combustible mixture would make less fuel to be burned in the premixed burning phase.

The reasons for the less premixed combustible mixture are higher viscosity and lower volatility of biodiesel as compared to those of diesel fuel [301].

4.8.3 Heat release rate

The rate of heat release was calculated from the pressure crank angle data using the Sorenson's heat release model elaborately discussed earlier. Heat release per crank angle was calculated using the equation (3.21). The heat release curve for various test fuels is shown in Figure 4.77 and Figure 4.78 for SME and KME blends respectively. For biodiesel, the maximum heat release rate at the premixed combustion phase was lower than that of diesel, and occurred earlier, while the heat release rate of diffusion combustion phase was higher for biodiesel, in comparison with that of diesel fuel, especially at the high engine load. This trend was similar to that reported by Zhu et al., [303].

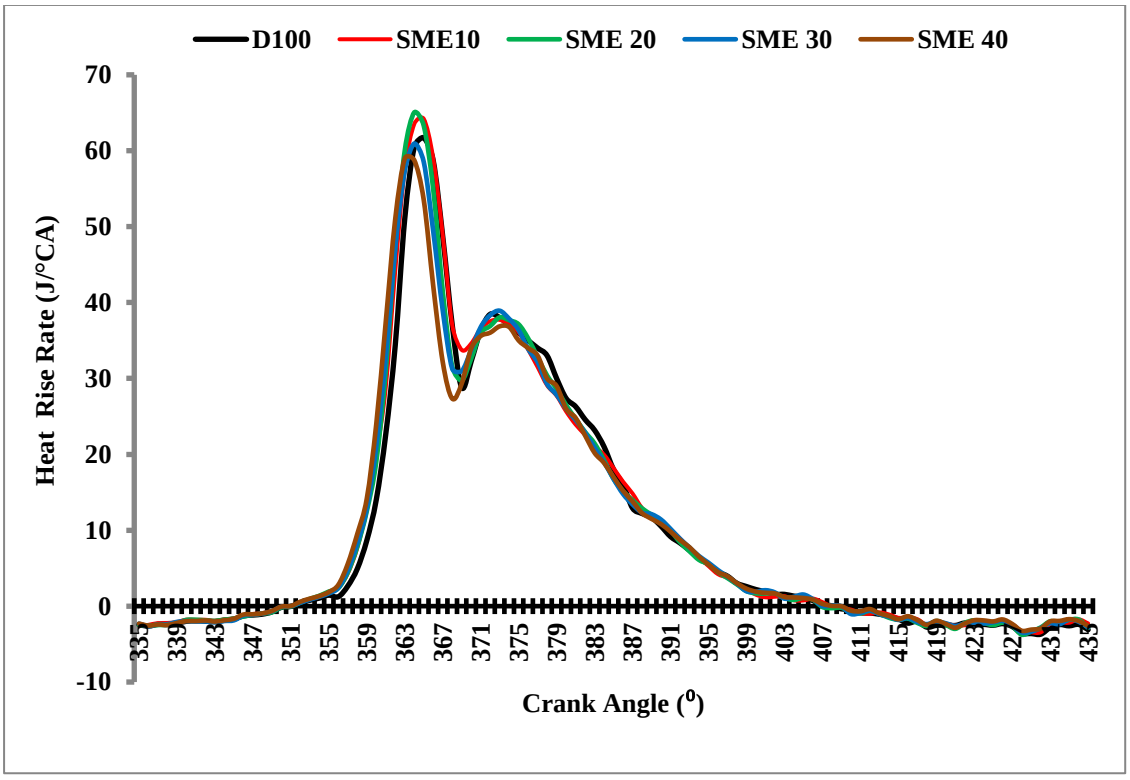

Figure 4.77: Heat release rate diagram for SME Fuel Blends

The heat release rate diagram shows negligible heat release until toward the end of compression when a slight loss of heat during the delay period (which is due to heat transfer to the walls and to fuel vaporization and heating) is evident. Due to heat absorbed by the injected fuel from the cylinder, the heat release rate is slightly negative during the ignition delay period. The initial phase of combustion, called the premixed combustion, is very rapid because of the combustion of the fuel that has mixed with air during the ignition delay. After this phase, the combustion continues slowly until most of the fuel is burned. This phase of combustion is called mixing-controlled combustion.

The final combustion phase is the late or post combustion, which continued until the end of the expansion stroke. In this third stage a small but distinguishable rate of heat release persisted throughout much of the expansion stroke. The heat released during this period usually amounts to about 20% of the total fuel energy. All the fuel blends tested experienced rapid premixed burning followed by diffusion combustion, which was typical for naturally aspirated engines. After the ignition delay period, the premixed fuel/air mixture burns rapidly, releasing heat at a very rapid rate, after which diffusion combustion takes place, where the burning rate is been controlled by the availability of combustible fuel/air mixture [302].

The heat release rate in the premixed combustion phase depends on the ignition delay, mixture formation and the combustion rate in the initial stages of combustion [276]. It could be observed from the Figure 4.77 and Figure 4.78 that the occurrence of maximum heat release rate was found to be little earlier for biodiesel and its diesel blends than that of diesel, as a result of the bulk modulus characteristics of biodiesel. The Figure 4.77 demonstrated that the peak heat release rate of diesel was 61.72 J/°CA. SME10, SME20, SME30 and SME40 display peak heat release rates of 63.51 J/°CA, 65.05 J/°CA, 60.94 J/°CA and 57.69 J/°CA

respectively. Notably, the crank angle corresponding to the peak heat release is lowered for SME blends from 365 ^{o}CA to 363 ^{o}CA.

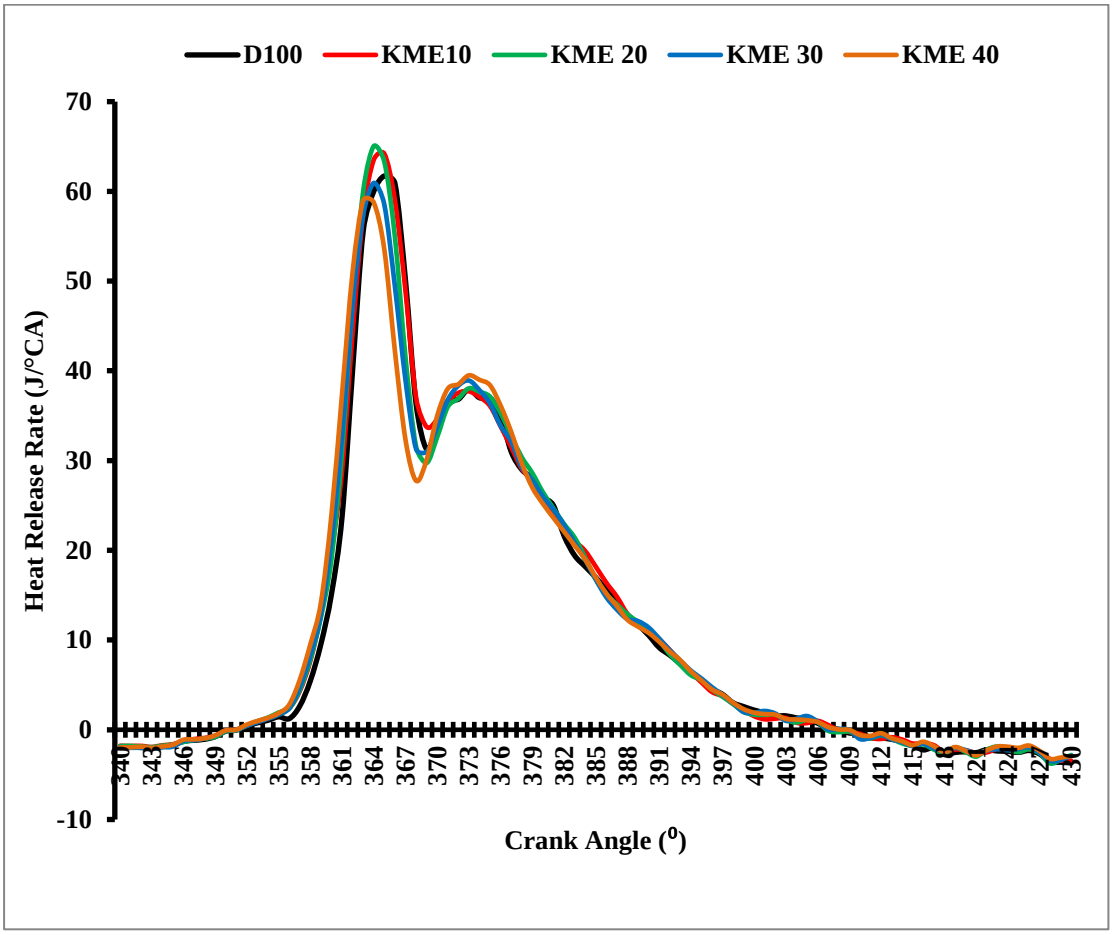

Figure 4.78: Heat release rate diagramfor KME Fuel Blends

As the percentage of SME in the blend increases, the peak HRR increased up to 20%, however further increase in volume fraction of SME showed the decreased peak HRR. These results are similar to the [276]. It may be observed from Figure 4.78 that the peak heat release rate of KME10, KME20, KME30 and KME40 exhibited peak heat release rates of 69.62, 70.71, 62.82, and 60.04 J/°CA respectively. Notably, the crank angle corresponding to the peak heat release was lower for KME and its blends. Therefore it may be stated that KME and its blends exhibited an earlier and slower rate of heat release compared to the baseline data of diesel.

4.8.4 Cumulative heat release rate

The CHR was calculated and illustrated in Figure 4.79 and Figure 4.80. These figures show the tendency of earlier heat release for biodiesel blends but combustion for diesel fuel quickly exceeds the CHR for biodiesel blends although combustion for diesel fuel starts later. The effect of two-stage heat release can be clearly observed. Relatively higher surface tension of biodiesel increases the droplet size distribution of the injected fuel, compared to diesel. This increased droplet size distribution required higher heat for vaporization, which resulted in relatively slower evaporation of test fuels. Slower evaporation delayed the formation of combustible mixture therefore delaying the SOC. Hence, SOC retards with increase in biodiesel content in the test fuel. This delay in SOC also shifts the position of maximum cylinder pressure. On increasing the biodiesel percentage in the test fuel, effect of slower evaporation dominates the effect of fuel borne oxygen; hence similar trend was also observed for the position of maximum cylinder pressure [306] also reported similar trends as observed in Figure 4.79 and Figure 4.80. They concluded that the chemical kinetics of diesel is faster than biodiesel hence mineral diesel shows earlier SOC compared to biodiesel blends.

It may be observed SME and KME blends exhibited higher CHR in compared to the base line diesel in both the cases as shown if figures. Cumulative heat released for D100 was 1172.4 J whereas SME10, SME20, SME30, SME40, KME10, KME20, KME30 and KME40 exhibited 1215.68 J, 1201.77 J, 1168.62 J, 1177.40 J, 1208.65 J, 1200.88 J, 1188.29J and 1179.14 J respectively. B10 showed highest CHR but further addition of volume fraction of biodiesel (like B20, B30, and B40) showed diminishing trend in both figures.

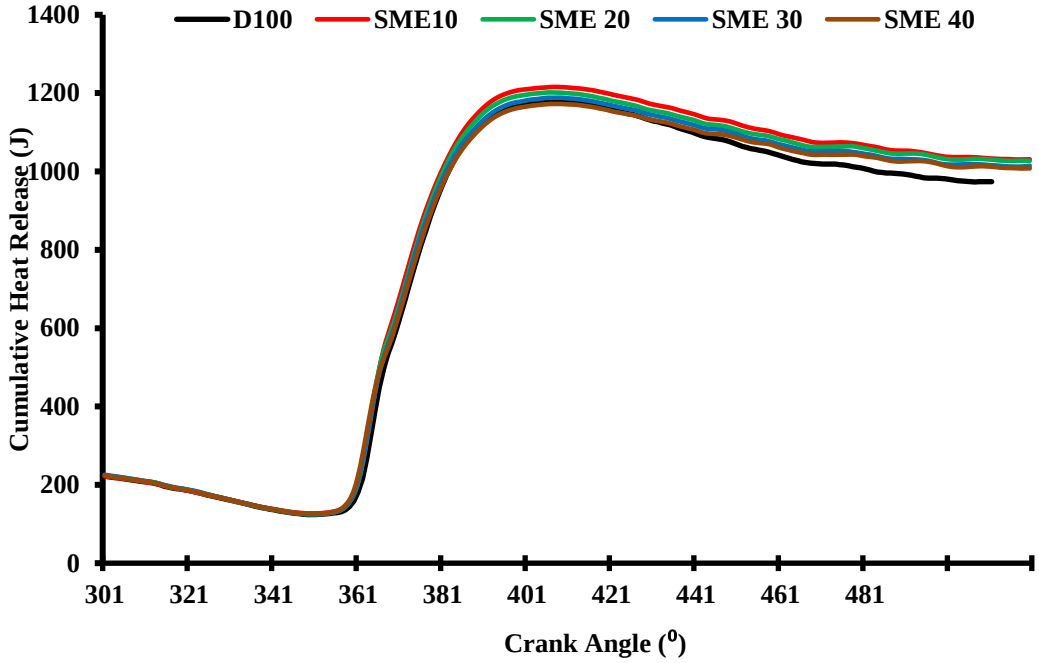

Figure 4.79: Cumulative heat release diagram for SME Fuel Blends

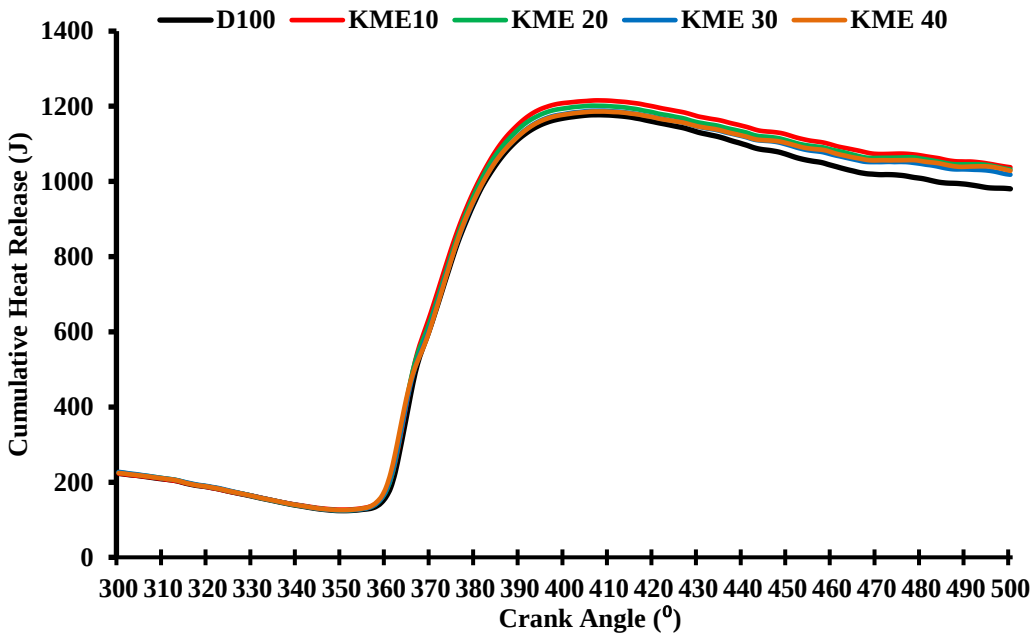

Figure 4.80: Cumulative heat release diagram for KME Fuel Blends

The reduction in total heat release was reported mainly on account of poor combustion and reduced heating values but it is marginally higher than base line diesel. Results in the similar spirits were reported by Dhar et al., [41]; Qi et al., [307] and Arora et al., [308]. The

combustion duration can be calculated based on the duration between the start of combustion and 90% CHR.

4.8.5 Mass fraction burnt

Mass fraction burnt (MFB) in each individual engine cycle is a normalized quantity with a scale of 0 to 1, describing the process of chemical energy release as a function of crank angle. Fractional pressure rise technique has been applied for MFB calculation. The variation of MFB with crank angle of all the tested fuels at 1500 rpm and full load condition has been shown in Figure 4.81 and Figure 4.82 for SME and KME respectively. It was observed that MFB increased with the increasing biodiesel percentage. This was attributed to the high concentration of oxygen molecule in biodiesel blend, which resulted in high rate of burning. Positions of 10% and 90% MFB have been used to define SOC and EOC, respectively. Therefore, the difference between the crank angle positions of 10% MFB and 90% MFB is the combustion duration period.

Mass fraction burnt was calculated as per the equation (3.31), discussed in the previous sections. The ignition delay of individual test fuels and total combustion duration was calculated from the mass fraction burnt. Ignition delay was calculated as the difference between the crank angle corresponding to the beginning of fuel injection and the crank angle for MFB=0.05. Similarly, the total combustion duration was calculated as the crank angle corresponding to MFB of 0.05 to 0.95. The total combustion duration was reduced for SME10 and SME20 to 19° and 20° of crank rotation respectively as compared to the 21° crank rotation for the baseline data.

However, SME30 and other higher blends exhibited higher total combustion durations. Notably, diffusion phase combustion duration was found to increase with increase in biodiesel

volume fraction in the test fuels suggesting smoother engine operation and equally evident to the pressure rise rate diagrams.

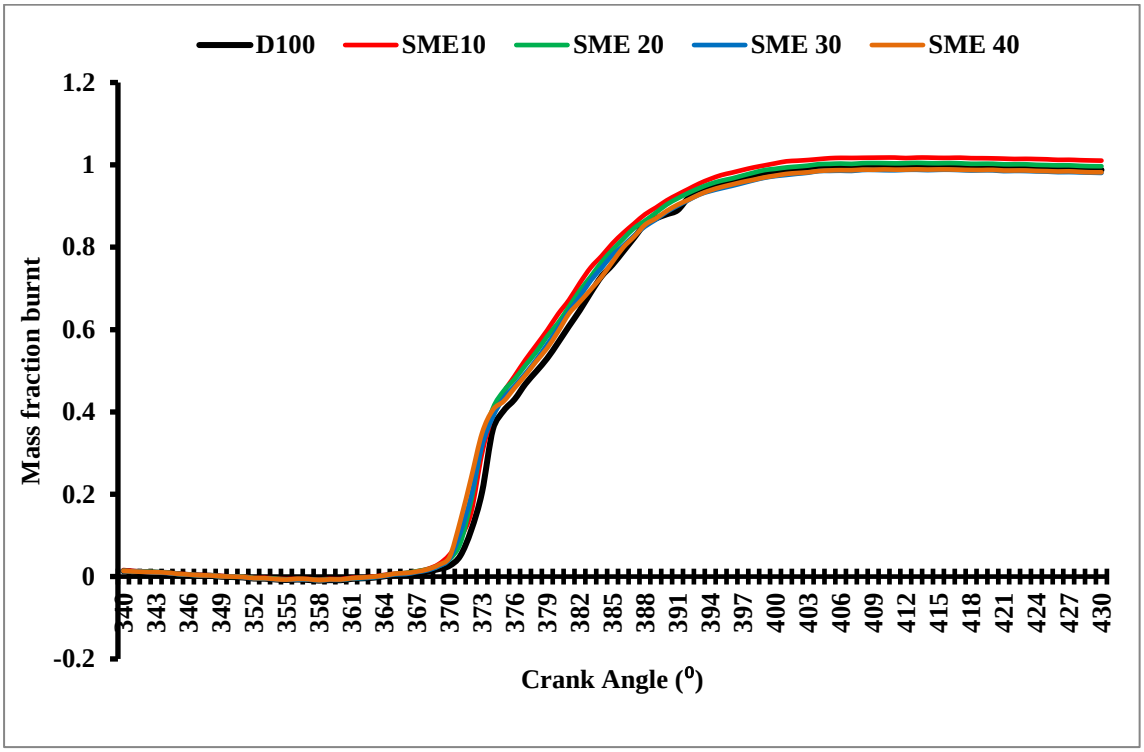

Figure 4.81: Mass fraction burnt for SME Fuel Blends

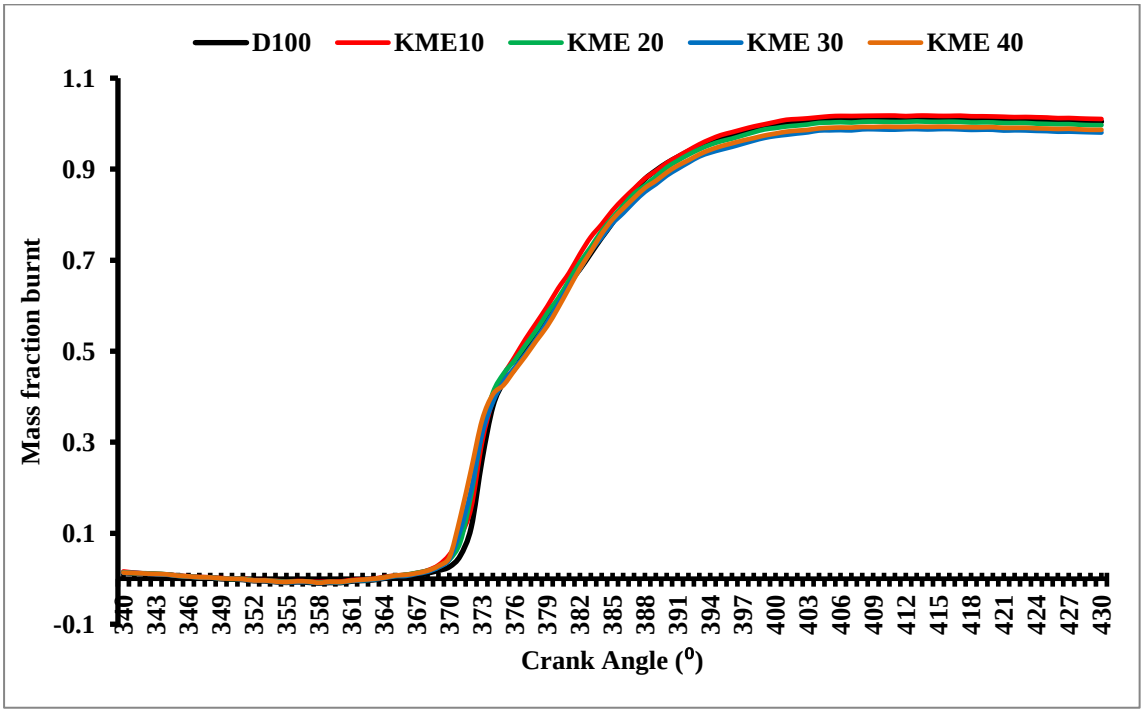

Figure 4.82: Mass fraction burnt for KME Fuel Blends

4.8.6 Ignition delay:

Ignition delay (ID) is an important parameter in combustion phenomenon. Biodiesel and its blends showed shorter IDs as compared to diesel fuel due to higher cetane number of biodiesel. High cetane number makes auto ignition easily and gives short ID. A lot of parameters such as fuel type, fuel quality, air/fuel ratio, engine speed, quality of fuel atomization, intake air temperature and pressure influence the ID [260,308]. The fuel type is an important parameter affecting the ID [301]. For a fuel like biodiesel having lower ignition delay, the ignition starts earlier and maximum cylinder pressure is lesser and is attained earlier than the fuel having higher ignition delay like diesel.

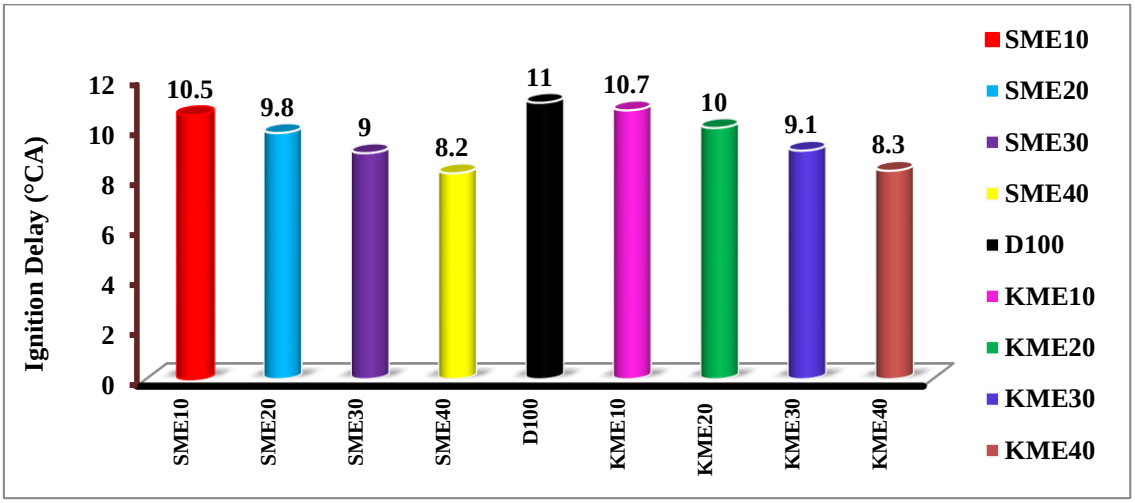

Figure 4.83: Ignition delay for various test fuels

The physical and chemical properties of the fuels will affect the ignition delay period. The ignition quality of a fuel is usually characterized by its cetane number. Higher cetane number generally meant shorter ignition delay as well as the compressibility of biodiesel and its blends are lower than that of diesel fuel. When biodiesel was used as fuel, the earlier fuel injection has occurred in engines with mechanical injection systems. When biodiesel is injected, the liquid fuel pressure rise produced by the pump is faster as a consequence of its lower compressibility, and also the pressure waves can propagate quicker toward the

injectors. The difference in this property has provided that the injection timing of biodiesel and its blends is effectively advanced relative to that of diesel fuel. Figure 4.83 is illustration of the SME and KME fuel blends with respect the diesel. Figure suggested almost linear reduction in ignition delay with increasing biodiesel volume fraction in the test fuel with baseline diesel.

Table 4.8: Various combustion characteristics of the test fuels

S. No	Test Fuel	Maximum Pressure (bar)	Peak Pressure Rise (bar/°C)	Peak HRR (J/°CA)	CHR (J)	Ignition delay (°CA)
1	Diesel	**63.8**	**4.95**	**61.72**	**1172.4**	**11**
2	SME10	**66.72**	**4.51**	**63.51**	**1215.68**	**10.5**
3	SME 20	**65.63**	**4.45**	**65.05**	**1201.77**	**9.8**
4	SME 30	**65.1**	**4.32**	**60.94**	**1168.62**	**9**
5	SME 40	**64.5**	**4.28**	**57.69**	**1177.4**	**8.2**
6	KME10	**69.06**	**4.62**	**69.62**	**1208.65**	**10.7**
7	KME20	**68.12**	**4.58**	70.71	1200.88	**10**
8	KME30	**65.81**	**4.32**	62.82	1188.29	**9.1**
9	KME40	**65.1**	**4.32**	60.04	1179.14	**8.3**

As an outcome of an exhaustive engine trial and the subsequent analyses, it may be satisfactorily stated that Sal methyl ester and Kusum methyl ester are an excellent diesel engine fuel. Up to 20% blend of SME and KME in diesel may be applied in any unmodified diesel engine with improved performance, emission (except NO_x) and combustion characteristics. 30% blend of SME and KME also showed marginally lower performance and combustion with improved emission.

CHAPTER 5

CONCLUSION

5.1 Conclusions

The present research work aims to produce biodiesel from some underutilized non-edible feedstocks such as Sal and Kusum and compare the results with neat diesel. Several physico-chemical properties of the vegetable oils and their respective methyl esters such as kinematic viscosity, density, calorific value, acid value, flash point, cold filter plugging point and oxidation stability were determined in accordance to ASTM standards.

The present work also discusses the study of effect of additives on oxidation stability and cold flow properties of test fuels. Moreover, the effect of biodiesel-diesel blends (up to 40% biodiesel by volume) of Sal methyl ester and Kusum methyl esteron engine performance, emissions and combustion was studied in a single cylinder four stroke diesel engine.

Based on the exhaustive experimental study, the following conclusions can be drawn:

1. Sal and Kusum are potential feedstocks for biodiesel production in India.
2. Single stage transesterification process optimization for Sal biodiesel indicated maximum yield of 96.92%, and a two stage process for Kusum biodiesel showed maximum yield of 96.5% using RSM as the optimization tool.
3. The biodiesel blending with diesel changes the physico-chemical properties such as density, kinematic viscosity, flash point etc. The various physico-chemical properties were within prescribed limits of ASTM standard. However post processing is required using additives for the improvement of some physico chemical properties like CFPP of sal biodiesel and oxidation stability of Kusum biodiesel.
4. Two antioxidant namely TBHQ and Ecotive were added (0.1 % and 0.5 % by weight) in Kusum biodiesel. All the biodiesel samples passed the minimum limit of oxidation stability after 0.5% doping.

5. The one year storage stability study revealed that peroxide value, density, viscosity and acid number increased for all stored biodiesel (SME and KME) with storage period. The changes in physico-chemical properties were found to be prominent in peroxide value and acid value. While change in other properties were mostly insignificant.
6. Four additives namely kerosene, EVA, Cristol and Lubrizol were used as pour point depressant in both biodiesels. Cristol was found most suitable.
7. The improvement in engine performance and emission characteristics with lower percentage substitution (up to 20%) of biodiesel in diesel fuel was due to better combustion of fuel blends as compared to diesel fuel due to the inbuilt oxygen content of biodiesel coupled with higher cetane number whereas more than 20% blending of biodiesel exhibited lower BTE with lower emissions.
8. It was observed that the peak in-cylinder pressure at full load was lower for D100 which increases with increase in volume fraction of biodiesel in diesel. The combustion heat release rate and ignition delay for biodiesel was lower as compared to baseline diesel. Thus, it can be concluded that combustion and performance improvement of the diesel engine can be achieved up to 20% blending of biodiesel in diesel with lower emissions.

5.2 Scope for Future Work

1. Very limited work has been carried out on combustion characteristics based on the realistic multi dimensional experimental combustion modelling as most of the works were confined to simpler zero-dimensional heat release models. There is a scope to simulate results and compare to the experimental results for validation of

the computational model. A three dimensional geometrical model consistent with the actual engine set up may be designed and simulated in ANSYS software.

2. Spray modelling of various biodiesel and its comparison with baseline spray model of diesel using computational fluid dynamics may also be carried by the future researchers.
3. As far as non edible feedstock is concerned, the research work has only focused on a few sources of biodiesel. There is a need to carry out numerical analysis of biodiesel derived from other potential feedstocks. Moreover, numerical studies on vegetable oils and biodiesel combustion in diesel engines and its validation from the experimental results are a new thrust area of research. Setting up a geometrical model consistent with the actual engine set up and its simulation using computational fluid dynamics tools provides a wider flexibility in engine studies and fuel effects.
4. NO_x has been found to increase in most cases; so there is a need to explore NO_x reduction techniques such as EGR or SCR.

REFERENCES

[1] BP Energy Outlook 2035, (2015), http://www.bp.com/content/dam/bp/pdf/energy-economics/energy-outlook-2015/bp-energy-outlook-2035-booklet.pdf, accessed on 17 June 2016.

[2] A. Kumar, S. Sharma. Potential Non-Edible Oil Resources as Biodiesel Feedstock: An Indian Perspective, *Renewable and Sustainable Energy Reviews*. **15** (2011), 1791–1800. doi:10.1016/j.rser.2010.11.020.

[3] Indian Petroleum and Natural Gas Statistics, Ministry Of Petroleum & Natural Gas Economics and Statistics Division New Delhi, Govt. of India, (2014-15), http://www.indiaenvironmentportal.org.in/files/file/pngstat%202014-15.pdf, accessed on 18 June 2016.

[4] BP Statistical Review of World Energy, (2015), https://www.bp.com/content/dam/bp/pdf/energy-economics/statistical-review-2015/bp-statistical-review-of-world-energy-2015-full-report.pdf, accessed on 20 June 2016.

[5] BP Energy Outlook 2035 Country and regional insights - India, (2016), http://www.bp.com/content/dam/bp/pdf/energy-economics/energy-outlook-2016/bp-energy-outlook-2016-country-insights-india.pdf, accessed on 20 June 2016.

[6] R. Dhingra, J.G. Overly, G.A. Davis, S. Das, S. Hadley, B. Tonn. A Life-Cycle-Based Environmental Evaluation : Materials in New Generation Vehicles, *SAE International*. (2000), doi:10.4271/2000-01-0595.

[7] S. Murugan, Sai Gu Research and development activities in pyrolysis – Contributions from Indian scientific community – A review, *Renewable and Sustainable Energy Reviews*. 46 (2015), 282-295. 10.1016/j.rser.2015.02.050.

[8] H.S. Pali, N. Kumar. Combustion, Performance and Emissions of Shorea Robusta Methyl Ester Blends in a Diesel Engine, *Biofuels*. **7269** (2016), 1–10. doi:10.1080/17597269.2016.1153363.

[9] H.S. Pali, N. Kumar, Y. Alhassan. Performance and Emission Characteristics of an Agricultural Diesel Engine Fueled with Blends of Sal Methyl Esters and Diesel, *Energy Conversion and Management*. **90** (2015), 146–153. doi:10.1016/j.enconman.2014.10.064.

[10] F. Ma, M.A. Hanna. Biodiesel Production: A Review, *Bioresource Technology*. **70** (1999),

1–15. doi:10.1016/S0960-8524(99)00025-5.

[11] A. Demirbas. Importance of Biodiesel as Transportation Fuel, *Energy Policy*. **35** (2007), 4661–4670. doi:10.1016/j.enpol.2007.04.003.

[12] D.H. Qi, H. Chen, L.M. Geng, Y.Z. Bian. Experimental Studies on the Combustion Characteristics and Performance of a Direct Injection Engine Fueled with Biodiesel/Diesel Blends, *Energy Conversion and Management*. **51** (2010), 2985–2992. doi:10.1016/j.enconman.2010.06.042.

[13] E.R. Sacia, M. Balakrishnan, A.T. Bell. Biomass Conversion to Diesel via the Etherification of Furanyl Alcohols Catalyzed by Amberlyst-15, *Journal of Catalysis*. **313** (2014), 70–79. doi:10.1016/j.jcat.2014.02.012.

[14] E.J.M. Paiva, M.L.C.P. Da Silva, J.C.S. Barboza, P.C. De Oliveira, H.F. De Castro, D.S. Giordani. Non-Edible Babassu Oil as a New Source for Energy Production-A Feasibility Transesterification Survey Assisted by Ultrasound, *Ultrasonics Sonochemistry*. **20** (2013), 833–838. doi:10.1016/j.ultsonch.2012.11.003.

[15] M.S. Shehata. Emissions, Performance and Cylinder Pressure of Diesel Engine Fuelled by Biodiesel Fuel, *Fuel*. **112** (2013), 513–522. doi:10.1016/j.fuel.2013.02.056.

[16] I.M.R. Fattah, H.H. Masjuki, A.M. Liaquat, R. Ramli, M.A. Kalam, V.N. Riazuddin. Impact of Various Biodiesel Fuels Obtained From Edible and Non-Edible Oils on Engine Exhaust Gas and Noise Emissions, *Renewable and Sustainable Energy Reviews*. **18** (2013), 552–567. doi:10.1016/j.rser.2012.10.036.

[17] M. Lapuerta, O. Armas, R. Ballesteros, M. Carmona. Fuel Formulation Effects on Passenger Car Diesel Engine Particulate Emissions and Composition, *SAE International*, (2000). doi:10.4271/2000-01-1850.

[18] M. Mofijur, A.E. Atabani, H.H. Masjuki, M.A. Kalam, B.M. Masum. A Study on the Effects of Promising Edible and Non-Edible Biodiesel Feedstocks on Engine Performance and Emissions Production : A Comparative Evaluation, *Renewable and Sustainable Energy Reviews*, **23** (2013), 391–404. doi:10.1016/j.rser.2013.03.009.

[19] T.M.Y. Khan, A.E. Atabani, I.A. Badaruddin, A. Badarudin, M.S. Khayoon, S. Triwahyono. Recent Scenario and Technologies to Utilize Non-Edible Oils for Biodiesel Production, *Renewable and Sustainable Energy Reviews*. **37** (2014), 840–851. doi:10.1016/j.rser.2014.05.064.

[20] S.K. Padhi. Preparation and Characterization from Non Edible Oils, *Ph.D. Thesis NIT Rourkela*, 2010.

[21] S.K. Hoekman, A. Broch, C. Robbins, E. Ceniceros, M. Natarajan. Review of Biodiesel Composition, Properties, and Specifications, *Renewable and Sustainable Energy Reviews*. **16** (2012), 143–169. doi:10.1016/j.rser.2011.07.143.

[22] S. Sindelar. India Biofuels Annual 2015, *Global Agricultural Information Network Report* (2015), http://gain.fas.usda.gov/Recent%20GAIN%20Publications/Biofuels%20Annual_New%20Delhi_India_7-1-2015.pdf, accessed on 22 June 2016.

[23] E.G. Giakoumis, C.D. Rakopoulos, A.M. Dimaratos, D.C. Rakopoulos. Exhaust Emissions of Diesel Engines Operating Under Transient Conditions with Biodiesel Fuel Blends, *Progress in Energy and Combustion Science*. **38** (2012), 691–715. doi:10.1016/j.pecs.2012.05.002.

[24] B.S. Chauhan, N. Kumar, H.M. Cho. Performance and emission studies on an agriculture engine on neat Jatropha oil , *Journal of Mechanical Science and Technology* 24 (2010). doi:10.1007/s12206-010-0101-.5

[25] V. Vibhanshu, A. Karnwal, Amardeep, N. Kumar. Performance, Emission and Combustion, Analysis of Diesel Engine Fueled with Blends of Mahua Oil Methyl Ester and Diesel, *SAE International.* (2014). doi:10.4271/2014-01-2651.

[26] Amar Deep, A.Singh, V. Vibhanshu, A. Khandelwal, N. Kumar. Experimental Investigation of Orange Peel Oil Methyl Ester on Single Cylinder Diesel Engine, *SAE International*, (2013). doi: 10.4271/2013-24-0171.

[27] G. Knothe. Analyzing Biodiesel : Standards and Other Methods, *Journal of the American Oil Chemists' Society*, **83** (2006), 823–833, doi:10.1007/s11746-006-5033-y.

[28] A. Sanjid, Md. A. Kalam, H.H. Masjuki, et al. Performance and Emission of Multi-Cylinder Diesel Engine using Biodiesel Blends obtained from Mixed Inedible Feedstocks, *Journal of Cleaner Production*. **112** (2016), 4114–4122. doi:10.1016/j.jclepro.2015.07.154.

[29] D.H. Qi, L.M. Geng, H. Chen, Y.Z.H. Bian, J. Liu, X.C.H. Ren. Combustion and Performance Evaluation of a Diesel Engine Fueled with Biodiesel Produced from Soybean Crude Oil, *Renewable Energy*. **34** (2009), 2706–2713. doi:10.1016/j.renene.2009.05.004.

[30] N. Kumar, P.B. Sharma. Jatropha Curcus- A sustainable Source for Production of Biodiesel, *Journal of Scientific and Industrial Research*. **64** (2005), 883–889.

[31] R. Sarin, M. Sharma, S. Sinharay, R.K. Malhotra. Jatropha-Palm Biodiesel Blends: An Optimum Mix for Asia, *Fuel*. **86** (2007), 1365–1371. doi:10.1016/j.fuel.2006.11.040.

[32] N. Scarlat, J.-F. Dallemand, F. Monforti-ferrario, M. Banja, V. Motola. Renewable Energy Policy Framework and Bioenergy Contribution in the European Union – An Overview from National Renewable Energy Action Plans and Progress Reports, *Renewable and Sustainable Energy Reviews*. **51** (2015), 969–985. doi:10.1016/j.rser.2015.06.062.

[33] S. Kumar, A. Chaube, S.K. Jain. Critical Review of Jatropha Biodiesel Promotion Policies in India, *Energy Policy*. **41** (2012), 775–781. doi:10.1016/j.enpol.2011.11.044.

[34] S. Ahmed, M.H. Hassan, Md. A. Kalam, S.M.A. Rahman, Md. J. Abedin, A. Shahir. An Experimental Investigation of Biodiesel Production, Characterization, Engine Performance, Emission and Noise of Brassica Juncea Methyl Ester and its Blends, *Journal of Cleaner Production*. **79** (2014), 74–81. doi:10.1016/j.jclepro.2014.05.019.

[35] A.K. Agarwal. Biofuels (Alcohols And Biodiesel) Applications as Fuels for Internal Combustion Engines, **33** (2007), 233–271. doi:10.1016/j.pecs.2006.08.003.

[36] G. Kafuku, M. Mbarawa. Alkaline Catalyzed Biodiesel Production from Moringa Oleifera Oil with Optimized Production Parameters, *Applied Energy*. **87** (2010), 2561–2565. doi:10.1016/j.apenergy.2010.02.026.

[37] S. Naik, V. V Goud, P.K. Rout, K. Jacobson, A.K. Dalai. Characterization of Canadian Biomass for Alternative Renewable Biofuel, *Renewable Energy*. **35** (2010), 1624–1631. doi:10.1016/j.renene.2009.08.033.

[38] A. E. Atabani, A. S. Silitonga, I.A. Badruddin, T.M.I. Mahlia, H.H. Masjuki, S. Mekhilef. A Comprehensive Review on Biodiesel as an alternative Energy Resource and its Characteristics, *Renewable and Sustainable Energy Reviews*. **16** (2012), 2070–2093. doi:10.1016/j.rser.2012.01.003.

[39] M. A. Fazal, A.S.M.A. Haseeb, H.H. Masjuki. Biodiesel Feasibility Study: An Evaluation of Material Compatibility; Performance; Emission and Engine Durability, *Renewable and Sustainable Energy Reviews*. **15** (2011), 1314–1324. doi:10.1016/j.rser.2010.10.004.

[40] D. Kashyap, M. Glueck, L. Kumar, S. Maithel, S. Sethi, S. Srinivas, et al. Liquid Biofuels for Transportation: India Country Study on Potential and Implications for sustainable

Agriculture and Energy, Reoprt submitted by: *The Energy and Resources Institute India* New Delhi (2006).

[41] S. Dhar, P.R. Shukla. Low Carbon Scenarios for Transport in India: Co-benefits Analysis, *Energy Policy*. **81** (2015), 186–198. doi:10.1016/j.enpol.2014.11.026.

[42] A.E. Atabani, T.M.I. Mahlia, H.H. Masjuki, et al. A Comparative Evaluation of Physical and Chemical Properties of biodiesel Synthesized from Edible and Non-Edible Oils and Study on the Effect of Biodiesel Blending, *Energy*. **58** (2013), 296–304. doi:10.1016/j.energy.2013.05.040.

[43] E.F. Aransiola, T. V. Ojumu, O.O. Oyekola, T.F. Madzimbamuto, D.I.O. Ikhu-Omoregbe. A Review of Current Technology for Biodiesel Production: State of the Art, *Biomass and Bioenergy*. **61** (2014), 276–297. doi:10.1016/j.biombioe.2013.11.014.

[44] V.B. Borugadda, V. V. Goud. Biodiesel Production from Renewable Feedstocks: Status and Opportunities, *Renewable and Sustainable Energy Reviews*. **16** (2012), 4763–4784. doi:10.1016/j.rser.2012.04.010.

[45] M. Mofijur, H.H. Masjuki, M. A. Kalam, et al. Effect of Biodiesel from Various Feedstocks on Combustion Characteristics Engine Durability and Materials Compatibility: A Review, *Renewable and Sustainable Energy Reviews*. **28** (2013), 441–455. doi:10.1016/j.rser.2013.07.051.

[46] G. Dwivedi, M.P. Sharma. Prospects of Biodiesel from Pongamia in India, *Renewable and Sustainable Energy Reviews*. **32** (2014), 114–122. doi:10.1016/j.rser.2014.01.009.

[47] S. Sankaranarayanan, C. A. Antonyraj, S. Kannan. Transesterification of Edible, Non-Edible and Used Cooking Oils for Biodiesel Production Using Calcined Layered Double Hydroxides as Reusable Base Catalysts, *Bioresource Technology*. **109** (2012), 57–62. doi:10.1016/j.biortech.2012.01.022.

[48] Ileri, Erol Koçar, Gunnur. Experimental investigation of the effect of antioxidant additives on NOx emissions of a diesel engine using biodiesel, *Fuel*. **125** (2014), 44-49. doi: 10.1016/j.fuel.2014.02.007.

[49] G. Dwivedi, S. Jain, M.P. Sharma. Impact Analysis of Biodiesel on Engine Performance - A Review, *Renewable and Sustainable Energy Reviews*. **15** (2011), 4633–4641. doi:10.1016/j.rser.2011.07.089.

[50] M.J. Abedin, M.A. Kalam, H.H. Masjuki, et al. Production of Biodiesel from a Non-edible

Source and Study of its Combustion, and Emission Characteristics : A Comparative Study with B5, *Renewable Energy*. **88** (2016), 20–29. doi:10.1016/j.renene.2015.11.027.

[51] B.S. Chauhan, R.K. Singh, H.M. Cho, H.C. Lim. Practice of Diesel Fuel Blends Using Alternative Fuels: A Review, *Renewable and Sustainable Energy Reviews*. **59** (2016), 1358–1368. doi:10.1016/j.rser.2016.01.062.

[52] H. Omidvarborna, A. Kumar, D.S. Kim, Recent Studies on Soot Modeling for Diesel Combustion, *Renewable and Sustainable Energy Reviews*. **48** (2015), 635–647. doi:10.1016/j.rser.2015.04.019.

[53] D.Y.C. Leung, X. Wu, M.K.H. Leung. A Review on Biodiesel Production using Catalyzed Transesterification, *Applied Energy*. **87** (2010), 1083–1095. doi:10.1016/j.apenergy.2009.10.006.

[54] M.F. Milazzo, F. Spina, A. Vinci, C. Espro, J.C.J. Bart. Brassica Biodiesels : Past , Present and Future, *Renewable and Sustainable Energy Reviews*. **18** (2013), 350–389. doi:10.1016/j.rser.2012.09.033.

[55] I.M. Atadashi, M.K. Aroua, A.A. Aziz. High Quality Biodiesel and its Diesel Engine Application: A Review, *Renewable and Sustainable Energy Reviews*. **14** (2010), 1999–2008. doi:10.1016/j.rser.2010.03.020.

[56] E.M. Shahid, Y. Jamal. Production of Biodiesel: A Technical Review, *Renewable and Sustainable Energy Reviews*. **15** (2011), 4732–4745. doi:10.1016/j.rser.2011.07.079.

[57] A.L. Ahmad, N.H.M. Yasin, C.J.C. Derek, J.K. Lim. Microalgae as a Sustainable Energy Source for Biodiesel Production: A Review, *Renewable and Sustainable Energy Reviews*. 15 (2011) 584–593. doi:10.1016/j.rser.2010.09.018.

[58] M. Takase, T. Zhao, M. Zhang, et al. An Expatiate Review of Neem, Jatropha, Rubber and Karanja as Multipurpose Non-Edible Biodiesel Resources and Comparison of their Fuel, Engine and Emission Properties, *Renewable and Sustainable Energy Reviews*. **43** (2015), 495–520. doi:10.1016/j.rser.2014.11.049.

[59] S.K. Karmee. Liquid Biofuels from Food Waste: Current Trends, Prospect and Limitation, *Renewable and Sustainable Energy Reviews*. **53** (2016), 945–953. doi:10.1016/j.rser.2015.09.041.

[60] M. Balat. Potential Alternatives to Edible Oils for Biodiesel Production - A Review of Current Work, *Energy Conversion and Management*. **52** (2011), 1479–1492.

doi:10.1016/j.enconman.2010.10.011.

[61] M. Balat, H. Balat. Progress in Biodiesel Processing, *Applied Energy*. **87** (2010), 1815–1835. doi:10.1016/j.apenergy.2010.01.012.

[62] X. Deng, Z. Fang, Y.H. Liu, C.L. Yu, Production of Biodiesel from Jatropha Oil Catalyzed by Nanosized Solid Basic Catalyst, *Energy*. **36** (2011), 777–784. doi:10.1016/j.energy.2010.12.043.

[63] P.S. Nigam, A. Singh. Production of Liquid Biofuels from Renewable Resources, *Progress in Energy and Combustion Science*. **37** (2010). doi:10.1016/j.pecs.2010.01.003.

[64] J. Li, L. Li, J. Tong, Y. Wang, S. Chen. Research Development on Lipase-Catalyzed Biodiesel, *Energy Procedia*. **16** (2012), 1014–1021. doi:10.1016/j.egypro.2012.01.162.

[65] M.M. Gui, K.T. Lee, S. Bhatia, Feasibility of Edible Oil vs. Non-Edible Oil vs. Waste Edible Oil as Biodiesel Feedstock, *Energy*. **33** (2008), 1646–1653. doi:10.1016/j.energy.2008.06.002.

[66] M.M. Azam, A. Waris, N.M. Nahar. Prospects and Potential of Fatty Acid Methyl Esters of Some Non-traditional Seed Oils for Use as Biodiesel in India, *Biomass and Bioenergy*. **29** (2005), 293–302. doi:10.1016/j.biombioe.2005.05.001.

[67] L.F. Razon, R.R. Tan. Net Energy Analysis of the Production of Biodiesel and Biogas from the Microalgae: Haematococcus Pluvialis and Nannochloropsis, *Applied Energy*. **88** (2011), 3507–3514. doi:10.1016/j.apenergy.2010.12.052.

[68] S. Kumar, A. Chaube, S.K. Jain. Sustainability Issues for Promotion of Jatropha Biodiesel in Indian Scenario: A Review, *Renewable and Sustainable Energy Reviews*. **16** (2012), 1089–1098. doi:10.1016/j.rser.2011.11.014.

[69] J.C. Juan, D.A. Kartika, T.Y. Wu, T.Y.Y. Hin. Biodiesel Production from Jatropha Oil by Catalytic and Non-catalytic Approaches: An Overview, *Bioresource Technology*. **102** (2011), 452–460. doi:10.1016/j.biortech.2010.09.093.

[70] L.Y. Chen, Y.H. Chen, Y.S. Hung, T.H. Chiang, C.H. Tsai. Fuel Properties and Combustion Characteristics of Jatropha Oil Biodiesel-Diesel Blends, *Journal of the Taiwan Institute of Chemical Engineers*. **44** (2013), 214–220. doi:10.1016/j.jtice.2012.09.011.

[71] C.Y. Yang, Z. Fang, B. Li, Y.F. Long. Review and Prospects of Jatropha biodiesel Industry in China, *Renewable and Sustainable Energy Reviews*. **16** (2012), 2178–2190.

doi:10.1016/j.rser.2012.01.043.

[72] S.Y. No, Inedible Vegetable Oils and Their Derivatives for Alternative Diesel Fuels in CI Engines : A Review, *Renewable and Sustainable Energy Reviews*. **15** (2011), 131–149. doi:10.1016/j.rser.2010.08.012.

[73] S.K. Karmee, A. Chadha. Preparation of Biodiesel from Crude Oil of Pongamia Pinnata, *Bioresource Technology*. **96** (2005), 1425–1429. doi:10.1016/j.biortech.2004.12.011.

[74] M.N. Nabi, S.M.N. Hoque, M.S. Akhter. Karanja (Pongamia Pinnata) Biodiesel Production in Bangladesh, Characterization of Karanja Biodiesel and its Effect on Diesel Emissions, *Fuel Processing Technology*. **90** (2009), 1080–1086. doi:10.1016/j.fuproc.2009.04.014.

[75] A.M. Ashraful, H.H. Masjuki, M.A. Kalam, et al. Production and Comparison of Fuel Properties, Engine Performance, and Emission Characteristics of Biodiesel from Various Non-Edible Vegetable Oils: A Review, *Energy Conversion and Management*. **80** (2014), 202–228. doi:10.1016/j.enconman.2014.01.037.

[76] D.D.C. Barbosa, T.M. Serra, S.M.P. Meneghetti, M.R. Meneghetti. Biodiesel Production by Ethanolysis of Mixed Castor and Soybean Oils, *Fuel*. **89** (2010), 3791–3794. doi:10.1016/j.fuel.2010.07.016.

[77] A. Machado, D. Castro, R. Castilho, D. Maria, G. Freire. Characterization of Babassu, Canola, Castor Seed and Sunflower Residual Cakes for use as Raw Materials for Fermentation Processes, *Industrial Crops & Products*. **83** (2016), 140–148. doi:10.1016/j.indcrop.2015.12.050.

[78] S. Pinzi, P. Rounce, J.M. Herreros, A. Tsolakis, M.P. Dorado. The Effect of Biodiesel Fatty Acid Composition on Combustion and Diesel Engine Exhaust Emissions, *Fuel*. **104** (2013), 170–182. doi:10.1016/j.fuel.2012.08.056.

[79] M. Kilic, B.B. Uzun, E. Putun, A.E. Putun. Optimization of Biodiesel Production from Castor Oil Using Factorial Design, *Fuel Processing Technology*. **111** (2013), 105–110. doi:10.1016/j.fuproc.2012.05.032.

[80] O.S. Valente, M.J. Da Silva, V.M.D. Pasa, C.R.P. Belchior, J.R. Sodre. a *Fuel*. **89** (2010), 3637–3642. doi:10.1016/j.fuel.2010.07.041.

[81] C. Mishra, N. Kumar, P. Mishra, B. Kar. In-Cylinder Combustion and Emission Characteristics of an Agricultural Diesel Engine Fuelled with Blends of Diesel and

Oxidatively Stabilized Calophyllum Methyl Ester, *SAE International*, (2016). doi:10.4271/2016-28-0140.

[82] M.F. Awalludin, O. Sulaiman, R. Hashim, W.N. Aidawati. An Overview of the Oil Palm Industry in Malaysia and its Waste Utilization through Thermochemical Conversion, Specifically via Liquefaction, *Renewable and Sustainable Energy Reviews*. **50** (2015), 1469–1484. doi:10.1016/j.rser.2015.05.085.

[83] C. Mishra, N. Kumar, Sidharth, B.S. Chauhan. Performance and Emission Studies of a Compression Ignition Engine on blends of Calophyllum Oil and Diesel, *Journal of Biofuels.* **3** (2012), 50-57. doi:10.5958/j.0976-3015.3.1.005.

[84] S. Puhan, N. Vedaraman, B. V Rambrahamam, G. Nagarajan. Mahua (Madhuca Indica) Seed Oil : A Source of Renewable Energy in India, *Journal of Scientific & Industrial Research*. **64** (2005), 890–896.

[85] H. Raheman, S. V. Ghadge. Performance of Compression Ignition Engine with Mahua (Madhuca Indica) Biodiesel, *Fuel*. **86** (2007), 2568–2573. doi:10.1016/j.fuel.2007.02.019.

[86] D. K. Bora, L.M. Das, M.K.G. Babu. Storage stability of mahua oil methyl ester, *Journal of Scientific & Industrial Research.* **68** (2009), 149–152.

[87] S. Puhan, N. Vedaraman, B.V.B. Ram, G. Sankarnarayanan, K. Jeychandran. Mahua Oil (Madhuca Indica seed oil) Methyl Ester as Biodiesel-Preparation and Emission Characterstics, *Biomass and Bioenergy*. **28** (2005), 87–93. doi:10.1016/j.biombioe.2004.06.002.

[88] A.W. Wagutu, S.C. Chhabra, C.L. Thoruwa, T.F. Thoruwa, R.L.A. Mahunnah. Indigenous Oil Crops as a Source for Production of Biodiesel in Kenya, *Bulletin of the Chemical Society of Ethiopia*. **23** (2009), 359–370. doi:10.4314/bcse.v23i3.47660.

[89] Alan C. Hansen, Qin Zhang, Peter W.L. Lyne. Ethanol-diesel fuel blends - a review, *Biosource Technology.* **96** (2004) 277-285. DOI: 10.1016/j.biortech.2004.04.007.

[90] S.S. Ragit. Process Standardization, Characterization and Experimental Investigation on the Performance of Biodiesel Fuelled C . I . Engine, *Ph.D. Thesis Thapar University* 2011.

.[91] V. Sathyaselvabala, T. Kadathur, D. Kirupha, V. Ponnusamy, S. Subramanian. Bioresource Technology Removal of Free Fatty Acid in Azadirachta Indica (Neem) Seed Oil using Phosphoric Acid Modified Mordenite for Biodiesel Production, *Bioresource Technology*. **101** (2010), 5897–5902. doi:10.1016/j.biortech.2010.02.092.

[92] A.S. Ramadhas, S. Jayaraj, C. Muraleedharan. Biodiesel Production from High FFA Rubber Seed Oil, *Fuel*. **84** (2005), 335–340. doi:10.1016/j.fuel.2004.09.016.

[93] A.S. Reshad, P. Tiwari, V. V Goud. Extraction of Oil from Rubber Seeds for biodiesel Application : Optimization of Parameters, *Fuel*. **150** (2015), 636–644. doi:10.1016/j.fuel.2015.02.058.

[94] N. Usta, B. Aydoğan, A.H. On, E. Uğuzdŏan, S.G. Özkal. Properties and Quality Verification of Biodiesel Produced from tobacco Seed Oil, *Energy Conversion and Management*. **52** (2011), 2031–2039. doi:10.1016/j.enconman.2010.12.021.

[95] C.R. Cardoso, T.J.P. Oliveira, J. A. Santana Junior, C.H. Ataíde. Physical Characterization of Sweet Sorghum Bagasse, Tobacco Residue, Soy Hull and fiber Sorghum Bagasse Particles: Density, Particle Size and Shape Distributions, *Powder Technology*. **245** (2013), 105–114. doi:10.1016/j.powtec.2013.04.029.

[96] B. Hajra, A.K. Pathak, C. Guria. Optimal Synthesis of Methyl Ester of Sal Oil (Shorea Robusta) using Ion-Exchange Resin Catalyst, *International Journal of Industrial Chemistry*. **5** (2014), 95–106. doi:10.1007/s40090-014-0024-6.

[97] H.S. Pali, N. Kumar, Y. Alhassan, Amardeep. Process Optimization of Biodiesel Production from Sal Seed Oil using Response Surface Methodology [RSM] and Diesel, *SAE International*. (2015). doi:10.4271/2015-01-1297.

[98] S. Kumar, R.C. Pradhan, P. Ghosh, et al. Shorea Robusta (Dipterocarpaceae) Seed and its Oil as Food, *International Journal of Food and Nutritional Sciences*, **4** (2015), 1–4.

[99] A.S. Silitonga, H.H. Masjuki, T.M.I. Mahlia, et al. Schleichera Oleosa L Oil as Feedstock for Biodiesel Production, *Fuel*. **156** (2015), 63–70. doi:10.1016/j.fuel.2015.04.046.

[100] Y.C. Sharma, B. Singh. An Ideal Feedstock, Kusum (Schleichera Triguga) for Preparation of Biodiesel: Optimization of Parameters, *Fuel*. **89** (2010), 1470–1474. doi:10.1016/j.fuel.2009.10.013.

[101] A.E. Atabani, A.S. Silitonga, H.C. Ong, et al. Non-Edible Vegetable Oils : A Critical Evaluation of Oil Extraction, Fatty Acid Compositions, Biodiesel Production, Characteristics, Engine Performance and Emissions Production, *Renewable and Sustainable Energy Reviews*. **18** (2013), 211–245. doi:10.1016/j.rser.2012.10.013.

[102] A. Kumar, S. Sharma. An Evaluation of Multipurpose Oil Seed Crop for Industrial Uses (Jatropha Curcas L.): A Review, *Industrial Crops and Products*. **28** (2008), 1–10.

doi:10.1016/j.indcrop.2008.01.001.

[103] Xuan Wu, Dennis Y.C. Leung. Optimization of biodiesel production from camelina oil using orthogonal experiment, *Applied Energy*. 88 (2011) 3615–3624. 10.1016/j.apenergy.2011.04.041.

[104] G. Knothe. A Comprehensive Evaluation of the Cetane Numbers of Fatty Acid Methyl Esters, *Fuel*. **119** (2014), 6–13. doi:10.1016/j.fuel.2013.11.020.

[105] A. Demirbas. Use of Algae as Biofuel Sources, *Energy Conversion and Management*. **51** (2010), 2738–2749. doi:10.1016/j.enconman.2010.06.010.

[106] G. Knothe. Biodiesel and Renewable Diesel: A Comparison, *Progress in Energy and Combustion Science*. **36** (2010), 364–373. doi:10.1016/j.pecs.2009.11.004.

[107] I.M. Atadashi, M.K. Aroua, A. R. Abdul Aziz, N.M.N. Sulaiman. Production of Biodiesel using High Free Fatty Acid Feedstocks, *Renewable and Sustainable Energy Reviews*. **16** (2012), 3275–3285. doi:10.1016/j.rser.2012.02.063.

[108] N. Kumar, Varun, S.R. Chauhan. Performance and Emission Characteristics of Biodiesel from Different Origins : A review, *Renewable and Sustainable Energy Reviews*. **21** (2013), 633–658. doi:10.1016/j.rser.2013.01.006.

[109] Y.C. Sharma, B. Singh, S.N. Upadhyay. Advancements in Development and Characterization of Biodiesel: A Review, *Fuel*. **87** (2008), 2355–2373. doi:10.1016/j.fuel.2008.01.014.

[110] N.N.A.N. Yusuf, S.K. Kamarudin, Z. Yaakub. Overview on the Current Trends in Biodiesel Production, *Energy Conversion and Management*. **52** (2011), 2741–2751. doi:10.1016/j.enconman.2010.12.004.

[111] N.-C. Shang, R.-Z. Liu, Y.-H. Chen, C.-Y. Chang, R.-H. Lin. Characterization of Fatty Acid Methyl Esters in Biodiesel Using High-Performance Liquid Chromatography, *Journal of the Taiwan Institute of Chemical Engineers*. **43** (2012), 354–359. doi:10.1016/j.jtice.2011.11.005.

[112] A. Demirbas. Progress and Recent Trends in Biodiesel Fuels, *Energy Conversion and Management*. **50** (2009), 14–34. doi:10.1016/j.enconman.2008.09.001.

[113] S. Shiung, R. Keey, A. Jusoh, C. Tung, F. Nasir, H.A. Chase. Progress in Waste Oil to Sustainable Energy , with Emphasis on Pyrolysis Techniques, *Renewable and Sustainable Energy Reviews*. **53** (2016), 741–753. doi:10.1016/j.rser.2015.09.005.

[114] W. Qu, Q. Zhou, Y.Z. Wang, J. Zhang, et al. Pyrolysis of Waste Tire on ZSM-5 Zeolite with Enhanced Catalytic Activities, *Polymer Degradation and Stability*. **91** (2006), 2389–2395. doi:10.1016/j.polymdegradstab.2006.03.014.

[115] M.Y. Koh, G.T.I. Mohd. A Review of Biodiesel Production from Jatropha Curcas L. Oil, *Renewable and Sustainable Energy Reviews*. **15** (2011), 2240–2251. doi:10.1016/j.rser.2011.02.013.

[116] A. Demirbas. Biodiesel Fuels from Vegetable Oils via Catalytic and Non-Catalytic Supercritical Alcohol Transesterifications and Other Methods: A Survey, *Energy Conversion and Management*. **44** (2003), 2093–2109. doi:10.1016/S0196-8904(02)00234-0.

[117] S. Jain, M.P. Sharma. Stability of Biodiesel and its Blends : A Review, *Renewable and Sustainable Energy Reviews.* **14** (2010), 667–678. doi:10.1016/j.rser.2009.10.011.

[118] S. Jain, M.P. Sharma. Bioresource Technology Kinetics of Acid Base Catalyzed Transesterification of Jatropha Curcas Oil, *Bioresource Technology*. **101** (2010), 7701–7706. doi:10.1016/j.biortech.2010.05.034.

[119] J. Van Gerpen. Biodiesel Processing and Production, *Fuel Processing Technology*. **86** (2005), 1097–1107. doi:10.1016/j.fuproc.2004.11.005.

[120] S. Silitonga, E. Atabani, T.M.I. Mahlia, H.H. Masjuki, I.A. Badruddin, S. Mekhilef. A Review on Prospect of Jatropha Curcas for Biodiesel in Indonesia, *Renewable and Sustainable Energy Reviews*. **15** (2011), 3733–3756. doi:10.1016/j.rser.2011.07.011.

[121] C.Y. Lin, C.L. Fan. Fuel Properties of Biodiesel Produced from Camellia Oleifera Abel Oil through Supercritical-Methanol Transesterification, *Fuel*. **90** (2011), 2240–2244. doi:10.1016/j.fuel.2011.02.020.

[122] C.L. Teo, H. Jamaluddin, N.A.M. Zain, A. Idris. Biodiesel Production via Lipase Catalysed Transesterification of Microalgae Lipids from Tetraselmis sp., *Renewable Energy*. **68** (2014), 1–5. doi:10.1016/j.renene.2014.01.027.

[123] D.L. Manuale, V.M. Mazzieri, G. Torres, C.R. Vera, J.C. Yori. Non-Catalytic Biodiesel Process with Adsorption-based Refining, *Fuel*. **90** (2011), 1188–1196. doi:10.1016/j.fuel.2010.10.047.

[124] D.K. Gupta, A. Sharma, V. Pathak, N. Kumar. Synthesis of Linseed oil Biodiesel using a Non-Catalytic Supercritical Transesterification Process, *SAE International Journal of*

Fuels and Lubricants. **7** (2014), 2014–01–1955. doi:10.4271/2014-01-1955.

[125] A. Deshpande, G. Anitescu, P. A. Rice, L.L. Tavlarides. Supercritical Biodiesel Production and Power Cogeneration: Technical and Economic Feasibilities, *Bioresource Technology*. **101** (2010), 1834–1843. doi:10.1016/j.biortech.2009.10.034.

[126] V. Rathore, G. Madras. Synthesis of Biodiesel from Edible and Non-Edible Oils in Supercritical Alcohols and Enzymatic Synthesis in Supercritical Carbon Dioxide, *Fuel*. **86** (2007), 2650–2659. doi:10.1016/j.fuel.2007.03.014.

[127] J. Gandure, C. Ketlogetswe, A. Temu. Fuel Properties of Biodiesel Produced from Selected Plant Kernel Oils Indigenous to Botswana : A Comparative Analysis, *Renewable Energy*. **68** (2014), 414–420. doi:10.1016/j.renene.2014.02.035.

[128] B.B. Uzun, M. Kiliç, N. Özbay, A.E. Pütün, E. Pütün. Biodiesel Production from Waste Frying Oils: Optimization of Reaction Parameters and Determination of Fuel Properties, *Energy*. **44** (2012), 347–351. doi:10.1016/j.energy.2012.06.024.

[129] K.T. Tan, K.T. Lee, A. R. Mohamed. Potential of Waste Palm Cooking Oil for Catalyst-Free Biodiesel Production, *Energy*. **36** (2011), 2085–2088. doi:10.1016/j.energy.2010.05.003.

[130] D.Y.C. Leung, B.C.P. Koo, Y. Guo. Degradation of biodiesel under different storage conditions, *Bioresource Technology*. **97** (2006), 250-256. doi: 10.1016/j.biortech.2005.02.006.

[131] X. Wu, D.Y.C. Leung. Optimization of Biodiesel Production from Camelina Oil using Orthogonal Experiment, *Applied Energy*. **88** (2011), 3615–3624. doi:10.1016/j.apenergy.2011.04.041.

[132] Y. Yücel. Optimization of Biocatalytic Biodiesel Production from Pomace Oil using Response Surface Methodology, *Fuel Processing Technology*. **99** (2012), 97–102. doi:10.1016/j.fuproc.2012.02.008.

[133] S. Jain, M.P. Sharma. Oxidation and Thermal Behavior of Jatropha Curcas Biodiesel Influenced by Antioxidants and Metal Contaminants, *International Journal of Engineering, Science and Technology*. **3** (2011), 65–75.

[134] S. Sharma, N. Kumar, S. Jain, S. Kumar. Scope of Fe-ZSM5 Zeolite Based Urea-SCR with Fish Oil Bio-Diesel Fuel in Compressed Ignition Engine, *SAE International*. (2014). doi:10.4271/2014-01-1541.

[135] A. Srivastava, R. Prasad. Triglycerides-based Diesel Fuels, *Renewable and Sustainable Energy Reviews.* **4** (2000), 111–133. doi:10.1016/S1364-0321(99)00013-1.

[136] A. Murugesan, C. Umarani, R. Subramanian, N. Nedunchezhian. Bio-diesel as an Alternative Fuel for Diesel Engines-A Review, *Renewable and Sustainable Energy Reviews*. **13** (2009), 653–662. doi:10.1016/j.rser.2007.10.007.

[137] C.T. Chong, S. Hochgreb. Spray Combustion Characteristics of Palm Biodiesel, *Combustion Science and Technology*. **184** (2012), 1093–1107. doi:10.1080/00102202.2012.663999.

[138] A. Dhar, R. Kevin, A.K. Agarwal. Production of Biodiesel from High-FFA Neem Oil and its Performance, Emission and Combustion Characterization in a Single Cylinder DICI Engine, *Fuel Processing Technology*. **97** (2012), 118–129. doi:10.1016/j.fuproc.2012.01.012.

[139] G.R. De Souza, A.M. Dos Santos, S.L. Ferreira, K.C. Ribeiro Martins, D.L. Módolo. Evaluation of the Performance of Biodiesel from Waste Vegetable Oil in a Flame Tube Furnace, *Applied Thermal Engineering*. **29** (2009), 2562–2566. doi:10.1016/j.applthermaleng.2008.12.026.

[140] M. Gülüm, A. Bilgin. Density, Flash Point and Heating Value Variations of Corn Oil Biodiesel – Diesel Fuel Blends, *Fuel Processing Technology*. **134** (2015), 456–464. doi:10.1016/j.fuproc.2015.02.026.

[141] A. Demirbas. Biodiesel Production from Vegetable Oils via Catalytic and Non-Catalytic Supercritical Methanol Transesterification Methods, *Progress in Energy and Combustion Science*. **31** (2005), 466–487. doi:10.1016/j.pecs.2005.09.001.

[142] F. Saloua, C. Saber, Z. Hedi. Methyl Ester of [Maclura Pomifera (Rafin.) Schneider] Seed Oil: Biodiesel Production and Characterization, *Bioresource Technology*. **101** (2010), 3091–3096. doi:10.1016/j.biortech.2009.11.100.

[143] G. Knothe, A.C. Matheaus, T.W. Ryan. Cetane Numbers of Branched and Straight-Chain Fatty Esters Determined in an Ignition Quality Tester, *Fuel*. **82** (2003), 971–975. doi:10.1016/S0016-2361(02)00382-4.

[144] A. Karmakar, S. Karmakar, S. Mukherjee. Properties of Various Plants and Animals Feedstocks for Biodiesel Production, *Bioresource Technology*. **101** (2010), 7201–7210. doi:10.1016/j.biortech.2010.04.079.

[145] M. Lapuerta, J.M. Herreros, L.L. Lyons, R. García-Contreras, Y. Briceño. Effect of the Alcohol Type used in the Production of Waste Cooking Oil Biodiesel on Diesel Performance and Emissions, *Fuel*. **87** (2008), 3161–3169. doi:10.1016/j.fuel.2008.05.013.

[146] H. Falahati, A. Y. Tremblay. The Effect of Flux and Residence Time in the Production of Biodiesel from Various Feedstocks using a Membrane Reactor, *Fuel*. **91** (2012), 126–133. doi:10.1016/j.fuel.2011.06.019.

[147] M. Hájek, F. Skopal, J. Machek. Determination of Free Glycerol in Biodiesel, *European Journal of Lipid Science and Technology*. **108** (2006), 666–669. doi:10.1002/ejlt.200600004.

[148] K. Bansal, J. McCrady, A. Hansen, K. Bhalerao. Thin Layer Chromatography and Image Analysis to Detect Glycerol in Biodiesel, *Fuel*. **87** (2008), 3369–3372. doi:10.1016/j.fuel.2008.04.033.

[149] S. Fernando, P. Karra, R. Hernandez, S.K. Jha. Effect of Incompletely Converted Soybean Oil on Biodiesel Quality, *Energy*. **32** (2007), 844–851. doi:10.1016/j.energy.2006.06.019.

[150] Z. Wen, X. Yu, S.T. Tu, J. Yan, E. Dahlquist. Synthesis of Biodiesel from Vegetable Oil with Methanol Catalyzed by Li-Doped Magnesium Oxide Catalysts, *Applied Energy*. **87** (2010), 743–748. doi:10.1016/j.apenergy.2009.09.013.

[151] A. Obadiah, R. Kannan, A. Ramasubbu, S.V. Kumar. Studies on the Effect of Antioxidants on the Long-Term Storage and Oxidation Stability of Pongamia Pinnata (L.) Pierre Biodiesel, *Fuel*. **99** (2012), 56–63. doi:10.1016/j.fuproc.2012.01.032.

[152] I.M. Atadashi, M.K. Aroua, A.R.A. Aziz, N.M.N. Sulaiman. The Effects of Water on Biodiesel Production and Refining Technologies : A Review, *Renewable and Sustainable Energy Reviews*. **16** (2012), 3456–3470. doi:10.1016/j.rser.2012.03.004.

[153] D.M. Fernandes, R.H.O. Montes, E.S. Almeida, et al. Storage Stability and Corrosive Character of Stabilised Biodiesel Exposed to Carbon and Galvanised Steels, *Fuel*. **107** (2013), 609–614. doi:10.1016/j.fuel.2012.11.010.

[154] P.J. Singh, J. Khurma, A. Singh. Preparation, Characterisation, Engine Performance and Emission Characteristics of Coconut Oil Based Hybrid Fuels, *Renewable Energy*. **35** (2010), 2065–2070. doi:10.1016/j.renene.2010.02.007.

[155] A. Dhar, A.K. Agarwal. Experimental Investigations of Effect of Karanja Biodiesel on Tribological Properties of Lubricating Oil in a Compression Ignition Engine, *Fuel*. **130**

(2014), 112–119. doi:10.1016/j.fuel.2014.03.066.

[156] G. Knothe. Structure Indices in FA Chemistry. How Relevant is the Iodine Value?, *Journal of the American Oil Chemists' Society*. **79** (2002), 847–854. doi:10.1007/s11746-002-0569-4.

[157] V.C. Eze, A.P. Harvey, A.N. Phan. Determination of the Kinetics of Biodiesel Saponification in Alcoholic Hydroxide Solutions, *Fuel*. **140** (2015), 724–730. doi:10.1016/j.fuel.2014.10.001.

[158] D.Y.C. Leung, B.C.P. Koo, Y. Guo. Degradation of Biodiesel under Different Storage Conditions, *Bioresource Technology*. **97** (2006), 250–256. doi:10.1016/j.biortech.2005.02.006.

[159] G. Karavalakis, S. Stournas, D. Karonis. Evaluation of the Oxidation Stability of Diesel/Biodiesel Blends, *Fuel*. **89** (2010), 2483–2489. doi:10.1016/j.fuel.2010.03.041.

[160] B.R. Moser. Biodiesel Production, Properties, and Feedstocks, *In Vitro Cell.Dev.Biol. — Plant.* **45** (2009) 229–266. doi:10.1007/s11627-009-9204-z.

[161] E. Cristina, R. Maia, D. Borsato, et al. Study of the Biodiesel B100 Oxidative Stability in Mixture with Antioxidants, *Fuel Processing Technology*. **92** (2011), 1750–1755. doi:10.1016/j.fuproc.2011.04.028.

[162] S. Schober, M. Mittelbach. The Impact of Antioxidants on Biodiesel Oxidation, *European Journal of Lipid Science and Technology*. **106** (2004), 382–389. doi:10.1002/ejlt.200400954.

[163] A.K. Agarwal, D. Khurana, Long-Term Storage Oxidation Stability of Karanja Biodiesel with the use of Antioxidants, *Fuel Processing Technology*. **106** (2012), 447–457. doi:10.1016/j.fuproc.2012.09.011.

[164] V. Marques, J. Angeiras, B. Silva, L. Stragevitch, R.L. Longo. Thermochemistry of Biodiesel Oxidation Reactions : A DFT Study, *Fuel*. **90** (2011), 811–817. doi:10.1016/j.fuel.2010.09.017.

[165] M. Naik, L.C. Meher, S.N. Naik, L.M. Das. Production of Biodiesel from High Free Fatty Acid Karanja (Pongamia Pinnata) Oil, *Biomass and Bioenergy*. **32** (2008), 354–357. doi:10.1016/j.biombioe.2007.10.006.

[166] S. Jain, M.P. Sharma. Optimization of Long-Term Storage Stability of Jatropha Curcas Biodiesel using Antioxidants by Means of Response Surface Methodology, *Biomass and*

Bioenergy. **35** (2011), 4008–4014. doi:10.1016/j.biombioe.2011.06.032.

[167] T. Issariyakul, A.K. Dalai. Biodiesel from Vegetable Oils, *Renewable and Sustainable Energy Reviews*. **31** (2014), 446–471. doi:10.1016/j.rser.2013.11.001.

[168] Z. Yaakob, B.N. Narayanan, S. Padikkaparambil, S. Unni K., M. Akbar P. A Review on the Oxidation Stability of Biodiesel, *Renewable and Sustainable Energy Reviews*. **35** (2014), 136–153. doi:10.1016/j.rser.2014.03.055.

[169] M. Canakci, J. Van Gerpen. A Pilot Plant to Produce Biodiesel from High Free Fatty Acid Feedstocks, *ASAE Meeting* Paper No. 01-6049. St. Joseph, Mich.: ASAE. (2001).

[170] P.S. Wang, J. Thompson, T.E. Clemente, J.H. Van Gerpen. Improving the Fuel Properties of Soy Biodiesel, *Transactions of the ASABE*. **53** (2010), 1853–1858.

[171] P. Bondioli, A. Gasparoli, L. Della Bella, S. Tagliabue, G. Toso. Biodiesel Stability under Commercial Storage, *European Journal of Lipid Science and Technology*. **105** (2003) 735–741. doi:10.1002/ejlt.200300783.

[172] J. Pullen, K. Saeed. Experimental Study of the Factors Affecting the Oxidation Stability of Biodiesel FAME Fuels, *Fuel Processing Technology*. **125** (2014), 223–235. doi:10.1016/j.fuproc.2014.03.032.

[173] D.H. Qi, C.F. Lee. Influence of Soybean Biodiesel Content on Basic Properties of Biodiesel-Diesel Blends, *Journal of the Taiwan Institute of Chemical Engineers*. **45** (2014), 504–507. doi:10.1016/j.jtice.2013.06.021.

[174] B.R. Moser. Impact of Fatty Ester Composition on Low Temperature Properties of Biodiesel-Petroleum Diesel Blends, *Fuel*. **115** (2014), 500–506. doi:10.1016/j.fuel.2013.07.075.

[175] P.V. Bhale, N. V. Deshpande, S.B. Thombre. Improving the Low Temperature Properties of Biodiesel Fuel, *Renewable Energy*. **34** (2009), 794–800. doi:10.1016/j.renene.2008.04.037.

[176] Y.H. Chen, Y.M. Luo. Oxidation Stability of Biodiesel Derived from Free Fatty Acids Associated with Kinetics of Antioxidants, *Fuel Processing Technology*. **92** (2011), 1387–1393. doi:10.1016/j.fuproc.2011.03.003.

[177] B.S. Chauhan, N. Kumar, H.M. Cho. A study on the Performance and Emission of a Diesel Engine Fueled with Jatropha Biodiesel Oil and its Blends, *Energy*. **37** (2012), 616–622. doi:10.1016/j.energy.2011.10.043.

[178] M.M. Rashed, M.A. Kalam, H.H. Masjuki, M. Mofijur, M.G. Rasul, N.W.M. Zulkifli. Performance and Emission Characteristics of a Diesel Engine Fueled with Palm, Jatropha, and Moringa Oil Methyl Ester, *Industrial Crops and Product*s. **79** (2016), 70–76. doi:10.1016/j.indcrop.2015.10.046

[179] A. Nalgundwar, B. Paul, S. Kumar. Comparison of Performance and Emissions Characteristics of DI CI Engine Fueled with Dual Biodiesel Blends of Palm and Jatropha, *Fuel*. **173** (2016), 172-179. doi:10.1016/j.fuel.2016.01.022.

[180] J. Huang, Y. Wang, J. Qin, A.P. Roskilly. Comparative Study of Performance and Emissions of a Diesel Engine using Chinese Pistache and Jatropha Biodiesel, *Fuel Processing Technology*. **91** (2010), 1761–1767. doi:10.1016/j.fuproc.2010.07.017.

[181] S. Bari. Performance, Combustion and Emission Tests of a Metro-Bus Running on Biodiesel-ULSD Blended (B20) Fuel, *Applied Energy*. **124** (2014), 35–43. doi:10.1016/j.apenergy.2014.03.007.

[182] T. Ganapathy, R.P. Gakkhar, K. Murugesan. Influence of Injection Timing on Performance, Combustion and Emission Characteristics of Jatropha Biodiesel Engine, *Applied Energy*. **88** (2011), 4376–4386. doi:10.1016/j.apenergy.2011.05.016.

[183] M. Mofijur, H.H. Masjuki, M. A. Kalam, A. E. Atabani. Evaluation of Biodiesel Blending, Engine Performance and Emissions Characteristics of Jatropha Curcas Methyl Ester: Malaysian Perspective, *Energy*. **55** (2013), 879–887. doi:10.1016/j.energy.2013.02.059.

[184] A. Dhar, A.K. Agarwal. Performance, Emissions and Combustion Characteristics of Karanja Biodiesel in a Transportation Engine, *Fuel*. **119** (2014), 70–80. doi:10.1016/j.fuel.2013.11.002.

[185] H. Raheman, A.G. Phadatare. Diesel Engine Emissions and Performance from Blends of Karanja Methyl Ester and Diesel, *Biomass and Bioenergy*. **27** (2004), 393–397. doi:10.1016/j.biombioe.2004.03.002.

[186] B.S. Chauhan, N. Kumar, H.M. Cho, H.C. Lim. A Study on the Performance and Emission of a Diesel Engine Fueled with Karanja Biodiesel and its Blends, *Energy*. **56** (2013), 1–7. doi:10.1016/j.energy.2013.03.083.

[187] P.K. Sahoo, L.M. Das, M.K.G. Babu, S.N. Naik. Biodiesel Development from High Acid Value Polanga Seed Oil and Performance Evaluation in a CI Engine, *Fuel*. **86** (2007), 448–454. doi:10.1016/j.fuel.2006.07.025.

[188] P.K. Sahoo, L.M. Das, Process Optimization for Biodiesel Production from Jatropha, Karanja and Polanga oils, *Fuel*. **88** (2009), 1588–1594. doi:10.1016/j.fuel.2009.02.016.

[189] S. Godiganur, C.H.S. Murthy, R. Prathap, 6BTA 5 . 9 G2-1 Cummins Engine Performance and Emission Tests using Methyl Ester Mahua (Madhuca Indica) Oil / Diesel Blends, *Renewable Energy*. **34** (2009), 2172–2177. doi:10.1016/j.renene.2008.12.035.

[190] S. Puhan, N. Vedaraman, G. Sankaranarayanan, B.V.B. Ram. Performance and Emission Study of Mahua Oil (Madhuca Indica Oil) Ethyl Ester in a 4-Stroke Natural Aspirated Direct Injection Diesel Engine, *Renewable Energy*. **30** (2005), 1269–1278. doi:10.1016/j.renene.2004.09.010.

[191] S. Puhan, N. Saravanan, G. Nagarajan, N. Vedaraman. Effect of biodiesel Unsaturated Fatty Acid on Combustion Characteristics of a DI Compression Ignition Engine, *Biomass and Bioenergy*. **34** (2010), 1079–1088. doi:10.1016/j.biombioe.2010.02.017.

[192] B. Hajra, M. Kumar, A.K. Pathak, C. Guria. Surface Tension and Rheological Behavior of Sal Oil Methyl Ester Biodiesel and its Blend with Petrodiesel Fuel, *Fuel*. **166** (2016), 130–142. doi:10.1016/j.fuel.2015.10.109.

[193] V.K. Chhibber, H.C. Joshi, S.K. Saxena. Sal (Shorea Robusta), an Environmentfriendly and Ecofriendly Alternative Vegetable Oil Fuel in Comparison to the Diesel Oil, *Advances in Pure and Applied Chemistry*. **1** (2012), 36–39.

[194] K. Muralidharan, D. Vasudevan, K.N. Sheeba. Performance, Emission and Combustion Characteristics of Biodiesel Fuelled Variable Compression Ratio Engine, *Energy*. **36** (2011), 5385–5393. doi:10.1016/j.energy.2011.06.050.

[195] P.C. Jena, H. Raheman, G. V. Prasanna Kumar, R. Machavaram. Biodiesel Production from Mixture of Mahua and Simarouba Oils with High Free Fatty Acids, *Biomass and Bioenergy*. **34** (2010), 1108–1116. doi:10.1016/j.biombioe.2010.02.019.

[196] N. Kumar. Production of Biodiesel from High FFA Rice Bran Oil and its Utilization in a Small Capacity Diesel Engine, *Journal of Scientific and Industrial Research*. **66** (2007), 399–402.

[197] K. Bonet-Ragel, A. Canet, M.D. Benaiges, F. Valero. Synthesis of Biodiesel from High FFA Alperujo Oil Catalysed by Immobilised Lipase, *Fuel*. **161** (2015), 12–17. doi:10.1016/j.fuel.2015.08.032.

[198] Z. Yaakob, M. Mohammad, M. Alherbawi, Z. Alam, K. Sopian. Overview of the

Production of Biodiesel from Waste Cooking Oil, *Renewable and Sustainable Energy Reviews*. **18** (2013), 184–193. doi:10.1016/j.rser.2012.10.016.

[199] X. Yuan, J. Liu, G. Zeng, J. Shi, J. Tong, G. Huang. Optimization of Conversion of Waste Rapeseed Oil with High FFA to Biodiesel using Response Surface Methodology, *Renewable Energy*. **33** (2008), 1678–1684. doi:10.1016/j.renene.2007.09.007.

[200] P. Goyal, M.P. Sharma, S. Jain. Optimization of Esterification and Transesterification of High FFA Jatropha Curcas Oil Using Response Surface Methodology, *Journal of Petroleum Science Research.* **1** (2012), 36–43.

[201] M. Azim, K. Ismail, et al. Microwave-assisted Pyrolysis of Palm Kernel Shell: Optimization using Response Surface Methodology (RSM), *Renewable and Sustainable Energy Reviews*. **55** (2013), 357–365. doi:10.1016/j.renene.2012.12.042.

[202] A. Abuhabaya, J. Fieldhouse, D. Brown. The Effects of using Biodiesel on CI (Compression Ignition) Engine and Optimization of its Production by using Response Surface Methodology, *Energy*. **59** (2013), 56–62. doi:10.1016/j.energy.2013.06.056.

[203] S. Jeong, J. Lee. Optimization of Pretreatment Condition for Ethanol Production from Oxalic Acid Pretreated Biomass by Response Surface Methodology, *Industrial Crops & Products*. **79** (2016), 1–6. doi:10.1016/j.indcrop.2015.10.036.

[204] A.K. Agarwal, A. Dhar. Experimental Investigation of Preheated Jatropha Oil Fuelled Direct Injection Compression Ignition Engine—Part 2: Engine Durability and Effect on Lubricating Oil, *Journal of ASTM International*. **7** (2010), 1-15. doi:10.1520/JAI102415.

[205] Md. J. Hussan, M.H. Hassan, Md. A. Kalam, L.A. Memon. Tailoring key Fuel Properties of Diesel-Biodiesel-Ethanol Blends for Diesel Engine, *Journal of Cleaner Production*. **51** (2013), 118–125. doi:10.1016/j.jclepro.2013.01.023.

[206] S. Kerschbaum, G. Rinke, K. Schubert. Winterization of Biodiesel by Micro Process Engineering, *Fuel*. **87** (2008), 2590–2597. doi:10.1016/j.fuel.2008.01.023.

[207] C. Boshui, S. Yuqiu, F. Jianhua, W. Jiu, W. Jiang. Effect of Cold Flow Improvers on Flow Properties of Soybean Biodiesel, *Biomass and Bioenergy*. **34** (2010), 1309–1313. doi:10.1016/j.biombioe.2010.04.001.

[208] E. Porpatham, A. Ramesh, B. Nagalingam. Effect of Compression Ratio on the Performance and Combustion of a Biogas Fuelled Spark Ignition Engine, *Fuel*. **95** (2012), 247–256. doi:10.1016/j.fuel.2011.10.059.

[209] M.N. Nabi, M.M. Rahman, M.S. Akhter. Biodiesel from Cotton Seed Oil and its Effect on Engine Performance and Exhaust Emissions, *Applied Thermal Engineering*. **29** (2009), 2265–2270. doi:10.1016/j.applthermaleng.2008.11.009.

[210] M. El-kasaby, M.A. Nemit-allah. Experimental Investigations of Ignition Delay Period and Performance of a Diesel Engine Operated with Jatropha Oil Biodiesel, *Alexandria Engineering Journal*. **52** (2013), 141–149. doi:10.1016/j.aej.2012.12.006.

[211] M.J. Abedin, H.H. Masjuki, M.A. Kalam, A. Sanjid, S.M.A. Rahman, I.M.R. Fattah. Performance, Emissions, and Heat Losses of Palm and Jatropha Biodiesel Blends in a Diesel Engine, *Industrial Crops & Products*. **59** (2014), 96–104. doi:10.1016/j.indcrop.2014.05.001.

[212] A.A. De Paulo, R. Silvestre, S.B. Rahde, F.D. Vecchia, M. Seferin, C. Alexandre. Performance and Emission Evaluations in a Power Generator Fuelled with Brazilian Diesel and Additions of Waste Frying Oil Biodiesel, *Applied Thermal Engineering*. **98** (2016), 288–297. doi:10.1016/j.applthermaleng.2015.12.036.

[213] A. Sanjid, H.H. Masjuki, M. a. Kalam, S.M.A. Rahman, M.J. Abedin, S.M. Palash. Production of Palm and Jatropha Based Biodiesel and Investigation of Palm-Jatropha Combined Blend Properties, Performance, Exhaust Emission and Noise in an Unmodified Diesel Engine, *Journal of Cleaner Production*. **65** (2014), 295–303. doi:10.1016/j.jclepro.2013.09.026.

[214] M. Mani, C. Subash, G. Nagarajan. Performance, Emission and Combustion Characteristics of a DI Diesel Engine using Waste Plastic Oil, *Applied Thermal Engineering*. **29** (2009), 2738–2744. doi:10.1016/j.applthermaleng.2009.01.007.

[215] M. Kousoulidou, G. Fontaras, L. Ntziachristos, Z. Samaras. Biodiesel Blend Effects on Common-rail Diesel Combustion and Emissions, *Fuel*. **89** (2010), 3442–3449. doi:10.1016/j.fuel.2010.06.034.

[216] I.B. Bankovic-Ilic, O.S. Stamenkovic, V.B. Veljkovic. Biodiesel Production from Non-edible Plant Oils, *Renewable and Sustainable Energy Reviews*. **16** (2012), 3621–3647. doi:10.1016/j.rser.2012.03.002.

[217] P. Hidalgo, G. Ciudad, M. Mittelbach, R. Navia. Biodiesel Production by Direct Conversion of Botryococcus Braunii Lipids : Reaction Kinetics Modelling and Optimization, *Fuel*. **153** (2015), 544–551. doi:10.1016/j.fuel.2015.03.039.

[218] L. Yu, Y. Ge, J. Tan, et al., Experimental Investigation of the Impact of Biodiesel on the Combustion and Emission Characteristics of a Heavy Duty Diesel Engine at Various Altitudes, *Fuel*. **115** (2014), 220–226. doi:10.1016/j.fuel.2013.06.056.

[219] E. Bakeas, G. Karavalakis, G. Fontaras, S. Stournas. An Experimental Study on the Impact of Biodiesel Origin on the Regulated and PAH Emissions from a Euro 4 Light-Duty Vehicle, *Fuel*. **90** (2011), 3200–3208. doi:10.1016/j.fuel.2011.05.018.

[220] L. Shi, Y. Cui, K. Deng, H. Peng, Y. Chen. Study of Low Emission Homogeneous Charge Compression Ignition (HCCI) Engine using Combined Internal and External Exhaust Gas Recirculation (EGR), *Energy*. **31** (2006), 2665–2676. doi:10.1016/j.energy.2005.12.005.

[221] P.Q. Tan, Z.Y. Hu, D.M. Lou, Z.J. Li. Exhaust Emissions from a Light-Duty Diesel Engine with Jatropha Biodiesel Fuel, *Energy*. **39** (2012), 356–362. doi:10.1016/j.energy.2012.01.002.

[222] S.M. Palash, H.H. Masjuki, M. A. Kalam, B.M. Masum, A. Sanjid, M.J. Abedin. State of the Art of NOx Mitigation Technologies and their Effect on the Performance and Emission Characteristics of Biodiesel-Fueled Compression Ignition Engines, *Energy Conversion and Management*. **76** (2013), 400–420. doi:10.1016/j.enconman.2013.07.059.

[223] K. Varatharajan, M. Cheralathan. Effect of Aromatic Amine Antioxidants on NOx Emissions from a Soybean Biodiesel Powered DI Diesel Engine, *Fuel Processing Technology*. **106** (2013), 526–532. doi:10.1016/j.fuproc.2012.09.023.

[224] C.H. Cheng, C.S. Cheung, T.L. Chan, S.C. Lee, C.D. Yao, K.S. Tsang. Comparison of Emissions of a Direct Injection Diesel Engine Operating on Biodiesel with Emulsified and Fumigated Methanol, *Fuel*. **87** (2008), 1870–1879. doi:10.1016/j.fuel.2008.01.002.

[225] E. Alptekin, M. Canakci, A.N. Ozsezen, A. Turkcan, H. Sanli. Using Waste Animal Fat Based Biodiesels–Bioethanol–Diesel Fuel Blends in a DI Diesel Engine, *Fuel*. **157** (2015), 245–254. doi:10.1016/j.fuel.2015.04.067.

[226] M. Lapuerta, O. Armas, J.J. Hernandez. Diagnosis of DI Diesel Combustion from In-cylinder Pressure Signal by Estimation of Mean Thermodynamic Properties of the Gas, *Applied Thermal Engineering*. **19** (1999), 513–529. doi:10.1016/S1359-4311(98)00075-1.

[227] M.T. Garcia, F.J.J. Aguilar, J.A.B. Villanueva, E.C. Trujillo. Analysis of a New Analytical Law of Heat Release Rate (HRR) for Homogenous Charge Compression Ignition (HCCI

) Combustion Mode Versus Analytical Parameters, *Applied Thermal Engineering*. **31** (2011), 458–466. doi:10.1016/j.applthermaleng.2010.09.025.

[228] X. Lu, J. Ma, L. Ji, Z. Huang. Simultaneous Reduction of NOx Emission and Smoke Opacity of Biodiesel-Fueled Engines by Port Injection of Ethanol, *Fuel*. **87** (2008), 1289–1296. doi:10.1016/j.fuel.2007.07.006.

[229] D.C. Rakopoulos. Heat Release Analysis of Combustion in Heavy-duty Turbocharged Diesel Engine Operating on Blends of Diesel Fuel with Cottonseed or Sunflower Oils and their Bio-diesel, *Fuel*. **96** (2012), 524–534. doi:10.1016/j.fuel.2011.12.063.

[230] D.C. Rakopoulos, C.D. Rakopoulos, E.G. Giakoumis. Impact of Properties of Vegetable Oil , Bio-Diesel , Ethanol and n -butanol on the Combustion and Emissions of Turbocharged HDDI Diesel Engine Operating under Steady and Transient Conditions, *Fuel*. **156** (2015), 1–19. doi:10.1016/j.fuel.2015.04.021.

[231] NTFP Enterprise and Forest Governance. Sal Seed, published by *Center for people's Forestry* ISBN:978-81- 906691-7-7.

[232] H.S. Pali, N. Kumar. Biodiesel Production from Sal (Shorea Robusta) Seed Oil, *NIET Journal of Engineering & Technology*. **5** (2014), 24–29.

[233] H.S. Pali, N. Kumar. Effect of Blending of Ethanol in Kusum Oil on Performance and Emission Characteristics of a Single Cylinder Diesel Engine, *SAE International*. (2014), doi:10.4271/2014-01-1396.

[234] S.T. Keera, S.M. El Sabagh, A. R. Taman. Transesterification of Vegetable Oil to Biodiesel Fuel using Alkaline Catalyst, *Fuel*. **90** (2011), 42–47. doi:10.1016/j.fuel.2010.07.046.

[235] A. Javidialesaadi, S. Raeissi. Biodiesel Production from High Free Fatty Acid-Content Oils : Experimental Investigation of the Pretreatment Step, *APCBEE Procedia*. **5** (2013), 474–478. doi:10.1016/j.apcbee.2013.05.080.

[236] M.W. Mumtaz, A. Adnan, F. Anwar, et al. Response Surface Methodology: An Emphatic Tool for Optimized Biodiesel Production using Rice Bran and Sunflower Oils, *Energies*. (2012), 3307–3328. doi:10.3390/en5093307.

[237] E. Betiku, A.E. Taiwo. Modeling and Optimization of Bioethanol Production from Breadfruit -vis Response Surface Methodology and Starch Hydrolyzate vis- a Artificial Neural Network, *Renewable Energy*. **74** (2015), 87–94.

doi:10.1016/j.renene.2014.07.054.

[238] H. V Lee, R. Yunus, J.C. Juan, Y.H. Taufiq-Yap. Process Optimization Design for Jatropha-based Biodiesel Production using Response Surface Methodology, *Fuel Processing Technology*. **92** (2011), 2420–2428. doi:10.1016/j.fuproc.2011.08.018.

[239] S. Sinha, A.K. Agarwal, S. Garg, Biodiesel development from rice bran oil: Transesterification process optimization and fuel characterization, Energy Conversion and Management. 49 (2008) 1248–1257. doi:10.1016/j.enconman.2007.08.010.

[240] D.C. Rakopoulos, C.D. Rakopoulos, R.G. Papagiannakis, D.C. Kyritsis. Combustion Heat Release Analysis of Ethanol or n-butanol Diesel Fuel Blends in Heavy-duty DI Diesel Engine, *Fuel*. **90** (2011), 1855–1867. doi:10.1016/j.fuel.2010.12.003.

[241] W. Ying, H. Li, Z. Jie, Z. Longbao. Study of HCCI-DI Combustion and Emissions in a DME Engine, *Fuel*. **88** (2009), 2255–2261. doi:10.1016/j.fuel.2009.05.008.

[242] H.S. Pali, N. Kumar, C. Mishra. Some Experimental Studies on Combustion, Emission and Performance Characteristics of an Agricultural Diesel Engine Fueled with Blends of Kusum Oil Methyl Ester and Diesel, *SAE International*. (2014). doi:10.4271/2014-01-1952.

[243] J.B. Heywood, Internal Combustion Engine Fundamentals, Book:*Mc-Graw Hills publication* (1988).

[244] X. Lu, Y. Hou, L. Zu, Z. Huang. Experimental Study on the Auto-Ignition and Combustion Characteristics in the homogeneous Charge Compression Ignition (HCCI) Combustion Operation with Ethanol / n -heptane Blend Fuels by Port Injection, *Fuel*. **85** (2006), 2622–2631. doi:10.1016/j.fuel.2006.05.003.

[245] K.Z.Mendera, A. Spyra, M. Smereka. Mass Fraction Burned Analysis, *Journal of KONES Internal Combustion Engines*. **3-4** (2002), 193–201.

[246] G. Knothe. Dependence of Biodiesel Fuel Properties on the Structure of Fatty Acid Alkyl Esters, *Fuel Processing Technology*. **86** (2005), 1059–1070. doi:10.1016/j.fuproc.2004.11.002.

[247] M.S. Krzystof Z.Mendera, Andrzej, Mass fraction burned analysis, *Journal of KONES Internal Combustion Engines*. (1988),193–201. http://ilot.edu.pl/KONES/2002/02/str193.pdf.

[248] W. Zhang, W. Yuan, X. Zhang, M. Coronado. Predicting the Dynamic and Kinematic

Viscosities of Biodiesel-Diesel Blends using Mid- and Near-Infrared Spectroscopy, *Applied Energy*. **98** (2012), 122–127. doi:10.1016/j.apenergy.2012.03.013.

[249] P. Nakpong, S. Wootthikanokkhan. High Free Fatty Acid Coconut Oil as a Potential Feedstock for Biodiesel Production in Thailand, *Renewable Energy*. **35** (2010), 1682–1687. doi:10.1016/j.renene.2009.12.004.

[250] A. Bouaid, N. El, K. Hahati, M. Martinez, J. Aracil. Biodiesel Production from biobutanol. Improvement of Cold Flow Properties, *Chemical Engineering Journal*. **238** (2014) 234–241. doi:10.1016/j.cej.2013.10.022.

[251] E.C. Zuleta, L. A. Rios, P.N. Benjumea. Oxidative Stability and Cold Flow Behavior of Palm, Sacha-Inchi, Jatropha and Castor Oil Biodiesel Blends, *Fuel Processing Technology*. **102** (2012), 96–101. doi:10.1016/j.fuproc.2012.04.018.

[252] A. Atmanli, B. Yüksel, E. Ileri, A. Deniz Karaoglan. Response Surface Methodology based Optimization of Diesel-n-butanol-Cotton Oil Ternary Blend Ratios to Improve Engine Performance and Exhaust Emission Characteristics, *Energy Conversion and Management*. **90** (2015), 383–394. doi:10.1016/j.enconman.2014.11.029.

[253] M. Charoenchaitrakool, J. Thienmethangkoon. Statistical Optimization for Biodiesel Production from Waste Frying Oil through Two-Step Catalyzed Process, *Fuel Processing Technology*. **92** (2011), 112–118. doi:10.1016/j.fuproc.2010.09.012.

[254] R. Wang, W.W. Zhou, M.A. Hanna, et al. Biodiesel Preparation, Optimization, and Fuel Properties from Non-edible Feedstock, Datura Stramonium L., *Fuel*. **91** (2012), 182–186. doi:10.1016/j.fuel.2011.07.001.

[255] Y. Alhassan, N. Kumar, I.M. Bugaje, H.S. Pali, P. Kathkar. Co-solvents Transesterification of Cotton Seed Oil into Biodiesel: Effects of reaction Conditions on Quality of Fatty Acids Methyl Esters, *Energy Conversion and Management*. **84** (2014), 640–648. doi:10.1016/j.enconman.2014.04.080.

[256] M. Atapour, H. Kariminia, P.M. Moslehabadi. Optimization of Biodiesel Production by Alkali-Catalyzed Transesterification of used Frying Oil, *Process Safety and Environmental Protection*. **92** (2013), 179–185. doi:10.1016/j.psep.2012.12.005.

[257] R. Gautam, N. Kumar, P. Sharma. Experimental Investigation on Use of Jatropha Oil Ethyl Easter and Diesel Blends in Small Capacity Diesel Engine, *SAE International*. (2013), doi: 10.4271/2013-24-0172.

[258] S.Z. Hassan, M. Vinjamur. Parametric Effects on Kinetics of Esterification for Biodiesel Production : A Taguchi Approach, *Chemical Engineering Science*. **110** (2014), 94–104. doi:10.1016/j.ces.2013.11.049.

[259] M. Atapour, H.R. Kariminia. Characterization and Transesterification of Iranian Bitter Almond Oil for Biodiesel Production, *Applied Energy*. **88** (2011), 2377–2381. doi:10.1016/j.apenergy.2011.01.014.

[260] C. Wityi, M. Shioji, S. Nakao, et al. Ignition and Combustion Characteristics of various Biodiesel Fuels (BDFs), *Fuel*. **158** (2015), 279–287. doi:10.1016/j.fuel.2015.05.049.

[261] Y. Alhassan, N. Kumar, I.M. Bugaje. Bioresource Technology Hydrothermal Liquefaction of De-Oiled Jatropha Curcas Cake using Deep Eutectic Solvents (DESs) as Catalysts and Co-solvents, *Bioresource Technology*. **199** (2016), 375–381. doi:10.1016/j.biortech.2015.07.116.

[262] Á. Pérez, A. Casas, C.M. Fernández, M.J. Ramos, L. Rodríguez. Winterization of Peanut Biodiesel to Improve the Cold Flow Properties, *Bioresource Technology*. **101** (2010), 7375–7381. doi:10.1016/j.biortech.2010.04.063.

[263] T.Q. Chastek. Improving Cold Flow Properties of Canola-Based Biodiesel, *Biomass and Bioenergy*. **35** (2011), 600–607. doi:10.1016/j.biombioe.2010.10.024.

[264] M. Lapuerta, O. Armas, J. Rodríguez-Fernández. Effect of Biodiesel Fuels on Diesel Engine Emissions, *Progress in Energy and Combustion Science*. **34** (2008), 198–223. doi:10.1016/j.pecs.2007.07.001.

[265] A. Karnwal, M.M. Hasan, N. Kumar, A.N. Siddiquee, Z.A. Khan. Multi-Response Optimization of Diesel Engine Performance Parameters using Thumba Biodiesel-Diesel Blends by Applying the Taguchi Method and Grey Relational Analysis, *International Journal of Automotive Technology*. **12** (2011), 599–610. doi: 10.1007/s12239-011-0070-4.

[266] M. Canakci, A.N. Ozsezen, E. Arcaklioglu, A. Erdil. Prediction of Performance and Exhaust Emissions of a Diesel Engine Fueled with Biodiesel Produced from Waste Frying Palm Oil, *Expert Systems with Applications*. **36** (2009), 9268–9280. doi:10.1016/j.eswa.2008.12.005.

[267] A. Dhar, A.K. Agarwal. Effect of Karanja Biodiesel Blend on Engine Wear in a Diesel Engine, *Fuel*. **134** (2014), 81–89. doi:10.1016/j.fuel.2014.05.039.

[268] E. Buyukkaya. Effects of Biodiesel on a DI Diesel Engine Performance, Emission and Combustion Characteristics, *Fuel*. **89** (2010), 3099–3105. doi:10.1016/j.fuel.2010.05.034.

[269] M. Gumus, S. Kasifoglu. Performance and Emission Evaluation of a Compression Ignition Engine using a Biodiesel (Apricot Seed Kernel Oil Methyl Ester) and its Blends with Diesel Fuel, *Biomass and Bioenergy*. **34** (2010), 134–139. doi:10.1016/j.biombioe.2009.10.010.

[270] K. Anand, R.P. Sharma, P.S. Mehta. Experimental Investigations on Combustion, Performance and Emissions Characteristics of Neat Karanji Biodiesel and its Methanol Blend in a Diesel Engine, *Biomass and Bioenergy*. **35** (2011), 533–541. doi:10.1016/j.biombioe.2010.10.005.

[271] C.D. Bannister, J.G. Hawley, H.M. Ali, et al. The Impact of Biodiesel Blend Ratio on Vehicle Performance and Emissions, *Proceedings of the Institution of Mechanical Engineers Part D Journal of Automobile Engineering*. **224** (2015), 2020. doi:10.1243/09544070JAUTO1270.

[272] J. Sadhik Basha, R.B. Anand. Performance, Emission and Combustion Characteristics of a Diesel Engine using Carbon Nanotubes Blended Jatropha Methyl Ester Emulsions, *Alexandria Engineering Journal*. **53** (2014), 259–273. doi:10.1016/j.aej.2014.04.001.

[273] M. Mohon, W. Wang, M. Alawi. Performance and Emissions of a Diesel Engine Fueled by Biodiesel-Diesel, Biodiesel-Diesel-Additive and Kerosene-Biodiesel Blends, **84** (2014), 164–173. doi:10.1016/j.enconman.2014.04.033.

[274] A. Sharma, N. Kumar, V. Vibhanshu, Amardeep. Emission Studies on a VCR Engine using Stable Diesel Water Emulsion, *SAE International*. (2013). doi:10.4271/2013-01-2665.

[275] R. Gautam, N. Kumar, P. Sharma. Experimental Investigation on use of Jatropha Oil Ethyl Easter and Diesel Blends in Small Capacity Diesel Engine, *SAE International*. (2013). doi:10.4271/2013-24-0172.

[276] P. Behera, S. Murugan. Combustion, Performance and Emission Parameters of used Transformer Oil and its Diesel Blends in a DI Diesel Engine, *Fuel*. **104** (2013), 147–154. doi:10.1016/j.fuel.2012.09.077.

[277] M. Mofijur, H.H. Masjuki, M.A. Kalam, A.E. Atabani, M.I. Arbab, S.F. Cheng, et al. Properties and Use of Moringa Oleifera Biodiesel and Diesel Fuel Blends in a Multi-

Cylinder Diesel Engine, *Energy Conversion and Management*. **82** (2014), 169–176. doi:10.1016/j.enconman.2014.02.073.

[278] C. Sayin. Engine Performance and Exhaust Gas Emissions of Methanol and ethanol-Diesel Blends, *Fuel*. **89** (2010), 3410–3415. doi:10.1016/j.fuel.2010.02.017.

[279] K. Khiari, S. Awad, K. Loubar, L. Tarabet, R. Mahmoud, M. Tazerout. Experimental Investigation of Pistacia Lentiscus Biodiesel as a Fuel for Direct Injection Diesel Engine, *Energy Conversion and Management*. **108** (2016), 392–399. doi:10.1016/j.enconman.2015.11.021.

[280] Amardeep, N. Kumar. Performance and Emission Studies of Diesel Engine Fuelled with Orange Peel Oil and n-butanol Alcohol Blends, *SAE International*. (2015). doi:10.4271/2015-26-0049.

[281] M.N. Nabi, M.S. Akhter, M.M.Z. Shahadat. Improvement of Engine Emissions with Conventional Diesel Fuel and Diesel-Biodiesel Blends, *Bioresource Technology*. **97** (2006), 372–378. doi:10.1016/j.biortech.2005.03.013.

[282] L. Panichelli, E. Gnansounou. Impact of Agricultural-based Biofuel Production on Greenhouse Gas Emissions from Land-Use Change : Key Modelling Choices, *Renewable and Sustainable Energy Reviews*. **42** (2015), 344–360. doi:10.1016/j.rser.2014.10.026.

[283] T.M. Yunus, I. Anjum, A. Badarudin, et al. Effects of Engine Variables and Heat Transfer on the Performance of Biodiesel Fueled IC Engines, *Renewable and Sustainable Energy Reviews*. **44** (2015), 682–691. doi:10.1016/j.rser.2015.01.025.

[284] C.D. Rakopoulos, D.C. Rakopoulos, D.T. Hountalas, E.G. Giakoumis, E.C. Andritsakis. Performance and Emissions of Bus Engine using Blends of Diesel Fuel with Bio-diesel of Sunflower or cottonseed Oils Derived from Greek Feedstock, *Fuel*. **87** (2008), 147–157. doi:10.1016/j.fuel.2007.04.011.

[285] C. Sayin, A. Necati, M. Canakci. The Influence of Operating Parameters on the Performance and Emissions of a DI Diesel Engine using Methanol-Blended-Diesel Fuel, *Fuel*. **89** (2010), 1407–1414. doi:10.1016/j.fuel.2009.10.035.

[286] D.L. Flowers, S.M. Aceves, J. Martinez-frias, R.W. Dibble. Prediction of Carbon Monoxide and Hydrocarbon Emissions in Iso-Octane HCCI Engine Combustion using Multizone Simulations, *Proceedings of the Combustion Institute*. **29** (2002), 687–694. doi:10.1016/S1540-7489(02)80088-8.

[287] F. Payri, V.R. Bermúdez, B. Tormos, W.G. Linares. Hydrocarbon Emissions Speciation in Diesel and Biodiesel Exhausts, *Atmospheric Environment*. **43** (2009), 1273–1279. doi:10.1016/j.atmosenv.2008.11.029.

[288] M. Canakci, J.H. Van Gerpen. The Performance and Emissions of a Diesel Engine Fueled with Biodiesel from Yellow Grease and Soybean Oil, ASAE Meeting Paper No. 01-6050. St. Joseph, Mich.: ASAE. (2001).

[289] D.R. Tree, K.I. Svensson. Soot Processes in Compression Ignition Engines, P*rogress in Energy and Combustion Science*. **33** (2007), 272–309. doi:10.1016/j.pecs.2006.03.002.

[290] K. Varatharajan, M. Cheralathan, R. Velraj. Mitigation of NOx Emissions from a Jatropha Biodiesel Fuelled DI Diesel Engine using Antioxidant Additives, *Fuel*. **90** (2011), 2721–2725. doi:10.1016/j.fuel.2011.03.047.

[291] M. A. Hess, M.J. Haas, T. A. Foglia. Attempts to Reduce NOx Exhaust Emissions by Using Reformulated Biodiesel, *Fuel Processing Technology*. **88** (2007), 693–699. doi:10.1016/j.fuproc.2007.02.001.

[292] A.J. Torregrosa, A. Broatch, A. García, L.F. Mónico. Sensitivity of Combustion Noise and NOx and Soot Emissions to Pilot Injection in PCCI Diesel Engines, *Applied Energy*. **104** (2013), 149–157. doi:10.1016/j.apenergy.2012.11.040.

[293] A. Atmanli, E. Ileri, B. Yuksel. Experimental Investigation of Engine Performance and Exhaust Emissions of a Diesel Engine Fueled with Diesel–n-butanol–Vegetable Oil Blends, *Energy Conversion and Managemen*t. **81** (2014), 312–321. doi:10.1016/j.enconman.2014.02.049.

[294] S.K. Hoekman, C. Robbins. Review of the Effects of Biodiesel on NOx Emissions, *Fuel Processing Technology*. **96** (2012), 237–249. doi:10.1016/j.fuproc.2011.12.036.

[295] R.D. Lanjekar, D. Deshmukh. A Review of the Effect of the Composition of Biodiesel on NOx Emission , Oxidative Stability and Cold Flow Properties, *Renewable and Sustainable Energy Reviews*. **54** (2016), 1401–1411. doi:10.1016/j.rser.2015.10.034.

[296] M. Zheng, T. Li, X. Han. Direct Injection of Neat n-butanol for Enabling Clean Low Temperature Combustion in a Modern Diesel Engine, *Fuel*. **142** (2015), 28–37. doi:10.1016/j.fuel.2014.10.075.

[297] D.B. Hulwan, S. V. Joshi. Performance, Emission and Combustion Characteristic of a Multicylinder DI Diesel Engine Running on Diesel-Ethanol-Biodiesel Blends of High

Ethanol Content, *Applied Energy*. **88** (2011), 5042–5055. doi:10.1016/j.apenergy.2011.07.008.

[298] H. Song, B.T. Tompkins, J. A. Bittle, T.J. Jacobs. Comparisons of NO Emissions and Soot Concentrations from Biodiesel-Fuelled Diesel Engine, *Fuel*. **96** (2012), 446–453. doi:10.1016/j.fuel.2012.01.004.

[299] M. Lapuerta, O. Armas, J.J. Hernández, A. Tsolakis. Potential for Reducing Emissions in a Diesel Engine by Fuelling with Conventional Biodiesel and Fischer-Tropsch Diesel, *Fuel*. **89** (2010), 3106–3113. doi:10.1016/j.fuel.2010.05.013.

[300] B. Tesfa, R. Mishra, C. Zhang, F. Gu, A. D. Ball. Combustion and Performance Characteristics of CI (compression Ignition) Engine Running with Biodiesel, *Energy*. **51** (2013), 101–115. doi:10.1016/j.energy.2013.01.010.

[301] M. Gumus. A Comprehensive Experimental Investigation of Combustion and Heat Release Characteristics of a Biodiesel (Hazelnut Kernel Oil Methyl Ester) Fueled Direct Injection Compression Ignition Engine, *Fuel*. **89** (2010), 2802–2814. doi:10.1016/j.fuel.2010.01.035.

[302] E. Rajasekar, S. Selvi. Review of Combustion Characteristics of CI engines Fueled with Biodiesel, *Renewable and Sustainable Energy Reviews*. **35** (2014), 390–399. doi:10.1016/j.rser.2014.04.006.

[303] L. Zhu, C.S. Cheung, W.G. Zhang, Z. Huang. Combustion, Performance And Emission Characteristics of a DI diesel Engine Fueled with Ethanol-Biodiesel Blends, *Fuel*. **90** (2011), 1743–1750. doi:10.1016/j.fuel.2011.01.024.

[304] P.K. Sahoo, L.M. Das. Combustion Analysis of Jatropha, Karanja and Polanga based Biodiesel as Fuel in a Diesel Engine, *Fuel*. **88** (2009), 994–999. doi:10.1016/j.fuel.2008.11.012.

[305] S. Sivalakshmi, T. Balusamy. Effect of Biodiesel and its Blends with Diethyl Ether on the Combustion, Performance and Emissions from a Diesel Engine, *Fuel*. **106** (2013), 106–110. doi:10.1016/j.fuel.2012.12.033.

[306] G. Singh, A.P. Singh, A.K. Agarwal. Experimental Investigations of Combustion, Performance and Emission Characterization of Biodiesel Fuelled HCCI Engine using External Mixture Formation Technique, *Sustainable Energy Technologies and Assessments*. **6** (2014), 116–128. doi:10.1016/j.seta.2014.01.002.

[307] D.H. Qi, H. Chen, L.M. Geng, Y.Z. Bian. Effect of Diethyl Ether and Ethanol Additives on the Combustion and Emission Characteristics of Biodiesel-Diesel Blended Fuel Engine, *Renewable Energy*. **36** (2011), 1252–1258. doi:10.1016/j.renene.2010.09.021.

[308] R. Arora, S. Behera, S. Kumar. Bioprospecting Thermophilic / Thermotolerant Microbes for Production of Lignocellulosic Ethanol : A Future Perspective, *Renewable and Sustainable Energy Reviews*. **51** (2015), 699–717. doi:10.1016/j.rser.2015.06.050.

APPENDIX-I

Technical Specifications of AVL 437 Smoke Meter

Accuracy and Reproducibility	± 1% full scale reading
Heating Time	Approx. 20 min
Light source	Halogen bulb 12 V / 5W
Colour temperature	3000 K ± 150 K
Detector	Selenium photocell dia. 45 mm , Max. Sensitivity in light In Frequency range: 550 to 570 nm. Below 430 nm and above 680 nm sensitivity is less than 4% related to the maximum sensitivity
Maximum Smoke	250ºC Temperature at entrance

APPENDIX-II

Technical Specifications of AVL Di-Gas Analyzer

Measurement principle	CO, HC, CO_2	Infrared measurement
	O_2	Electrochemical measurement
	NO (option)	Electrochemical measurement
Operating temperature	+5 to +45ºC	Keeping measurement accuracy
	+1 to +50ºC	Ready for measurement
	+5 to +35ºC	with integral NO sensor (Peaks of : +40ºC)
Storage temperature	-20 to +60ºC	
	-20 to +50ºC	With integrated O_2 sensor
	-10 to. +45ºC	With integrated NO sensor
	0 to +50ºC	With water in filter and / or pump
Air humidity	90% max.,	non-condensing
Power drawn	150 VA	
Dimensions	432 x 230 x 470 mm	(w x h x l)
Weight	16 Kg	

Measurement Ranges of AVL Di-Gas Analyzer

Parameter	Measurement Range	Resolution
CO	0-10% vol	0.01% vol
CO_2	0-20% vol	0.1% vol
HC	0-20000 ppm vol	1 ppm
NO_X	0-5000 ppm vol	1 ppm
O_2	0-25% vol	0.01% vol

APPENDIX-III

Infra-red Correlation Chart

	Type of Vibration	**Frequency (cm^{-1})**	**Intensity**
C-H	Alkanes (stretch)	3000-2850	s
	-CH3 (bend)	1450 and 1375	m
	-CH2- (bend)	1465	m
	Alkenes (stretch)	3100-3000	m
	(out-of-plane bend)	1000-650	s
	Aromatics (stretch)	3150-3050	s
	(out-of-plane bend)	900-690	s
	Alkyne (stretch)	~3300	s
	Aldehyde	2900-2800	w
C-C	Alkane not interpretatively useful		
C=C	Alkene	1680-1600	m-w
	Aromatic	1600 and 1475	m-w
C≡C	Alkyne	2250-2100	m-w
C=O	Aldehyde	1740-1720	s
	Ketone	1725-1705	s
	Carboxylic Acid	1725-1700	s
	Ester	1750-1730	s
	Amide	1670-1640	s
	Anhydride	1810 and 1760	s
	Acid Chloride	1800	s
C-O	Alcohols, Ethers, Esters, Carboxylic Acids, Anhydrides	1300-1000	s
O-H	Alcohols, Phenols		
	Free	3650-3600	m
	H-bonded	3500-3200	m
	Carboxylic Acids	3400-2400	m

N-H	Primary and Secondary Amines and Amides		
	(stretch)	3500-3100	m
	(bend)	1640-1550	m-s
C-N	Amines	1350-1000	m-s
C=N	Imines and Oximes	1690-1640	w-s
C≡N	Nitriles	2260-2240	m
X=C=Y	Allenes, Ketenes, Isocyanates, Isothiocyanates	2270-1950	m-s
N=O	Nitro (R-NO2)	1550 and 1350	s
S-H	Mercaptans	2550	w
S=O	Sulfoxides	1050	s
	Sulfones, Sulfonyl Chlorides, Sulfates, Sulfonamides	1375-1300	s s
C-X	Fluoride	1400-1000	s
	Chloride	800-600	s
	Bromide, Iodide	<667	s

Curriculum Vitae

Personal details:			
Full Name:	**Harveer Singh Pali**		
Father's Name:	Shri Shivraj Singh		
Nationality:	Indian	**Gender/Date of Birth:**	**Male/8th, October 1980**
Address:	C-253, Sector P3, Greater Noida, Pin- 201308, India		
Research Gate:	**http://www.researchgate.net/profile/HARVEER_S_Pali/**		
Languages Known:	Professional proficiency in **English, Hindi and Sanskrit**		
Contact No:	**9971695452**	**Email:**	harvirpali@gmail.com hspali@niet.co.in,

Core Skills

- **Published** more than **30 Research papers** in **various National and International Forums**.
- **Net (Impact Factor: 10.33), (h-index: 3), (i 10-index: 2), (Citations: 62).**
- **Reviewer** of **Elsevier, Taylor & Francis, SAE, ASME and Inderscience**
- **Ph.D.** in **Mechanical Engineering** from **Delhi Technological University**, Delhi. (***Topic:*** **"Performance, Emission and Combustion Characteristics of a Biodiesel Fuelled Diesel Engine"**)
- **M.Tech.** – Mechanical Engineering (CAD) secured 73.66% with **First** Division.
- **MBA** - Human Resourse (Personal) secured 61.33% with **First** Division.
- **B.E.** – Mechanical & Industrial Engineering secured 74.68% with **First** Division.

M.Tech./B.Tech. Project Supervised

- **M. Tech Project : 04**
- **B. Tech Project : 31**

Research Publications (Net Impact Factor : 10.33)

- **International Journals : 15**
- **National Journals : 03**
- **International/National Conferences : 13**
- **Book : 01**
- **Best Paper Award : 01**

Positions of Responsibility

- **Organizing Secretary:** International Science & Fusion Technology" (ISFT-2016).
- **Convener: SAE -** Inter-Institutional Technical Contest & Symposium Enzinius, 2015**.**
- **Organizing Secretary:** International Conference & Exhibition on "Cutting Edge Technological Challenges in Mechanical Engineering" (CETCME-2015)

Work Experience: (13years = 03 Year Industry + 10 years Academics)

WorkEx-1 (20 July 2007 to present):
Profile: Assistant Professor (Senior Scale Selection Grade) at **NIET**, Greater Noida, Uttar Pradesh.
WorkEx-2 (12th May 2004 to 15th July 2007):
Profile: R & D Engineer at **K.C.ENGINEERS PVT.LTD., AMBALA CANTT (HR).**
WorkEx-3 (1st July 2003 to 10th May 2004):

Profile: Guest Lecturer at Department of Chemical Technology (Fertilizer) in Government Polytechnic Lakhimpur Kheri, U.P.

Research Publication(s):

International Journals

1. **Harveer Singh Pali***, N. Kumar, **(2016)** Combustion, Performance and Emission of *Shorea Robusta* Methyl Ester Blends in Diesel Engine, *Biofuels*. **doi: 10.1080/17597269.2016.1153363** (Publisher: Taylor & Francis; **Scopus indexed**)
2. **Harveer Singh Pali***, N. Kumar, **(2016)** Comparative assessment of sal and kusum biodiesel properties, *Energy Sources Part A: Recovery, Utilization and Environmental Effects*. **http://dx.doi.org/10.1080/15567036.2015.1136974**. (Publisher: Taylor & Francis; **SCI indexed**)
3. N. Kumar**, Harveer Singh Pali***, **(2016)** Some Experimental Studies on Use of Biodiesel as an Extender in SI Engine, *SAE Technical Paper* 2016-01-1269. **doi:10.4271/2016-01-1269**. (Publisher: SAE International; **Scopus indexed**)
4. **Kumar N.,* Pali H. S. (2016)** Effects of n-butanol blending with Jatropha methyl esters on compression Ignition engine, *Arabian Journal for Science and Engineering*, **doi-10.1007/s13369-016-2127-1** (Publisher: Springer; **SCI indexed**) **(Impact Factor: 0.728).**
5. **Pali H. S.,*** Kumar N., Singh K., **(2016)** Optimisation of Process Parameters of EDM on Al6082/SiC Metal Matrix Composite. *SAE Technical Paper* 2016-01-0533. **doi:10.4271/2016-01-0533**. (Publisher: SAE International; **Scopus indexed**).
6. Gautam R.,* Kumar N., **Pali H. S.,** Kumar P., **(2016)** Experimental studies on the use of methyl and ethyl esters as an extender in a small capacity diesel engine, *Biofuels*.

http://dx.doi.org/10.1080/17597269.2016.1187538 (Publisher: Taylor & Francis; **Scopus indexed**).

7. **Harveer Singh Pali***, N. Kumar, Y. Alhassan (**2015**). Performance and emission characteristics of an agricultural engine with Sal methyl ester and diesel, *Energy Conversion and Management,* **90** 146-153. **http://dx.doi.org/10.1016/j.econman.2014.10.064 (Elsevier, Impact Factor : 4.8)**
8. **Harveer Singh Pali***, Naveen Kumar, Alhassan Y, Deep A, "Process Optimization of Biodiesel Production from Sal Seed Oil using Response Surface Methodology [RSM] and Diesel". SAE Technical Paper 2015-01-1297; **2015**. **doi:10.4271/2015-01-1297.**
9. Naveen Kumar*, Sidharth, **Harveer Singh Pali**, "Blending of Higher Alcohols with Vegetable Oil Based Fuels for Use in Compression Ignition Engine". SAE Technical Paper 2015-01-0958; **2015**. **doi:10.4271/2015-01-0958.**
10. **Harveer Singh Pali***, Kumar, N., Alhassan, Y., and Deep, A., [2015] "Process Optimization of Biodiesel Production from Sal Seed Oil using Response Surface Methodology [RSM] and Diesel", *SAE Technical Paper* 2015-01-1297, **doi:10.4271/2015-01-1297**.
11. **Harveer Singh Pali***, Kumar, N., and Mishra, C., [2014] "Some Experimental Studies on Combustion, Emission and Performance Characteristics of an Agricultural Diesel Engine Fueled with Blends of Kusum Oil Methyl Ester and Diesel", *SAE Technical Paper* 2014-01-1952, **doi:10.4271/2014-01-1952**.
12. **Harveer Singh Pali***, Kumar, N., and Mishra, C.,[2014] "Effect of Blending of Ethanol in Kusum Oil on Performance and Emission Characteristics of a Single Cylinder Diesel Engine," *SAE Technical Paper* 2014-01-1396, **doi:10.4271/2014-01-1396.**
13. Alhassan Y,* Kumar N, Bugaje IM, **Harveer Singh Pali**, Katchkar P., [2014] "Co-solvents transesterification of cotton seed oil into biodiesel: effects of reaction conditions on quality of fatty acids methyl esters". *Energy Conversion and Management*. 84:640–8. **http://dx.doi.org/10.1016/j.enconman.2014.04.080 (Elsevier, Impact Factor : 4.8).**
14. Naveen Kumar*, Bansal, S., and **Harveer Singh Pali**, [2015] "Blending of Higher Alcohols with Vegetable Oil Based Fuels for Use in Compression Ignition Engine," *SAE Technical Paper* 2015-01-0958, **doi:10.4271/2015-01-0958**.
15. Vipul Vibhanshu,* N.Kumar, C. Mishra, S. Sinha, **Harveer Singh Pali**, Sidarth Basal [2013]"Experimental Investigation of Diesel Engine Fueled with Jatropha Oil Blend with Ethanol" *SAE Technical Paper*. 2013-24-0105, **doi: 10.4271/2013-24-0105**, (saefuel.saejournals.org and ISSN: 1946-3960).

National Journals

1. **Harveer Singh Pali**,* Chinmay Mishra and Naveen Kumar, "Production and Physico-Chemical Characterisation of Kusum Oil Methyl Ester as an Alternative fuel in Diesel Engine " *Journal of Biofuels*, vol.4, pp. 38-46, 2013, **doi: 10.5958/j.0976-4763**.4.1.005 (ISSN 0976-3015).

2. **Harveer Singh Pali**,* Naveen Kumar, [2014] "Biodiesel Production from Sal (Shorea Robusta) Seed Oil", *NIET Journal of Engineering &Technology*, vol. 5, pp. 24 – 29. (ISSN 2229-5828)
3. **Harveer Singh Pali**,* [2013] "Performance Characteristics of Biodiesel Blend in CI Engine Using Artificial Neural Network (Karanja Oil)" *NIET Journal of Engineering &Technology*, vol. 1, pp 46 – 53. (ISSN 2229-5828).

Peer Reviewed International and National Conferences

1. **Harveer Singh Pali**,* Naveen Kumar, Comparative assessment of Sal and Kusum methyl ester in CI engine. International Symposium on Fusion of Science and Technology (**ISFT-2016**), New Delhi, India, January 18-22,2016.
2. **Harveer Singh Pali**,* Naveen Kumar, Vipul Vibhanshu, "Performance and Emission Characteristics of Castor Seed oil Biodiesel on Medium Capacity Diesel Engine" (paper no. 147) Proceedings of International Conference STME – 2013 Delhi Technological University, Delhi, October 25 -26, 2013. (ISBN 978-93-83083-35-0)
3. **Harveer Singh Pali**,* C. Mishra, A. Yahaya, Sidharth and N. Kumar, "Sal Seed Oil: A potential feedstock for biodiesel production" (paper code- ISTE 121) Proceedings of ISTE Delhi section Convention Delhi Technological University, Delhi, September 5-6, 2013.
4. **Harveer Singh Pali**,* Rohit Singh, Shubham jain, Saumitra Shekhar, Rohit Kumar, " Castor oil as a Potential fuel for Diesel Engine" Proceedings of International Conference MANFEX 2013, Amity University, Noida, May 30 -31, 2013. (ISBN 978-93-83083-17-6)
5. Y.Alhassan, N. Kumar, **Harveer Singh Pali**,* "Catalytic Hydrothermal Liquefaction of Waste Banana Peels for Heavy Oil Production: Process Optimization" International Conference & Exhibition on "Cutting Edge Technological Challenges in Mechanical Engineering" (CETCME-2015). March, 21-22, 2015.
6. Naveen Kumar, **Harveer Singh Pali**,* "Kusum Oil As A Potential Fuel For CI Engines" Proceedings of International Conference on Alternative Fuels for I. C. Engines (ICAFICE) at MNIT Jaipur, February 6-8, 2013. (ISBN)
7. A.K.Yadav,* A.F.Sherwani, M.N.Karimi and **H.S.Pali** , "Performance & Emission Analysis of Blends of Mahua Oil Methyl Ester in a Compression Ignition Engine" (Paper ID - IC030) Proceedings of International Conference on Alternative Fuels for I. C. Engines (ICAFICE) at MNIT Jaipur, February 6-8, 2013. (ISBN)
8. Kausambi Singh,* **Harveer Singh Pali**, S. P. Divedi, "Study Of Microstructure And Mechanical Properties Of Aa6082/7.5% Sic Composite Produced By Electromagnetic Stir Casting Process" Proceedings of International Conference MANFEX 2013, Amity University, Noida, May 30 -31, 2013. (ISBN 978-93-83083-17-6).
9. Shailesh Singh,* Shashi Prakash Divedi, **Harveer Singh Pali**, "Composite Produced By

Electromagnetic Stir Casting Process" Proceedings of International Conference MANFEX 2013, Amity University, Noida, May 30 -31, 2013. (ISBN 978-93-83083-17-6).

10. Vivek Singh,* Sandeep Chauhan, **H. S. Pali**, " Stress Analysis Of A Spur Gear Tooth Using Solidworks And Stress Reduction By Stress Relief Hole" (paper code- ISTE 146) Proceedings of ISTE Delhi section Convention Delhi Technological University, Delhi, September 5-6, 2013.
11. Shailesh Singh,* Shashi Prakash Dwivedi, **Harveer Singh Pali**, " Wear Characterization of Aa6082/Sic Composite Produced By Mechanical Stir Casting Process" (paper code- ISTE 110) Proceedings of ISTE Delhi section Convention Delhi Technological University, Delhi, September 5-6, 2013.
12. **Harveer Singh Pali**,* S.N.Pandit, P. Pachauri, "Performance Characteristics of Diesel Engine with Jatropha Oil" Proceeding of National Conference on Emerging Trends in Mechanical Engineering (ETME-2011) organized by Department of Mechanical Engineering, IIMT College of Engineering & Technology, Gr. Noida, 2011 .
13. **Harveer Singh Pali**,* P. Pachauri, "Optimization and Simulation of Engine Performance Using Artificial Neural Network" Proceeding of National Conference on Emerging Trends in Computer Science Engineering (ETCSE-2012) organized by NIET, Gr. Noida, 2012.

REVIEWER

1- Energy Conversion & Management
2- Biofuels
3- International Journal of Global Warming
4- SAE International
5- ASME

WORKSHOP & COURSES ATTENDED

- One Week Faculty Development Programme on "Thermal Engineering Applications" ITS Engineering College, Greater Noida, From January 04-09, 2016.
- One Week Faculty Development Programme on "Modeling and Simulation for Mechanical System-MSMS-2016" NIET Greater Noida, From June 06-10, 2016.
- Interactive workshop on "Student Centric Teaching for Mechanical Engineering Course EME102/202", in Skyline Institute of Engineering & Technology, Gr. Noida , from 30-08-2008 to 31-08-2008.
- One Week short term course on "Independent Study Techniques" in National Institute of Technical Teacher's Training and Research, Chandigarh, from March 10-14, 2008.
- One Week training program on "Programming and Machine operation" in Lakshmi Machine Works Ltd., Machine Tool Division in Coibatore from September 05-09, 2005.
- National Seminar on "Advanced Manufacturing Processes" in Noida Institute of

Engineering & Technology Gr. Noida, from 20-02-2010 to 21-02-2010.

- One Week interactive workshop on "Innovative Teaching Techniques" organized by the WIPRO Mission 10X in Noida Institute of Engineering & Technology Gr. Noida, from 17- 21, August 2009.

Educational Qualification:

Degree	Year	Specialization/ Subjects	Board/University	Division
Ph. D	2012-16	Mechanical Engineering	Delhi Technological University, Delhi	-
M.Tech	2008-10	Mechanical Engineering	UP Technical University, Lucknow	First
MBA	2006-08	HR (General)	Algappa University, Tamilnadu	First
B.Tech	1999-2003	Mechanical & Industrial Engineering	M.J.P. Rohilkhand, Bareilly	First

Membership of International Societies and Organizations:

a) Member – Society of Automotive Engineers **(SAE International)**.
b) Member – American Society of Mechanical Engineering **(ASME)**.
c) Member - Centre for Advanced Studies & Research in Automotive Engineering **(CASRAE)**
d) Member – Indian Society of Technical Education **(ISTE)**.
e) Member – **Mission 10X(WIPRO)**
f) Faculty Advisor **– SAE collegiate Club NIET.**
g) Founder Member **– ISFT India**

Foreign Research Collaboration:

Visited the National Research Institute for Chemical Technology, (NARICT) Zaria, Nigeria for research collaboration in Algae biodiesel production and attend International Training Workshop on Biodiesel Production Technology.

Place: Greater Noida **(HARVEER SINGH PALI)**